Vol. 122 Nos. 1-6

September-October 1958

PROCEEDINGS OF THE ACADEMY OF SCIENCES

OF THE USSR

(DOKLADY AKADEMII NAUK SSSR)

Physical Chemistry Section

A publication of the Academy of Sciences of the USSR

IN ENGLISH TRANSLATION

Year and issue of first translation:
Vol. 112, Nos. 1-6 Jan.-Feb. 1957

Annual subscription	*$160.00*
Single issue	*35.00*

CONSULTANTS BUREAU INC.
227 W. 17th ST., NEW YORK 11, N. Y.

Printed in the United States of America

PROCEEDINGS OF THE ACADEMY OF SCIENCES OF THE USSR

Physical Chemistry

Volume 122, Numbers 1-6 September-October 1958

CONTENTS

	PAGE	ISSUE	RUSS. PAGE
A Study of the Electrode Process on Zinc Amalgams by the Method of Radioactive Indicators. G.M. Budov and V.V. Losev.	617	1	90
A Mass-Spectrometric Study of the Photo-Ionization and Photodissociation of Amine Vapors. F.I. Vilesov, B.L. Kurbatov and A.N. Terenin	623	1	94
The Production of Geometrically Ordered Structures in Amorphous Polymers. V.A. Kargin, N.F. Bakeev and Kh. Vergin	627	1	97
The Dipole Moments of Certain Organosilicon Compounds. G.N. Kartsev, Ia. K. Syrkin, V.F. Mironov and E.A. Chernyshev.	631	1	99
The Part Played by Ozone in the Initiation of the Oxidation of Saturated Gaseous Hydrocarbons. N.A. Kleimenov and A.B. Nalbandian	635	1	103
The Kinetics of Ion Exchange Between Metal and Slag. Iu.P. Nikitin and O.A. Esin	639	1	106
The Heat of Combustion of Tetrahydropyran. S.M. Skuratov and M.P. Kozina . . .	643	1	109
The Mechanism of the Cross-Linking of Polymer Chains under the Influence of Gamma Radiation. Ying Sheng-k'ang, A.N. Pravednikov and S.S. Medvedev	645	2	254
Convection Diffusion in Liquid Solutions under Turbulent Conditions. I.P. Krichevskii and Iu. V. Tsekhanskaia	649	2	258
The Influence of the Adsorption of Volatile Inhibitors on the Electrochemical Behavior of Iron. I.L. Rozenfel'd and V.P. Persiantseva.	651	2	260
A Study of the Structure of the Products of the Carbonization of Materials Containing Carbon, by the Methods of Electronic Paramagnetic Resonance and X-Ray Structural Analysis. N.N. Tikhomirova, B.V. Lukin, L.L. Razumova and V.V. Voevodskii.	655	2	264
The Polarography of the Tropyllium Ion. S.I. Zhdanov and A.N. Frumkin	659	3	412
Low Pressure Adsorption Isotherms for Nitrogen. M.G. Kaganer	663	3	416
An Investigation of the Low Temperature Oxidation of Methane Initiated by Oxygen Atoms Formed in the Thermal Decomposition of Ozone. N.A. Kleimenov and A.B. Nalbandian	667	3	420
The Scale of the Structural Etching in the Electrochemical Polishing of Metals. S.I. Krichmar.	671	3	424
The Problem of the Hydration of Ions in Aqueous Solutions. O.A. Osipov and I.K. Shelomov.	675	3	428

CONTENTS (continued)

	PAGE	ISSUE	RUSS. PAGE
The Thermodynamic Equilibrium of Surfaces of Strong Dislocation. V.I. Skobelkin	679	3	431
An X-Ray Diascopic Investigation of the Mechanism of Internal Diffusion. D.P. Timofeev and A.A. Voskresenskii	683	3	434
A Study of the Adsorption of Benzene Vapors on Palladium Films. V.D. Iagodovskii	687	3	437
Investigation of the Kinetics of Recombination of Triphenylmethyl Radicals by the Electron Paramagnetic Resonance Method. F.S. D'iachkovskii, N.N. Bubnov and A.E. Shilov	691	4	629
Germanium Electrode with a p-n Junction. E.A. Efimov and I.G. Erusalimchik	695	4	632
Effect of CaF_2 on the Distribution of Phosphorus in Liquid Iron and Iron Lime Slag. I.Iu. Kozhevnikov, O.V. Travin and E.N. Iakho	697	4	635
Effect of Inorganic and Organic Cations on the Reduction of the $PtCl_4^{=}$ Anion by a Dropping Mercury Electrode. N.V. Nikolaeva-Fedorovich, L.A. Fokina and O.A. Petrii	701	4	639
Effect of Oxide Films and Adsorptionally Active Media on Creep of Copper Wire. V.S. Ostrovsky, T.A. Amfiteatrova and B.Ia. Iampol'skii	705	4	643
Elastic Properties of Disperse Systems and the Phenomenon of Thixotropy. V.P. Pavlov and G.V. Vinogradov	709	4	646
Equilibrium Distribution of Deuterium in the Hydrogen Exchange with Liquid Hydrogen Chloride. Ia.M. Varshavskii, S.E. Vaisberg and B.A. Trubitsyn	713	5	831
Thermodynamic Properties of Cu–Ni and Fe–Co Solid Solutions. Ia.I. Gerasimov, A.A. Vecher and V.A. Geiderikh	717	5	834
Three-Center Orbitals in the Structure of Cyclopropane and Other Three-Membered Ring Compounds. M.E. Diatkina and Ia.K. Syrkin	721	5	837
Adsorption of Water Vapor on Crystalline Silver and Lead Halide Dust Particles. N.N. Moskvitin, M.M. Dubinin and A.I. Sarakhov	725	5	840
The Effect of Replacing Hydrogen with Deuterium on the Polarizability of Molecules. I.B. Rabinovich and Z.V. Volokhova	729	5	844
Equilibrium Ionization Generated by Dust Particles. Iu.S. Saiasov	735	5	848
The Effect of Concentration on the Degree of Radiolytic Transformation of Aqueous Sodium Nitrate. V.A. Sharpatyi, V.D. Orekhov and M.A. Proskurnin	739	5	852
Radiolysis of Heptane. A.M. Brodskii, Iu.A. Kolbanovskii, E.D. Filatova and A.S. Chernysheva	741	6	1035
Combustion in an Adiabatically Heated Gaseous Mixture. S.G. Zaitsev and R.I. Soloukhin	745	6	1039
Preparation and Electrochemical Properties of Crystalline Modifications of Lead Dioxide. L.G. Kiseleva and B.N. Kabanov	749	6	1042
Interaction of Shock Waves with Flame Fronts. S.M. Kogarko, V.I. Skobelkin and A.N. Kazakov	753	6	1046
The Role of Surface Properties of a Semiconductor in Adhesion Phenomena. V.P. Smilga and B.V. Deriagin	757	6	1049
P.M.R. Spectra of Some Polymers Irradiated at 77°K. Iu.D. Tsvetkov, N.N. Bubnov, M.A. Makul'skii, Iu.S. Lazurkin and V.V. Voevodskii	761	6	1053

A STUDY OF THE ELECTRODE PROCESS ON ZINC AMALGAMS BY THE METHOD OF RADIOACTIVE INDICATORS

G. M. Budov and V. V. Losev

(Presented by Academician A. N. Frumkin April 30, 1958)

The principal difficulty which arises in studying the anodic dissolution and electrodeposition of metals is that the rate of the strictly electrochemical step of discharge and ionization of the reacting particles is in many instances so high as to make the transfer, either of reacting particles to the electrode surface, or of reaction products away from this surface, the limiting factor which fixes the rate of the entire reaction under ordinary conditions. It naturally follows that stationary polarization curves obtained under these conditions would fail to directly reflect the kinetics of ionization and discharge. Thus, in the study of the mechanism of rapid electrode processes, especial significance attaches to those measurements of the exchange current (one of the important parameters characterizing the ionization and discharge) which are so carried out that only the electrochemical step can exert an influence on the kinetics of the electrode process. We will consider the kinetics of the ionization and discharge processes in the anodic dissolution of a metal amalgam into a solution containing the simple ions of this same metal: $Me \rightarrow Me^{n+} + n(e)$. According to the theory of retarded discharge [1], the relation between potential and current density in anodic polarization is expressed by the equation.*

$$i = k'C_a e^{\beta F\varphi/RT} - k''C_p e^{-\alpha F\varphi/RT}, \tag{1}$$

in which C_a and C_p are the bulk concentrations in the amalgam and the solution, and α and β are transfer coefficients, for which it is assumed that $\alpha + \beta = n$. At the equilibrium potential, φ_e, the rates of the anodic and the cathodic processes become equal to the exchange current and:

$$i_0 = k'C_a e^{\beta F\varphi_e/RT} = k''C_p e^{-\alpha F\varphi_e/RT}. \tag{2}$$

When account is taken of those concentration differences which exist between the surface and the body of the solution at high $\underline{i}$ values, (1) and (2) give rise to:

$$i = i_0\left[(1 - i/i_d^a)\, e^{\beta F\Delta\varphi/RT} - (1 + i/i_d^k)\, e^{-\alpha F\Delta\varphi/RT}\right], \tag{3}$$

in which i^a_d and i^k_d are the limiting anodic and cathodic currents, and $\Delta\varphi = \varphi - \varphi_e$. By combining (2) with the Nernst Equation, an expression for the relation between the exchange current and the concentrations of the amalgam and of the solution** is readily obtained:

---

* The assumption is made that the over-all electrode reaction consists of a series of consecutive single-electron steps, and that the slowest of these limits the rate of the entire reaction [2, 3]. It is further presumed that the solution contains an excess of an indifferent electrolyte, so that no account need be taken of the existence of a ψ_1-potential [1], and the activity coefficients of the metal ions can be considered as constant.

** An equation of this type was first obtained for the discharge of hydrogen ions and the ionization of hydrogen atoms [1]. Equation (4) differs from those expressions which are usually employed for relating the exchange current and the concentrations of the amalgam and the solution [4, 5], in so far as these equations were derived by supposing the slow step of the electrode process to be the simultaneous splitting off $\underline{n}$ electrons, the normalization relation $\alpha + \beta = 1$ being employed in place of the relation $\alpha + \beta = n$ which was adopted above. It is not difficult to show that the physical meaning of the coefficients α and β is not the same in the two cases [2, 3].

$$i_0 = kC_a^{\alpha/n} \cdot C_p^{\beta/n}. \quad (4)$$

It follows from (4) that measurements of i_0 at various concentrations of the amalgam and the solution permit the determination of those coefficients α and β which characterize the slow step and which cannot be directly evaluated from the usual polarization curves for rapid electrode processes. Determination of the parameters i_0, α and β, when combined with measurements on the limiting currents, also permits the development of the entire polarization curve through Equation (3), in which there is taken into account not only the delay in discharge and ionization, but the concentration polarization as well.

For measuring exchange currents on amalgam electrodes, there have been employed not only nonstationary methods (alternating current [4, 6-8], galvanostatic [9, 10], potentiostatic [11, 12]) but also the method of radioactive indicators [13, 14]. This latter is distinguished by the fact that the measurements of the exchange current are carried out under conditions most closely approximating those prevailing at equilibrium.*

It was the aim of the present work to make measurements of the exchange currents on zinc amalgams by the method of radioactive indicators, to carry out polarization measurements and to determine the limiting anodic and cathodic currents. When combined, such measurements made it possible to readily separate out that interval of concentrations of amalgam and solution within which the rate of exchange is limited by the discharge-ionization step and not by the diffusion of the radioactive particles, and, in addition, allow a comparison of the experimentally determined polarization curves with those calculated from Equation (3) by using the values of the parameters i_0, α, β, and i_d obtained under fixed experimental conditions.

The technique which was employed was a refinement of that described earlier in [2].** Measurements of the exchange current were carried out in an atmosphere of nitrogen at 25°, and involved amalgams of concentrations 0.00008-0.97 M, in 0.0001-0.20 M $ZnSO_4$ solutions which were acidified with H_2SO_4 (0.005 M) and contained added

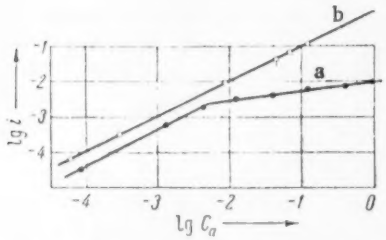

Fig. 1. Dependence of the exchange current (a) and the limiting anodic current (b) on the amalgam concentration, at C_p = 0.025 M $ZnSO_4$.

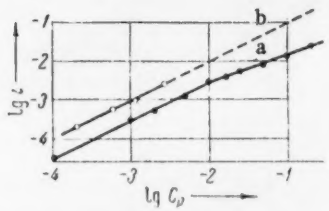

Fig. 2. The dependence of the exchange current (a) and the limiting cathodic current (b) on the $ZnSO_4$ concentration, at C_a = 0.13 M $ZnSO_4$.

$MgSO_4$ to maintain constancy of the ionic strength (2 M). Over a wide interval of $ZnSO_4$ concentrations (0.01-0.20 M), preliminary measurements showed the exchange current to be but weakly dependent on the rate of agitation (200-500 rev/min). The slight increase in the exchange current which accompanied an increase in the rate of agitation clearly resulted from an increase in the amalgam surface. All of these experiments were carried out at an agitation rate of 400 rev/min.

* Even with intensive agitation of the amalgam and the solution, it is possible that at very high exchange currents there is a breakdown in that equilibrium distribution of the radioactive particles between the two phases whose existence is the fundamental requirment for the correctness of the measurements; it can then be true that the experimentally measured rate of transfer of the radioactive particles through the interface between the phases will be fixed by the rate of diffusion of these particles in one of the phases [14].

** Into the cell there was introduced a magnetic glass stirrer of the propellet type and a burette with an attachment for saturating added portions of the solution with nitrogen. With one portion of the amalgam which had been tagged with Zn^{65} it was possible to measure several values of the exchange current corresponding either to different solution concentrations or to different temperatures.

The results of measurements of the exchange current are presented in Figs. 1 and 2, together with data on the limiting anodic and cathodic currents. The slopes of the straight lines log i^a_d vs log C_a and log i^k_d vs log C_p are equal respectively to 0.96 and 0.97, i.e., the limiting currents were directly proportional to the corresponding concentrations. It is to be seen from Figs. 1 and 2 that the log i_0 vs log C_a, and the log i_0 vs log C_p, curves consist of two segments of different slope, these slopes being close to unity in the region of low concentrations where the corresponding segments are parallel to the straight lines representing the limiting currents. It is clear that the transfer of radioactive particles into solution is limited in this region of concentrations by diffusion rather than by the ionization-discharge step so that the corresponding experimental values of i_0 are low in comparison with the true exchange currents. At higher concentrations, there is observed a more gradual rise in the exchange current with increasing concentration; on increasing the $ZnSO_4$ concentration from 0.01 to 0.20 M (with C_a = 0.13 M), the exchange current rises from 2.8 to 22.5 ma/ cm^2; on increasing the amalgam concentration from 0.013 to 0.970 M (with C_p = 0.025 M) the exchange current rises from 2.9 to 8.3 ma/ cm^2. For this region of concentrations, values of the coefficients $\alpha = 0.52 \pm 0.04$ and $\beta = 1.40 \pm 0.05$, were determined from the slopes of the straight lines log i_0 vs log C_a, and log i_0 vs log C_p by the use of Equation (4).

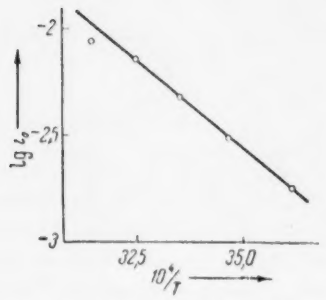

Fig. 3. The dependence of the exchange current on the temperature, at C_p = 0.025 M $ZnSO_4$ and C_a = 0.13 M Zn.

The values which we obtained for the exchange currents are in satisfactory agreement with the data of V. A. Pleskov and N. B. Miller [13], although somewhat lower than those found by other authors through the use of nonstationary methods [4, 6, 9, 10, 11].* The values of the transfer coefficients α and β agree well with the data of Gerisher [4]. The fact that the sum of the experimental values of α and β is close to 2, and that the i_0 values are independent of the rate of agitation of the solution, indicates that the rate of exchange in this region of concentrations is limited by the ionization-discharge step and not by the diffusion of the radioactive particles. This conclusion is confirmed by the results of a study of the temperature dependence of the exchange current (at C_p = 0.025 M) for two different amalgam concentrations corresponding to the two different segments of the log i_0 vs log C_a curve (Fig. 1). For the interval 3-45°, the log i_0 vs 1/ T relation at C_a = 0.13 M is sketched in Fig. 3. The energy of activation as calculated from the slope of this straight line amounts to 7.4 kcal, whereas in the diffusion region at concentration C_a = 0.00013 M, its value is approximately 5 kcal.

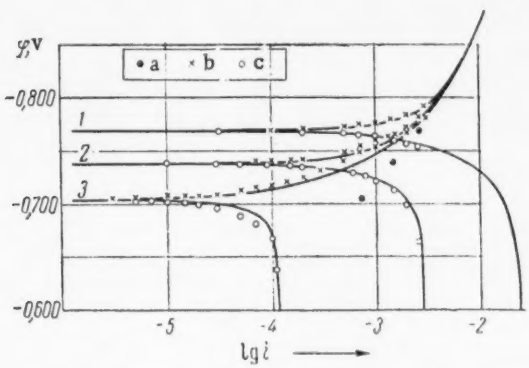

Fig. 4. Polarization curves for various amalgam concentrations: 1) C_a = 0.026 M Zn, 2) C_a = 0.0029 M Zn; 3) C_a = 0.00011 M Zn (C_p = 0.025 M $ZnSO_4$). a) Exchange current; b) points on the cathodic branch of the polarization curve; c) points on the anodic branch of the polarization curve. The full curves are calculated according to Equation (3).

In addition to the measurements of the exchange current, polarization curves were also obtained in this same cell at the same rate of agitation. In Fig. 4 the results of these measurements have been represented by circles and crosses, and exchanged currents corresponding to these concentrations have been plotted;** theoretical polarization curves calculated from Equation (3) by using

* It is possible that these deviations arise from differences in the anode compositions, and in the ionic strengths of the solutions which were employed.

** The values of i_0 corresponding to diluted solutions were determined by extrapolating that portion of the log i_0 vs log C_a curve (Fig. 1) which marks out the kinetic region.

the experimentally determined values of i_0, the coeffients α and β, and the values of the limiting currents, are here represented by the full curves.* It is to be seen from this figure that the experimental points agree well with the theoretical curves. This is additional confirmation of the fact that the values of i_0, α and β which were employed in the calculations (and which had been arrived at by the independent radiochemical method) were trustworthy, i.e., that these actually characterized the ionization-discharge step and were not, to a detectable degree, distorted by the diffusion effect.

An analysis of Equation (5) for the anodic polarization curves shows that $i_d^a / i_0 \sim 0.1$ in the case of Curve 3 so that the first term in the denominator is small in comparison with the second and the rate of the anodic process is limited by diffusion, whereas $i_d^a / i_0 \sim 10$ for Curve 1, and it is possible to neglect the second member of the denominator at moderate values $\Delta\varphi$, ionization-discharge being the limiting step. Thus, by an increase in the concentration of the amalgam alone (by approximately 200-fold), other conditions being held constant, there is brought about a transition from the diffusion zone into the kinetic. This results from the fact that the exchange current and the limiting anodic current are differently related to the amalgam concentration C_a, the limiting current being linearly dependent on C_a, whereas the exchange current rises much more slowly as C_a is increased (Equation (4) and Fig. 4).** It follows from the results which have been obtained that this effect might be utilized for selecting those concentrations of the reacting substances under which it would be possible to markedly diminish the influence of the diffusional step on the rate of rapid electrode processes, and on the measured values of the exchange current, in particular.

We wish to express our deep thanks to Academician A. N. Frumkin for his valuable advice in evaluating the results of this work.

LITERATURE CITED

[1] A. N. Frumkin, V. S. Bagotskii, Z. A. Iofa and B. N. Kabanov, The Kinetics of Electrode Processes [in Russian], Moscow, 1952.

[2] V. V. Losev, Proc. Acad. Sci. USSR, 100, 111 (1955); Trans. Ins. Phys. Chem., vol. 6, 20 (1957).

[3] V. V. Losev and A. M. Khopin, Trans. Fourth Electrochemical Conference (in press).

[4] H. Gerischer, Zs. phys. Chem., 202, 292, 302 (1953).

[5] A. G. Stromberg, J. Phys. Chem., 29, 409 (1955).

[6] B. V. Ershler and K. I. Rozental', Trans. of a Conference on Electrochemistry, 1953, p. 446.

[7] J. E. B. Randles and K. W. Somerton, Trans. Farad. Soc., 48, 951 (1952).

[8] G. C. Barker, R. L. Faircloth and A. W. Gardner, Nature, 181, 247 (1958).

[9] P. Delahay et al., J. Am. Chem. Soc., 75, 2486, 4205 (1953); 76, 874 (1954); 77, 6448 (1955).

[10] H. Gerischer, Zs. Elektrochem., 59, 604 (1955); Zs. Phys. Chem., 10, 264 (1957).

[11] H. Gerischer and W. Vielstich, Zs. Phys. Chem., 3, 16 (1955); 4, 10 (1955).

[12] W. Vielstich and P. Delahay, J. Am. Chem. Soc., 79, 1874 (1957).

*For the calculation of the anodic curves, use was made of an approximation relation which was obtained from (3):

$$i = i_d^a \frac{e^{\beta F \Delta\varphi / RT} - e^{-\alpha F \Delta\varphi / RT}}{i_d^a / i_0 + e^{\beta F \Delta\varphi / RT}} . \qquad (5)$$

**Such a phenomenon can clearly lead to the transition from reversible to irreversible waves in obtaining anodic polarograms in amalgams [15].

[13] N. B. Miller and V. A. Pleskov, Proc. Acad. Sci. USSR, 74, 323 (1950); Trans. of a Conference on Electrochemistry, 1953, p. 165.

[14] S. Froneus, Acta Chem. Scand., 7, 764 (1953); 8, 412, 961 (1954); 10, 490 (1956).

[15] V. V. Losev, J. Phys. Chem., 30, 1402 (1956).

The Electrochemical Institute of the
Academy of Sciences of the USSR
The L. Ia. Karpov Physicochemical Institute

Received April 29, 1958

A MASS-SPECTROMETRIC STUDY OF THE PHOTO-IONIZATION AND PHOTODISSOCIATION OF AMINE VAPORS

F. I. Vilesov, B. L. Kurbatov and Academician A. N. Terenin

In a paper reporting the results of our measurements of the photo-ionization potentials of the vapors of organic compounds [1], it was suggested that when the molecules are exposed to the influence of long-wavelength radiation in the ultraviolet region of the spectrum in vacuo, elementary photo-ionization of the molecule takes place with the removal of an electron.

On the other hand, it is known that when molecular vapors are exposed to short-wave radiation with wavelengths of up to 1050 Å (energy of the quantum 11.8 ev), photodissociation of the molecules also takes place, and this has been studied in a number of works (see, for example, [2]).

In order to carry out a detailed study of these processes, we constructed a mass spectrometer of the 90-degree type with an average ion trajectory radius of 126 mm.* The mass analysis was automatic and exponential and the spectrum was recorded by means of a PS-01 recorder. The ion source was constructed in such a way that it was possible to bring about the ionization of the gas under study by means of electrons or photons separately, or by means of both simultaneously. The electron beam, as a rule, was directed along the slit of the ion source, while the photon beam was perpendicular to the slit.

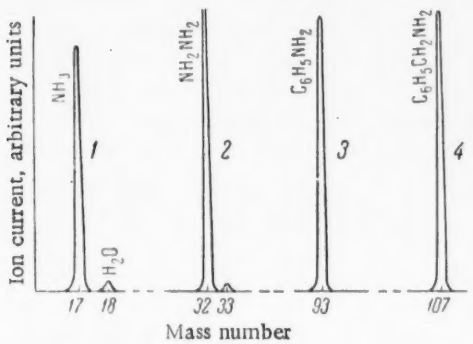

Fig. 1. The mass spectra of amines, obtained with ionization under the influence of light.
1) Ammonia; 2) hydrazine; 3) aniline; 4) benzylamine.

With the difficult to irradiate space in the ionization chamber irradiated by means of unresolved light from a hydrogen lamp (discharge current 2 amps, voltage 1000 volts) through a LiF window (transparent up to 1050 Å), the ion current on the collector was of the order of 10^{-13} - 10^{-14} amps with the pressure of the gas under study in the ion source equal to 10^{-4} - $5 \cdot 10^{-5}$ mm mercury.

The following amines were studied: ammonia NH_3, hydrazine NH_2-NH_2, benzylamine $C_6H_5-CH_2-NH_2$, aniline $C_6H_5-NH_2$. The mass spectra obtained with radiation of these compounds are given in Fig. 1. They reveal only elementary photo-ionization of the molecules according to the scheme:

$$AB + h\nu \rightarrow AB^+ + e.$$

This result confirms our suggestion that in the work previously described [1] the observed photo-ionization currents were in fact produced only by the elementary photo-ionization of the molecules and that, in any case, ionization processes involving breakdown of the type

$$AB + h\nu \rightarrow A^+ + B^- \quad \text{or} \quad AB + h\nu \rightarrow A^+ + B + e$$

* The magnet was kindly placed at our disposal by Professor N. I. Ionov, to whom we have to express our deep gratitude for friendly service.

have a low probability (less than 1% of the main process).

When the vapors of aniline and benzylamine are irradiated, not with photons, but with electrons with energies of approximately 11.5 ev, more complex mass spectra, produced by processes involving breakdown of the molecules into ions, are obtained.

It follows from this that the use of even a monochromatic photon beam is more suitable for carrying out the mass-spectrometric analysis of complex organic compounds than the use of an electron beam.

The use of monochromatic light, by means of which ionization potentials may be determined with an accuracy of 0.02-0.03 ev, will make it possible to carry out further analysis at the photo-ionization thresholds and in this way to identify even different isomers.

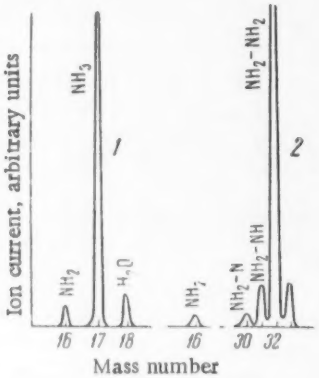

Fig. 2. The mass spectra of radicals produced with photodissociation. 1) Ammonia; 2) hydrazine.

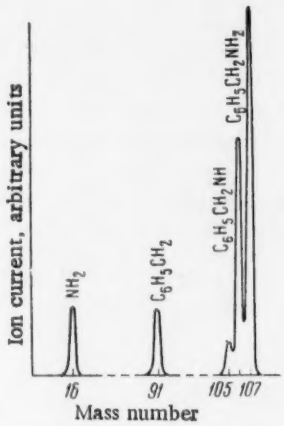

Fig. 3. The mass spectra of radicals produced with photodissociation of benzylamine.

The studies which we made on photodissociation were carried out as follows. First of all the mass spectrum of the vapor of the substance under study was recorded using high-energy electrons without optical excitation. The energy of the electrons was then reduced to the value at which all the peaks produced by radicals disappeared, and the hydrogen lamp irradiation was switched on. When this was done, peaks appeared in the mass spectrum as a result of the formation of radicals by photodissociation of the molecules and subsequent ionization by electron collision. Figures 2 and 3 give the spectra obtained for ammonia, hydrazine, aniline and benzylamine vapor.

Ammonia. Figure 2 (Spectrum 1) shows two peaks with masses of 17 and 16, corresponding to the ions NH_3^+ and NH_2^+, so that, in addition to the photo-ionization of the molecule, photodissociation takes place according to the scheme

$$NH_3 + h\nu \rightarrow NH_2 + H.$$

Hydrazine. In the case of hydrazine (Fig. 2, Spectrum 2) an intense peak is observed corresponding to the radical NH_2-NH, together with weak peaks corresponding to the radicals NH_2 and NH_2-N, which indicates that the probability of the removal of a hydrogen atom is greater than that of breakdown of the molecule into two parts at the weaker N – N bond [3].

The photodissociation of ammonia and hydrazine has been studied by Neuimin and Terenin [2] who showed that the following processes take place:

$$NH_3 + h\nu_v \rightarrow NH_2^* + H \rightarrow NH_2 + H + h\nu_f$$

$$NH_2 - NH_2 + h\nu_v \rightarrow NH_2^* + NH_2 \rightarrow NH_3 + NH_2 + h\nu_f.$$

At the same time it was observed that the fluorescence of the NH_2 radical in the case of hydrazine was much

weaker than in the case of ammonia, and this is in accordance with the mass spectra obtained for hydrazine in the present work.

Benzylamine. It can be seen from Fig. 3 that an intense peak is obtained with mass number 106, corresponding to the ion $C_6H_5-CH_2-NH^+$, which is evidently formed by photodissociation according to the scheme:

$$C_6H_5-CH_2-NH_2+h\nu \rightarrow C_6H_5-CH_2-NH+H.$$

In addition, weak peaks are present with masses of 16 and 91, produced by the ionized radicals $C_6H_5-CH_2$ and NH_2, which are evidently formed by photolysis of the benzylamine according to the scheme:

$$C_6H_5-CH_2-NH_2+h\nu \rightarrow C_6H_5-CH_2+NH_2.$$

Aniline. The study of aniline vapor showed no photodissociation into radicals. We made repeated attempts, based on the methods of earlier work [2], to obtain an NH_2^+ radical fluorescence spectrum by irradiating the vapor of benzylamine and aniline with light from a powerful hydrogen lamp passed through a LiF window. We did not, however, obtain any positive results. The absence of photodissociation with excitation of the NH_2 radical may be explained by the fact that the benzene ring, which has a large number of vibrational degrees of freedom, drains off the excess energy absorbed by the $C-NH_2$ bond and also deactivates the excited NH_2 particle. This tapping of the energy is particulary important in the case of the aniline molecule, in which the NH_2 group is linked directly to the benzene ring. The presence of the NH_2 radical in the mass spectrum for benzylamine indicates that removal of the NH_2 radical is taking place in this case, and this is related to the fact that the CH_2 group, as is known, is insulating and hinders the direct transfer of energy from the NH_2 and the $C-NH_2$ bond into the benzene ring. When the radiation is sufficiently powerful, it is possible to detect the formation of the excited NH_2 radical in benzylamine vapor from its fluorescence spectrum.

At the same time, this viewpoint is in good agreement with the low quantum yield for the photo-ionization close to the threshold for these molecules (3-5%) compared with the molecules of other compounds (30-50%).

LITERATURE CITED

[1] F. I. Vilesov, A. N. Terenin, Proc. Acad. Sci., 115, No. 4 (1957).*

[2] G. G. Neuimin, A. N. Terenin, Bull. AN SSSR, OMEN, Phys. Ser., No. 4, 529 (1936).

[3] A. Gaydon, The Dissociation Energy and Spectra of Diatomic Molecules, IL (1949).**

Institute of Physics, A. A. Zhdanov
State University, Leningrad

Received May 30, 1958

*Original Russian pagination. See C.B. translation.

**Russian translation.

THE PRODUCTION OF GEOMETRICALLY ORDERED STRUCTURES IN AMORPHOUS POLYMERS

Academician V. A. Kargin, N. F. Bakeev and Kh. Vergin

On the basis of experimental data obtained recently by a number of authors, it has been suggested that the existing theories which regard the structure of amorphous polymers as involving chaotically entangled twisted chains do not correspond to the actual structure of amorphous polymers. V. A. Kargin, A. I. Kitaigorodskii and G. L. Slonimskii [1] consider that the molecular arrangement of the chains in amorphous polymers may be produced, as a rule, either by unfolded chains collected in bundles or by chains coiled up into globules. The peculiar features of the physical and mechanical properties of amorphous polymers can be readily explained starting from such a model.

The existence of molecular bundles formed by the linking together of parallel unfolded chains in amorphous polymers has been shown for the case of polyacrylic acid and its salts [2].

In the present work we undertook an electron microscope study of the structure of certain amorphous polymers exhibiting different molecular chain arrangements. The materials studied were polymers of arsenic (salvarsan), polyacrylamide, and a copolymer based on methyl methacrylate and methacrylic acid. We have thus studied polymers containing different polar groups in the chain and consequently exhibiting different intra- and intermolecular forces.

The specimens for study were prepared by placing a solution of the polymer on a thin support and then evaporating the solvent. The concentrations of the solutions were chosen over a range from 0.01 to 0.0001%. The studies were carried out with a direct electron-optical magnification of 18000-20000.

The electron microscope studies showed that salvarsan, polyacrylamide and a copolymer based on methyl methacrylate and methacrylic acid form, in dilute solution, separate secondary aggregates in the form of molecular bundles of different shapes and dimensions as described above. Electron microscope photographs of such bundles are shown in Figs. 1 a, 2 a and 3 a respectively.

In the case of salvarsan and polyacrylamide we observed the production of geometrically regular structures in the form of rectilinear molecular bundles. The regular external shape of these bundles is remarkable. The dimensions of the bundles are naturally determined by the magnitude of the molecular weight and by the intermolecular forces. For salvarsan, on the basis of the transverse dimensions of the molecular bundles, the dimensions of the separate chains, and the distance between them (assuming closest packing) we find that one bundle consists of from 10-50 molecular chains. If, however, we take into account the fact that we are starting from a planar image, and that the bundle naturally possesses the dimensions of volume, we may assume at least a quadratic value for the number of chains inside the bundle.

The data obtained show that a bundle formed from molecular chains arranged parallel to one another retains the flexibility shown by a separate isolated chain. Evidence for this is provided by the fact that at a certain spacing the bundles are no longer directed along a straight line but show a coordinated bending at a definite angle. This bending is not the result of a gradual smooth inflexion of the bundle, but has a more "articulate" character. This bending can be pictured as resulting only from the high degree of order in the arrangement of the molecular chains. In actual fact the process of arranging the chains in order will lead to the production of stresses inside the bundles as a result of the thermal motion of the separate macromolecules. As a result, stresses will accumulate inside the bundles and will lead to the coordinated twisting at a definite angle, generally all at once.

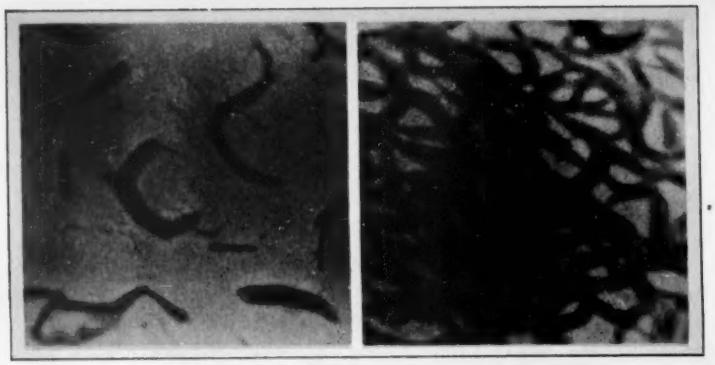

a b

Fig. 1. Salvarsan. × 50000.

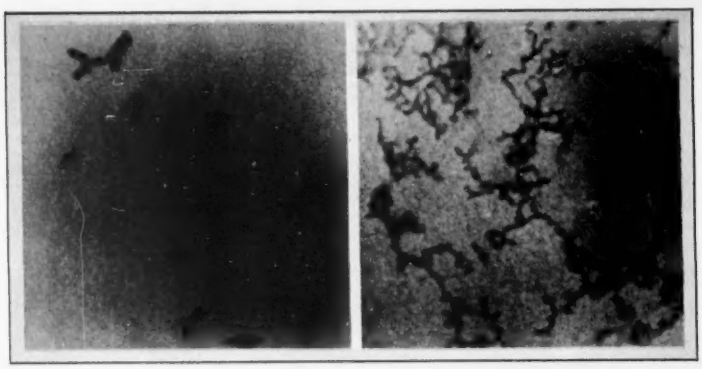

a b

Fig. 2. Polyacrylamide. a) × 30000; b) × 50000.

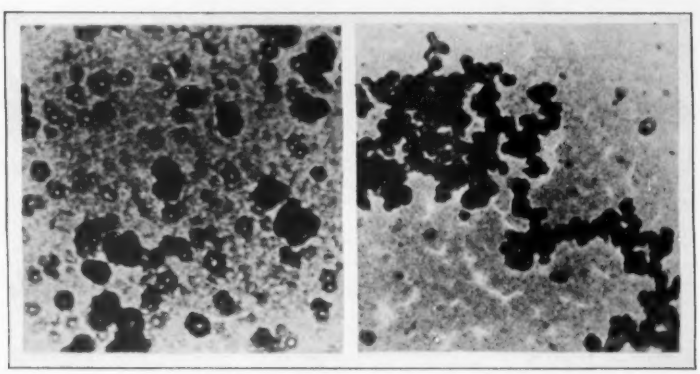

a b

Fig. 3. Copolymer bases on methyl methacrylate and methacrylic acid. a) × 60000; b) × 40000.

It is necessary to mention that the twisting of the bundles at a definite angle which results from the production of internal stresses may be the reason for the formation of geometrically ordered structures in amorphous polymers. This is the case for the copolymer based on methyl methacrylate and methacrylic acid which we have studied. In the case of this copolymer we observed the formation of geometrically regular polyhedra as a result of the twisting of the molecular bundles. It may be supposed that this mechanism is responsible for the production of regular structures in amorphous polymers which is also observed in biological systems.

Figures 1 b, 2 b and 3 b show photomicrographs of the polymers under study, obtained from concentrated solutions. The unfolded secondary structures of which the molecular bundles form the units, indicate that the bundles preserve their individuality at the fairly high concentrations at which interaction takes place between the bundles.

It has thus been shown that in the case of the amorphous polymers which have been studied, an ordered arrangement of molecular chains is produced leading to the formation of rectilinear bundles. The high degree of order of the chains in the bundles is also indicated directly by the coordinated twisting of the bundles themselves, which is of an "articulated" character. On the basis of the results obtained in the case of the copolymer formed by methyl methacrylate and methacrylic acid, it has been shown that the formation of geometrically regular structures in amorphous polymers as a result of the regular twisting of the bundles is possible.

Confirmation has thus been obtained for the suggestion previously put forward, that the structure of amorphous polymers should be regarded as a system of ordered molecular bundles.

The authors take this opportunity to express their thanks to Professor M. Ia. Kraft and his co-workers for the salvarsan which they kindly make available.

LITERATURE CITED

[1] V. A. Kargin, A. I. Kitaigorodskii and V. L. Slonimskii, Colloid J., 19, 131 (1957).*

[2] V. A. Kargin, N. F. Bakeev, Colloid J., 19, 133 (1957).*

M. V. Lomonosov State University,
Moscow.

Received July 7, 1958

*Original Russian pagination. See C.B. translation.

THE DIPOLE MOMENTS OF CERTAIN ORGANOSILICON COMPOUNDS

G. N. Kartsev, Corresponding Member AN SSSR Ia. K. Syrkin,
V. F. Mironov and E. A. Chernyshev

We have measured the dipole moments of a number of organosilicon compounds using the heterodyne method at 25° in benzene. The extrapolated polarizations were calculated using the Hedestrand formula. In the case of compounds containing silicon, it is necessary to take into account the atomic polarization, since neglect of this quantity may introduce an error into the value of the dipole moment. In a number of works the atomic polarization has been taken as equal to 5% of the electronic polarization or has not been taken into account at all. The known atomic polarizations for a number of substances ($SiCl_4$ 5.3 [1]; Si_2H_6 4; SiH_4 2; SiF_4 5.4 [2]; $(CH_3)_3SiCH_2CH_2 \cdot C_6H_5$ 6.5; $(CH_3)_3SiCH_2CH_2C_6H_4NO_2$ 10; $(CH_3)_3Si-O-Si(CH_3)_3$ 7.9 cm^3 [3]) show that these quantities should be taken into account in the calculation of the dipole moments. In the case of SiH_4 and $SiCl_4$ the atomic polarization amounts to 16 and 18% of the electronic polarization. We have examined the relationship between the total polarization of $(CH_3)_3SiCH_2CH_2C_6H_4NO_2$ (-para) and the temperature within the range from 280.5 to 333° K and have found that the total polarization is given satisfactorily by the equation:

$$P_{total} = 77 \times 126950/T. \quad (1)$$

From this, using the Debye equation, it is found that the atomic polarization is equal to approximately 10 cc, which in this case amounts to 15% of P_{el}. In this connection we evaluated P_{el} and introduced the appropriate corrections in the determination of the dipole moments. We used for P_{el} the refraction for the yellow sodium line without extrapolation to infinite wavelength, in order to compensate to a certain extent for the reduced values of the atomic polarization.

The experimental data obtained are given in Table 1.

A distinctive feature of silicon compounds is the increased polarity compared with the corresponding bonds for carbon. From the existing data we may take the moment of the Si−H bond as 1 D and that of the Si−C bond as 0.6 D [1]. In both cases the positive end of the dipole is directed towards the silicon. In the bonds Si−O and Si-Hal the influence of the ionic state is greater. The electropositive nature of silicon is also apparent from the fact that its ionization potential is considerably lower than that of carbon (186 kcal. and 258 kcal. respectively). Another distinguishing feature shown by silicon is that, unlike carbon, in which the outer $2s^2\ 2p^2$ electrons are in a shell with no d-orbits, silicon has its outer $3s^2\ 3p^2$ electrons in a shell in which there are empty d-orbits. It has been shown by various data that the electron affinity of the silicon atom is equal to 62 ± 11 kcal. Thus, in addition to the polar bonds $Si^+ - X^-$, a state with the reverse direction of the moment is inherent in silicon. A fact which is in accordance with this is that $N(SiH_3)_3$ is a much weaker base than $N(CH_3)_3$. In addition, data are available which indicate that in $N(SiH_3)_3$ the nitrogen atom and the three silicon atoms surrounding it lie in the same plane, as in those cases where the central atom forms 3 σ-bonds (sp^2) and one π-bond.

Attention should be paid to the fact that the difference in the moments of CH_3SiCl_3 and $HSiCl_3$ amounts to 0.97 D, whereas the difference for CH_3CCl_3 and $HCCl_3$ is equal to only 0.35 D. We see that the difference between the moments of $(CH_3)_2SiCl_2$ and H_2SiCl_2 is equal to 0.7 D. This is related to the high value of the Si−H moment. When we go to the next element of the fourth group − germanium − the polarity naturally increases. According to our data the moment of CH_3GeCl_3 is equal to 2.63 D, whereas the moment of CH_3SiCl_3 is equal to 1.87 D and that of CH_3CCl_3 is equal to 1.57 D. A comparison of the moment of $(CH_2)_3SiCH = CHCl$ (1.71 D) with the moment of vinyl chloride (1.44 D) shows that in the first compound the moment of the C−Cl bond is closer to its normal

value. In vinyl chloride the conjugation of the chlorine with the CH_2 group, which is capable of attracting electrons, reduces the moment of the C^+-Cl^- bond. In $(CH_3)_3SiCH=CH_2$ the carbon of the CH_2 group already carries a slight negative charge from the Si^+-C^- bond. The somewhat reduced value for the moment of $(CH_3)_3SiCH = = CCl_2$ (1.64 D) is caused by the presence of two chlorine atoms on one carbon atom. The compound $Cl_3SiCH = = CHCl$ is probably a mixture of cis- and trans-isomers with the trans-form predominating, since a moment of approximately 2.3 D would be expected for the cis-isomer, with a moment of approximately 0.3 D for the trans-isomer. A considerable difference is observed in the moments of Cl_3SiCH_2Cl (1.61 D) and $Cl_3SiCHClCH_3$ (2.30 D) although vectorially the moments should be identical. The replacement of the C–H bond by the $C-CH_3$ in organosilicon compounds often shows a profound influence on the moment. Indeed the moment of $(CH_3)_2SiCl_2$ is equal to 1.88 D whereas the moment of $(CH_3)(C_2H_5)SiCl_2$ amounts to 2.31 D, i.e., it is 0.43 D greater. Yet in this case also it would seem that the replacement of the C–H bond by the $C-CH_3$ bond should have no influence on the resultant vector. Of the three compounds

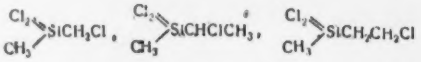

the greatest moment is observed for the last, in which the chlorine is situated in the β-position. It may be suggested that in the chain of bonds $Si-CH_2-CH_2-Cl$ an alternating polarity develops [5]. If this is the case, then the odd or even nature of the number of links may have an influence on the reactivity. In actual fact, substituents in the β-position have a considerable influence on kinetics. This "silicon" effect is well known in the chemistry of organosilicon compounds. Thus, the β-chlorine atom in $Cl_3SiCH_2CH_2Cl$ may be titrated with 0.5 N aqueous alkali. We are of the opinion that the alternating polarity, which has an influence on the dipole moment, is revealed in the kinetics of the reaction, which takes place via a five-membered cyclic complex (with six electrons in the field of five nuclei).

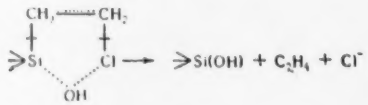

With an odd number of methylene groups present the reaction takes place under more severe conditions.

It follows from the moment of $(CH_3)_2Si(CH_2-CH=CH_2)_2$, equal to 0.54 D, that the moment of the $Si-CH_2-CH=CH_2$ group has a value of approximately 0.65 D either as a result of alternating polarity or as a result of a displacement of electrons towards the CH_2 group on the double bond. A comparison of these data with the moment of $(C_2H_5)_3SiCH_2-CH=CH_2$, which is almost zero, indicates an increase in polarity from the $Si-CH_3$ group to the $Si-C_2H_5$ group. The same specific feature of organosilicon compounds appears in this case also, namely a change in the properties when the number of links in the hydrocarbon chain increases from one to two. A comparison of $Cl_3SiCH_2CH_2Cl$ and $Cl_3SiCH_2CH_2CHCl_2$ shows that the presence of two chlorine atoms on one carbon atom brings about a reduction in the moment of 0.16 D, which is less, certainly, than in the case of CH_3Cl and CH_2Cl_2. From the compound CH_3SiCl_3 the moment of the $SiCl_3$ group may be evaluated as 2.07 D; from the moment of $HSiCl_3$ it may be evaluated as 1.90 D. From $(CH_3)_2SiCl_2$ the moment of the $SiCl_2$ group may be evaluated as 2.11 D. The compound Cl_3SiCH_2Cl has a moment of 1.61 D. At the same time the vector sum of the moments Cl_3Si 2.07 D; C–Si 0.6 D; C–Cl 1.46 D; C–H 0.4 D leads to a resultant moment of 2.26 D. It has been shown that the compound $Cl_3SiCHClCH_3$ with the same vector sum has a moment of 2.3 D, i.e., very close to the calculated value. The discrepancy in the case of Cl_3SiCH_2Cl should be the subject of further study.

As a result of the fact that it is possible for the free 3d-orbits of silicon to take part in bond formation, a state Si^- may exist with five bonds. This circumstance plays a certain part in aromatic derivatives, for example in the bonds between silicon and a benzene ring. From the value of the moment of $(CH_3)_3SiC_6H_5$ 0.42 D, the moment of the group $Si-C_6H_5$ may be evaluated as 0.62 D. From the compound $(CH_3)_2Si\cdot(CH_2-CH=CH_2)$ with $\mu = 0.54$ D, and the moment of the Si-allyl group, which is equal to 0.65 D, it is possible to calculate the moment

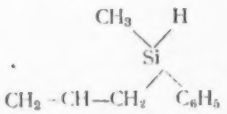

of , and good agreement with the experimental value is obtained. The moment of the

TABLE 1

Spec. No.		P_{total}, cc	R_D	$\sim P_{ar}$, cc	$\mu \cdot 10^{18}$, D
1	Cl_3SiCH_2Cl	93,8	34,5	5,0	1,61
2	$Cl_3SiCH_2CH_2Cl$	91,4	38,5	5,1	1,51
3	$Cl_3SiCH_2CH_2CH_2Cl$	129,1	43,3	5,2	1,97
4	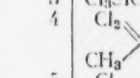	109,2	34,2	5,7	1,82
5	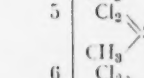	123,9	38,5	5,8	1,96
6	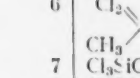	118,5	38,7	5,8	1,87
7	$Cl_3SiCH{=}CHCl$	60,1	38,4	5,5	0,88
8	$(CH_3)_3SiCH{=}CHCl$	106,4	39,4	6,0	1,71
9	$(CH_3)_3SiCH{=}CCl_2$	108,0	44,0	8,0	1,64
10	$(CH_3)_3SiCH{=}CH_2$	38,6	34,6	4,0	0
11	$Cl_3SiCH_2CHCl_2$	89,1	43,4	7,5	1,35
12	$Cl_3SiCHClCH_3$	154,1	38,6	5,2	2,30
13	$Cl_3SiCH_2CHClCH_3$	138,7	43,2	5,3	2,08
14	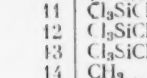	149,9	34,1	5,0	2,34
15	CH_3SiCl_3	106,2	29,1	4,5	1,87
16	$(CH_3)_2SiCl_2$	108,5	29,6	4,5	1,89
17	CH_3GeCl_3	183,2	31,7	8,0	2,63
18	$(CH_3)_2Si(CH_2CH{=}CH)_2$	58,3	47,2	5,0	0,54
19	$(C_2H_5)_3SiCH_2CH{=}CH_2$	59,6	53,0	5,0	~0,2
20	$(CH_3)_3SiCH_2C_6H_5$	66,9	54,7	5,9	0,55
21	$(CH_3)_3SiCH_2CH_2C_6H_5$	65,5	59,3	6,0	0
22	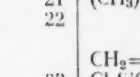	66,0	54,5	5,0	0,55
23	$Cl_3SiC_6H_5$	155,0	48,9	4,8	2,21
24	$Cl_3SiCH_2C_6H_5$	125,5	54,5	4,9	1,78
25	$Cl_3SiCH_2CH_2C_6H_5$	131,5	58,1	5,0	1,81
26	$Cl_3SiCH_2C_6H_4Br$ (-para)	136,0	60,9	5,5	1,83
27	$(CH_3)_3SiCH_2C_6H_4NO_2$ (-ortho)	343,2	60,8	10	3,62
28	$(CH_3)_3SiCH_2CH_2C_6H_4NO_2$ (-ortho)	349,3	65,4	10	3,63
29	$(CH_3)_3SiCH_2C_6H_4NO_2$ (-para)	563,5	62,4	10	4,86
30	$(CH_3)_3SiCH_2CH_2C_6H_4NO_2$ (-para)	504,3	67,0	10	4,55
31	$(C_2H_5)_3SiC_6H_4Br$ (-para)	143,3	71,4	7,0	1,77
32	$(C_2H_5)_3SiCH_2C_6H_4Br$ (-para)	173,1	76,0	7,1	2,08
33	$(C_2H_5)_3SiCH_2CH_2C_6H_4Br$ (-para)	162,3	80,6	7,2	1,89

compound $(CH_3)_3SiCH_2CH_2C_6H_5$ is probably close to zero, since the total polarization remains constant in the temperature range 288-318° K. The moment of $Cl_3SiC_6H_5$ differs sharply from the additive value for the moments of $SiCl_3$ (2.07) and $Si-C_{ar}$. This is evidently connected with the withdrawal of electrons towards the chlorine atoms via the ring and via the silicon atom, and also with the ability of the silicon atom to become negatively charged as a result of the empty orbit as described above. This shows that it is insufficient to evaluate the polarity of bonds from the electronegativities alone. Depending on the valence states, the same atom in different bonds may be both the positive and the negative end of a dipole. When we go from $Cl_3SiC_6H_5$ to $Cl_3SiCH_2C_6H_5$, the chain of conjugation is broken down and the moment is nearer to the additive value. The same applies to the moment of $Cl_3SiCH_2CH_2C_6H_5$. The moment of the two compounds containing the nitro group in the ortho-position (27 and 28, Table 1) are the same. We would point out that the moments of ortho-nitrotoluene and ortho-$(CH_3)_3SiC_6H_4NO_2$ are the same (3.66 and 3.67 D). The experimental values found for the moments of the para-bromo derivatives $(C_2H_5)_3SiC_6H_4Br$, $(C_2H_5)_3SiCH_2C_6H_4Br$ and $(C_2H_5)_3SiCH_2CH_2C_6H_4Br$ are greater than the values calculated from the vector sums. It is possible that in this case the inductive influence of the moments of the Si^+-C_{ar} and $C^+_{ar}-Br^-$ bonds has some effect.

LITERATURE CITED

[1] R. I. W. LeFevre and D. A. A. S. N. Rao, Austr. J. Chem., 7, No. 2, 135 (1954).

[2] C. P. Smyth, Dielectric Behavior and Structure, N. Y., 1955, p. 420.

[3] R. S. Holland and C. P. Smyth, J. Am. Chem. Soc. 77, 268 (1955).

[4] A. P. Altshuller and L. Rosenblum, J. Am. Chem. Soc., 77, 272 (1955).

[5] K. Fajans, Chem. and Eng. News, 27, 900 (1949).

M. V. Lomonosov Institute of
Fine Chemical Technology, Moscow

Received May 15, 1958

THE PART PLAYED BY OZONE IN THE INITIATION OF THE OXIDATION OF SATURATED GASEOUS HYDROCARBONS

N. A. Kleimenov and A. B. Nalbandian

(Presented by Academician V. N. Kondrat'ev, April 24, 1958)

Ozone, like many other active materials added in small quantities to hydrocarbon – oxygen mixtures, lowers the reaction temperature considerably. The literature contains contradictory reports on the mechanism of this action shown by ozone. Many workers consider [1-4] that the oxidation of saturated hydrocarbons in the presence of ozone involves the direct reaction of the ozone molecule with the fuel. In recent years, however, a number of works have appeared [5, 6] in which it has been established, taking the oxidation of carbon monoxide as an example, that low-temperature oxidation processes in the presence of ozone are initiated by atomic oxygen which is formed by thermal decomposition of the ozone. In a recently published work [7] on the oxidation of methane in the presence of small quantities of ozone, we have, on various grounds, including the fact that the ozone decomposition temperature coincides with the temperature at which the oxidation of methane starts to proceed at a measurable rate, concluded that the initiation of the oxidation reaction is, in fact, brought about by oxygen atoms.

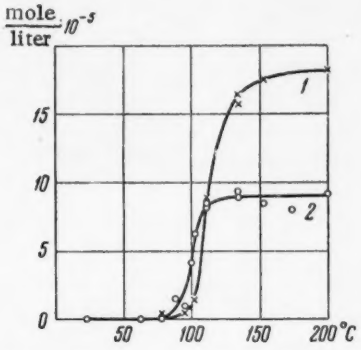

Fig. 1. The effect of temperature on the oxidation of hydrogen. Original mixture: H_2 = 50%, O_2 = 50%; ozone concentration 0.41%. Total pressure 760 mm mercury, time of contact 21 seconds.
1) Quantity of zone decomposed;
2) quantity of water formed.

The present communication reports certain new data on the oxidation of propane and hydrogen, which, it seems to us, confirm the suggestion previously put forward that the mechanism of the action of the zone involves oxygen atoms. The experiments were carried out at atmospheric pressure in a flow-through apparatus. The products of the oxidation of the propane – peroxides and aldehydes – were recovered in a trap containing water and afterwards analyzed by the usual methods: the sum of the peroxides was determined iodometrically, while the aldehydes were determined by the hydroxylamine method. In the experiments on the oxidation of hydrogen, the rate of flow of the reaction gases leaving the reaction vessel was adjusted by means of a glass valve until the pressure was equal to a fraction of a millimeter of mercury, after which the water formed in the reaction was frozen out in a trap cooled by liquid nitrogen. The water formed was allowed to evaporate into a calibrated volume and the quantity present determined, using a membrane monometer.

The experimental data on the oxidation of hydrogen by ozonized oxygen are given in Fig. 1, from which it can be seen that appreciable decomposition of the ozone starts at a temperature of 85°. The oxidation of the hydrogen starts at the same temperature. When the contact time is increased from 21 to 40 seconds, the temperature at which the ozone starts to decompose is reduced by 20-25°. At the same time the temperature at which the oxidation of the hydrogen starts is reduced by the same amount.

A similar picture is observed for the oxidation of propane. In this case, as in the oxidation of methane and and hydrogen, the start of the oxidation coincides with the start of the ozone decomposition, as can be seen from Fig. 2.

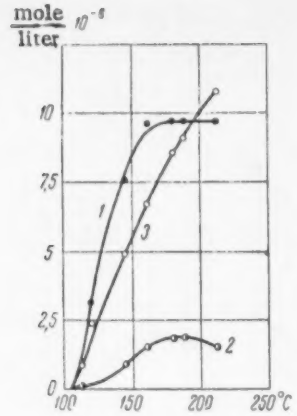

Fig. 2. The effect of temperature on the oxidation of propane. Original mixture: C_3H_8 = 62%; O_2 = 38%; ozone concentration 2.09%. Time of contact 6 seconds. 1) Quantity of ozone decomposed; 2) quantity of organic peroxides formed; 3) quantity of aldehydes formed.

Thus, for the three substances studied – methane, propane and hydrogen – the start of the oxidation reaction coincides with the start of the ozone decomposition. This fact is evidently related to the formation of some sort of active particles – atoms or excited molecules of oxygen – which initiate the chain oxidation.

The subsequent experiments were directed to an examination of the nature of the initiation process. If the initiation of an oxidation reaction is brought about by excited oxygen molecules, then the addition of an inert gas will increase the rate of deactivation of the excited oxygen molecules and lower the rate of reaction to a similar extent.

The experiments on the oxidation of hydrogen were carried out with the reaction mixture kept in the reaction zone for 16 seconds at a temperature of 206° to ensure complete decomposition of the ozone during the reaction time. In the absence of an inert gas, at a total pressure $P_{H_2}+O_2+O_3$ = 100 mm mercury, the rate of reaction, as measured by the quantity of water formed, was equal to $2.2 \cdot 10^{-7}$ moles/second. When the same mixture was diluted by a factor of 7.4 to give $P_{H_2}+O_2+O_2+N_2$ = 740 mm mercury, the reaction rate was found to be equal to $2.5 \cdot 10^{-7}$ moles/second, i.e., practically unchanged. These data enable us to assume that excited oxygen molecules do not play an important part in the oxidation reaction, and that consequently the initiation of the reaction must be brought about by the action of atomic oxygen.

In order to convince ourselves of the accuracy of the conclusions reached, we carried out experiments on the initiation of the reaction by means of atomic oxygen directly created in the mixture of methane and oxygen. For this purpose we used photochemical initiation. The reaction mixture was irradiated at room temperature with ultraviolet light produced by a hydrogen discharge tube separated from the reaction zone by a fluorite window. The experiments were carried out in flow-through and circulatory apparatus at various pressures. The reaction products leaving the reaction vessel were frozen out in a trap immersed in liquid nitrogen. It was established by special experiments that methane is completely transparent under the conditions of our experiments. The value of the oxygen pressure chosen in all the experiments was such that complete absorption of the Schumann region of the spectrum was achieved.

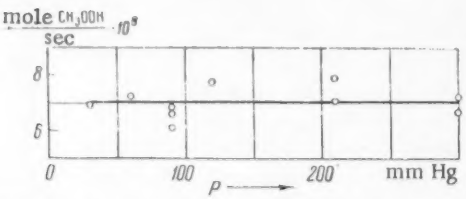

Fig. 3. The influence of dilution of the methane–oxygen mixture with nitrogen on the rate of formation of methyl hydroperoxide by the photochemical oxidation of methane under the influence of irradiation by the Schumann region of the spectrum. Original mixture: CH_4 = 75%, O_2 = 25%. Pressure $P_{CH_4} + P_{O_2}$ = 30 mm mercury, t = 20°.

When the experiment was carried out with circulation of the methane – oxygen mixture (75% CH_4 and 25% O_2) at a pressure of 15 mm mercury for 5 hours, the reaction products being frozen out at the temperature of liquid nitrogen, approximately 9% of the original methane was oxidized to methyl hydroperoxide and approximately 7% to formaldehyde. A closer examination of the relationship between these products and the time of contact led us to the conclusion that the formaldehyde is in all probability a secondary product formed by the further photochemical decomposition of the hydroperoxide.

In order to confirm that in the photochemical reaction the initiation is again brought about by oxygen atoms and not by excited molecules, the formation of which is possible at $\lambda < 2000$ A, we used the same method involving dilution of the mixture with the inert gas nitrogen. The dilution coefficient was varied up to 10. These experiments were carried out using a methane – oxygen mixture. The data from this series of experiments are given in Fig. 3. The fact that the rate of oxidation of the methane remains constant over a wide range of dilutions of the methane – oxygen mixture with nitrogen indicates that in these experiments, also, the initiation process does not

involve exited oxygen molecules. The data described in the present communication and in our previous paper lead us to the conclusion that in the oxidation of saturated gaseous hydrocarbons by ozonized oxygen, the reaction is initiated by oxygen atoms formed by the thermal decomposition of the ozone.

LITERATURE CITED

[1] M. M. Otto, Ann. Chim. Phys., 13, 109 (1898).

[2] C. C. Schubert and R. N. Pease, J. Am. Chem. Soc., 76, 2044 (1956).

[3] C. C. Schubert and R. N. Pease, J. Chem. Phys., 24, 919 (1956).

[4] C. C. Schubert and R. N. Pease, J. Am. Chem. Soc., 78, 5553 (1956).

[5] D. Garvin, J. Am. Chem. Soc., 76, 1523 (1954).

[6] P. Harteck and S. Dondes, J. Chem. Phys., 26, 1734 (1957).

[7] N. A. Kleimenov, I. N. Antonova, A. M. Markevich, A. B. Nalbandian, J. Phys. Chem., 30, 794 (1956); J. Chim. Phys., 54, No. 4 (1957).

Received April 17, 1958

THE KINETICS OF ION EXCHANGE BETWEEN METAL AND SLAG

Iu. P. Nikitin and O. A. Esin

(Presented by Academician A. N. Frumkin, April 11, 1958)

The rate of ion exchange between liquid metals (Fe – C, Fe–Si, Fe–P, Ag) and molten slags has been studied by the method previously described [1]. The values found for the diffusion resistance R_g were used to evaluate the diffusion coefficients D for iron and silver ions using the relationship [2]:

$$R_D = \frac{RT}{n^2F^2}\frac{1}{C}\sqrt{\frac{2}{D\omega}}, \qquad (1)$$

where C is the concentration of the potential-determining ions in the slag; ω – circular current frequency, R – the gas constant, T – the absolute temperature, F – the Faraday, and n – charge on the ion.

It was found that for slags containing 31% CaO, 54% SiO_2, 15% Al_2O_3, the diffusion coefficients for iron ions at 1500° C lie between 2.4 and 3.1 · 10^{-6} $cm^2 \cdot sec^{-1}$. The values obtained are close to those found earlier (D = 3.5 · 10^{-6}) at the same temperature by a radioactive isotope method [3].

The diffusion coefficient for silver ions in molten sodium borate (15% Na_2O, 85% B_2O_3) was found to be equal to 0.6 · 10^{-7} $cm^2 \cdot sec^{-1}$/840° and 1.42 · 10^{-7} $cm^2 \cdot sec^{-1}$ at 940°. From this the activation energy of the diffusion process, calculated using the usual exponential equation, was found to be equal to 23 kcal /g-atom. The fact that the values of D_{Ag^+} are lower than those of $D_{Fe^{2+}}$ is evidently due to the relatively high viscosity and low temperatures.

The values of the reaction resistance R_r were used to calculate the exchange currents i_0 using the expression [2]:

$$i_0 = \frac{RT}{nF}\cdot\frac{1}{R_r}. \qquad (2)$$

For alloys of iron with carbon, silicon and phosphorus, and slags containing CaO, SiO_2, Al_2O_3, Na_2O, B_2O_3, P_2O_5 and small concentrations of FeO and Fe_2O_3, it was found that a practically linear relationship exists between i_0 and the total percentage concentration of iron oxides (see Fig. 1). A similar relationship has been observed at low concentrations of the potential- determining ions for a number of metals in aqueous and organic solutions [2, 4, 5]. As is well known [2], this fact indicates that the discharge of the ion is the step determining the rate of the exchange.

The addition of Na_2O to the slag leads to an increase in the concentration of FeO in the slag and to an increase in the exchange current. This is in accordance with the results previously obtained, when it was found that the addition of Na_2O increases the density of the negative charge on Fe–C and Fe–P electrodes [6] and reduces the inter-phase tension at the phase boundary under study [7].

Measurements made using liquid pig iron (4.3% C) and a slag containing 31% CaO, 54% SiO_2 and 15% Al_2O_3 have shown that at a temperature of 1350°C and an iron ion concentration of 0.36% the exchange current amounts to to 22 milliamps / cm^2, while at a temperature of 1550° and iron ion concentration of 0.52% it is equal to 50 milliamps / cm^2. From this, taking into account the linear relationship between i_0 and C, we find that the activation energy for the reaction (E_1):

$$Fe\ (pig\ iron) = Fe^{2+}\ (slag) + 2e \qquad (a)$$

is equal to 23.5 kcal / g-atom, while for the reverse process E_2 = 13 kcal / g-atom. This difference between E_1 and E_2 is evidently due to the fact that the carbon in the metallic alloy produces intense reducing conditions at the interphase boundary. We have not yet studied the influence of the change in potential with change in the temperature and the ion concentration [8] on the value of the activation energy [9].

Table 1 gives the results obtained for a silver electrode in oxide melts. They enable us to evaluate the activation energy for the forward reaction (E_1)

$$Ag\ (metal) = Ag^{+}\ (slag) + e \qquad (b)$$

and for the reverse reaction (E_2) involved in the exchange. These are found to be E_1 = 12.8 and E_2 = 22.8 kcal / g-atom. This difference between the values of E_1 and E_2 for silver seems unusual and requires further study. It is possible that it is caused by a stable linkage between the Ag^+ cations and the anions in the borate melt.

TABLE

Electrolyte comp.	t, °C	i_0, ma/cm²	C, μf/cm²
14,48% Na_2O, 85,4% B_2O_3, 0,12% Ag_2O	940	75	16,8
14,43% Na_2O, 85,4% B_2O_3 0,17% Ag_2O	840	46	16,8
30% CaO, 70% P_2O_5, 0,01% Ag_2O	1040	19	16,5

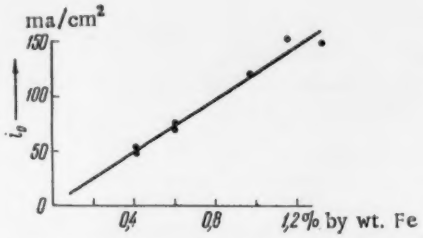

Fig. 1. Graph showing the variation in the exchange current between iron alloys and slags with change in the concentration of iron ions in the slag.

The values for the capacity of the double layer are approximately the same in all three cases and are close to those obtained earlier for Fe−C. This suggests that there is again an excess negative charge on the surface of the silver in contact with the borate.

Attention is drawn to the fact that in spite of the high temperature and relatively high concentration of potential-determining iron ions in the slag, the values of i_0 in the melts studied (Fe−C, Fe−Si, Fe−P) are close to those obtained in aqueous solutions. The iron ions are evidently more firmly bound in the slag than the metal cations in aqueous solution. At the same time the silicon, carbon and phosphorus are concentrated in the interphase boundary [1], which leads to a reduction in the concentration of iron atoms at the metal surface, i.e., to a peculiar isolation of the metal surface from the slag. A similar effect has been observed in aqueous solutions in the study of the influence of surface-active agents on the value of the exchange current (which is decreased) [4].

Support for these suggestions is also provided by the low reaction resistance between pig iron (4.3% C) and a slag containing calcium carbide (10.8% CaC_2, 55% CaO, 19.8% SiO_2, 3.6% Al_2O_3, 10.8% MgO and 0.143% Fe) at a temperature of approximately 1500°. In this case the potential is probably determined not by the transfer of iron but by the transfer of carbon:

$$2C\ (metal) + 2E = C_2^{2-}\ (slag) \qquad (c)$$

The high concentration of carbon in the surface layer of the pig iron and the slag facilitate rapid ion exchange and reduce i_0 sharply. The capillary activity of CaC_2 at such a boundary results from the reduction in the interphase tension [10].

In this connection it may be thought that for pure iron and other metals the exchange current with the slag should be greater at high temperatures. This is also indicated by a comparison of the values of i_0 for Ag and Fe−C. The exchange currents for these are approximately equal, in spite of the lower temperature and the lower concentration of Ag^+ ions in the slag.

LITERATURE CITED

[1] Iu. P. Nikitin, O. A. Esin, Proc. Acad. Sci., 116, 63 (1957).*

[2] B. V. Ershler, K. I. Rozental', Proc. of the Conference on Electrochemistry, Izd. AN SSSR, 1953, p. 446.**

[3] E. S. Vorontsov, O. A. Esin, Bull. AN SSSR, OTN, No. 3, 1958.

[4] V. A. Pleskov, N. B. Miller, Proc. of the Conference on Electrochemistry, Izd. AN SSSR, 1953, p. 165.**

[5] H. Gerischer, K. E. Staubach, Zs. Phys. Chem., 6, 118 (1956).

[6] O. A. Esin, Iu. P. Nikitin, Proc. of the Conference on the Phys.-Chem. Principles of Steel Production, Izd. AN SSSR, 1957, p. 446.**

[7] O. A. Esin, J. Phys. Chem., 30, No. 3 (1956).

[8] A. N. Frumkin, V. S. Bagotskii, Z. A. Iofa, B. N. Kabanov, The Kinetics of Electrode Processes, M., 1952.**

[9] M. I. Temkin, Proc. of the Conference of Electrochemistry, Izd. AN SSSR, 1953, p. 181.**

[10] S. I. Popel', O. A. Esin, Iu. P. Nikitin, Coll. Works of the S. M. Korov Ural Polytechnical Inst., Sverdlovsk, No. 49, 82 (1952).**

S. M. Kirov Ural Polytechnical Institute,
Sverdlovsk

Received March 15, 1958

---

* Original Russian pagination. See C. B. Translation.

** In Russian.

THE HEAT OF COMBUSTION OF TETRAHYDROPYRAN

S. M. Skuratov and M. P. Kozina

(Presented by Academician A. N. Frumkin, June 30, 1958)

In the Thermochemical Bulletin* No. 3 for 1957, values were published for the heats of formation of tetrahydrofuran and tetrahydropyran obtained in two laboratories.

Tetrahydrofuran	(*l*)	598.8	Springall, Mortimer and Fletcher (England)
Tetrahydropyran	"	753.2	
Tetrahydrofuran		598.0	Skuratov, Kozina (USSR)**
Tetrahydropyran		750.1	

For tetrahydrofuran the difference is comparatively small, but for tetrahydropyran it amounts to 0.5%. This difference cannot be explained by the errors of the calorimetric measurements and is evidently due to the fact that the material is insufficiently pure.

TABLE 1

Expt. No.	Wt. of sample (in vacuo)	$\frac{CO_2 \text{ found}}{CO_2 \text{ calc}}$	ΔH_c^0 kcal/mole
1	0,4946	0,9996	750,45
2	0,4780	1,0004	750,42
3	0,5305	0,9997	750,50
4	0,5143	0,9997	750,63
5	0,5940	1,0002	750,71
6	0,5953	1,0005	750,54
7	0,6342	1,0004	750,45
8	0,4877	0,9998	750,32
9	0,5334	0,9997	750,67
Average	—	1,0000∓0,0001	750,52∓0,04

As a result of correspondence with the English authors we decided to repeat the determination of the heat of combustion of tetrahydropyran in both laboratories. In their repeat determination the English authors obtained a value for the heat of combustion of tetrahydropyran equal to 752.8 ± 0.9 kcal / mole [2], i.e., practically the same as the value given in the Thermochemical Bulletin. The authors make the observation that the specimen which we used was evidently impure.

* The Bulletin is issued annually by the Experimental Thermodynamics Subcommittee of the International Union of Pure and Applied Chemistry and its aim is to give information regarding the thermochemical work being carried out in different laboratories. Data of a preliminary nature may be published in the Bulletin.

** See [1].

In the present communication we give the results of a repeat determination of the heat of combustion of tetrahydropyran which we have carried out. We purified the tetrahydropyran by various methods (bromination, boiling with dilute hydrochloric acid, freezing out; all the specimens were thoroughly dried and fractionally distilled over metallic sodium before combustion). The heats of combustion of the specimens obtained agreed within the limits of experimental error. The chief criterion for the purity of the material used was the close agreement between the quantity of carbon dioxide found by analysis in the products of combustion (accuracy of the analysis 0.01%) and the quantity of carbon dioxide calculated from the weight of the original material taken. Table 1 gives the results obtained. Column 4 of Table 1 gives the standard heat of combustion of tetrahydropyran in the liquid state. It can be seen from the data presented that the tetrahydropyran used by us may be considered sufficiently pure. The error in the calorimetric measurements and the gas analyses was evaluated as the mean square deviation. The value which we have obtained agrees with that published by us earlier [1] and differs from the figure given in [2] by 0.3%.

LITERATURE CITED

[1] S. M. Skuratov, A. A. Strepikheev, M. P. Kozina, Proc. Acad. Sci., 117, No. 3, 452 (1957).*

[2] R. C. Cass and S. E. Fletcher, et al., J. Chem. Soc., 1958, 1406.

Received July 1, 1958

* Original Russian pagination. See C. B. Translation.

THE MECHANISM OF THE CROSS-LINKING OF POLYMER CHAINS UNDER THE INFLUENCE OF GAMMA RADIATION

Ying Sheng-K'ang, A.N. Pravednikov and Academician S.S. Medvedev

When a γ-quantum interacts with a molecule, an electron is knocked out of one of the orbits so that a positive ion is formed. When the ion is discharged by a thermal electron, highly excited molecules are formed and these break down with the formation of free radicals. The formation of cross-linkages should therefore involve secondary processes in which the radicals take part.

Study of the kinetics of the cross-linking process has shown that the rate of the process is constant with time and proportional to the first degree of the intensity of the radiation. The simplest theory of the mechanism of cross-linking is that the formation of cross-linkages during radiolysis takes place as a result of the recombination of polymeric radicals formed by rupture of the C−H bonds, and also as a result of the addition of polymeric radicals to the double bonds of the polymeric molecule. The rate of cross-linking in this case will evidently be equal to

$$v = k_1 n^2 + k_2 nA$$

(n and A are the concentrations of the radicals and double bonds, respectively). This scheme leads to the relationships observed experimentally only when n = constant and A = constant.

The accumulation of double bonds in the polymer during irradiation indicates that a stationary state relative to the concentration of double bonds and free radicals is not attained. The fact that the rate of cross-linking is constant with time therefore indicates that the part played by the recombination of the radicals and the addition of the radicals to the double bonds is insignificant, and this is evidently connected with the extremely low rates of diffusion of polymeric molecules in a solid polymer.

For an understanding of the mechanism of the processes leading to the formation of cross-linkages, it is necessary to examine the reactions involving radicals which take place in the irradiated polymer, in particular those reactions in which atomic hydrogen takes part.

The atomic hydrogen which is formed as a result of the rupture of C−H bond in the polymeric molecule under the influence of the radiation has at first an increased energy. This atom may lose this excess energy or may react according to one of the schemes given below:

1. Reaction with another hydrogen atom

$$H + H \rightarrow H_2 \qquad (1)$$

2. Reaction with the free radicals formed during the irradiation

$$\sim CH_2 - \dot{C}H - CH_2 \sim + H \begin{cases} \nearrow \sim CH_2 - CH_2 - CH_2 \sim \\ \searrow \sim CH_2 - CH = CH \sim + H_2 \end{cases} \qquad (2)$$

3. Reaction with double bonds

$$\sim CH_2 - CH = CH \sim + H \rightarrow CH_2 - \dot{C}H - CH_2 \sim. \qquad (3)$$

4. Removal of a hydrogen atom from the polymer molecule

$$\sim CH_2 - CH_2 - CH_2 \sim + H \rightarrow \sim CH_2 - \dot{C}H - CH_2 \sim + H_2. \qquad (4)$$

The rates of the reactions in which the "hot" hydrogen atom takes part will be determined not so much by the values of the activation energies for these reactions as by the probability of collision of the hydrogen atom with one or other of the groupings. In carbon-chain polymers the concentration of CH_2 groups is greater by several orders of magnitude than the concentrations of H atoms, free radicals or double bonds, so that the "hot" hydrogen atom will react predominantly according to reaction (4) with the formation of a polymeric radical in direct proximity to the site of the C–H bond rupture. The recombination of the primary radical and the radical formed according to reaction (4), which are situated so closely together, leads to the formation of the cross-linkages. The rate of cross-linking by this mechanism is evidently independent of the temperature of the specimen.

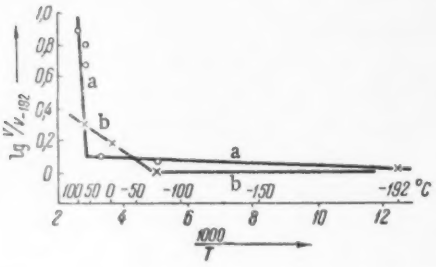

Fig. 1. The influence of temperature on the rate of cross-linking of polyethylene and polyvinyl chloride by irradiation with γ-rays. a) polyethylene, 35 Mr; b) polyvinyl chloride, 24 Mr. The number of cross-linkages (in arbitrary units) was calculated from data obtained by experiments on the swelling of the specimens in toluene (polyethylene) and dichloroethane (polyvinyl chloride). V and $V_{-192°}$ are the rates of cross-linking at temperatures t and −192°, respectively.

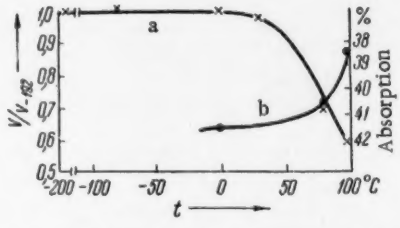

Fig. 2. The influence of temperature on the rate of cross-linking in a polymer with the structure $\left(\begin{array}{c}-C_3H_6-CH- \\ \quad\quad\quad\quad | \\ \quad\quad\quad\quad CH_3\end{array}\right)_n$ (a) and on the rate of formation of trans-vinyl double bonds (absorption in the region of 964 cm^{-1}) (b). The rate of cross-linking was calculated from data on the swelling in toluene. V and $V_{-192°}$ are the rates of cross-linking at temperatures t and −192°, respectively.

Reactions involving atomic hydrogen which has "lost" its excess energy will obey the usual laws. The rates of diffusion of gases in polymers are comparatively low, so that, taking into account the fact that the concentration of radicals and C=C bonds in the polymers during irradiation is also very low, it can be seen the "cold" hydrogen atoms will react in polymers of the polyethylene type for the most part according to reaction (4).

The radicals which are formed according to reaction (4) when "cold" hydrogen atoms are involved can recombine with primary radicals only at a comparatively short distance from the site where the H atom is formed. The rate of cross-linking in this case will evidently depend on the temperature of the specimen, since an increase in the temperature will lead on the one hand to an increase in the probability that reaction (4) will take place at short distances from the site of C–H bond rupture, and on the other hand – as a result of an increase in the mobility of the polymer chains – to recombination reactions involving radicals formed at comparatively large distances from the place where the primary radical is situated.

The removal of the hydrogen atom from the polymer chain (Reaction (4)) is accompanied by a change in the configuration of the corresponding part of the chain from tetrahedral to planar. In the case of polymers this change is coupled with a displacement of parts of the polymer chains, which should lead to an increase in the activation energy for the reaction (compared with the activation energies for analogous reactions involving compounds of low molecular weight). A particularly marked increase in the activation energy, and consequent reduction in the rate of cross-linking, should be observed in the change to a glassy polymer.

TABLE 1

The Influence of Heat on the Degree of Cross-Linking of Irradiated Polymers. $t_{irrad.} = 25°$

Radiation dose, Mr	Subsequent treatment	l_0/l **	n_{ht}/n_{uht} *	Remarks
		Polyvinyl chloride		
98	Without heating	0.613	1.76	Further cross-linking
98	Heating for 4 hours at 90°	0.685		
		Polystyrene		
185	Without heating	0.334	1.56	Further cross-linking
185	Heating for 4 hours at 95°	0.365		
204	Without heating	0.353	0.662	Reduction in degree of cross-linking
204	Heating for 4 hours at 140°	0.325		
195	Without heating	0.340	0.400	Reduction in degree of cross-linking
195	Heating for 2 hours at 145°	0.283		
225***	Specimen soluble			A gel fraction is formed

* The number of cross-linkages n (in arbitrary units) was calculated from data on the degree of swelling of the specimen V, using the equation $n_{ht}/n_{uht} = (V_{uht}/V_{ht})^{5/3}$; the indices ht and uht denote heated and unheated specimens respectively. The swelling of the polyvinyl chloride was carried out in dichloroethane, that of polyethylene in toluene.

** l_0/l is the ratio of the length of the original specimen to the length of the swollen irradiated specimen.

*** Temperature of irradiation 130-135°.

It can be seen from Fig. 1 that the rates of cross-linking for polyethylene and polyvinyl chloride at temperatures below the temperature of glass formation T_g (−80° and + 80°, respectively) are practically independent of temperature, i.e., in this case the "cold" hydrogen atoms take practically no part in the reactions leading to the formation of cross-linkages. At temperatures above T_g the rate of cross-linking increases with increase in the temperature (the "cold" hydrogen atoms are drawn into the cross-linking reactions).

TABLE 2

The Influence of the Presence of Side Groups on the Rate of Cross-Linking of Polymers. $t_{irrad.} = 25°$.

Radiation dose, Mr	Polymer	l_0/l *	n_{ipps}/n_{ps}**
200	Polystyrene	0.345	
200	Polystyrene with isopropyl groups introduced	0.422	2.74

* See Table 1.

** n is the number of cross-linkages (in arbitrary units). The indices ps and ipps denote polystyrene and polystyrene with isopropyl groups introduced, respectively.

TABLE 3

The Influence of Heat on the Degree of Cross-Linking of Irradiated Polysytrene Containing Isopropyl Groups. $t_{irrad.} = 25°$

Radiation dose, Mr	Subsequent treatment	l_0/l*	n_{ht}/n_{uht}*
204	Without heating	0.410	
204	Heating for 4 hours at 100°	0.414	1.0

* See Table 1.

In a glassy polymer the "cold" hydrogen atoms should also take part in reaction (4), but the radicals thus formed, as a result of steric hindrance, cannot recombine with the primary radical, and remain in the polymer in a "frozen" condition. As a result, when specimens of polystyrene (T_g = 80°) or polyvinyl chloride which have been irradiated at room temperature are kept for some time at 90-100°, further cross-linking is observed (Table 1). When polystyrene is heated at a higher temperature (140-145°) a decrease in the degree of cross-linking is observed; the reason for this decrease will be examined below.

The removal of a hydrogen atom from a side group (methyl, isopropyl, etc.) does not involve a displacement of parts of the polymer chains in the transition state and therefore has practically the same activation energy as the corresponding reactions in compounds of low molecular weight, while glass formation by the polymer should have no influence on the rate of this reaction. In polymers which contain a sufficiently large number of such groups, therefore, the "cold" hydrogen atoms will also take part in the cross-linking reactions below the temperature of glass formation.

In order to confirm this, a study was made of the action of γ-radiation on polymers with the structure $\left(\begin{array}{c}-C_3H_6-CH_2-\\ \quad\quad\quad\quad|\\ \quad\quad\quad\quad CH_3\end{array}\right)_n$ obtained by decomposing a mixture of diazomethane and diazoethane in the presence of $B(OCH_3)_3$. The high rates of cross-linking of this polymer in the glassy state ($T \approx -80°$) is 2.5 times greater than the rate of cross-linking in polyethylene under these conditions, and the fact that the rate of cross-linking is constant within the temperature range −190° to +35° indicates that in polymers of this type not only the "hot" hydrogen atoms but also the "cold" atoms are practically all intercepted at a very short distance from the site of primary radical formation.

An increase in the rate of cross-linking by a factor of 2.7 is also observed when isopropyl groups are introduced into polystyrene in the para-position (by treating polystyrene with isopropyl chloride in the presence of $AlCl_3$ (Table 2)).

The high rates of reaction (4) in the case of polymers containing side groups are also confirmed by the fact that when isopropylated polystyrene, irradiated in the glassy state at a temperature greater than T_g, is heated, no further cross-linking takes place (Table 3).

When copolymers of the type $\left(\begin{array}{c}-C_3H_6-CH_2-\\ \quad\quad\quad|\\ \quad\quad\quad CH_3\end{array}\right)_n$ are irradiated at 35-100°, a sharp decrease in the rate of cross-linking is observed, accompanied by an increase in the rate of accumulation of trans-vinyl double bonds (calculated from the absorption in the region of 964 cm^{-1}) (Fig. 2). This effect is evidently caused by a chain transfer reaction, as a result of which radicals of the isopropyl type are converted into tert-butyl radicals. When the latter react with radicals of the isopropyl type, they disproportionate to a considerable extent [1], and this also leads to a reduction in the rate of cross-linking and to an increase in the rate of accumulation of double bonds in the polymer.

There are reports in the literature [2] that the irradiation of isotactic polypropylene leads not to cross-linking but to destruction of the polymer molecules. This conclusion, however, is in all probability erroneous. The reduction in molecular weight is evidently caused not by radiochemical effects but by the thermal destruction of the polymer which takes place when the specimen is heated to ~ 150° for the determination of its molecular weight. We have obtained similar results by heating polystyrene, irradiated at room temperature, to 140-145° or by irradiating polystyrene at 135°. The data given in Table 1 show that whereas the degree of cross-linking increases when the specimen is heated at 90-95°, it is reduced appreciably when the specimen is heated at 140-145°. The results obtained give grounds for considering that the formation of a free radical inside the chain is a definite stage in the process of the thermal destruction of polymers.

LITERATURE CITED

[1] J. Kraus and J. Calvert, J. Am. Chem. Soc., 79, 5921 (1957).

[2] R. Black and B. Lyons, Nature, 180, 1346 (1957).

L. Ia. Karpov Physicochemical
Scientific Research Institute

Received May 18, 1958

CONVECTION DIFFUSION IN LIQUID SOLUTIONS UNDER TURBULENT CONDITIONS

I. P. Krichevskii and Iu. V. Tsekhanskaia

(Presented by Academician S. I. Vol'fkovich, May 8, 1958)

V. G. Levich [1] has deduced an equation for convection diffusion in liquid solutions at the surface of a rotating disc for turbulent conditions:

$$I \approx \frac{0{,}01\ c_0 s}{\alpha \mathrm{Pr}^{1/3}} (a\omega) \left(\frac{\nu}{a^2\omega}\right)^{1/4}, \qquad (1)$$

where I is the diffusion current, s – the area of the disc, a – the radius of the disc, c_0 – the concentration of the substance in the bulk of the solution, ω – angular rate of rotation of the disc, ν – the kinematic viscosity of the solution, and α is a universal constant.

Equation (1) was deduced in accordance with the theories of L. D. Landau [2] and V. G. Levich [3] on the nature of turbulent motion in liquids next to solid surface and contradicts the ideas put forward by L. Prandtl [4] and T. Karman [5].

As far as the authors are aware, the only experimental check which has been made of Equation (1) is the work of I. A. Bagatskaia [6], who proved that the diffusion current is proportional to the diffusion coefficient raised to the $^3/_4$ power, and not to the first power as required by the theory of L. Prandtl and T. Karman.

TABLE 1

The Value of the Universal Constant α Which Enters Into V. G. Levich's Equation for Convection Diffusion Under Turbulent Conditions

Solution	C_0, mmoles alkali · cm^{-3}	I, mmoles alkali · $cm^{-2} \cdot sec^{-1}$	t, °C	$\nu \cdot 10^2$, $cm^2 \cdot sec^{-1}$	$D \cdot 10^5$, $cm^2 \cdot sec^{-1}$	$Re = \frac{a^2\omega}{\nu}$	α
Water-ammonia	0,5	0,040	67,5	0,45	6,0	119000	0,16
	0,5	0,052	67,5	0,45	6,0	179000	0,16
	0,5	0,023	40,0	0,65	3,5	82500	0,15
	0,5	0,032	40,0	0,65	3,5	124000	0,14
	0,5	0,016	30,0	0,80	2,6	67000	0,14
	0,5	0,018	30,0	0,80	2,6	100000	0,14
Water-hexamethyleneimine	0,2	0,0035	40,0	0,75	1,0	71500	0,14
	0,2	0,0055	40,0	0,75	1,0	107000	0,13
	0,2	0,0055	40,0	0,75	1,0	251000	0,13
	0,2	0,0030	30,0	0,9	0,72	59600	0,12
	0,2	0,0045	30,0	0,9	0,72	89300	0,11
	0,2	0,0045	30,0	0,9	0,72	209000	0,11
Water-triethylamine	0,2	0,0020	17,0	1,06	0,43	50600	0,14
	0,2	0,0027	17,0	1,06	0,43	75800	0,11

The authors decided to obtain experimental confirmation of the accuracy of Equation (1) by proving that the universal constant α which occurs in this equation is in fact constant. A second aim of the work was the

determination of the numerical value of α, which is in itself of considerable interest.

In order to obtain experimental confirmation of Equation (1), the authors measured the rate at which terephthalic acid, which is practically insoluble in water, [7] dissolves in dilute water – triethylamine, water – hexamethyleneimine and water – ammonia solutions using a rotating disc and turbulent conditions. The apparatus used for measuring the rate of dissolution and the method of carrying out the experiment are described in [8].

The results of the diffusion current measurements, together with all the data necessary for calculating the value of α, are given in Table 1. The error in the determination of the diffusion currents under turbulent conditions amounted to 3-6 %.

The authors calculated the values of the diffusion coefficients of ammonia and hexamethyleneimine at different temperatures from data on the rate of dissolution of terephthalic acid in dilute aqueous solutions of ammonia and hexamethyleneimine under laminary conditions using V. G. Levich's equation [2]:

(2)

The value of the diffusion coefficient of triethylamine at 17° was taken as equal to $0.43 \cdot 10^{-5}$ cm$^2 \cdot$ sec^{-1} [8]. The kinematic viscosity of dilute aqueous solutions of ammonia was taken as equal to the kinematic viscosity of water [9], that of triethylamine solutions was taken from the data given in [10], while the kinematic viscosity of hexamethyleneimine – water was determined using a Höppler viscosimeter. In this way the mean value of α was found to be 0.13. The probable error in the separate measurements of α was $\pm$ 0.01, while the probable error of the mean value of α was $\pm$ 0.003. The value of α thus remains constant irrespective of the nature of the diffusing substance while the diffusion coefficients change by a factor of fifteen (from $6.0 \cdot 10^{-5}$ to $0.43 \cdot 10^{-5}$ cm$^2 \cdot$ sec^{-1}) and the Reynolds numbers change from $\sim 5 \cdot 10^4$ to $\sim 2.5 \cdot 10^5$.

The fact that the universal constant α which enters into Equation (1) is in fact constant confirms the accuracy of the views of L. D. Landau and V. G. Levich on the nature of the turbulent motion in liquids close to a solid surface.

LITERATURE CITED

[1] V. G. Levich, Physicochemical Hydrodynamics, Izd. AN SSSR, 1952.*

[2] L. D. Landau, E. M. Lifshits, The Mechanics of Compact Media, M., 1944.*

[3] V. G. Levich, Acta Physicochim. URSS, 19, 117 (1943).

[4] L. Prandtl, Phys. Zs., 11, 1072 (1910); 29, 487 (1927).

[5] T. Karman, Coll. Problems of Turbulence, M., 1936.*

[6] I. A. Bagotskaia, Proc. Acad. Sci., 85, 1057 (1952).

[7] J. D'Ans, E. Lax, Taschenbuch für Chemiker and Physiker, Berlin, 1943.

[8] I. R. Krichevskii, Iu. V. Tsekhanskaia, J. Phys. Chem., 30, 2315 (1956).

[9] E. N. Dorsey, Properties of Ordinary Watersubstance (N.Y., 1940).

[10] F. Kohler, Monatsh. f. Chem., 82, 913 (1951).

Scientific Research and Design
Institute for the Nitrogen Industry

Received May 7, 1958

*In Russian.

THE INFLUENCE OF THE ADSORPTION OF VOLATILE INHIBITORS ON THE ELECTROCHEMICAL BEHAVIOR OF IRON

I. L. Rozenfel'd and V. P. Persiantseva

(Presented by Academician P. A. Rebinder, May 4, 1958)

In recent years a new and extremely efficient method has been worked out for the protection of apparatus and instruments from atmospheric corrosion. The essential feature of the method is the introduction, into an enclosed space containing the instrument, of chemical compounds with a definite vapor pressure, so-called volatile inhibitors, which saturate the atmosphere of the enclosed space and provide complete protection against corrosion. Almost no studies have been devoted to the mechanism of the action of these inhibitors, although many theories and conjectures regarding its nature have been put forward [1].

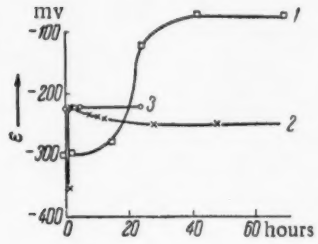

Fig. 1. The relationship between the stationary potential of an iron electrode and the conditions of benzylamine adsorption.
1) Electrode kept in benzylamine vapor before deposition of film of 0.01 N Na_2SO_4; 2) electrode kept in benzylamine vapor after deposition of film of 0.01 N Na_2SO_4; 3) film consisting of a 25% solution of benzylamine in 0.01 N Na_2SO_4; deposited on the electrode (film thickness 160μ).

From the electrochemical theory of the corrosion of metals, the most probable explanation was that the retarding action of the volatile inhibitors was related to the ability of the compounds adsorbed on the metal surface to alter the kinetics of the electrode reactions involved in the corrosion processes [2].

We have studied the adsorption process by electrochemical methods (measurement of the stationary potentials) which have simultaneously made it possible to obtain data on the direction of the change in the electrochemical kinetics.

The usual methods for the study of inhibitors under conditions where they are introduced in advance into the electrolyte, i.e., conditions which differ greatly from the actual conditions encountered in the use of a volatile inhibitor adsorbed from the gaseous phase, cannot, as will be shown below, be used to establish the specific features of the action of such compounds.

In the present work we made use of a method for studying electrochemical kinetics in thin layers of electrolytes developed by one of the authors [3]. Improvements were introduced into the method of working which made it possible to deposit films of electrolyte on the electrode surface after adsorption of inhibitor on the electrode surface from the gaseous phase, without disturbing the hermetically enclosed space.

Studies were made of the volatile inhibitors benzylamine (C_7H_9N) and morpholine (C_4H_9NO). It was first of all established by experiment that these compounds effectively protect iron from corrosion.

Figure 1 shows the relationship between the potential of the iron and the time for which the electrode is kept beforehand in an atmosphere saturated with benzylamine (Curve 1). It can be seen from the Figure that adsorption of the inhibitor shifts the stationary potential in a positive direction. As the time for which the electrode is kept in the atmosphere saturated with inhibitor vapor is increased, the observed effect increases, and after a definite time reaches a constant value, the time in the case of benzylamine being approximately 40-50 hours. After

this period of time, the surface is evidently completely saturated with inhibitor. The shift in the potential amounts to more than 200 mv.

It is interesting to note that the adsorption of the same inhibitor from the gas phase, when this takes place after a thin layer of electrolyte has already been deposited on the metal surface, leads to a much smaller effect (see Curve 2). In the second case the potential of the iron is shifted by only 50-60 mv.

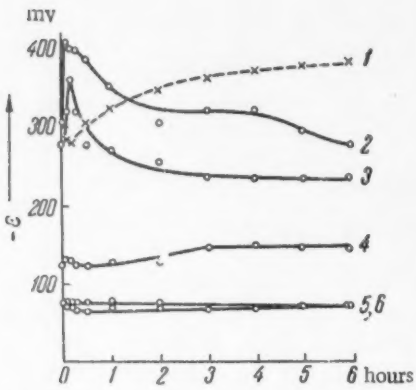

Fig. 2. The relationship between the stationary potential of an iron electrode and the time for which the electrode is kept beforehand in benzylamine vapor. Electrolyte – 0.01 N H_2SO_4 (thickness of layer 160 μ). 1) Without volatile inhibitor. Time for which electrode was kept beforehand in contact with benzylamine vapor before deposition of the electrolyte film; 2) 1 hour; 3) 17 hours; 4) 24 hours; 5, 6) 42-72 hours.

The adsorption of the volatile inhibitor from a concentrated solution of the inhibitor (25%) in 0.01 N sodium sulfate again does not shift the stationary potential of the iron by the same amount as that observed when the inhibitor is adsorbed from the gaseous phase (see Curve 3). This is evidently caused by the preferential adsorption of SO_4^{--} ions.

It must therefore be concluded that the adsorption of the inhibitor from the gaseous phase leads to a greater shift in potential and consequently to a greater degree of electrode passivation.

The strength of the adsorption of the inhibitor on the metal surface and the stability of the passive state may be characterized to a certain extent by data on the change in potential of the metal with time after the electrolyte film has been deposited on its surface.

Figure 2 gives curves showing the relationship between the change in the stationary potential of iron with time and the length of time for which the metal is kept beforehand in an atmosphere of volatile inhibitor (benzylamine).

The potential of the electrode which is not exposed beforehand to an atmosphere of the volatile inhibitor becomes less noble with time (Curve 1). Practically no change in the initial potential of the electrode takes place when the electrode is kept for a short time in the inhibitor vapor. With the passage of time the potential of the iron starts to become less noble (Curves 2 and 3) as a result of activation of the electrode surface by the electrolyte, and also possibly as a result of the adsorptive removal of oxygen

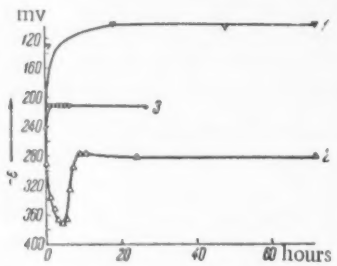

Fig. 3. The relationship between the stationary potential of an iron electrode and the conditions of morpholine adsorption. 1) Electrode kept in morpholine vapor before deposition of film of 0.01 N Na_2SO_4; 2) electrode kept in morpholine vapor after deposition of film of 0.01 N Na_2SO_4; 3) film of a 25% solution of morpholine in 0.1 N Na_2SO_4 deposited on the electrode (film thickness 160 μ).

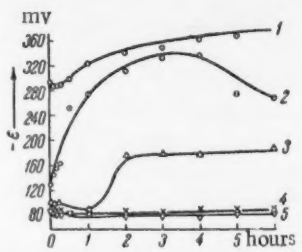

Fig. 4. The relationship between the change in stationary potential with time for which the electrode is kept beforehand in morpholine vapor. Electrolyte 0.01 N Na_2SO_4, layer thickness 160 μ. 1) Without volatile inhibitor. Time for which electrode is kept beforehand in contact with morpholine vapor before deposition of electrolyte film; 2) 1 hour; 3) 17 hours; 4, 5) 42-72 hours.

by sulfate ions from the electrode surface. (It is interesting to note that at first the surface of the electrode acquires more negative potentials than when inhibitor is absent. The latter phenomenon is possibly related to the preliminary adsorption of an organic cation which is formed by hydrolysis of the inhibitor and which facilitates the adsorption of anions).

Later, as a result of adsorption of the inhibitor through the film from the gaseous phase, the passivating properties of the inhibitor begin to have an effect and the potential of the electrode is shifted to more positive values (Curves 2, 3).

As the time for which the electrode is kept beforehand in an atmosphere of inhibitor vapor is increased, the potential of the metal becomes more stable (Curves 4, 5, 6) and the activating influence of the electrolyte is not observed. The potential is shifted by a considerable amount to more positive values (Curves 5 and 6), indicating the stability of the passive state.

A similar effect on the electrochemical behavior of an iron electrode is shown by the adsorption of morpholine. The relationship between the potential and the time for which the electrode is kept beforehand in an atmosphere saturated with morpholine vapor (Fig. 3, Curve 1) is similar to that examined above. The time requiredfor the limiting saturation of the surface to be attained with morpholine inhibitor, however, is approximately half of that required for benzylamine. Even when the electrode is kept for only a short time in the vapor of this compound, the potential is shifted by a considerable amount (by 180-200 mv) to more positive values. As in the case of benzylamine, adsorption of morpholine through the film brought about a much smaller effect (Curve 2). Moreover, in the initial period the potential of the iron becomes less noble, as a result of the activation of the surface by the electrolyte under conditions where the adsorption of the inhibitor evidently is still weak or else has not taken place at all. After a certain time the potential of the electrode starts to become more noble as a result of the adsorption of morpholine vapor by the electrolyte film and the subsequent adsorption of the inhibitor from the solution by the electrode. With the passage of time the potential becomes established at a constant value but it does not attain the same values as are reached by the electrode when preliminary adsorption of inhibitor from the gaseous phase has taken place. The adsorption of morpholine from a solution in which the inhibitor concentration was very high (25%) also gave a smaller effect (Curve 3). The potential of such an electrode in a film of 0.01 N Na_2SO_4 is close to the potential of an electrode exposed beforehand to the action of morpholine vapor for a very short period of time. In this case the potential does not change with change in the time for which the electrode is kept under the solution and does not reach the values characteristic of an electrode whose surface has become completely saturated from the gaseous phase.

The strength of the binding between the morpholine and the metal surface, and its passivating properties, are characterized by the curves showing the change in potential with time after deposition of a film of 0.01 N Na_2SO_4 on an electrode previously exposed to the influence of morpholine vapor (Fig. 4). When saturation of the electrode surface by the inhibitor is not complete (time of exposure 1 and 17 hours), the potential remains unstable (Curves 2 and 3). When the electrode is kept in contact with the volatile inhibitor for 48 hours, however, the potential is shifted by a considerable amount to more positive values and remains stable (Curves 4 and 5). The latter fact indicates that the passive state of the electrode in the presence of morpholine is extremely stable. We thus come to the conclusion that the volatile inhibitors are adsorbed by the metal surface and alter its electrochemical properties to a considerable extent. The greatest shift in stationary potential is observed when the electrode adsorbs the inhibitor beforehand from the gaseous phase. This results in maximum saturation of the surface by the inhibitor and an extremely stable passive state.

LITERATURE CITED

[1] H. R. Baker, Ind. and Eng. Chem. 46, 12, 2592 (1954); E. G. Strond, W. H. J. Vernon, J. Appl. Chem., 2, 4, 166 (1952); A. Wachter, T. Sky and N. Stillman, Corrosion, 7, 9, 284 (1951); S. D. Beskov, S. A. Balezin, V. P. Barannik, Corrosion Inhibitors, Coll. No. 2, M., 1957.*

[2] I. L. Rozenfel'd, Corrosion Inhibitors in Neutral Media, Izd. AN SSSR, 1953.*

[3] I. L. Rozenfel'd, T. I. Pavlutskaia, Zav. Lab. 21, 4, 37 (1955).

Institute of Physical Chemistry,
USSR Academy of Sciences

Received April 10, 1958

*In Russian.

A STUDY OF THE STRUCTURE OF THE PRODUCTS OF THE CARBONIZATION OF MATERIALS CONTAINING CARBON, BY THE METHODS OF ELECTRONIC PARAMAGNETIC RESONANCE AND X-RAY STRUCTURAL ANALYSIS

N. N. Tikhomirova, B. V. Lukin, L. L. Razumova and
Corresponding Member AN SSSR V. V. Voevodskii

In recent years the method of electronic paramagnetic resonance (e.p.r.) has shown that the products of the carbonization of various organic compounds contain free radicals in concentrations amounting to 10^{19}-10^{20} g^{-1} [1]. The method of e.p.r. absorption makes it possible to detect free radicals directly in the system under study and to measure their concentration; by analysis of the shape and width of the absorption line it is possible to reach certain conclusions regarding the properties of the free valences and also regarding their interaction with surrounding atoms.

In order to examine the possibilities presented by a study of the structure of carbonized substances by a combination of the methods of e.p.r. and x-ray structural analysis, we have made a study of the structural changes which take place in the carbonization of polyvinyl chloride (PVC) and polyvinylidene chloride (PVDC). The carbonization was carried out in an inert atmosphere in the temperature range 350-700°C. The e.p.r. spectra of all the specimens were recorded in high vacuum using an e.p.r.-spectrometer operating at a frequency of 9370 megacycles/sec. The signal was recorded on an oscillograph screen or on a recorder ribbon in the form of the first derivative of the absorption curve. A thin-walled glass ampoule containing the specimen was placed in the resonator, connected to a high-vacuum apparatus, and the specimen exhausted directly in the resonator. In all the specimens studied the g-factor (2.0036) was close to the g-factor for a free electron (2.0023). The chief parameter measured was the width of the line (the distance between the points of maximum slope on the absorption curve).

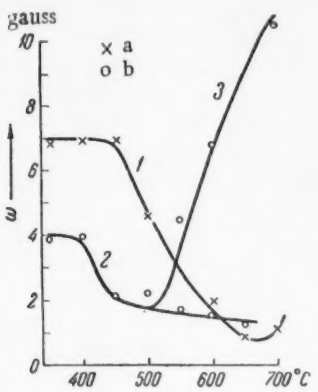

Fig. 1. Curves showing the change in width of the e.p.r. line for the products of the carbonization of polyvinyl chloride (a) and polyvinylidene chloride (b) with change in the carbonization temperature.

It is known that in systems consisting of "light atoms" (H, C, O, N) the width of the e.p.r. lines from the unpaired electrons is determined for the most part by the dipole interactions of the magnetic moments of the unpaired electrons with one another and by their interactions with the moments of the H or N nuclei. The first type of interaction leads to the so-called spin-spin broadening, the second to an increase in the total width of the line as a result of the appearance of a superfine structure (s.f.s.) for the e.p.r. line. On the other hand it is known that when a sufficiently intense exchange interaction takes place between unpaired electrons, or when unpaired electrons are delocalized along a system of conjugated chemical bonds, the local fields produced by the above interactions are neutralized, and this leads to a contraction of the e.p.r. line and to a change in its shape (change from Gaussian to Lorentzian [2]). In the case of systems in which interaction with nuclear moments and exchange interaction take place simultaneously, a reduction is observed in the total width of the line together with a smoothing out of the superfine structure [3]. The analysis of the width and shape of the e.p.r. line may thus give valuable information regarding the

site at which the unpaired electrons are localized and also regarding the structure of the substance under study.

The e.p.r. absorption signal, which indicates the presence of free radicals, appears in the very first stages of the carbonization of PVC and PVDC (starting at 350°). Figure 1 shows the relationship between the change in width of the e.p.r. signal (ω) and the carbonization temperature for both substances. For PVC the width of the line decreases in the carbonization process from 7.0 gauss (350-450°) to 0.8 gauss (650°). With further increase in the carbonization temperature the line starts to become wider (1.2 gauss at 700°) and when the ignition is carried out at above 900°, the broadening of the line becomes so great that it is difficult to observe the signal.

The relatively large width of the line (7 gauss) in PVC indicates the considerable influence of the superfine splitting on the hydrogen nuclei. Such large widths are characteristic of certain natural forms of carbon.* In the case of specially prepared carbon containing no H atoms (by the carbonization of C_3O_2), the e.p.r. gives a very narrow line (~0.6 gauss) which confirms the suggestion outlined above that the broadening of the e.p.r. line results from the effect of the superfine structure on the hydrogen [5].

In the case of PVDC (Fig. 1, Curves 2 and 3), particularly in the initial stages of carbonization, the width of the e.p.r. line is considerably less than that obtained for the products of the carbonization of PVC. From a temperature of 550° onwards a second broad e.p.r. absorption signal appears (Fig. 1, Curve 3).

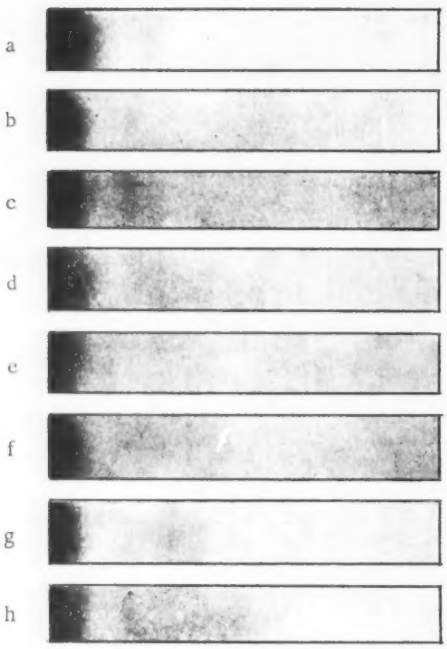

Fig. 2. X-ray diagrams for the products of the carbonization of polyvinyl chloride (a) 350°; b) 450°; c) 500°; d) 600°) and polyvinylidene chloride (e) 350°; f) 450°; g) 600°; h) 700°).

In order to examine the peculiar features of the e.p.r. curves for PVC and PVDC, we made use of information on the molecular structure of the specimens under study obtained by x-ray structural methods. The x-ray diagram for the products of the carbonization of PVC (350°) (Fig. 2a) shows the presence of carbon networks in the specimen (from the (10) line which is present in the x-ray diagram) and also indicates that the networks are separated by irregular structures (from the absence of the (002) line in the x-ray diagram and the presence of an extensive background in the center of the x-ray diagram). According to generally accepted theories, free radicals in coals are formed in side chains as a result of the rupture of C–C or C–H bonds [6]. It may therefore be expected that in a structure with extremely wide spaces between the networks with little conjugation, the radicals will be fairly far from the conjugated bond system in the carbon networks and the exchange interaction of the unpaired electron with the conjugated π-bonds of the condensed rings will not be very great.

It can be seen from the x-ray structural data that increase in the temperature of ignition up to 450° produces little change in the nature of the structure of the carbonization products from PVC (Fig. 2b). The magnitude of the e.p.r. line also remains practically unchanged.

Further carbonization of PVC (500-600°) leads to the appearance of the (002) line in the x-ray diagrams, to a reduction in the background inside this ring, (which indicates a decrease in the disorder of the structure), and to a reduction in the (10) line as a result of an increase in the dimensions of the networks (Fig. 2, c and d). These changes are related to a shortening of the side chains and to an increase in the conjugation within them. An

* E.p.r. lines with widths of this order of magnitude have been obtained in studies which we have carried out using a number of poor natural coals; analogous data are given in paper [4].

improvement in the conditions for conjugation of the unpaired electrons with the π-bonds of the aromatic rings may also take place as a result of the approach of the free radicals to the network packets. The improved conditions lead to exchange interaction and consequently to a further reduction in the e.p.r. line. At the same time the magnitude of the superfine splitting is reduced, since the relative concentration of hydrogen is lower in the high-temperature carbonization products.

The ignition of PVC at higher temperatures leads to a considerable increase in the dimensions of the carbon chains and in the order of their arrangement. As a result of these changes in the system, conductance electrons appear. The interaction of an unpaired electron with the conductance electrons evidently also leads to the experimentally observed broadening of the e.p.r. lines for the PVC specimen obtained at a temperature of more than 700°.

In PVDC, even at 350°, small networks are present (see Fig. 2e) and the regularity of this structure, judging by the presence of the diffuse ring and the comparatively slight background inside it, is considerably greater than that in an analogous specimen from PVC. The smaller width of the e.p.r. absorption line for carbonized PVDC indicates the greater conjugation of this system compared with that of carbonized PVC.

As has already been pointed out, increase in the temperature of PVDC carbonization above 500° leads to the appearance of a second e.p.r. signal, whose width increases as the carbonization temperature increases. It is interesting to note that in the case of petroleum cokes ignited at various temperatures, splitting of the signal into two parts coincided with a sharp increase in the electronic conductivity. For cokes ignited at comparatively low temperatures (up to 700°), a single narrow e.p.r. signal (2-4 gauss) is observed, together with an extremely low electrical conductivity ($< 3.10^{-4}$ ohm$^{-1}\cdot$ cm^{-1}). When the temperature at which the coke is treated is increased to ~800°, a second broad e.p.r. signal (150 gauss) appears and the electrical conductivity increases to $\sim 13^{-3}$ ohm$^{-1}\cdot$ $\cdot$ cm^{-1}. Increase in the temperature to 1100-1300° leads to such an extensive broadening of the signal that the e.p.r. line is hardly observed, and the electrical conductivity increases to $\sim 2.10^{-3}$ ohm$^{-1}\cdot$ cm^{-1}.

In our opinion, the presence of two e.p.r. signals at high temperatures provides evidence for the existence in the specimen of two types of unpaired electron, differing evidently in the sites at which they are localized and in the structure of the surrounding bond lattice. It may be assumed that the narrow signal, as in the case of PVC, is produced by the free valences localized on side chains with intense exchange interaction between one another throughout the system of conjugated side chains. If we develop the ideas outlined above regarding the width of the e.p.r. line in carbonaceous materials, it is possible to relate the appearance of a broad signal to the presence of free valences close to the separate large carbon networks or packets in which the conductivity electrons appear.

LITERATURE CITED

[1] J. E. Bennett, D. J. E. Ingram, and J. M. Tapley, J. Chem. Phys., 23, 215 (1955); D. E. G. Austen, D. J. E. Ingram and J. M. Tapley, Trans. Farad. Soc., 54, 400 (1958); J. Uebersfeld, Ann. Phys., 1, 436 (1956); F. H. Winslow, W. O. Baker and W. A. Jager, J. Am. Chem. Soc., 77, 4751 (1955).

[2] P. W. Anderson and P. R. Weiss, Rev. Mod. Phys., 9, 269 (1953).

[3] P. W. Anderson, J. Phys. Soc. Japan, 9, 316 (1954).

[4] A. Étienne and J. Uebersfeld, J. Chim. Phys., 51, 328 (1954).

[5] D. Wobschall, H. Akamatu and S. Mrozowski, Bull. Am. Phys. Soc., 3, No. 2 (1958).

[6] D. J. E. Ingram and J. M. Tapley, Phil. Mag., 45, 1221 (1954).

Received June 28, 1958

THE POLAROGRAPHY OF THE TROPYLIUM ION

S. I. Zhdanov and Academician A. N. Frumkin

The polarogram of the tropylium ion ($C_7H_7^+$) on a LiCl background contains three waves (Fig. 1, 3), the third of which occurs at $\varphi_{1/2} \approx -1.5$ v (against the normal calomel electrode) and corresponds to the discharge of the H^+ ions arising from the hydrolysis of the tropylium salt [1]. The nature of the remaining waves will be considered in the present work. Tropylium perchlorate served as the starting material for this investigation.

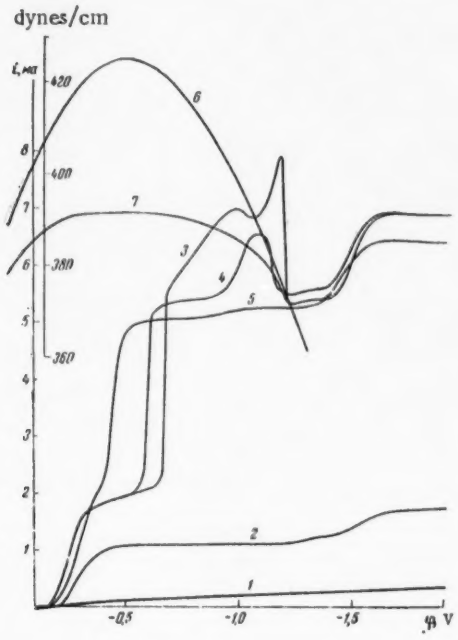

Fig. 1. Polarization and electrocapillary curves for the tropylium ion. Solution compositions: [LiCl] = 0.1 M; [$C_7H_7ClO_4$]: 1) 0, 2) $2 \cdot 10^{-4}$; 3) $5 \cdot 10^{-3}$ M; [gelatine]: 1-3) 0; 4) $1.48 \cdot 10^{-3}$; 5) $9.1 \cdot 10^{-3}$ %. Curve 6 was obtained in a 0.1 M $HClO_4$ solution, Curve 7, in a 0.1 M $HClO_4$ + 0.01 M $C_7H_7ClO_4$ solution; t = 25°. Curve 5 falls below Curve 4 because of the dilution of the solution with respect to tropylium by the gelatine solution.

When $[C_7H_7^+] < 3 \cdot 10^{-4}$ M, the polarogram contains only the first waves at $\varphi_{1/2} \approx -0.30$ v (Fig. 1, 2) and the limiting current is proportional to $\sqrt{h}$, where h is the heighth of the mercury column above the drop, these facts pointing to the diffusional nature of the wave. The slope of this wave is approximately 80 mv. According to microcoulometric data, 1 Faraday of electricity is expended per 1 mole of $C_7H_7^+$ reduced. Over the working interval of concentrations (10^{-4} - 1 M), $\varphi_{1/2}$ is independent of $[H^+]$. Thus, the following mechanism seems most likely to be that which represents the reduction of the $C_7H_7^+$:

$$C_7H_7^+ + e \rightarrow \dot{C}_7H_7 \quad \text{(radical);} \qquad (1)$$

$$2\dot{C}_7H_7 \rightarrow C_7H_7 - C_7H_7 \text{ (ditropylium).} \qquad (2)$$

These conclusions are confirmed by the data of Doering and Krauch [2] who have prepared ditropylium by the reduction of tropylium salt with zinc dust.

From a comparison of the polarization and the electrocapillary curves* for tropylium (Fig. 1), it follows that the $C_7H_7^+$ ion is reduced in the adsorbed state. It can here be supposed that the adsorbed $\dot{C}_7H_7$ radical is bound to the metal surface through an electron. So considered, the discharge of the tropylium ion proves to be similar to the discharge of metallic cations which are joined to a metallic lattice, the water molecules of the hydrate cloud being replaced by the electrons of the metal.

By assuming that the ionic structure is to a certain degree retained in the adsorbed tropylium radical, it is possible to understand the relative stability of this radical; this stability tends to increase the stationary surface concentration of the radical in the course of the electrode process and the accompanying dimerization reaction. In the case of the halide derivatives, it is known that re-

*The electrocapillary curves were obtained by M.A. Gerovich (deceased) and N.S. Polianovskaia in the Department of Electrochemistry of the University of Moscow.

duction usually proceeds with the union of two electrons, and that this leads to a replacement of the halide by hydrogen without a duplication of the number of carbon atoms in the molecule [3].

The increase in the first wave ceases when $[C_7H_7^+] \sim 3 \cdot 10^{-4}$ M. Further increase in $[C_7H_7^+]$ leads to the appearance of a second wave at $\varphi_{1/2} \sim -0.7$ v (Fig. 1, 3). Under these conditions, i_{lim} for the first wave becomes proportional to $\underline{h}$, a fact which points to the adsorptional nature of the wave. The sum of the i_{lim} values for the first two waves is proportional to $\sqrt{h}$ * and to $[C_7H_7^+]$, i.e., this sum is fixed by the diffusion of the $C_7H_7^+$. Microcoulometric measurement show that the process remains monoelectronic at the potential of the second wave.

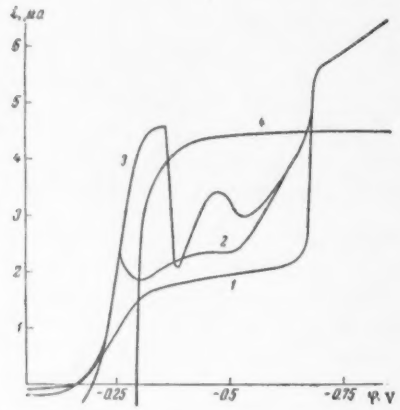

Fig. 2. The effect of KI on the polarization curves of tropylium. Solution compositions: 0.1 M LiCl + 10^{-3} M $C_7H_7ClO_4$ + KI. KI: 1) 0; 2) $5 \cdot 10^{-5}$; 3) $5 \cdot 10^{-4}$ M; 4) 0.1 M KI + 10^{-3} M $C_7H_7ClO_4$ + $5 \cdot 10^{-3}$% gelatine; t = 25°.

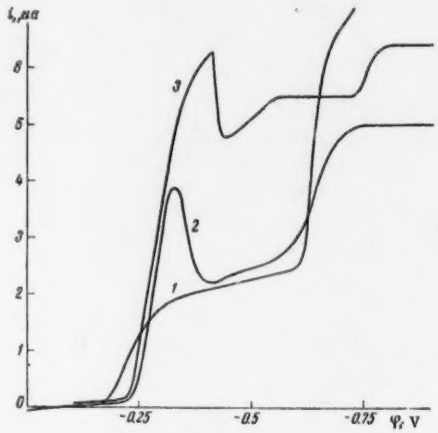

Fig. 3. The effect of β-naphthol on the polarization curve of tropylium. Solution compositions: 1) 0.1 M KCl + 10^{-3} M $C_7H_7ClO_4$ (t = 25°); 2) 0.1 M KCl + 10^{-3} M $C_7H_7ClO_4$ + saturated β-naphthol (t = 25°); 3) 0.1 M KCl + 10^{-3} M $C_7H_7ClO_4$ + saturated β-naphthol (t = 50°).

Following the well-known paper of Brdicka [4] in which the theory of adsorption waves in reversible systems was developed from work on methylene blue, it was discovered that these waves could be produced by a large number of organic and inorganic compounds. In most cases, even at times when proof of the reversibility of a process is lacking, the appearance of an adsorptional prewave is ascribed to the acquisition of energy through the adsorption of a reduction product, just as in the Brdicka theory.

The adsorption wave of tropylium shows characteristics which definitely distinguish it from a Brdicka wave:

1. From the i_{lim} value for an adsorption wave, it is possible on the basis of the Brdicka theory to calculate the maximum number of molecules which are adsorbed per unit of electrode surface and the area which is occupied by the individual molecule. In our case, such a calculation leads to a value of 5.6 $Å^2$ per C_7H_7 radical, which is too low. Low values have also been obtained by other authors [5, 6].

2. As a result of diminished adsorbability, a Brdicka wave disappears with rising temperature [4, 7]. The adsorption wave of tropylium increases with rising temperature, the temperature coefficient of i_{lim} being approximately 1.5% per degree, over the interval 25-95°.

3. A Brdicka wave disappears on the addition of those surface active substances which are more strongly adsorbed on mercury than are the products of reduction [4, 8, 9]. Such surface active substances have the opposite effect on the adsorption wave of tropylium. The addition of surface active anions leads to an increase in the value of i_{lim} for the adsorption wave, either over a limited range of potentials, or over the entire potential range of the adsorption wave up to the i_{lim} value for the second wave (Fig. 2). In this respect, the activity of the anions increases in the sequence Br^-, CNS^-, I^-.

* As a result of this, the height of the second wave itself diminishes with increasing $\underline{h}$, a fact that was accepted in [1] as indication of the wave's kinetic nature.

Experiment points to a similar action with the neutral molecules of such organic substances as β-naphthol (Fig. 3), camphor, hydroquinone, paratoluidine, and gelatine (Fig. 1), and even with cations, including the cations of tropylium itself at sufficiently high concentrations (Fig. 4). Such effects have also been observed by other workers [10-13].

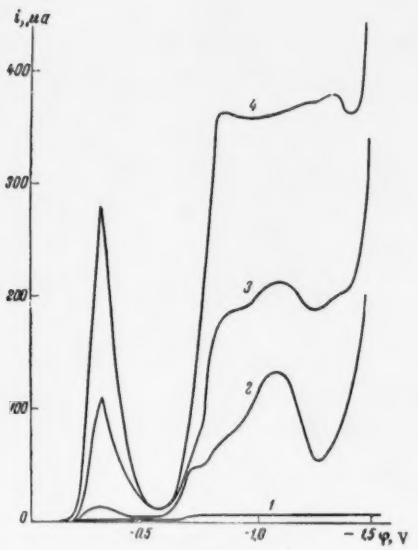

Fig. 4. Polarization curves for tropylium at various concentrations.
1) 0.1 M LiCl + 10^{-3} M $C_7H_7ClO_4$; 2) 0.35 M HCl + 0.011 M $C_7H_7ClO_4$; 3) 1 M HCl + 0.05 M $C_7H_7ClO_4$; 4) 1 M HCl + 0.1 M $C_7H_7ClO_4$.

Thus, the adsorption wave of tropylium is not of the same type as a Brdicka wave. It is clear that the adsorption wave of tropylium arises because of a retardation of the electrode process by the adsorbed film of ditropylium.* The height of this adsorption wave is fixed by the number of $C_7H_7^+$ ions which must be reduced in order to cover the surface of the electrode with a dense film of ditropylium, plus the number of $C_7H_7^+$ ions whose reduction products desorb from the surface. The desorption is clearly accelerated by increasing the temperature and this fact accounts for the existence of a positive temperature coefficient for i_{lim}.

It is striking that the adsorption of a depolarizer leads, as Kemula and Cisak [15] have shown, to the appearance of an adsorption prewave in the irreversible reduction of the halogen derivatives of cyclohexane, i.e., that the result is a promotion of the process rather than a retardation, such as would follow from the Brdicka theory for reversible processes.

The adsorption of ditropylium is due, according to M. A. Gerovich [16], to the interaction of the metal with the π-electrons; its strength diminishes with an increase in the negative potential, with the result that the retardation is removed and the second wave appears (Fig. 1).

Surface active substances which adsorb more strongly than the ditropylium impede the formation of an adsorbed film of the latter, but do not have so marked an effect on the kinetics of the electrode processes in the cases which we have investigated. Experiment proves that complete elimination of the retardation is not always attained by the addition of surface active substances. In such cases, a minimum current is to be observed on the first wave of the tropylium (Fig. 2, 2 and 3; Figs. 3 and 4).

In the absence of surface active substances, complex polarographic maxima, which are readily supressed by gelatine (Curves 4 and 5), develop on the second tropylium wave (Fig. 1, 3). Near the potential for the desorption of the tropylium, the maximum current increases and then sharply diminishes. Formerly, this fall-off in the current was incorrectly interpreted [1] as indicating a cessation of process (1) in desorption. Further studies are needed here.

In the presence of iodine I^- ions, and of gelatine which has been added for the supression of the maximum, it is possible to determine the wave form for tropylium without distortion from the adsorption of ditropylium. Under these conditions, the tropylium wave is not symmetrical, the lower portion of the curve being steeper than the upper. Such a wave form conforms to the supposition that the electrode step, (1), is reversible and that it is followed by the rapid dimerization of the product of the reduction (2)** [17].

The product of the complete hydrolysis of the tropylium salt, tropylium oxide [2], shows a single mono-electron irreversible (slope, 87 mv) reduction wave at $\varphi_{1/2} = -2.09$ v.

---

* A similar argument has recently been given by Schmid and Reiley [14] to account for the appearance of an adsorption prewave in the irreversible reduction of sodium vanadate.

** In this case, a solution of the problem was carried to completion by V. S. Krylov and B. M. Grafov. For the upper and the lower segments of the curve, two different wave equations were obtained which gave a good description of the experimental curve.

The authors take this opportunity to express their thanks to M. E. Vol'pin for having supplied the sample of tropylium perchlorate.

LITERATURE CITED

[1] M. E. Vol'pin, S. I. Zhdanov and D. N. Kursanov, Proc. Acad. Sci. USSR, 112, 264 (1957).*

[2] W. E. v. Doering and H. Krauch, Angew. Chem., 68, 661 (1956).

[3] I. M. Kolthoff and J. J. Lingane, Polarography, N. Y., (1952).

[4] R. Brdicka, Coll. Czech. Chem. Comm., 12, 522 (1947).

[5] A. Trifonov, Bull. Chem. Inst. Bulgarian Acad. Sci., 4, 21 (1956).

[6] L. Stárka, A. Vystrcil and B. Stárková, Coll. Czech. Chem. Comm., 23, 206 (1958).

[7] M. Voriskova, Coll. Czech. Chem. Comm., 12, 607 (1947).

[8] K. Wiesner, Coll. Czech. Chem. Comm., 12, 594 (1947).

[9] S. Wawzonek and J. D. Fredrikson, J. Am. Chem. Soc., 77, 3985 (1955).

[10] I. M. Kolthoff and J. J. Lingane, Polarography, 1, N.Y., 1952, p. 580.

[11] A. Vlcek, Coll. Czech. Chem. Comm., 19, 221 (1954).

[12] P. Silvestroni, Ricerca Sci., 24, 1695 (1954).

[13] A. S. Zagainova and A. G. Stromberg, Proc. Acad. Sci. USSR, 105, 747 (1955).

[14] R. W. Schmid and C. N. Reiley, J. Am. Chem. Soc., 80, 2087 (1958).

[15] W. Kemula and A. Cisak, Roczn. Chem., 31, 837 (1957).

[16] M. A. Gerovich, Proc. Acad. Sci. USSR, 105, 1278 (1955).

[17] J. Koutecky and V. Hanus, Coll. Czech. Chem. Comm., 20, 124 (1955).

Received July 19, 1958

*Original Russian pagination. See C.B. translation.

LOW PRESSURE ADSORPTION ISOTHERMS FOR NITROGEN

M. G. Kaganer

(Presented by Academician M. M. Dubinin May 13, 1958)

Until recently, the investigation of the adsorption of gases at low pressures has been almost completely neglected. With the development of the thermodynamics of adsorption, experimental data in this region has acquired great significance, particularly for the calculation of surface pressures and the entropies of gas molecules which are adsorbed on solid surfaces. Such data are also indispensable for the study of heterogeneous surfaces. Measurements of the adsorption of gases at low pressures also have practical significance, especially for vacuum techniques. Thus, in metallic Dewar flasks for liquefied gases, adsorbents are used to take up the residual gases at pressures of 10^{-5}-10^{-6} mm of Hg.

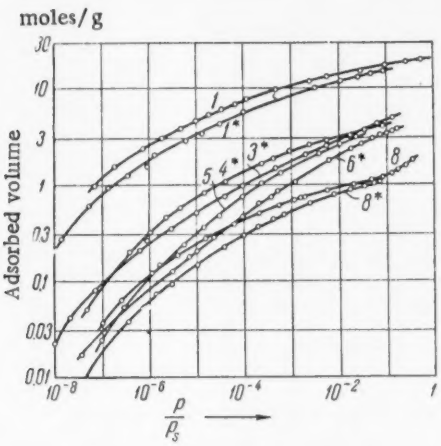

Fig. 1. Adsorption isotherms for nitrogen at 77.6 and 90.1°K, and at pressures ranging from $1 \cdot 10^{-5}$ to $5 \cdot 10^{2}$ mm of Hg. The figures on the curves correspond to the numeration of the specimens in Table 1.

A number of papers on adsorption at low pressures have recently appeared in which the work was essentially limited to that region of relative pressures in which $p/p_s > 10^{-6}$. The present paper aims at establishing the laws which apply to adsorption over that range of low pressures which extends up to region of applicability of Henry's Law. For this purpose, isotherms were developed for the adsorption of nitrogen by several adsorbents at 77.6 and 90.1° K, and at pressures down to $p/p_s = 1 \cdot 10^{-8}$. These measurements were carried out by the volume method.* At pressures below $1 \cdot 10^{-3}$ mm of Hg, equilibrium was attained within 15-25 hours. A correction for the thermomolecular effect was applied in determining the pressures [1]. The experimental results are shown in Fig. 1.

The characteristics of the investigated adsorbents are given in Table 1. The measurements on the lump silica gel, KSM, and on the alumino gel, A-2, had been made earlier [2]. Data on barium sulfate, a non-porous adsorbent, are also presented in this table [3]. The specific surfaces of these adsorbents were determined by the method which has been proposed by the authors [2].

The principal source of difficulty involved in establishing general relationships at low degrees of surface coverage is the great effect exerted by surface non-uniformities on adsorptive properties in this region. Here the adsorption principally proceeds on the more active portions of the surface, particularly in the ultra-fine pores. It is well-known that adsorption must follow Henry's Law when $p \to 0$. In most experimental work, this region has not been approached. In certain investigations, proportionality between the amount of adsorption and the pressure was obtained at comparatively high pressures [4, 5], this being clearly due to the fact that the experiments were

* A. I. Danilina participated in carrying out these experiments.

TABLE 1

Adsorbent Characteristics

No.	Specimen designation	T, °K	S, m²/g	α	β	D
1	Coking charcoal	77,6	1561	6,38	7,96	0,0215
1*	" "	90,1	1604	6,22	10,6	0,0335
2	Silica gel KSM, lump	77,6	629	5,42	4,84	0,0247
3*	Silica gel KSM, granulated	90,1	426	5,84	20,7	0,0448
4*	Silica gel S-U	90,1	393	5,39	5,95	0,0290
5	Silica aerogel	77,6	338	4,96	13,2	0,0414
6*	Silica gel, coarsely porous	90,1	333	5,32	39,5	0,0564
7	Alumino gel A-2	77,6	143	5,67	6,69	0,0281
8	Active alumina	77,6	114	5,70	7,15	0,0275
8*	" "	90,1	113	5,71	11,5	0,0357
9	Barium sulfate	77,4	9,4	5,98	3,20	0,0169

of too short a duration for the attainment of equilibrium. Several equations have been recommended for the presentation of data in the low pressure region. Most investigators [6-9] consider the Freundlich Equation to be the most acceptable of these. In a number of instances, good approximations can be had from the equation of M.M. Dubinin and L. V. Radushkevich [10-12], and from the Langmuir Equation [13].

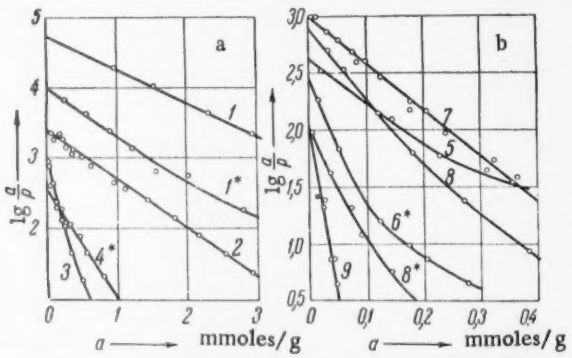

Fig. 2. Adsorption isotherms for nitrogen in the coordinates of the Williams-Henry Equation. The figures on the curves correspond to the numeration of the specimens in Table 1.

From the forms of the isotherms of Fig. 1, it follows that our data do not conform to the Freundlich Equation. The more precise version [2] of the equation of M. M. Dubinin and L. V. Radushkevich [14] has the form:

$$\lg \theta = -D\left(\lg \frac{p}{p_s}\right)^2, \qquad (1)$$

in which θ is the degree of surface coverage. The experimental data follow Equation (1) at relative pressures ranging from 0.005-0.03 to 10^{-5} - 10^{-4}. For the adsorbents Nos. 5 and 6, the points corresponding to the lowest pressures fall on straight lines when plotted in the coordinates log θ, $(\log p/p_s)^2$.

For each of the investigated adsorbents, experiment has shown that the initial segment of the isotherm can be represented with sufficient precision by a straight line in the coordinates log (a/ p), a of the Williams-Henry Equation:

$$\lg \frac{a}{p} = A - Ba \qquad (2)$$

here a is the amount of adsorbed gas, p is the corresponding pressure, and A and B are constants. In Fig. 2 the initial segments of our isotherms are shown plotted in these coordinates. At pressures below $1\text{-}2 \cdot 10^{-3}$ mm of Hg, the points fall on straight lines. Equation (2) can also be written as:

$$\lg \frac{\theta}{p/p_s} = \alpha - \beta\theta, \tag{3}$$

in which α and β are dimensionless constants.

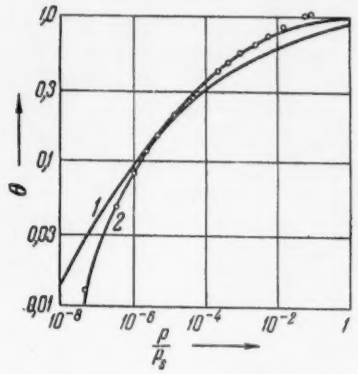

Fig. 3. Adsorption isotherms for nitrogen on the silicagel S-U at 90.1° K.
1) Equation (1); 2) Equation (3).

Equation (3) can serve for representing the adsorption isotherms for θ values ranging from 0 to 0.1-0.3, whereas Equation (1) embraces the θ region which goes from 0.1-0.5 to 0.75-0.9. Thus, the two equations cover almost the entire field of monomolecular adsorption. By way of an example, the adsorption isotherm for the silica gel S-U is presented in Fig. 3. The transition from Equation (1) to Equation (2) occurs here at a θ value of approximately 0.2 as is to be seen from the figure. The situation is similar for the other adsorbents which have been investigated. Exceptions to this last statement are to be found in the silica gels Nos. 3 and 6, in which the transition embraces the rather wide interval θ = 0.03-0.3, and in the coking charcoal, where the transition region at 90.1° K is θ = 0.1-0.6. In these three latter cases, it should be noted that the experimental points in the transition region lie on a straight line corresponding to new a D values when plotted in the coordinates $\log \theta$, $(\log \frac{p}{p_s})^2$.

In certain instances, such, for example, as in the calculation of the entropies of adsorbed molecules, it is necessary to extrapolate the experimental data to p = 0. The results of the present work show that a trustworthy method for carrying out this extrapolation is the construction of adsorption isotherms in the coordinates $\log \frac{a}{p}$, a. When $p \to 0$, a/p tends toward a definite limit which can be readily determined graphically.

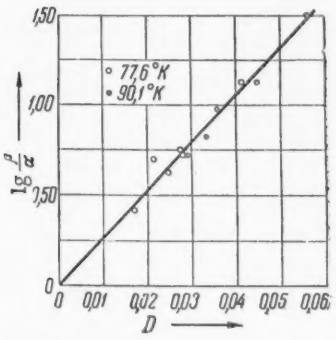

Fig. 4. The relation between the constants of Equations (1) and (3).

The linear Henry region appears on these isotherms at very low pressures. For practical purposes (with an accuracy of about 1%), the linear relation is valid for $p/p_s \leq 10^{-7}\text{-}10^{-8}$; this corresponds to a coverage of $\theta < 0.01$.

The coefficients α and β of Equation (3), and the quantity D of Equation (1), differ from the various adsorbents, as is to be seen from Table 1. Thus, the absolute isotherms (per 1 m^2 of surface) for the adsorption of nitrogen by the various adsorbents, including the finely porous, fail to coincide in the monomolecular region. According to the measurements, the coefficient α increases, as a rule, with a diminution of the mean pore dimensions, whereas β and D diminish. Increasing the temperature leads to an increase in the value of β and to a diminution in the value of α, the coefficient D being thereby increased (according to the theory, the latter is proportional to the square of the absolute temperature). Through these investigations it has been established that the coefficients α, β and D are mutually related through a definite functional equation. In Fig. 4, values of $\log \beta/\alpha$ are plotted as functions of D. It can be considered that the resulting straight line is generally applicable for the adsorption of nitrogen by various adsorbents at below-critical temperatures. The relation covered by this line can be represented by the equation

$$\frac{\lg \beta}{\alpha} = 26{,}2\,D \tag{4}$$

The data of Table 1 lead to what appears, at first glance, to be a paradox: the more coarsely porous is the adsorbent, the larger is the coefficient β which characterizes the departure of the low-pressure adsorption isotherm from the Henry Law. The explanation of this situation is as follows. When prepared in the usual manner, adsorbents, including such coarsely porous materials as silica aerogel (with mean pore dimensions of about 200 Å), contain a certain number of ultra-fine pores in which it is possible, in principle, to have adsorption at the very lowest pressures. Thus, the α values which characterize the adsorption in a given region, are approximately the same for various adsorbents. With the coarsely porous adsorbents, the number of fine pores is relatively small, and thus when a small fraction of the surface has been covered the value of the ratio $\theta/(p/p_s)$ rapidly falls to that corresponding to the coarse pores. Adsorbents Nos. 5 and 6 can be referred to as examples (Fig. 2b). Specially prepared homogeneous, coarsely porous, adsorbents are completely free of fine pores, and these substances must show relatively low values of α and β, and rather high values of D. It is clear that Relation (4) remains valid here.

On the basis of what has been said, it is possible to propose a method using three experimental points for the construction of adsorption isotherms which would be valid in the monomolecular region down to $\theta = 0$. Two of these points must have been obtained in the region $\theta = 0.5$-0.75, and one at $\theta = 0.1$. In the case of the adsorption of nitrogen at its boiling point, two of these measurements should have been at pressures of 0.5-5.0 mm of Hg, and one at $p = 1\text{-}2 \cdot 10^{-3}$ mm of Hg. By plotting the first two of these points in a graph with the coordinates log a, $(\log p/p_s)^2$, and drawing a straight line through them, it is possible to determine a_m, the amount of gas which is adsorbed in the monomolecular layer, and D. With the aid of Equation (4), the constants α and β of Equation (3) are then found by substituting the values of a/a_m and p/p_s for the third point.

By making use of these rules, it is possible to avoid the performance of long and tedious measurements at low pressures.

LITERATURE CITED

[1] S. Chu Liang, J. Appl. Phys., 22, 148 (1951).

[2] M. G.Kaganer, Proc. Acad. Sci. USSR, 116, 251 (1957).*

[3] B. V. Il'in, A. V. Kiselev, et al, Proc. Acad. Sci. USSR, 74, 827 (1950).

[4] H. Rowe, Phil. Mag., 1, 1042 (1926).

[5] A. Magnus, and A. Müller, Zs. Phys. Chem., A, 148, 241 (1930).

[6] O. Winkler, Zs. Techn. Phys. 14, 319 (1933).

[7] W. C. Frankenburg, J. Am. Chem. Soc., 66, 1827 (1944).

[8] J. de Dios Lopez-Gonzalez, F. G. Carpenter and V. R. Dietz, J. Res. Nat. Bur. Stand., 55, 11 (1955).

[9] M. H. Armbruster and J. B. Austin, J. Am. Chem. Soc., 66, 159 (1944).

[10] M. M. Dubinin, E. D. Zaverina and L. V. Radushkevich, J. Phys. Chem., 21, 1351 (1947).

[11] M. M. Dubinin and E. D. Zaverina, J. Phys. Chem., 23, 469 (1949).

[12] V. P. Dreving, A. V. Kiselev and O. A. Likhacheva, J. Phys. Chem., 25, 710 (1951).

[13] M. L. Corrin, J. Phys. Chem., 59, 313 (1955).

[14] M. M. Dubinin and L. V. Radushkevich, Proc. Acad. Sci. USSR, 55, 331 (1947).

The Scientific Research Institute for
Oxygen Machine Construction

Received May 13, 1958

*Original Russian pagination. See C.B. translation.

AN INVESTIGATION OF THE LOW TEMPERATURE OXIDATION OF METHANE INITIATED BY OXYGEN ATOMS FORMED IN THE THERMAL DECOMPOSITION OF OZONE

N. A. Kleimenov and A. B. Nalbandian

(Presented by Academician V. N. Kondrat'ev May 23, 1958)

In preceding papers [1] it has been shown that the oxidation of methane by ozonized oxygen is initiated by oxygen atoms which result from the thermal decomposition of the ozone. Under these conditions, methyl hydroperoxide and formaldehyde are the principal reaction products. Importance attaches to the study of the relation existing between the yield of these products and the several variables: the mixture composition, the ozone concentration, the time of contact, etc., and to a comparison of these relations and the results which have been obtained on the mercury-sensitized oxidation of methane and its higher homologs, where the alkyl radicals serve as the initial active centers and initiate the chain oxidation.

Experiments on oxidation by ozonized oxygen were carried out under atmospheric pressure in a flow system, at contact times ranging from 6 to 32 seconds. In this work there was employed aerated methane which had been carefully freed from carbon dioxide and traces of unsaturated hydrocarbons. The oxygen was taken from a tank and was carefully dried by being passed through sulfuric acid. Ozone was obtained by passing a part of the oxygen which had been introduced into the reactor through three ozonators which were connected in series. Analysis for ozone and methyl hydroperoxide was by the iodometric method. Formaldehyde was determined either polarographically, or by the hydroxylamine method.

EXPERIMENTAL RESULTS AND DISCUSSION

In Fig. 1 there are presented kinetic curves for the formation of methyl hydroperoxide, these having been obtained with mixtures of three different compositions at T = 150°. Some of these experiments were carried out at a constant concentration of ozone in the initial mixture; others were performed under such conditions that the discharge gases contained a definite quantity of undecomposed ozone. It is clear that the peroxide yield increased according to a linear law over the investigated interval of contact times.

In Fig. 2 there is shown the relation between the ozone concentration and the yield of peroxide and formaldehyde in equimolar methane-oxygen mixtures at temperatures of 150 and 180°, the contact time being 21 seconds. From this figure it is to be seen that the amount of product peroxide and formaldehyde was proportional to the ozone initially present in the mixture. It should be noted that this linear relation was maintained as long as the discharge gases contained ozone. This proportionality broke down at higher temperatures (200°, and above), when the ozone entering the reactor decomposed before reaching the end of the vessel.

A special series of experiments was set up to determine the effect of methane on the yield of methyl hydroperoxide. These experiments were carried out at T = 150°, and at a constant time of contact (t = 21 sec.); in them the ozone content of the initial mixture was 1.08%. In each of these experiments the oxygen concentration was held constant, and the concentration of the methane varied by replacing a portion of this gas by nitrogen. The data showed the amount of product peroxide to increase linearly with the methane concentration. Analysis of the discharge gases showed that the amount of decomposing ozone remained constant in these experiments. Similar results were obtained at T = 180°.

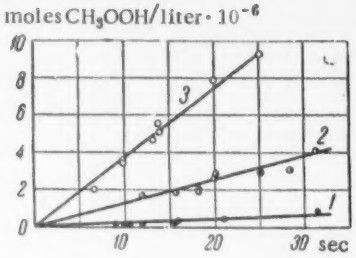

Fig. 1. The relation between the yield of methyl hydroperoxide and the time of contact for mixtures of three different concentrations. T = 150°. Concentration of ozone in the initial mixture, 0.32% by volume: 1) 10% CH_4 + 90% O_2; 2) 50% CH_4 + 50% O_2; 3) 90% CH_4 + 10% O_2.

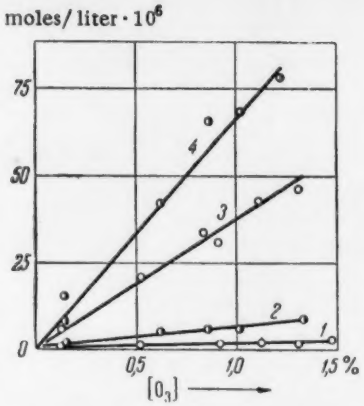

Fig. 2. The relation between the concentration of ozone in the initial mixture and the yield of methyl hydroperoxide (1, 2), and of formaldehyde (3, 4), at two different temperatures. 1, 3 at 150°; 2, 4 at 181°. Time of contact 21 sec. Composition of mixture: 50% CH_4 + 50% O_2.

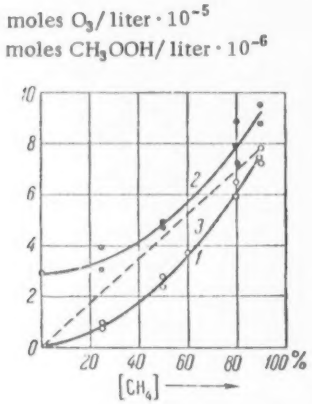

Fig. 3. The relation between the compositions of methane-oxygen mixtures, the yield of methyl hydroperoxide (1), and the decomposition of ozone (2). 3 — yield of methyl hydroperoxide, reduced to a constant amount of decomposing ozone. T = 150°. Time of contact 21 sec. Concentration of ozone in the initial mixture, 0.28% by volume.

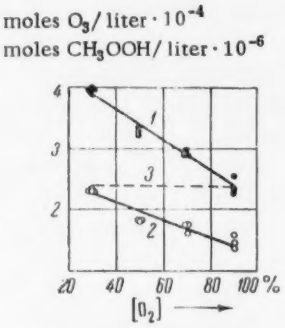

Fig. 4. The relation between the oxygen concentration, the yield of methane (1), and the decomposition of ozone (2), at a constant methane concentration of 10% and a constant ozone concentration of 0.3% by volume. T = 150°. Contact time, 21 sec.

It is to be seen from Fig. 3 (Curve 1) that the linear relation between the amount of product peroxide and the methane concentration broke down when the oxygen concentration was not held constant in the course of the experiments and the mixture composition was varied by replacing oxygen by methane. A detailed study showed that such departures from linearity were related to the fact that the amount of decomposing ozone increased with increasing methane concentration, and that, as a result, the amount of product peroxide was increased. Curve 2 of Fig. 3 shows how the amount of decomposing ozone rose with increasing methane concentration. If the experimental data are now recalculated on the basis of a fixed amount of decomposing ozone, the amount of ozone in a reaction mixture containing 90% methane being taken as unity, a straight-line relation between the amount of product peroxide and the concentration of the methane is once more obtained (Fig. 3, 3). From these experiments it

follows that the decomposition of the ozone was increased by replacing a part of the oxygen by methane. Such an effect was not observed on replacing the methane by nitrogen. This indicates that methane and nitrogen were about the same in their effect on the decomposition of ozone. Oxygen affects the breakdown of the ozone to a much smaller degree than either methane or nitrogen. This is in agreement with the results of other workers [2] who have studied the rate of decomposition of ozone, and its dependence on added amounts of various gases.

In Fig. 4 there is shown the relation between the yield of peroxide and the amount of oxygen. In this series of experiments, the concentration of methane in the initial mixture was held constant and a part of the oxygen was replaced by nitrogen. It is to be seen from Fig. 4 that the yield of peroxide (Curve 1) fell with increasing content of oxygen in the mixture. In this case, however, closer study showed that the amounts of decomposing ozone differed in the various points, despite the fact that the ozone concentration was held constant in the initial mixture (Fig. 4, 2). As the concentration of the oxygen increased, i.e., as the amount of nitrogen diminished, the amount of decomposing ozone decreased. Recalculating the experimental data to a fixed amount of decomposing ozone, the amount of the latter in the point corresponding to 90% oxygen being taken as unity, there is obtained the straight line 3 which is horizontal to the axis of abcissas. This indicates that the amount of product peroxide was independent of the oxygen concentration over the investigated interval of oxygen concentrations (from 30 to 90%).

In the course of this work it appeared that the ratio between the reaction products – peroxide and formaldehyde – was strongly dependent on the S/V ratio. With a decrease in the S/V ratio, the ratio of methyl hydroperoxide to formaldehyde increased. At low S/V values, the amount of the peroxide can become considerably greater than that of the formaldehyde. From these data the conclusion can be drawn that the peroxide radicals were lost on the walls of the vessel with the formation of formaldehyde. In addition, a part of the formaldehyde arose from the peroxide, which, under certain conditions, can partially break down into formaldehyde and water.

Comparing the principal results which have been obtained here (the proportionality between the reaction rate and the methane concentration, the lack of a relation between this rate and the oxygen concentration of the mixture, the proportionality to the concentration of the atoms of oxygen, etc.) with those which have been obtained on the photochemical oxidation of methane, ethane and propane [3-7], where similar products were found and identical relations established over the same temperature interval, it can be affirmed that the mechanism of oxidation is the same in both instances, although the initiators are different (oxygen atoms in the first case, and alkyl radicals in the second). In both cases the reaction proceeds through the same step. It is clear that methyl radicals are also formed through the action of oxygen on methane (according to the reaction: $\dot{O} + CH_4 \rightarrow \dot{C}H_3 + \dot{O}H$), and that these carry the basic chain forward. Further development of the chain then follows through:

low temperatures	$CH_3 + O_2 \rightarrow CH_3OO$,
	$CH_3OO + CH_4 \rightarrow CH_3OOH + CH_3$;
medium temperatures	$CH_3OO + CH_4 \rightarrow CH_3OOH + CH_3$,
	$CH_3OO \rightarrow CH_2O + OH$;
high temperatures	$CH_3OO \rightarrow CH_2O + OH$.

LITERATURE CITED

[1] N. A. Kleimenov, I. N. Antonova, A. M. Markevich and A. B. Nalbandian, J. Phys. Chem., 30, 794 (1956); J. Chim. Phys., 54, 321 (1957); N. A. Kleimenov and A. B. Nalbandian, Proc. Acad. Sci. USSR, 122, No. 1 (1958).*

[2] E. H. Riesenfeld, and E. Wasmuth, Zs. phys. Chem., 143 A, 397 (1929); V. Beretta and H. J. Schumacher, Zs. phys. Chem., 17 B, 417 (1932); W. D. Grath and R. G. W. Norrish, Proc. Roy. Soc., 242, 265 (1957).

[3] A. B. Nalbandian, J. Phys. Chem., 22, 1443 (1948).

[4] A. B. Nalbandian, Proc. Acad. Sci. USSR, 66, 413 (1949).

[5] N. F. Fok, V. V. Bereslavskii, A. B. Nalbandian and V. Ia. Shtern, Proc. Acad. Sci. USSR, 67, 499 (1949).

*See C.B. translation.

[6] N. F. Fok and A. B. Nalbandian, Proc. Acad. Sci. USSR, 85, 1093 (1952); 86, 589 (1952); 89, 125 (1953).

[7] N. F. Fok and A. B. Nalbandian, Monog., Problems of Chemical Kinetics, Catalysis and Reactivity, [in Russian], Acad. Sci. USSR Press, 1955.

Received May 21, 1958

THE SCALE OF THE STRUCTURAL ETCHING IN THE ELECTROCHEMICAL POLISHING OF METALS

S. I. Krichmar

(Presented by Academician A. N. Frumkin May 17, 1958)

Despite the high degree of perfection of the metallic surfaces which result from electrochemical polishing, the existence of structural etching in many of these has been shown in a number of papers [1, 2]. G. S. Vozdvizhenskii [2] has shown that even when structural etching cannot be detected by direct microscopic investigation, its existence can be proven by other methods (the method of maximum gloss [3], etc.).

Electropolishing is directly related, just as are the other processes of anodic dissolution, to the breakdown of the faces of those crystals which make up the surface that is under treatment. Depending on the circumstances, the electrochemical non-uniformity of these faces can make itself manifest in the form of a more or less pronounced microetching. It is known to be the rule that surface etching in electrochemical polishing cannot be detected by microscopic examination. We have shown that the conditions which arise in this case are those favoring the suppression of the usual structural etching [4]. The possibility is not to be excluded, however, that the appearance of the crystal structure of the metal could take place on a finer, submicroscopic, scale, where the effect of those factors which tend to repress distortion is considerably less.

From the data which are presented in [4], it is to be seen that, after etching, the smoothing out of the microrelief of a pure metal surface by electropolishing is not different from the smoothing out of the traces left by mechanical treatment. This gives reason to suppose that the conditions which are realized here are those which not only favor the smoothing out, but also impede, within certain limits, the appearance of the individual peculiarities of the separate crystalline components of the surface. As has been noted in [4], these conditions are most frequently met in the region of the limiting current where similarity in the volt-ampere characteristics of the various structural elements arises as the result of the formation either of a saturated layer of reaction products or, on occasion, of a solid film.

In considering the dissolving anode it is necessary, however, to take account of the fact that regions of supersaturation will exist near very small crystalline inclusions. This must lead to an increase in both the concentration gradient and the current density in these sectors. Dissolving will then proceed more intensively as long as this gradient has not been leveled off as the result of the increase in the distance between the anode surface of such sectors and the effective outer boundary of the diffusion layer. In the case of the formation of a solid film on the anode surface, transfer of matter will be realized through the pores in the latter. Even in this case, the presence of surface sectors in which the concentration is enhanced must lead to a more intensive dissolution of the metal. It follows from what has been said that the electrochemical polishing of metals cannot impede the decrystallization of crystal formations, the dimensions of these latter exerting a marked influence in increasing the solubility of the metal.

We will now evaluate the scale of etching. We will consider the simplest case of the behavior of a pure metal anode in an electrolyte which does not form passive films over the potential range which is under study. At low potentials, the current density on the various sectors of the anode (i_1), and the mean value of this density over the anode (i), can be represented by the following equations:

$$i_1 = nFD \operatorname{grad} C_1, \tag{1}$$

$$i = nFD \operatorname{grad} C = nFD\left(\frac{\partial C}{\partial x}\right)_{x=0} \simeq nFD\,\frac{C_{av} - C_0}{\delta}, \qquad (2)$$

in which D is the effective diffusion coefficient, δ is the mean effective depth of the diffusion layer on the anode, and δ_1 is this depth evaluated at a certain element of the surface. It is obvious that it is possible to find extremal points on most of these surface elements at which $(\partial C_1/\partial y) = (\partial C_1/\partial z) = 0$* (Fig. 1). Thus to a certain degree of approximation, it is possible to write:

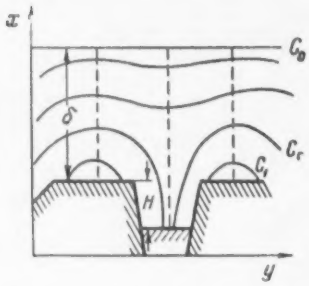

Fig. 1. Schematic representation of the distribution of the concentration of the reaction products at the surface of an electrode which is undergoing etching (deformed layer removed).

$$i_{1\max} \simeq nFD\,\frac{C_1 - C_0}{\delta_{1\max}} = nFD\,\frac{C_1 - C_0}{\delta + H}, \qquad (3)$$

where H is the deviation of the anode from flatness, a quantity which fixes the scale of etching, and C_{av} and C_1 are, respectively, the mean value of the concentration over the anode, and the value of the concentration at the surface element. When the dissolution is sufficiently gradual, there is equalization of the current densities on the various sectors. On equating (2) and (3) there results:

$$H = \delta\,(C_1 - C_0)\,(C_{av} - C_0)^{-1}. \qquad (4)$$

As has already been shown, the value of C_1 depends on the deviation of the potential of the sector from the mean anode potential, as determined by the crystalline properties of the individual sectors (ϵ_a) and by the effect of the crystal dimension in enhancing the solubility (ϵ_r). We have:

$$\varepsilon = \pm \varepsilon_a + \varepsilon_r, \qquad (5)$$

where ϵ is the total deviation of the potential of the sector from the statistical mean electrode potential. For ϵ we have:

$$\varepsilon = \frac{RT}{nF} \ln \frac{\gamma_1 C_1'}{\gamma_{av} C_{av}'}, \qquad (6)$$

in which C_{av} and C_1, and γ_{av} and γ_1 are, respectively, the ionic concentrations and activity coefficients of the reaction products. In most cases of electrochemical polishing, the reaction products are weakly dissociated. Taking the first ionization step into account, there results:

$$\varepsilon = \frac{RT}{2nF} \ln \frac{C_1}{C_{av}}. \qquad (7)$$

For ϵ_r we can write:

$$\varepsilon_r = 2\sigma M\,(nF\rho r)^{-1}, \qquad (8)$$

where σ is the surface tension at the metal – solution interface and r is the effective radius of the crystalline inclusion.

Combining (5), (7) and (8) we obtain for small ϵ:

$$C_1 \simeq C_{av}[1 \pm 2nF\varepsilon_a\,(RT)^{-1} + 4\sigma M\,(RT\rho r)^{-1}]. \qquad (9)$$

After setting (9) into (4) we will have:

$$H = \delta C_{av}(C_{av} - C_0)^{-1}\,[4\sigma M\,(RT\rho r)^{-1} \pm 2nF\varepsilon_a\,(RT)^{-1}]. \qquad (10)$$

* It is supposed that the surface is free of traces of mechanical treatment (the deformed layer has been removed).

The crystal dimensions prevent an unlimited increase in H with a corresponding decrease in $\underline{r}$. It is thus possible to speak of the maximum dimensions of crystals in which etching is not retarded by the suppressing factors. Designating the effective radius of such a crystal by r_0, and setting this value into (1) in place of H, we obtain:

$$r_0 = \frac{\delta C_{av}}{RT(C_{av} - C_0)}\left[\sqrt{(nF\varepsilon_a)^2 + \frac{4\sigma MRT(C_{av} - C_0)}{\rho\delta C_{av}}} \pm nF\varepsilon_a\right]. \tag{11}$$

If ϵ_0 is sufficiently large, the first member of (10) can be neglected at low current densities. Then

$$r_0 = H = \pm 2nF\delta C_{av}\varepsilon_a (RT)^{-1} (C_{av} - C_0)^{-1}. \tag{12}$$

Since δ is of the order of 10^{-2} cm (in the case of natural convection [5, 6]) and the potential difference between the faces of a single crystal amounts to several tenths of a volt (in copper, for example), [7] it follows from (12) that $r_0 \approx 10^{-1}$ cm. In actuality, r_0 is considerably less, since a surface which has been given preliminary mechanical treatment will, as a rule, show a resulting texture and will therefore prove to be covered with crystal faces of essentially one single type [8]. Here, as experiment proves, ϵ_a can be of the order of a millivolt, which would correspond to a r_0 value of 10^{-2} - 10^{-3} cm.

The reaction products reach saturation as the limiting current is approached on the various, more positively charged, sectors of the surface. A further increase in the electrochemical potentials of these faces then becomes impossible. Under such conditions, ϵ_0 is diminished, and completely reduced to zero in the area of limiting current. Then:

$$r_0 \cong 2\left[\delta\sigma MC_{av}(C_{av} - C_0)^{-1} (\rho RT)^{-1}\right]^{1/2}. \tag{13}$$

It is to be seen from (13) that etching arises here as a result of the enhanced solubility of the small crystals.

These ideas are also uniformly applicable to the case in which the surface is covered with a thin passive layer, since such a layer almost completely reproduces the microrelief of the metal surface and those same concentration relations are established on the interface between the solid film and the electrolyte as when the solution is in contact with the pure metal.

In the case of a solution of copper in H_3PO_4, we have $\delta = 10^{-2}$ cm [5], $\sigma = 2 \cdot 10^3$ dynes/cm [9], M = 64 g/mole, ρ = 8 g/ cm^3 and $C_{av}/(C_{av} - C_1) = 1$ (this is the situation when $C_0 = 0$). For r_0 there is obtained a value of the order of magnitude of 10^{-4} cm. Increasing the temperature and diminishing the depth of the diffusion layer favors a further supression of the etching. In this case the linear dimensions of the etch figures are so small that it is almost impossible to detect them with the usual microscopic methods. This submicroscopic structure can, however, be revealed by other methods, as has been indicated above. Thus, an electromicroscopic study of an electrochemically polished aluminum surface (18000 ×) has shown that the surface has a porous structure [10] in which the pore dimensions do not exceed several tenths of a micron.

As for the upper limit of the smoothing that can be obtained in electrochemical polishing, this can be defined as the ratio of the dimensions of the non-uniformities and the depth of the diffusion layer, in the case of where the passivity is weak or completely lacking, or as the ratio of the dimensions of the nonuniformities to the thickness of the passive layer when the latter is thick (of the order of several microns or more).* Smoothing will not take place when the upper boundary of either the diffusion layer, or the thick passive layer, reproduces the surface relief. It is most likely that smoothing will be realized when H is of the same order as δ. Since δ is of the order of 10^{-2} - 10^{-3} cm for natural convection, the interface must be of this same order.

From what has been said it follows that electrochemical polishing can be considered as a process which can prevent structural etching and smooth out the nonuniformities in the microrelief only in the definite range of 10^{-3} to 10^{-5} cm.

*For example, the electropolishing of silver in cyanide baths [11].

LITERATURE CITED

[1] G. S. Vozdvizhenskii, Proc. Acad. Sci. USSR, 58, 1587 (1948); G. S. Vozdvizhenskii, G. N. Dezder'ev and V. A. Dmitriev, J. Phys. Chem., 25, 547 (1951).

[2] G. S. Vozdvizhenskii, G. N. Dezider'ev and V. A. Dmitriev, Proc. Acad. Sci. USSR, 65, 697 (1949).

[3] G. Tamman, Metal Working [in Russian], Moscow-Leningrad, 1955, page 118.

[4] S. I. Krichmar and V. P. Galushko, J. Phys. Chem., 30, 577 (1956).

[5] S. I. Krichmar, Proc. Acad. Sci. USSR, 100, 481 (1955).

[6] V. G. Levich, Physicochemical Hydrodynamics [in Russian], Acad. Sci. USSR Press, 1952, page 106.

[7] G. S. Vozdvizhenskii, V. A. Dmitriev and E. V. Rzhevskaia, J. Phys. Chem., 29, 280 (1955).

[8] G. S. Vozdvizhenskii, A. Sh. Valeev and V. A. Dmitriev, Proc. Conference on Electrochemistry [in Russian], Acad. Sci. USSR Press, 1953, page 151.

[9] S. I. Krichmar, Proc. Acad. Sci. USSR, 101, 237 (1955); Handbook of the Metallurgy of the Light Metals [in Russian], 1, 1940.

[10] P. V. Shchigolev, J. Phys. Chem., 29, 682 (1955).

[11] A. T. Vagramian and A. P. Popkov, Proc. Acad. Sci. USSR, 102, 297 (1955).

Received October 15, 1956

THE PROBLEM OF THE HYDRATION OF IONS IN AQUEOUS SOLUTIONS

O. A. Osipov and I. K. Shelomov

(Presented by Academician A. N. Frumkin May 17, 1958)

In the papers of D. Bernal and R. Fowler [1], and of O. Ia. Samoilov [2], it has been shown that various ions in aqueous solution differently affect the translatory movement of the water molecules which are immediately adjacent to them. The multiple-charged ions, and the small, singly charged ions, reduce this motion, and the large ions increase it, i.e., the small ions increase the orientation of the dipoles in the water, whereas the large molecules reduce this orientation. This effect is usually designated as "orientation hydration." An interpretation of this phenomena can be given in the electrostatic theory of the liquid state [3, 4].

At any point in the body of a polar liquid there acts an internal field, E, which, as we have shown in [3], can be approximated by the expression:

$$E = \frac{4}{3}\pi N \frac{d}{M}\mu, \quad (1)$$

in which M is the molecular weight of the polar liquid that is under study, d is its density and μ, its dipole moment, and N is Avogadro's number. Because of the association of water molecules which results from hydrogen bonding, the value of the dipole moment in the liquid state is considerably different from that in the gaseous condition, and proves to be equal to approximately 3 debyes when evaluated either by the Syrkin formula [5] or by the method proposed by one of us [6]. Calculation shows that

$$E \approx 4{,}2 \cdot 10^5 \, CGSE.$$

at room temperature. When a water molecule is replaced by an ion, the energy of the liquid will remain unaltered if the force which the ion will exert on the surrounding molecules is equal to the force which these molecules (without change in their orientation, of course) will exert on the ion, i.e., when these forces are in equilibrium. In other words, the strength of the field due to the ion at the centers of the neighboring molecules must be equal to the strength of the field due to these liquid molecules at the ion center, i.e., to the internal field:

$$E_i = E, \quad (2)$$

E_i being the ion field.

When $E_i > E$, there will be a reduction in the translatory motion of the water molecules adjacent to the ion, i.e., a positive hydration, and, on the other hand, when $E_i < E$, there is an increase in the mobility of these molecules, and a negative hydration.

According to the laws of electrostatics

$$E_i = \frac{Ze}{(r_i + r_{H_2O})^2}, \quad (3)$$

r_i being the ionic radius, and r_{H_2O} the effective radius of the water molecule. It is clear that the sign of the ionic hydration is fixed by the difference $E_i - E = \Delta E$. From the condition $\Delta E = 0$, it is possible to determine that ionic radius at which a positive hydration goes over into a negative hydration:

$$\frac{Ze}{(r_i^{crit} + r_{H_2O})^2} - \frac{4}{3}\pi N \frac{d}{M}\mu = 0, \quad (4)$$

from whence

$$r_i^{crit} = \sqrt{\frac{Ze}{\frac{4}{3}\pi N \frac{d}{M}\mu}} - r_{H_2O}. \quad (5)$$

Ascribing to the water molecule an approximately spherical form, the effective radius can be found from the equation

$$r_{H_2O} = \sqrt{\frac{3M}{4\pi N d}} = 1{,}93\text{Å}.$$

For univalent ions the critical radius is equal to 1.45 Å ($r_i^{crit.} = 3.38 - 1.95 = 1.45$) and for the divalent ions its value is 2.05 Å.

TABLE 1

Ion	r_i, Å	$\Delta u_{calc.}$, kcal/mole	$\Delta u_{exp.}$, kcal/mole
Li^+	0,78	+0,63	+0,63
Na^+	0,98	+0,39	+0,34
Ag^+	1,15	+0,23	+0,14
K^+	1,33	+0,08	—0,07
Tl^+	1,50	—0,04	—0,15
Cs^+	1,65	—0,12	—0,24
Cl^-	1,81	—0,21	—0,25
Br^-	1,96	—0,28	—0,3
I^-	2,20	—0,37	—0,37

According to the data of D. Bernal and R. Fowler, the ions beginning with rubidium (for which r_i = 1.49 Å) should be considered as unhydrated and this is in good agreement with the results of our calculations. Similar conclusions have also been reached by E. Kh. Fritsman [7] on the basis of a study of the spectra of aqueous solutions. O. Ia. Samoilov gives somewhat lower values for $r_i^{crit.}$, including potassium among the negatively hydrated ions.

We will now carry out a calculation for the supplementary orientation energy which is communicated to the surrounding water molecules by an ion. An associated liquid can be looked upon as a system of molecules which are distributed at potential minima where the barrier is of height u. On superimposing a field ΔE, the potential barrier of the molecules which surround the ion is, according to Ia. I. Frenkel [8], lowered by an amount Δu in the direction of the field, and increased by the same amount in the opposite direction. It is clear that the work of the field will be equal to

$$A = 2n \cdot \Delta u, \quad (6)$$

n being the coordination number of the ion in solution. On the other hand, according to the data of the literature [8]

$$A = \frac{\Delta E \mu}{2}, \quad (7)$$

where μ is the dipole moment of the water molecule. From Equations (6) and (7) we obtain

$$\Delta u = \frac{\Delta E \mu}{4n}. \quad (8)$$

But Δu is also the supplementary energy of orientation of the molecule in the ionic field. It has been shown by O. Ia. Samoilov [10, 11] that the coordination number in dilute solutions can be taken as equal to four. Then

$$\Delta u = \frac{\mu \cdot \Delta \varepsilon}{16}. \quad (9)$$

In Table 1 there are given the values of Δu calculated for certain ions according to Equation (9), comparison being made with data on Δu which have been obtained by O. Ia. Samoilov from a study of ion mobilities [2]. From these figures it follows that our calculated values of Δu are in good agreement with the experimental data, especially

so when account is taken of the fact that the second significant figure in the Samoilov data on Δu has only arithmetical significance.

LITERATURE CITED

[1] D. Bernal and R. Fowler, Usp. Fiz. Nauk 14, 586 (1934).

[2] O. Ia. Samoilov, Bull. Acad. Sci. USSR, Div. Chem. Sci., 1953, 242.*

[3] O. A. Osipov and I. K. Shelomov, J. Phys. Chem., 30, Vol. 3, 608 (1956).

[4] O. A. Osipov and I. K. Shelomov, J. Phys. Chem., 31, Vol. 8, 1766 (1957).

[5] Ia. K. Syrkin, Proc. Acad. Sci. USSR, 35, 45 (1942).

[6] O. A. Osipov, J. Phys. Chem., 31, Vol. 7, 1542 (1957).

[7] E. Kh. Fritsman, The Nature of Water. Heavy Water [in Russian], Leningrad, 1935, page 102.

[8] Ia. I. Frenkel, The Kinetic Theory of Liquids [in Russian], Acad. Sci. USSR, Press 1954, page 196.

[9] A. M. Evseev and V. P. Lebedev, J. Phys. Chem., 27, Vol. 7, 1068 (1953).

[10] O. Ia. Samoilov, Bull. Acad. Sci. USSR, Div. Chem. Sci., 1952, 398.*

[11] O. Ia. Samoilov, Bull. Acad. Sci. USSR, Div. Chem. Sci., 1952, 627.*

The Rostov-on-Don State University

Received December 18, 1957

*Original Russian pagination. See C.B. translation.

THE THERMODYNAMIC EQUILIBRIUM OF SURFACES OF STRONG DISLOCATION

V. I. Skobelkin

(Presented by Academician S. A. Vekshinskii June 30, 1958)

In the hydromechanics of recent years application has been made of various variational principles which are equivalent to the equations of motion corresponding to the given initial and boundary conditions. For the most general adiabatic movement of gases (without dislocations), these variational principles have been stated and proven in [1, 2]. But for motions involving surfaces of strong dislocation, there must exist not only a variational principle equilvent to the equations of motion, but also one which is equivalent to the second law of thermodynamics, and expresses the condition for the equilibrium of such a surface. In the usual case, the thermodynamic equilibrium of a physical system is fixed by the variational equation $\delta\Phi = 0$, with two or more of the system parameters being held constant. The function Φ, which depends on the physical (variational) constants characterizing the given phenomenon, is the Gibbs thermodynamic potential [3]. Thus, the position of the vector of spontaneous magnetizability of a ferromagnetic crystal is found from the condition that $\delta\Phi = 0$, $\Phi = \delta - TS$ being the free energy of the crystal [4]. In varying the position of the magnetization vector, the specific volume and the temperature are held constant.

The problem of thermodynamic equilibrium must always arise in hydromechanics when some variational principle is formulated to describe the movement of a gas. In actuality, infinitesimal deviations from the true movement corresponding to the given initial and boundary conditions must satisfy not only a variational equation which is equivalent to the equation of motion but also the variational equation

$$\Delta Q - T\delta S = 0, \tag{1}$$

which is equivalent to the second law of thermodynamics for the actual condition of the gas when the latter is in thermodynamic equilibrium. The variations which are permitted in (1) are the same as those which determine the actual movement of the gas (in contradiction to δ, the symbol Δ indicates that ΔQ is not a complete differential). Thus, the class of permissible variations is limited by Equation (1).

In hydromechanics, it is generally true that the Gibbs thermodynamic potentials cannot be obtained from Equation (1), since, under variation, all of the parameters change as the result of the movement. For this reason, and in view of the fact that ΔQ is not a complete differential, the variations Δ and δ of Equation (1) must be infinitesimally small. In the variational principles which are known at the present time and which have been applied to continuous motion, and in the principle of minimum flow potential [1, 2], in particular, Equation (1) is satisfied identically. In the case of motion involving a surface of strong dislocation, Equation (1) is no longer identically satisfied, but gives an additional condition defining the thermodynamic equilibrium of the gas which is passing through this surface.

Let us consider the case of gas motion in the presence of a shock wave, or a sharply defined reaction front, which separates the incident gas, 0, from the burned gas, 1. Such a reaction front can be looked upon as a special instance of a surface of strong dislocation. If the gas through which the surface of strong dislocation is to be propagated is designated by the index 0, and the gas on the other side of this surface is designated by 1, it is then possible to write the conservation laws for mass, energy and impulse as [5]:

$$\rho_0 D = \rho_1 v_{n1}, \tag{2}$$

$$p_0 + \rho_0 D^2 = \rho_1 v_{n1}^2 + p_1, \tag{3}$$

$$E_0(p_0, \tau_0) + p_0\tau_0 + \frac{1}{2} D^2 = E_1(p_1, \tau_1) + p_1\tau_1 + \frac{1}{2} v_{n1}^2, \tag{4}$$

p being the pressure, ρ the density, $\tau = 1/\rho$, D the rate of propagation of the surface of strong dislocation with respect to the gas 0, v_n the component normal to this surface of the velocity of movement of the gas relative to the surface, and E the total energy or the sum of the internal energy and the "energy of formation" or the energy of binding, a. For exothermic reactions, the difference $a_0 - a_1 = q$ is the heat of reaction [6] referred to unit mass of the gas 0. Eliminating the velocity from (2) - (3) and substituting into (4), the Giugonio Equation is obtained

$$E_0(p_0, \tau_0) - E_1(p_1, \tau_1) = -\frac{1}{2}(\tau_0 - \tau_1)(p_0 + p_1). \tag{5}$$

It will be supposed that a description of the movement of the gas under the given boundary conditions and the conditions (2) - (4) on the surface of strong dislocation (this surface will be designated by σ) is given by a certain variational equation. In particular, when the generalized current functions ψ and ϑ [2, 7] have been assigned on the surface which limits the region of flow, ω, and the conversion laws of (2) - (4) are satisfied on σ, which divides ω into the two regions ω_1 (isentropic flow) and ω_2 (nonisentropic flow), the actually established subsonic flow of an ideal gas will satisfy the variational equation

$$\Delta[\psi, \vartheta] = \delta I + \frac{1}{R}\int_{\omega_2} pdSd\omega - \int_{\sigma} [L]_\sigma \delta \vec{l}\, d\vec{\sigma} = 0, \tag{6}$$

in which $I = \int_{\omega} (p + \rho v^2)\, d\omega = \int_{\omega} Ld\omega$ is the flow potential in the discontinuous case [2], $d\vec{\sigma} = \vec{n}d\sigma$ is the vector element of surface, l is the arc of the stream line, ψ = const., ϑ = const., R is the gas constant and S is the entropy. In Equation (6), ψ and ϑ are subject to variation under the condition that the Bernoulli Equation in the altered constants be satisfied in ω_1 and ω_2. The symbol $[L]_\sigma$ will designate the difference between the values of L on the two sides of σ: $[L]_\sigma = L_1 - L_0$. To Equation (6) there must be appended the variational equation for the thermodynamic equilibrium, (1), in which ΔQ and δS are fixed by the same deviations from the actual state as those which are involved in (6).

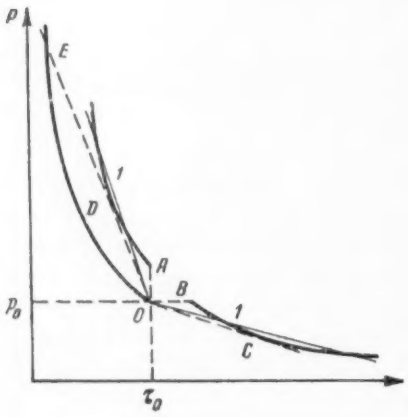

Fig. 1.

By way of an example we will consider the presonic flow of an ideal gas in a tube in the presence of a flame front which is being propagated at a definite velocity $D = D(p_0, \tau_0)$, in an isentropic gas with fixed Poisson constant. Fig. 1 represents the Giugonio adiabatic curves for a shock wave (OE), a detonation wave (AD), and for weak deflagration (BC).

For weak deflagration, Equations (2)-(3) give the Michelson line, $p - p_0 = \frac{D^2}{\tau_0^2}(\tau_0 - \tau)$, which is followed by the thermodynamic process in the reaction zone. Moving along this line to any point of the adiabatic curve BC, there is liberated a definite quantity of heat, q (the heat of reaction). Each state within the zone of combustion satisfies (2) - (4) with variable q. Integrating the equation $dQ = dE + pd\tau$ along the Michelson line, we obtain $\int dQ = E_0(p_0, \tau_0) - E_1(p_1, \tau_1) + \frac{1}{2}(\tau_0 - \tau_1)(p_0 + p_1)$, from which it follows, according to (5), that $\int dQ = q$. Consequently, in any variation of the state of gas 1, $\Delta Q = \Delta q = 0$, and Equation (1) leads to the condition $\delta S_1(p_1, \tau_1) = 0$. A change in the entropy S_1 under variation of the state of gas 1 (such a change is permissible with constraints) is possible only because of variations in τ_0 (or in p_0) ahead of the flame front. Thus, for those variations which are permitted by the boundary conditions, the conditions (2) - (4) on σ, and by the other constraints which are required in the given variational principle for the gas motion, $\delta S_1 = 0$

leads to the differential equation $\frac{dS_1(p_1, \tau_1)}{d\tau_0} = 0$ which, together with (2)- (4), gives a system of four algebraic equations for uniquely determining the parameters τ_0, τ_1, p_1 and v_{n1} of the gases 0 and 1 on the surface of the flame front. Thus, all of the parameters of the gases 0 and 1 are constant along the flame front and the movement of gas behind the front is isentropic (laminar).

In certain papers, particularly in [9-12], the presonic movement of a gas in the presence of a flame front has been hydrodynamically replaced by the movement of two incompressible fluids whose densities alter discontinuously on the front. The result is a strong vortex movement in the flow behind this front. From what has been said above, it follows that the two incompressible-fluids model of the movement does not satisfy the equation of thermodynamic equilibrium for the front, (1).

If the movement of the gas takes place in the presence of a shock wave, it is then necessary in determining ΔQ for the elementary particles behind the wave to investigate the nonequilibrium conditions prevailing in a transition layer, of the order of length of the mean free path of the gas molecule, where the energy dissipation takes place. The same is true in the case of a detonation wave. In these cases, the determination of ΔQ is only possible on the basis of a statistical theory of the fluctuations in the transition layer.

LITERATURE CITED

[1] V. I. Skobelkin, Proc. Acad. Sci. USSR, 108, No. 5 (1956).

[2] V. I. Skobelkin, J. Exp. Theo. Phys., No. 8 (1956).

[3] A. Sommerfeld, Thermodynamics and Statistical Physics, Foreign Lit. Press, 1955 [Russian translation].

[4] S. V. Vonsovskii, Modern Theory of Magnetism [in Russian], Moscow, 1953.

[5] G. Courant and K. Fredrichs, Supersonic Flow and Shock Waves, Foreign Lit. Press, 1950, pages 199-227, [Russian translation].

[6] L. D. Landau and E. M. Lifshits, The Mechanics of Continuous Media [in Russian], Moscow, 1954, pages 576-605.

[7] M. Z. v. Krzywoblocki, J. Aeronaut. Sci., 25, No. 1 (1958).

[8] Ia. B. Zel'dovich, The Theory of Shock Waves and an Introduction of Gas Dynamics [in Russian], Moscow-Leningrad, 1946.

[9] A. C. Scurlock, Mass. Inst. Techn. Meteor. Rep., No. 19 (1948).

[10] H. S. Tsien, J. Appl. Mech., 18, No. 2 (1951).

[11] G. C. Williams, H. C. Hattel and A. C. Scurlock, 3 Sympos. on Combust. and Flame and Explos. Phenom., Baltimore, 1949, p. 21.

[12] J. Fabri, R. Siestrunck and C. Fourê, Rech. Aeronaut., No. 25 (1952).

The M. V. Lomonosov State
University, Moscow

Received May 26, 1958

AN X-RAY DIASCOPIC INVESTIGATION OF THE MECHANISM OF INTERNAL DIFFUSION

D. P. Timofeev and A. A. Voskresenskii

(Presented by Academician M. M. Dubinin April 26, 1958)

The transfer of a substance which has been adsorbed in a porous sorbent out of a current of carrier gas proceeds by diffusion in the pore volumes and along their surfaces. The role of each of these components can be great or small, depending on the porosity of the sorbent, the nature of the surface, the nature of the adsorbing substance, the temperature, and on a number of other factors as well. Both types of transfer, i.e., diffusion in the gaseous phase and migration along the surface, proceed simultaneously and in the same direction, and the evaluation of the contribution of each is a matter of difficulty. In this work the attempt has been made to separate the flow in the gaseous phase from that occuring in the adsorbed phase.

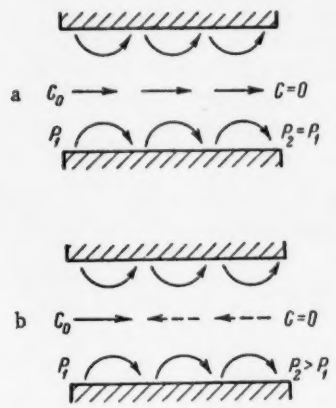

Fig. 1. Diagram showing the transfer of an adsorbed substance in the gaseous phase, and along the pore surface. a) In the absence of a countercurrent of nonadsorbing gas, b) with a countercurrent of nonadsorbing gas.

Fig. 1 schematically represents a pore of the sorbent, and illustrates the idea lying at the basis of the experimental work. Prior to the initiation of adsorption, this pore was filled with air, nitrogen, or some other poorly-adsorbing gas (which will be considered as nonadsorbing), at a uniform pressure equal to P_1. At one end of the pore there will now be established a concentration C_0 of the substance which is to be adsorbed; at the other end, let $C = 0$. A diffusion current from left to right will arise as a result of this concentration difference, part of the material moving through the gaseous phase and part along the pore surface (Fig. 1a). Now, let the pressure of the nonadsorbing gas be raised to P_2. The pressure difference $\Delta P = P_2 - P_1$ gives rise to a countercurrent of the nonadsorbing gas (Fig. 1b) and the conditions for transfer of matter in the gaseous phase are markedly altered. If, at the same time, $\Delta P \ll P_1$, the conditions for transfer in the adsorbed phase will remain practically unaltered.

If the adsorbed material is transferred principally along the pore surface, the rate of displacement of the adsorption front in a grain will not be especially retarded by the presence of a countercurrent of the nonadsorbing gas. On the other hand, a pronounced effect from the current of nonadsorbing gas is to be expected if the transfer of matter takes place principally in the gaseous phase. It is clear that the countercurrent will exert its influence only in those pores whose radii are large in comparison with the mean free path of the molecules. In the fine pores whose radii are smaller than this mean free path, the countercurrents will flow independently of one another. In our experiments at atmospheric pressure, the mean free path amounted to approximately 10^{-5} cm, so that retardation of transfer in the gaseous phase occurred only in pores of radii larger than 10^{-5} cm.

As a test material there was employed a granulated wood charcoal, steam activated, which had been obtained at 32% charring. The apparent specific gravity amounted to 0.898 g/ cm^3; the respective volumes of the

micro-, intermediate and macro- pores were 0.27, 0.11 and 0.21 cm^3/g. The constants in isothermal adsorption equation of Dubinin and Radushkevich were: $W_0 = 0.26$ cm^3/g, and $B = 0.42 \cdot 10^{-6}$. In Fig. 2 there is given the adsorption isotherm for the adsorption of ethyl bromide.

A grain of charcoal in the form of a cylinder, 5 mm in diameter and 6 to 9 mm in length, was inserted in an adsorption cell of plexiglass, such as is shown in Fig. 3. This grain was hermetically sealed in place by grinding its lateral surface against the walls of the tube. The grain was flushed out from the one end by a current of air-vapor mixture containing nitrogen with added ethyl bromide, and after a definite interval of time was irradiated with x-rays. The position of the adsorption front within the grain was recorded on the resulting x-ray diagram. In order to exclude effects from the variability in the structures and surface properties of various charcoal grains, a series of experiments was carried out on a single grain which was regenerated after treatment by being pumped out directly in the tube under high vacuum for 72 hours at room temperature. The completeness of regeneration was checked by x-raying. These experiments were performed at ethyl bromide concentrations of 20.7 and 75.9 mg/l, the velocity of the air-vapor mixture being 1.8 and 13.6 l / min · cm^2 and the temperature, 20 ± 0.5°. An x-ray tube with a copper target served as the source of x-rays. The potential on the anode was 30 kv, the current strength, 10 ma, and the distance to the object, 30 cm. The rate of passage of gas through the grain amounted to 28 cm^3/ min, which corresponded to a pressure drop of about 20 mm of Hg between the extremities of the grain. The nitrogen was introduced from a tank, after having been first passed through a column with cotton wadding, silica gel and activated charcoal.

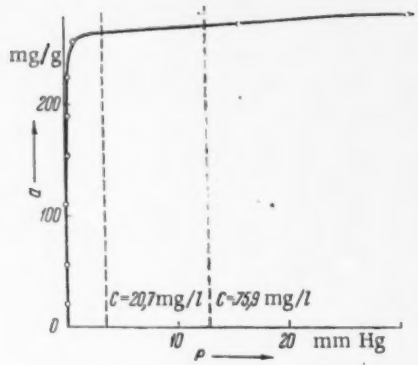

Fig. 2. Adsorption isotherm for the adsorption of ethyl bromide vapors on a activated charcoal. t = 20°.

The results from one series of experiments are represented in Fig. 4. In the first two horizontal lines there are shown positions of the adsorption front (blackened strip) within the grain when there was no current of the nonadsorbing gas; lines 3 and 4 give the positions of this front in the presence of a countercurrent of gas. Line 5 shows the results of desorption experiments where the grain was first treated in a current of the air-vapor mixture at a velocity of 1.8 l / min · cm^2 and an ethyl bromide concentration of 20.7 mg/l, after which the supply of ethyl bromide was cut off, i.e., the end was blown out with pure nitrogen alone, and gas scavenging of the grain with nitrogen at 28 cm^3/ min begun from the other direction. The time of the exposure of the grain to the current of air-vapor mixture, and the other experimental conditions, are indicated on the figure.

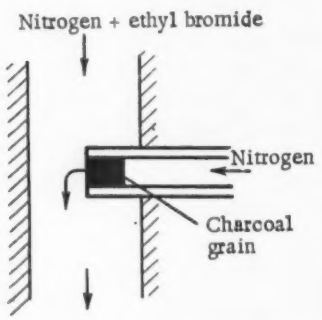

Fig. 3. Diagram of the sorption cell.

It follows from what has been said, that the depth of penetration of the grain was considerably less in the countercurrent of nonadsorbing gas that it was when no such current was present. This result cannot be explained in terms of a lowering of the concentration of the air-vapor mixture at the grain end due to the movement of nitrogen out of the grain since increasing the velocity of the mixture by more than 7-fold did not lead to any measurable alteration in the rate of movement of the adsorption front (see the photographs in lines 3 and 4). Neither can this be the result of some secondary phenomenon, such, for example, as the transfer of matter along the surface, followed by passage into the gaseous phase with subsequent reversal of movement in the current of nitrogen. Such a mechanism would not be consistent with the results of the desorption experiments. Full desorption of the ethyl bromide was not observed after 30 minutes even in the initial section of the grain. It should be noted that the pores with radii $r \geq 10^{-5}$ cm had surfaces amounting to many square meters per gram whereas the surfaces of the remaining, finer pores were of the order of hundreds of square meters per gram; in these latter the countercurrent exerted no influence on the gaseous phase transfer although transfer along their surfaces must have been much more extensive than in the case of pores for which $r > 10^{-5}$ cm.

After the elapse of 20-30 minutes from the beginning of an experiment, the depth of penetration of the grain in the presence of a countercurrent remained essentially constant and equal to ~ 0.7 mm, i.e., the initial rapid movement of the adsorption front slowed down markedly. This indicated that the transfer of adsorbed material occurred principally in the gaseous phase. From the Einstein-Smoluchowski relation, $x^2 = 2Dt$, (x is the path traversed by the particle in the time t, and D is the diffusion coefficient) it follows that the adsorption front would come to a stop (provided the transfer of matter was in the gaseous phase) when the linear rate of the countercurrent $w \geq 2D/x$. Under the above indicated conditions the linear rate of the gas in the grain amounted to 2.3 cm/sec, or to 3.7 cm/sec when account was taken of the porosity. Accepting the approximation $D = 0.1$ cm^2/sec, we find $x = 0.54$ mm, which is satisfactorily close to the experimental value (0.7 mm). With the passage of time the adsorption front was somewhat displaced in the direction of the diffusional current, as is quite natural, since transfer along the surface, or even in pores whose radii are less than the mean free path, is not retarded by a current of the nonadsorbing gas.

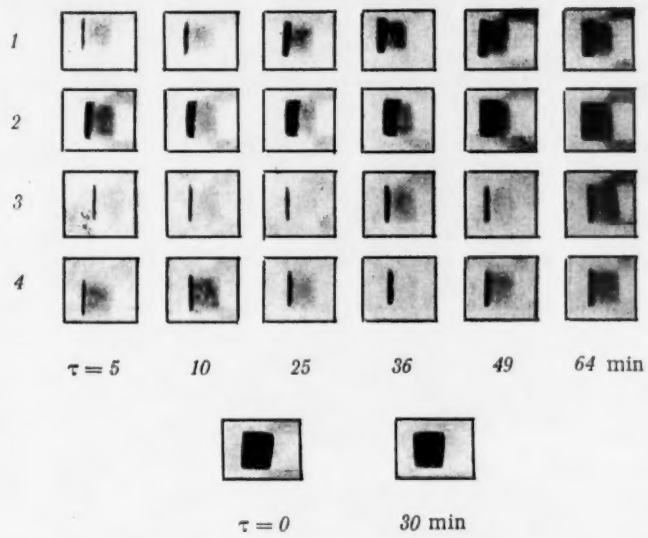

Fig. 4. The position of the adsorption front in the charcoal grain. 1, 2) Without a counter-current of nonadsorbing gas: 1) $C_0 = 20.7$ mg/l; 2) $C_0 = 75.9$ mg/l; 3, 4) with a countercurrent of nonadsorbing gas. Velocity of air-vapor mixture: 3) 1.8 l/min · cm^2; 4) 13.6 l/min · cm^2; 5) desorption. Velocity of nitrogen current at the extremity of the grain 1.8 l/min · cm^2; through the grain 28 cm^3/min.

On increasing the concentration of the air-vapor mixture from 20.7 to 75.9 mg/l there was observed a pronounced increase in the rate of movement of the adsorption front within the grain. Since the adsorption was thereby increased from 265 to 270 mg/g, i.e., by only 2%, so that the adsorption gradient within the grain was only slightly altered, this increase could only be explained by assuming that the principal form of transfer was diffusion in the gaseous phase.

Thus, on the basis of the results which have been obtained, it can be concluded that the transfer of matter in the gaseous phase is of fundamental significance for the system in question here, and that the role of the large pores in furnishing a transport path is very important in fixing the rate of internal diffusion.

The authors express their indebtedness to Academician M. M. Dubinin for his valuable remarks in evaluating the results of this work.

The Institute of Physical Chemistry of
the Academy of Sciences of the USSR

Received April 12, 1958

A STUDY OF THE ADSORPTION OF BENZENE VAPORS ON PALLADIUM FILMS

V. D. Iagodovskii

(Presented by Academician M. M. Dubinin May 14, 1958)

Because of their characteristic high surface purity, metals which have been sublimed in vacuum are frequently employed in studies on adsorption and catalysis. It has been shown in [1] that the palladium films which are obtained by vaporization in high vacuum possess high catalytic activity with respect to the redistribution of hydrogen in cyclohexadiene-1,3. In studying the kinetics of this latter reaction, the necessity arose for an investigation of the adsorption of benzene, one of the reaction products, on palladium films.

In the adsorption measurements, use was made of the inleakage method which has been worked out in detail by N. N. Kavtaradze [2]. The palladium films were prepared by the evaporation of metal from an electrically heated wire onto the walls of the adsorption vessel at a residual pressure of $5 \cdot 10^{-7}$ mm of Hg, the heated walls and the wire having been first carefully freed of sorbed gases. The film depth was estimated through the loss in weight of the palladium wire, it being assumed in these calculations that the film density was the same as that of the massive palladium. The apparent surface of the palladium film amounted to 100 cm^2. Benzene vapors were admitted into the adsorption vessel from a balloon of 10 l capacity where they were stored at a pressure of 3 mm of Hg, these vapors passing through a capillary 0.1 mm in diameter and 5 cm long. The krypton which was employed in determining the film surface by adsorption was introduced through this same capillary from another 10 l balloon. The pressure in the adsorption vessel was measured over 2-3 minute intervals on a Piriani gauge which was thermostated at 20° and which had been previously calibrated against krypton and benzene vapors by using a MacLeod gauge. In working up the results a correction for the thermal effusion was made according to the method of N. N. Kavtaradze [4] in each case where the temperature of the adsorption vessel differed from that of the Piriani gauge. Special experiments proved that adsorptional equilibrium was established quite rapidly under the rates of inleakage which were employed. The adsorption kinetics did not therefore interfere with the development of the isotherms. The amount of material adsorbed was determined from the difference in the rates of inleakage measured before and after the deposition of the palladium film on the walls of the adsorption vessel.

The adsorption of benzene vapors on the glass portions of the apparatus proved to be considerable, and was independently evaluated through the technique proposed by N. N. Kavtaradze. Near the capillary there was sealed an ampule which was cooled with liquid nitrogen. The weight of benzene which condensed into this ampule during several hours of inleakage of vapors through the capillary was in good agreement with that calculated through the Knudsen Equation:

$$\frac{dN}{dt} = \frac{1}{2} \frac{\beta}{V\sqrt{2\pi MRT}} \frac{1}{l} (p_1 - p_2), \quad \beta = 16 \frac{a^3}{3},$$

in which M is the molecular weight, a is the capillary radius, l is the capillary length, p_1 is the pressure of the benzene vapors in the ten liter balloon and p_2 the pressure of these vapors in the adsorption vessel. By comparing the amount of benzene which had been admitted into the adsorption vessel with the amount of benzene in the vapor phase, the adsorption of these vapors on the glass could be readily evaluated at various pressures.

Adsorption isotherms were obtained for the benzene vapors at 20° and at 79°, since it was over this temperature interval that study had been made of the disproportionation of hydrogen in cyclohexadiene. In Fig. 1 there are presented isotherms for the adsorption of benzene vapors on four palladium films at 20° (Curves 1-4), and a

similar isotherm at 79° (Curve 5). Repeated inleakage showed that a portion of the benzene which had been adsorbed in each experiment was readily removed from the surface, but that the major portion of it remained on the film even after evacuation to $1 \cdot 10^{-5}$ mm of Hg at the working temperature. Desorption occurred only when the film temperature was raised to 250°. On once more lowering the temperature to 20°, the entire amount of the earlier-adsorbed benzene was not again taken up. In all likelihood, this was due to a contraction in the total film surface as a result of heating, a supposition which was confirmed through the determination of the surface by the use of krypton (see below). In the pressure range $1 \cdot 10^{-2}$ - $2.6 \cdot 10^{-2}$ mm of Hg, the fraction of the benzene which was firmly adsorbed on each of the investigated film surfaces at 20° amounted to 75-80% of the total amount taken up.

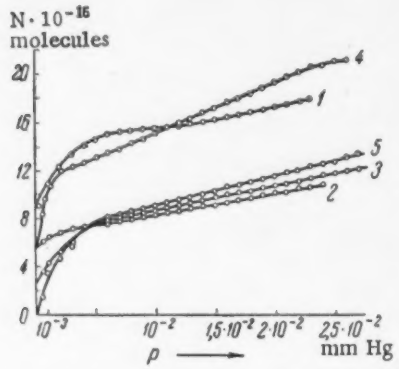

Fig. 1. Isotherms for the total adsorption of benzene vapors on palladium films at 20° (1, 2, 3, 4) and at 79° (5).

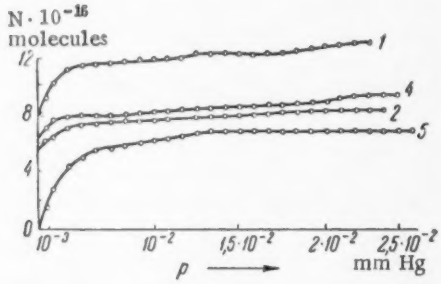

Fig. 2. The strong adsorption of benzene on palladium films at 20° (1, 2, 4), and at 79° (5).

Experiment showed (Fig. 2) that the amount of material adsorbed depended on the pressure, at pressures lower than $5 \cdot 10^{-3}$ mm of Hg. This dependence was more weakly expressed at higher pressures. In the case of films Nos. 1-4 at 20°, curves showing the relation between the adsorption and the pressure had a step-like form. It is clearly possible to assume that the surface involved in the firm adsorption of the benzene was nonuniform and consisted of two or three different kinds of sectors. Film 2 had been subjected to a preliminary sintering at 100°, and film 3 had been similarly treated at 300°. A comparison of the corresponding curves showed that the nature of the surface nonuniformities were but slightly dependent on the thermal treatment. Films Nos. 1 and 4 were prepared under similar conditions but the number of sectors showing differences in adsorption potential was not the same in these two cases. In studying the influence of the surface coverage of palladium on the infrared adsorption spectra of chemadsorbed carbon dioxide, Eischens, Francis and Pliskin [4] came to the conclusion that there were several types of surface sectors with different adsorption potentials, each of these sectors being relatively uniform in surface. This is in agreement with our data, and that despite marked differences in the methods which were employed in preparing the palladium sorbents.

For each film, with the exception of No. 1, plots in the coordinates of the BET Equation gave broken straight lines consisting of two linear segments. From the slope of the first of these segments, the number of firmly adsorbed benzene molecules, N', was obtained, and from the slope of the second linear portion, the total number of adsorbed benzene molecules, N". The results of the calculations are presented in Table 1. In the coordinates of the Langmuir Equation, $[(p/N - p$, where N is the number of molecules adsorbed at the pressure p) the isotherms also consisted of two linear segments, from whose slopes the same values were obtained for N' and for N" as those resulting from the BET Equation. It is to be seen from Table 1 that the surface available for the firm adsorption of the benzene contracted considerably as the result of sintering at 100° and at 300°. The isotherms for the total adsorption of benzene at 79°, and for film No. 1, followed both the Langmuir and the BET equations and did not show breaks in the respective coordinates of these equations.

In order to determine the surfaces of the sublimed palladium films and their temperature dependence, the adsorption of krypton was studied at −195°. In calculating the surface according to the BET Equation, the pressure of the saturated vapors of solid krypton [5] was substituted for p_s. It proved to be such that nonuniformity of the surface appeared even in the case where two straight lines of different slope were obtained in the coordinates $\frac{p}{N(p_s - p)}$ and p/p_s. In Table 2 there are presented values of the film surfaces before and after sintering to 300°; for com-

TABLE 1

The Number of Benzene Molecules Adsorbed on Palladium Films at 20° and at 79°

Nos.	T, °C	Preliminary treatment	Film weight, g	BET, $N' \cdot 10^{-16}$	$N^{\circ} \cdot 10^{-16}$
1	20	Without sintering	0.0054		17.3
2	20	With sintering at 100°	0.0042	8.8	13.9
3	20	With sintering at 300°	0.0059	11.05	19.25
4	20	Without sintering	0.0077	15.4	29.3
5	79	Without sintering	0.0025		11.5

TABLE 2

Values of the Total Surfaces of Pb Films in cm^2

σ_{Kr}, Å²	In terms of krypton				In terms of benzene			
	before sintering		after sintering at 300°		Nos.	preliminary treatment	S_{active}	S_{total}
	S_{active}	S_{total}	S_{active}	S_{total}				
14.7	447	909	320	718	1	Without sintering		700
22[5]	667	1340	480	1075	2	With sintering at 300°	346	547
					3	With sintering at 100°	446	761
					4	Without sintering	622	1160

parison, surface values from Table 1 are given for the four films, these having been calculated from the benzene adsorption by assuming the area occupied by one plane-oriented benzene molecule to be 40.3 Å² [6]. These data point to the good agreement between the surface values determined from benzene and from krypton, regardless of the choice of area values for Kr [5]. This becomes quite obvious when account is taken of the fact that the film surface areas were not reproducible, even when the films were prepared under identical conditions of sublimation. The specific film surfaces were of the order of 15 m^2/g which is near to that of specific surfaces of films that have been prepared by Beeck [7]. The geometric surface of the adsorption vessel was 100 cm^2. It follows from Table 2 that the surface area of the film was approximately 13 times greater than the geometric prior to thermal treatment, and 10 times greater than the geometric after such treatment. A comparison of the surfaces as determined from benzene and from krypton showed palladium to be a coarsely porous adsorbent.

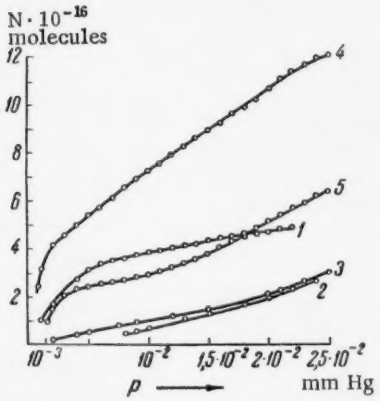

Fig. 3. Isotherms for the reversible adsorption of benzene. 1-4) at 20°; 1-4) palladium films which had not been subjected to thermal treatment; 2, 3) palladium films after preliminary thermal treatment; 5) at 79°.

Isotherms for the reversible adsorption of benzene vapors are shown in Fig. 3. The isotherms for films Nos. 1 and 4 which had not been subjected to any thermal treatment different markedly from the isotherms for films Nos. 2 and 3 which had been thermally treated. In this same figure there is given the isotherm 5 for reversible adsorption at 79°. The isotherms which were obtained on the thermally treated films were concave and could not be described by either the Langmuir, or the BET equation. The isotherms obtained with films Nos. 1 and 4 were convex in form,

but they, too, failed to follow the Langmuir and the BET equations. The convex form of these isotherms indicated a predominance of the adsorbate-surface interaction over the molecular interaction in the monolayer. The reversible adsorption isotherms which were obtained for benzene on the thermally treated palladium films (Nos. 2 and 3) could be described by the equation of A. V. Kiselev [8]:

$$\frac{\theta}{p(1-\theta)} = k_1 + k_1 k_n \theta,$$

which makes allowance for the interaction of the molecules in the adsorption layer. Here k_1 is a constant which characterizes the interaction of the adsorbed molecules with the surface, and k_n is another constant which covers the interaction between the molecules themselves. In the coordinates $\frac{\theta}{p(1-\theta)}$ and θ, the isotherm obtained with film No. 3 gavea straight line from which there were found the values: $k_1 = 6.1$ mm^{-1}, $k_n = 7.5$ mm^{-1}. For film No. 2 which had been sintered at a lower temperature, a broken straight line of two linear segments was obtained in these same coordinates. According to the first of these segments $k_1 = 9.4$ mm^{-1} and $k_n = 0.8$ mm^{-1}; from the second, $k_1 = 4.9$ mm^{-1} and $k_n = 7.5$ mm^{-1}. These results indicate that for the films in question, the molecular interaction in the monolayer was of considerable magnitude: in the case of film No. 3, $k_n > k_1$. In this situation there was also observed a "step-wise" nonuniformity in terms of the adsorption potential. In actuality, the value of K_1 for film No. 2 diminished by almost one half on going from low to high coverage, and the contribution of the intermolecular interaction increased almost 10-fold on the sector with the lower adsorption potential.

The authors express their indebtedness to N. N. Kavtaradze for his valuable advice and help in carrying out this work and to V. M. Griaznov for a discussion of the results.

LITERATURE CITED

[1] V. M. Griaznov and V. D. Iagodovskii, Proc. Acad. Sci. USSR, 116, No. 1, 81 (1957).*

[2] N. N. Kavtaradze, Candidate's Dissertation, Ins. Phys. Chem., Acad. Sci. USSR, 1956.**

[3] N. N. Kavtaradze, J. Phys. Chem., 28, 6, 1081 (1954).

[4] R. P. Eischens, S. A. Francis and W. A. Pliskin, J. Phys. Chem., 60, No. 2, 194 (1956).

[5] R. A. W. Haul, Angew. Chem., 68, No. 7, 238 (1956).

[6] I. A. Lygina, Candidate's Dissertation, Ins. Phys. Chem., Acad. Sci. USSR, (1958).**

[7] O. Beeck and A. W. Ritchie, Disc. Farad. Soc., 8, 159 (1950).

[8] A. V. Kiselev, Proc. Acad. Sci. USSR, 117, No. 6 (1957).*

Received May 5, 1958

*Original Russian pagination. See C.B. translation.

**In Russian.

INVESTIGATION OF THE KINETICS OF RECOMBINATION OF TRIPHENYLMETHYL RADICALS BY THE ELECTRON PARAMAGNETIC RESONANCE METHOD

F.S. D'iachkovskii, N.N. Bubnov and A.E. Shilov

(Presented by Academician V.N. Kondrat'ev, May 23, 1958)

Tsigler et al. [1] has studied the kinetics of dissociation of hexaphenylethane by the rate of oxygen and nitrogen oxide absorption; he found that the activation energy of the decomposition of hexaphenylethane into radicals (18-20 kcal) is considerably higher than its heat of dissociation (11-12 kcal). This means that the reverse reaction, that of recombination of triphenylmethyl radicals must proceed with an activation energy equal to the difference between the activation energy of dissociation and heat of dissociation of hexaphenylethane (6-8 kcal).

We have verified this conclusion by the electron paramagnetic resonance method (EPR) by measuring directly the rate of depolymerization of triphenylmethyl radicals in the solution. This was done in the following way: a sealed capillary containing a solution of hexaphenylethane in toluol heated to 100°C was quickly cooled to the temperature of the experiment in a thermostatic fluid placed in the resonator of the EPR spectrometer. In this way we obtained concentrations of triphenylmethyl radicals considerably higher than equilibrium concentrations and measured the rate of their recombination. By special experiments we have shown that with a thin-walled

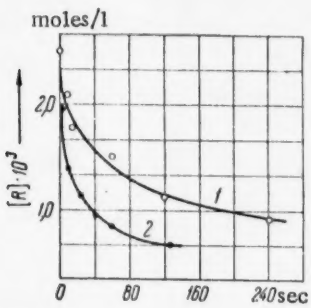

Fig. 1. Kinetics of depolymerization of triphenylmethyl radicals in toluol: 1) at −64°C; 2) at −35°C.

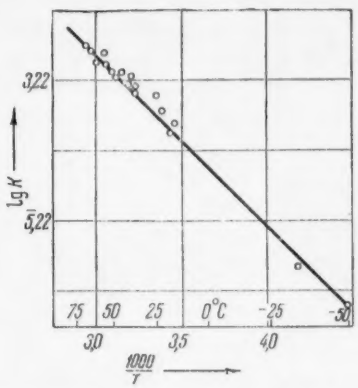

Fig. 2. Variation of the equilibrium constant of dissociation of hexaphenylethane in toluol as a function of temperature.

capillary with an internal diameter of about 1 mm, the temperature of the solution in the capillary becomes stabilized after a few seconds. The measurements were made with the EPR spectrometer with high-frequency modulation of the magnetic field. The solution of hexaphenylethane was obtained by shaking the triphenylchloromethane solution in toluol with zinc dust until the cessation of reaction with chlorine. The concentration of the hexaphenylethane prepared in this way was determined gasometrically by the amount of absorbed nitrogen oxide.

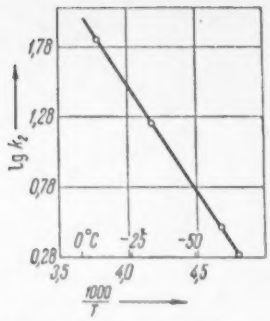

Fig. 3. Variation of the constant of the depolymerization rate of triphenylmethyl radicals in toluol as a function of temperature.

The concentration of triphenylmethyl radicals during the reaction was measured by the relative integral intensities of the EPR signals of the solution and of diphenylpicrylhydrazyl of a given concentration. Measurement of the depolymerization rate was made in the temperature range of −64° to −9°C. The rapid change of the signal at −9°C was registered by taking a motion picture of the oscillograph screen. Figure 1 represents two kinetic curves of recombination of triphenylmethyl radicals at −64 and −35°C. The figure shows that the recombination rate increases considerably with increasing temperature.

The kinetics of recombination of radicals, taking into account the reverse reaction, follows the kinetic relationship:

$$\frac{d[R]}{dt} = -k_2[R]^2 + k_1\left(\frac{a-[R]}{2}\right), \qquad (1)$$

where [R] is the concentration of radicals, k_2 is the constant of the recombination rate of radicals, k_1 is the constant of the dissociation rate of hexaphenylethane, and $(a - [R])/2$ is the concentration of nondissociated hexaphenylethane ($\underline{a}$ is the amount of absorbed NO). If we express $k_1 = k_2K$ [K is the equilibrium constant of the reaction $2(C_6H_5)_3C \rightleftharpoons (C_6H_5)_3C - C(C_6H_5)_3$] we can determine k_2 from Eq. (1). The equilibrium constant of dissociation of hexaphenylethane in toluol is determined from the equilibrium concentration of radicals in the temperature range of +60 to −50°C. Figure 2 represents the variation of the equilibrium constant as a function of temperature in log K and 1000/T coordinates. Calculation by the method of least squares gives the following value for log K:

$$\log K = 4.944 - 11200/4.5676T \text{ (K in mole/liter).}$$

The values of the equilibrium constant and of ΔH (11.2 kcal) are in very good agreement with the values determined by other methods [2]. The constant of the recombination rate of radicals can be calculated by integrating Eq. (1) or directly from Eq. (1), determining d[R]/dt by graphic differentiation of the kinetic curves. The second method is more convenient since it makes it possible to avoid indeterminancy in the choice of the initial concentration $[R]_0$ related to the decrease in the temperature at the first moment of the reaction. The fact that the reaction constant remained constant was taken as the criterion of the exactness of the kinetic equation (1) and as proof that the temperature remained constant during the reaction. Figure 3 represents the variation of the constant of the depolymerization rate as a function of temperature. It can be seen that the Arrhenius relationship holds very well. The rate constant is described by the following formula:

$$k_2 = 3.85 \cdot 10^7 \, e^{(-6950 \pm 500)/RT} \text{ (liter} \cdot \text{mole}^{-1} \text{ sec}^{-1}).$$

Thus, the result of direct determination of the depolymerization constant of triphenyl radicals was confirmed not only by the fact of the presence of activation energy in this reaction but also its value, equal to the difference between the activation energy of dissociation and the energy of the rupture of the bond C−C of hexaphenylethane.

Let us note that in spite of a considerable inertness of the $(C_6H_5)_3C$ radicals, which distinguishes them from other types of radicals − alkyl, for example − the value of the activation energy of depolymerization fits satisfactorily into the general relationship between the activation energy and the heat effect of the reaction: $E = 11.5 - 0.25\,Q$ [3], which is the case for the majority of radical reactions.

We express our thanks to V.V. Voevodskii, Corresponding Member of the Academy of Sciences USSR, for his interest in this work.

LITERATURE CITED

[1] K. Ziegler, A. Seib, et al., Ann. Chem. 551, 153 (1942); K. Ziegler, Trans. Faraday Soc. 30, 13 (1934).

[2] K. Ziegler and L. Ewald, Ann. Chem. 473, 163 (1929); E. Müller, J. Müller-Rodloff and W. Bunge, Ann. Chem. 520, 235 (1935); 521, 89 (1936).

[3] N.N. Semenov, Some Problems of Chemical Kinetics and Reaction Capacity [in Russian] (Moscow, 1954).

Institute of Physical Chemistry,
Academy of Sciences, USSR

Received May 14, 1958

GERMANIUM ELECTRODE WITH A p-n JUNCTION

E.A. Efimov and I.G. Erusalimchik

(Presented by Academician A.N. Frumkin, May 23, 1958)

It has been shown earlier [1, 2] that the process of anodic dissolution of germanium depends on the concentration of holes on the surface of the semiconductor. In connection with this result it appeared to be of interest to investigate the behavior of a germanium electrode with a p-n junction, which would allow us either to inject holes or to create areas impoverished in carriers.

In the present work we have made experiments using plates of germanium with electron type conductivity, with a specific resistance of 20 ohm · cm and a diffusion length of 1 mm. The original thickness of the plate was 250 μ. A p-n junction with a total area of about 0.04 cm^2 was created on one side of the plate by melting a piece of indium into the plate. An ohmic contact ring (base ring) was welded onto the same side of the electrode. The whole germanium plate and terminals was insulated with a silicone lacquer except for an area equal to the area of the p-n junction and opposite it. The electric circuit allowed us to measure the potential of the electrode at different current densities either when an inverse voltage was applied to the p-n junction or when the external circuit of the junction was open. All the tests were made in a 0.1-N HCl solution at 20°C in nitrogen atmosphere.

Figure 1 represents the polarization curves for the process of anodic dissolution of germanium obtained for current densities in the range of 10^{-6}-10^{-2} a/cm^2 for different ways of connecting the p-n junction in the circuit. Curve 2 shows the variation of the potential of the germanium anode when the positive pole of the source of current is connected to the ohmic contact ring and the external circuit of the p-n junction (between the base contact ring and the indium) is open. For current densities of about $3 \cdot 10^{-3}$ a/cm^2 this curve is displaced toward more positive values of the potential because the number of holes on the germanium surface becomes insufficient when the rate of the anodic process is high [2]. If an inverse voltage of 30 volts is applied to the p-n junction located on the opposite side of the plate, the polarization curve coincides with curve 2. This phenomenon is observed only for plates whose thickness is greater than 100 μ.

Since the rate of anodic dissolution of germanium is limited by the number of holes arriving on the surface of the semiconductor per unit time [1, 2], one would expect that any injection of holes into germanium would lead to decrease of the polarization of the electrode reaction. Curve 1 of Fig. 1 was obtained by connecting the positive pole of the source of the current, not to the base contact ring, but to the indium, i.e., to the p-region of germanium. Here the p-n junction is connected in the circuit in the direction of the current and injects holes toward the germanium-electrolyte separation line. These holes are consumed during the electrochemical reaction and increase the rate of the process of anodic dissolution of germanium. Therefore, the electrode reaction will proceed in this case almost at the same rate as in the case of p-type germanium. This explains the fact that curve 1 is almost identical to the analogous curve obtained for the process of anodic dissolution of the p-type germanium in our previous work [2].

Curve 3 was obtained with the same electrode as curve 2 but the thickness of the germanium plate was decreased down to 25 μ by chemical etching. The positive pole of the source of the current was connected to the base while the external circuit of the p-n junction was open. Under these conditions the process of anodic dissolution of germanium proceeds with higher polarization than in the case of thick germanium plates when $I > 10^{-3}$ a/cm^2 (curve 2). This phenomenon is due to the decrease of the number of holes generated in the whole volume of the semiconductor because of the decrease of geometric dimensions of the electrode.

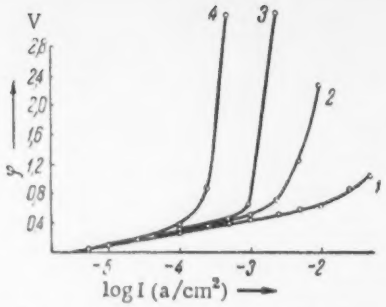

Fig. 1. Polarization curves for germanium electrode with a p-n junction. The explanations are in the text.

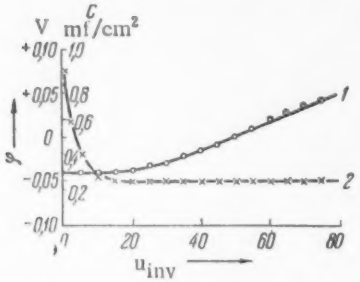

Fig. 2. Variation of capacitance and potential of the germanium electrode as a function of the inverse voltage applied to the p-n junction. Explanations are in the text.

If an inverse voltage of 30 volts is applied at the same time to the p-n junction of such electrodes, the curve $\varphi - \log I$ (Fig. 1, 4) will cease to be linear at high values of the potential and low current densities ($I \approx 10^{-4}$ a/cm^2). When the inverse voltage is applied to the p-n junction the width of the zone impoverished in carriers increases. This further decreases the volume of the semiconductor within which are generated the holes absorbed during the anodic reaction; this cannot fail to affect the value of the saturation current. It must be underlined that this effect is observed only with very thin plates.

The width of the impoverished layer of the volume charge for the welded p-n junction [3] is equal to:

$$D = \sqrt{2\varepsilon\mu\rho u_{inv}}, \qquad (1)$$

where ϵ is the dielectric constant, μ the mobility of the fundamental current carriers, ρ the specific resistance of germanium, and u_{inv} is the inverse voltage.

It follows that the increase of the value of u_{inv} can widen the region of the volume charge so much that it will extend to the surface of germanium in contact with the electrolyte. In order to follow the behavior of the electrode under these conditions we measured its potential (Fig. 2, 1) and its capacitance at a frequency of 5000 cps (Fig. 2, 2) for different values of inverse voltage on the p-n junction. The experiments were performed in a 0.1-N HCl solution on a germanium plate 25 μ in thickness. No external voltage was applied to the electrolytic cell.

Figure 2 shows that when u_{inv} is increased up to 15-20 volts the capacitance of the electrode drops rapidly and then becomes constant. The potential of the electrode, on the contrary, remains constant up to u_{inv} = 15-20 volts and then slowly increases. This shape of the curve is due to the fact that the volume charge of the p-n junction reaches the separation line germanium-electrolyte when $u_{inv} \approx$ 15-20 volts. In fact, according to Eq. (1), when u_{inv} = 20 volts and ρ = 20 ohm · cm, the width of the volume layer is ~20 μ, which corresponds to the thickness of the n-layer of germanium in the electrolyte used.

The decrease of the capacitance with the increase of the width of the volume charge up until it reaches the surface of the electrode is apparently due to the increase of the distance between the ionic coating of the layer and the centers of the positive charges on the surface of germanium, due to the fact that the holes are being pulled into the p-n junction. After the volume charge has reached the surface, the impoverished layer, deprived of current carriers, occupies the whole thickness of the plate. In this layer the ionized atoms of donors which cannot change their positions in the lattice are the carriers of positive charges. This is responsible for the fact that the values of the capacitance of the double layer remain constant for inverse voltages higher than 20 volts.

When the volume charge reaches the surface the process of self-solution of germanium is slowed down due to the insufficient number of holes, and the potential of the electrode acquires a more positive value (Fig. 2, 1).

LITERATURE CITED

[1] W. Brattain and C. Gorrett, Bell System Techn. J. 34, 129 (1955).

[2] E.A. Efimov and I.G. Erusalimchik, J. Phys. Chem. (USSR) 32, 413 (1958).

Received May 21, 1958

EFFECT OF CaF_2 ON THE DISTRIBUTION OF PHOSPHORUS IN LIQUID IRON AND IRON LIME SLAG

I.Iu. Kozhevnikov, O.V. Travin and E.N. Iakho

(Presented by Academician G.V. Kurdiumov, May 24, 1958)

From steel industry practice, it is known that the introduction of fluoride into the slag favors the formation of homogeneous slags, increases their fluidity, and consequently increases the rate of the physicochemical processes in the metal-slag system, particularly the process of dephosphorization. However, opinions about the effect of CaF_2 on the distribution of phosphorus are contradictory.

Winkler and Chipman [1] consider that CaF_2 is simply a solvent of the slag and has no significant effect on the equilibrium distribution of phosphorus. On the contrary, Herasimenko and Speight [2] have concluded, on the basis of the results published by Winkler [1], that the introduction of CaF_2 considerably modifies the equilibrium constants of the reaction of phosphorus, assuming that the compounds and the oxides present in liquid slags are completely ionized. To arrive at their conclusions, these authors had to assume that complex anions composed of F^- and PO_4^{3-} are formed in liquid slags. Flud and Griotkheim [3] later showed that this is not the case if one defines the physical model of an ionic solution as two independent solutions of anions and cations pushed within one another, for the calculation of the ionic shares of cations and anions [4].

The purpose of the present work is the investigation of the effect of CaF_2 on the distribution of phosphorus in liquid iron and iron-lime slag.

In molten oxides calcium fluoride gives a singly charged anion F^- ($R_{F^-} = 1.33$ A), whose radius is almost identical to the radius of the oxygen ion ($R_{O^{2-}} = 1.32$ A). Thus, two simple anions of the same size but of different charge are present in slags of the $CaO-FeO-CaF_2$ system. Therefore, the effect of F^- on the distribution of phosphorus is in principle different from the effect of complex anions such as SiO_4^{4-}, PO_4^{3-} and AlO_2^-.

For the present investigation, we used the method of successive saturation [5, 6]; the principle of this method consists in saturating iron at constant temperature with radioactive phosphorus P^{32} introduced into the slag. This method allowed us to: 1) create isothermic conditions for the metal-slag system, 2) determine accurately the state of equilibrium, 3) determine the variation of the phosphorus distribution index L_P with temperature for a slag of constant composition. It can be shown that under these conditions:

$$\frac{d \ln L_P}{dT} = \frac{\Delta H}{RT^2} = \frac{\Delta H^0 - \Sigma \Delta H_{mix}}{RT^2}, \quad (1)$$

where ΔH is the heat effect accompanying the passage of phosphorus from liquid iron into the slag of a given composition, ΔH^0 is the heat effect under standard conditions (between pure substances), $\Sigma \Delta H_{mix}$ is the sum of heat effects accompanying the mixing of phosphorus with molten metal of FeO, P_2O_5 slags.

By integrating Eq. (1) we obtain:

$$\log L_P = \log \frac{I_S}{I_M} = -\frac{\Delta H}{4{,}575T} + B, \quad (2)$$

where I_s and I_M are count rates for the slag and for the metal in equilibrium (imp/min); B is an entropy term numerically equal to the change of the entropy of the reaction during the passage of phosphorus from a 1% phosphorus solution in the metal into a 1% phosphorus solution in the slag. Consequently $B = -\Delta S^0/4.575$.

The change in the values of ΔH and ΔS^0 depends only on the composition of the slag since the solutions of phosphorus in iron up to concentrations of 1% obey Henry's law [7, 8]. This allows us to compare the results obtained for the CaO–FeO–CaF_2 system with the data of thermodynamic functions obtained for the reaction of dephosphorization of iron by iron-lime slags [6], and in this way to determine the pure effect of CaF_2.

TABLE

Designation of slag	Composition of slag in % weight						
	CaO	FeO	Fe_2O_3	CaF_2	P_2O_5	MgO	SiO_2
A	28,0	41,02	21,97	6,00	0,030	—	—
B	35,0	34,80	20,71	9,26	0,040	—	0,10

The variation of $\log L_P$ as a function of the temperature for the slags investigated (see the Table) is represented in Fig. 1. The experimental points follow with sufficient accuracy the straight lines described by the following equations:

$$\text{for slag A} \quad -\log L_P = 20900/T - 9.40; \tag{3}$$

$$\text{for slag B} \quad -\log L_P = 21300/T - 9.25. \tag{4}$$

From these equations and also from this equation:

$$\log L_P = 14000/T - 6.41 + 2.5\, N_{CaO}, \tag{5}$$

which describes the distribution of phosphorus between liquid iron and the slag of the CaO–FeO system [6], one can determine the effect of partial replacement of CaO by CaF_2. The results of this comparison at 1600°C are represented in Fig. 2; one can see that the introduction of CaF_2 in place of CaO decreases the distribution index of phosphorus. In order to explain this fact it is necessary to compare the values of ΔH and ΔS^0 for the passage of phosphorus from iron into the slag in the CaO–FeO, CaO–FeO–P_2O_5 and CaO–FeO–CaF_2 systems.

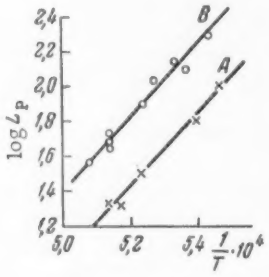

Fig. 1. Variation of $\log L_P$ as a function of 1/T for slags of the CaO–FeO–CaF_2 system: A) 6.0% CaF_2; B) 9.26% CaF_2.

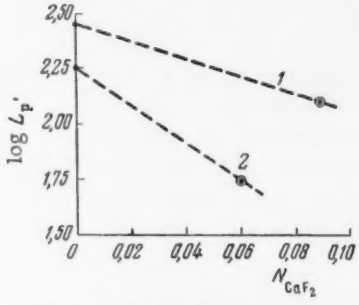

Fig. 2. Effect of partial replacement of CaO by fluoride in slags of the CaO–FeO–CaF_2 system on the distribution index of phosphorus (t = 1600°C): 1) $N_{CaO} + N_{CaF_2} = 0.534$; 2) $N_{CaO} + N_{CaF_2} = 0.452$.

At low phosphorus concentrations the following reaction takes place between iron and the iron-lime slags [6, 9]:

$$2[P] + 5(FeO) + 3(CaO) \rightleftarrows 2(PO_4^{3-}) + 3(Ca^{2+}) + 5[Fe]_{iron},$$
$$\Delta H_6 = -128000 \text{ cal}, \quad (6)$$

the product of this reaction being the phosphate ion. When the concentration of P_2O_5 in the iron-lime slag is higher than 3% either a homogeneous formation of calcium phosphate occurs:

$$2(PO_4^{3-}) + 3(Ca^{2+}) \rightleftarrows (Ca_3(PO_4)_2), \quad \Delta H_7 = -56000 \text{ cal}, \quad (7)$$

or an over-all reaction between iron and the slag of the $CaO-FeO-P_2O_5$ system.

$$2[P] + 5(FeO) + 3(CaO) \rightleftarrows (Ca_3(PO_4)_2), \quad \Delta H_8 = -184000 \text{ cal}. \quad (8)$$

The entropy change in this reaction is equal to −37.5 cal/deg · g-atom. If we compare the values of ΔH_8 and ΔS_8^0 with the change of the heat effect and the entropy occurring during the passage of phosphorus from iron into the slags of the $CaO-FeO-CaF_2$ systems (Fig. 3), equal, respectively, to −96000 cal/deg · g-atom and −42.5 cal/deg · g-atom, we can see that they are similar. Thus, the introduction of CaF_2 into the iron-lime slag decreases the value of L_P due to a sharp decrease of the ΔS^0 value, i.e., strong associations of ions (cations and anions) are created in the molten mass. The coincidence of the ΔH_8 value with the heat effect of the reaction of phosphorus in this case (calculated for 1 g-atom) allows us to assume that calcium phosphate is formed during the reaction (8). In other words, the introduction of CaF_2 into the slag favors the reaction (7) at very low concentrations of P_2O_5 in the slag, i.e., it stabilizes the calcium phosphate. This is due to the fact that the presence of the electrostatically weak fluorine ion decreases the polarizability of the Ca^{2+} cation in microregions of the molten slag containing PO_4^{3-} anions. This is equivalent to the intensification of the mutual reaction between the PO_4^{3-} and Ca^{2+} ions in the molten slag, which leads to the association of these ions into stable groupings even when the concentration of P_2O_5 is very low. In this case a similar grouping of ions can be composed of Ca^{2+}, PO_4^{3-} and F^- ions, whose structure and combination may correspond to the fluorine apatite $Ca_5(PO_4)_2F$ – a magmatic mineral present in igneous rocks [10]. The structure of the molecule of fluor-apatite is more complicated than that of the molecule of calcium phosphate. Correspondingly, the change of entropy during the passage of phosphorus from iron into the slags of the $CaO-FeO-CaF_2$ system is somewhat smaller than that of ΔS_8^0, while the value of the heat effect is greater than ΔH_8.

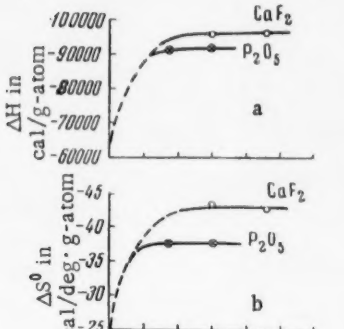

Fig. 3. Effect of the addition of CaF_2 and P_2O_5 to iron-lime slag on the values of the heat effect and entropy of dephosphorization of iron.

Thus, the introduction of CaF_2 into iron-lime slags leads to the formation of strong ionic groupings whose compositions correspond to the chemical combination of fluor-apatite, even at low concentrations of P_2O_5. It has been shown [9] that in molten $CaO-FeO-P_2O_5$, the stable ionic groupings correspond to the molecule of calcium phosphate. In such ionic groupings – molecules – present in liquid slags there operates only the principle of "depersonalization" of cations which basically insure the transfer of current [11, 13]. For example, it was found that in the case of calcium phosphate the conductivity is due to singly charged cations [11]. For $CaO-MgO-Al_2O_3-SiO_2$ the transport number of Ca^{2+} is less than unity and it decreases with the increase of Al_2O_3 concentration since in this case the current can be carried by the Al^{3+} cation [12].

The results obtained allow us to conclude that the theory of actual metallurgical slags, taking into account the description of their physical model, which serves as the basis of further calculation, must stem from the fact that stable groupings of ions whose formulas correspond to definite chemical combinations are formed in molten oxides. Therefore, the reaction must be written in the "molecular form." This considerably facilitates the interpretation of thermodynamic data of metallurgical reactions and simplifies the calculation of the activity of the

components in the slags. Such a model of liquid slags does not contradict the ionic nature of their structure, which has been confirmed by a great number of experimental investigations of electrochemical properties of liquid slags. The chemical compounds (phosphates, silicates) or stable groupings of ions in the slag can be dissociated into cation and complex anions only if the concentration of the acid oxides is very low. However, for actual metallurgical slags such a case is not characteristic. The only exception is fluorspar, which when added to the slag leads to the stabilization of ionic groupings containing PO_4^{3-} at very low P_2O_5 concentrations.

Taking into account the fact that CaF_2 sharply decreases the solubility of P_2O_5 in citric acid, thus decreasing the value of the phosphate slag as fertilizer, its use in the process of refining cast iron containing phosphorus must be considered as unwise. CaF_2 can be used only during the period of pure boiling in an open hearth furnace on the condition that the furnace be completely emptied.

LITERATURE CITED

[1] T.B. Winkler and J. Chipman, Metals Technol. April 13, Techn. Publ. No. 1987 (1946).

[2] P. Herasymenko and G.A. Speight, J. Iron and Steel Inst. 166, p. 4, 289 (1950).

[3] G. Flud and K. Griotkheim, Problems of Modern Metallurgy No. 3, 3 (1953).*

[4] M.I. Temkin, J. Phys. Chem. (USSR) 20, 1, 105 (1946).

[5] V.F. Surov, O.V. Travin and L.A. Shvartsman, Problems of Investigation of Metals and Physics of Metals No. 4, 616 (1955).*

[6] I.Iu. Kozhevnikov and L.A. Shvartsman, Proc. Acad. Sci. USSR 113, No. 2, 376 (1957).**

[7] A.A. Granovskaia and A.P. Liubimov, Collections of Works of Moscow Steel Inst. 32, 79 (1954).*

[8] D.B. Buki, F.D. Richardson and A. Vel, Problems of Modern Metallurgy No. 3, 18 (1953).

[9] I.Iu. Kozhevnikov and I.S. Kulikov, Bull. Acad. Sci. USSR, Div. Techn. Sci. No. 11, 196 (1957).

[10] A.G. Betekhtin, Mineralogy (1950).*

[11] V.I. Malkin and L.A. Shvartsman, Proc. Acad. Sci. USSR 102, No. 5, 961 (1955).

[12] V.I. Malkin and S.F. Khokhlov, Bull. Acad. Sci. USSR, Div. Techn. Sci. No. 3, 108 (1958).

[13] V.I. Malkin, S.F. Khokhlov and L.A. Shvartsman, Int. J. Appl. Rad. and Isotopes 2, No. 1 (1957).

Received May 24, 1958

*In Russian.

**Original Russian pagination. See C.B. translation.

EFFECT OF INORGANIC AND ORGANIC CATIONS ON THE REDUCTION OF THE $PtCl_4''$ ANION BY A DROPPING MERCURY ELECTRODE

N.V. Nikolaeva-Fedorovich, L.A. Fokina and O.A. Petrii

(Presented by Academician A.N. Frumkin, April 17, 1958)

During electrical reduction of some anions, such as S_2O_8'', $FeCy_6'''$, $HgCy_4''$, in dilute solutions one observes a sharp deceleration of the reaction which is due to electrostatic repulsion of anions by the negatively charged surface of the electrode during the passage from positive charges of the surface of the electrode to the negative at the point of zero charge [1]. The increase of the concentration of the supporting electrolyte increases the reaction rate and in some cases the deceleration is completely eliminated. This effect of the supporting electrolyte can be explained by the fact that when the concentration of the cations of the supporting solution increases, the electric field of the negative charges of the surface of the electrode becomes screened and repulsions of anions by the surface of the electrode decreases. The effect of organic cations such as $[(CH_3)_4N]^+$, $[(C_4H_9)_4N]^+$ and tribenzylamine is analogous to the action of inorganic cations and is manifested in the regions of their adsorption potentials [2].

However, different anions have different sensitivities with respect to the effect of additions of a supporting electrolyte [1]. Thus, for example, the addition of a 1 N KCl solution completely eliminated the deceleration of the reduction of the S_2O_8'' anion, while in the case of the reduction of $PtCl_4''$ in the presence of KCl at the same concentration the deceleration of the reaction is unaffected, although in a narrow range of potentials. Therefore, it was of interest to investigate the effect of the most active inorganic and organic cations on electrical reduction of the $PtCl_4''$ anion.

It is known that the effectiveness of cations of the supporting solution on the electrical reduction increases in the following order: $Li^+ < Na^+ < K^+ < Rb^+ < Cs^+$ and $Ca^{++} < Sr^{++} < Ba^{++}$; for example, in the case of electrical reduction of S_2O_8'' the reaction rate increases 40 times when one passes from 0.01-N LiCl to 0.01-N CsCl ($\varphi = -1.0$ volt with respect to the normal calomel electrode) [3]. Figure 1* represents the polarization curves for the reduction of the $PtCl_4''$ anion in the presence of 1-N alkali chlorides. As the figure shows, the addition of the supporting electrolyte leads to the increase of the reaction rate in the whole region of adsorption potentials of the cations of the supporting electrolyte [4]. The reaction rate, as in the case of the reduction of S_2O_8'' depends on the cation of the supporting solution, but even in the presence of 1 N CsCl the deceleration of the reaction is not completely eliminated. The organic cations $[(CH_3)_4N]^+$ and $[(C_2H_5)_4N]^+$ also increase the rate of electrical reduction of $PtCl_4''$. As the concentration of the additional element and the length of the organic chain are increased, for example, in the case of $[(C_2H_5)_4N]^+$, the effectiveness of the organic cations increases (Fig. 2). Organic cations are more effective additional elements than even the most effective of singly charged inorganic cations – Cs^+ – at the same concentration. However, the effectiveness of cations on the electrical reduction of anions is determined not only by their adsorbability but apparently also by the relationship between the dimensions of the cation and the position of the center of the activated complex of the discharging anion. Thus, the $[(C_4H_9)_4N]^+$ cation, which increases the reaction rate of reduction of S_2O_8'' [2] and $HgCy_4''$ [2] in the whole region

*All the figures show only the part of the polarization curve corresponding to negative charges of the surface, since for positive charges one observes strong deformation of the curve by the polarographic maxima.

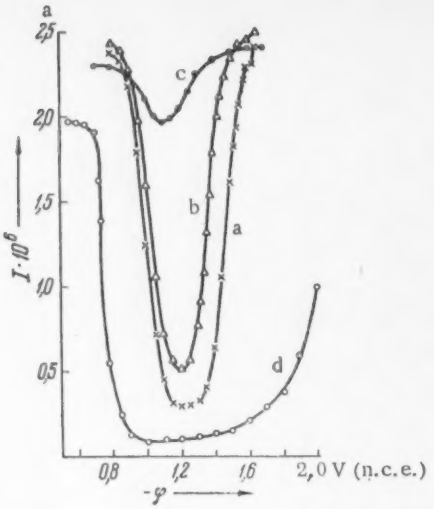

Fig. 1. Polarization curves of reduction of 10^{-3} N K_2PtCl_4 by a dropping mercury electrode with addition of: a) 1-N NaCl; b) 1-N KCl; c) 1-N CsCl; d) no addition.

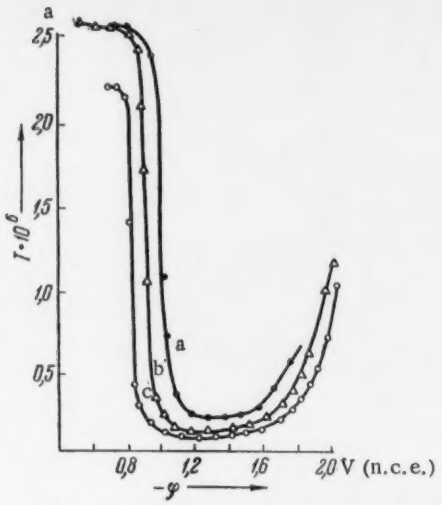

Fig. 2. Polarization curves of reduction of 10^{-3} N K_2PtCl_4 by a dropping mercury electrode with addition of: a) 10^{-3} N $[(C_2H_5)_4N]Br$; b) 10^{-3} N $[(CH_3)_4N]_2SO_4$; c) no addition.

of adsorption potentials of the cation, increases the rate of reduction of the $PtCl_4$" anion only at potentials more negative than −1.2 volts with respect to a normal calomel electrode (Fig. 3). The increase of the rate of the process disappears completely for more negative potentials due to desorption of the organic cation from the surface of the electrode. The potentials at which the accelerating action of $[(C_4H_9)_4N]^+$ on the reduction rate of $PtCl_4$" ceases coincides with the desorption potential determined from the curves representing the variation of the differential capacitance as a function of potential in the case of a mercury electrode [2]. In the region of potentials for which $[(C_4H_9)_4N]^+$ accelerates the rate of the reaction, the polarization curves are deformed by the catalytic wave of hydrogen evolution, which appears in the presence of traces of platinum. For potentials more positive than −1.2 volts, the reduction of $PtCl_4$" is decelerated. The relative deceleration of the reaction becomes more intense when the concentrations of $[(C_4H_9)_4N]^+$ and the supporting solution are increased (Figs. 3 and 4).

This effect of the $[(C_4H_9)_4N]^+$ cation on the reduction of $PtCl_4$" can be explained in the following way: the $PtCl_4$" anion has a flat (square planar) structure and is strongly adsorbed on the surface of mercury. As the result, during the reduction reaction, the electrons pass much closer to the electrode than during the reduction of S_2O_8" and $HgCy_4$" anions. Small, inorganic cations and relatively small, organic cations – $[(CH_3)_4N]^+$, for example – can approach the electrode so closely that the electric field of these cations affects the reduction of $PtCl_4$". The positive charge of the $[(C_4H_9)_4N]^+$ cation, being far from the surface of the electrode, is not effective up to the potential of −1.2 volts. The deceleration of the reaction within this region of potentials is due to the elimination of the accelerating effect of inorganic cations because at these potentials the inorganic cations adsorbed at the surface are pushed out by the tetrabutylammonium cation. The comparison of the polarization curves obtained in 10^{-3} N K_2PtCl_4 + 0.1 N Na_2SO_4 and in 10^{-3} N K_2PtCl_4 + 0.1 N Na_2SO_4 + 10^{-3} N $[(C_4H_9)Na]_2SO_4$ with the $I-\varphi$ curves obtained in the same solutions without the addition of 0.1 N Na_2SO_4 shows that the increase of the concentration of the inorganic cation leads to the increase of the effect of the relative deceleration of the reduction of $PtCl_4$" (Fig. 4). When the concentration of Na_2SO_4 is increased up to 1 N the region of potentials within which the reaction is decelerated remains the same as when 0.1 N Na_2SO_4 is added; however, the deceleration at the minimum of the curve is somewhat less, due to the fact that accelerating action of the inorganic cation starts at this ratio between the concentrations of the tetrabutylammonium cation (10^{-3} N) and the Na^+ (1 N) cation (Fig. 4). If one replaces Na^+ by a larger singly charged cation, Cs^+, for example, the deceleration decreases due to the expulsion of the inorganic cation from the surface of the electrode by the $[(C_4H_9)_4N]^+$ cation. However, this difference between Na^+ and Cs^+ disappears when the concentration of $[(C_4H_9)_4N]^+$ increases, so that when 10^{-3} N $[(C_4H_9)_4N]^+$ is added to the 10^{-3} N K_2PtCl_4 + 0.1 N NaCl and to 10^{-3} N K_2PtCl_4 + 0.1 N CsCl solution the curves $I-\varphi$ for the reduction of $PtCl_4$" completely coincide.

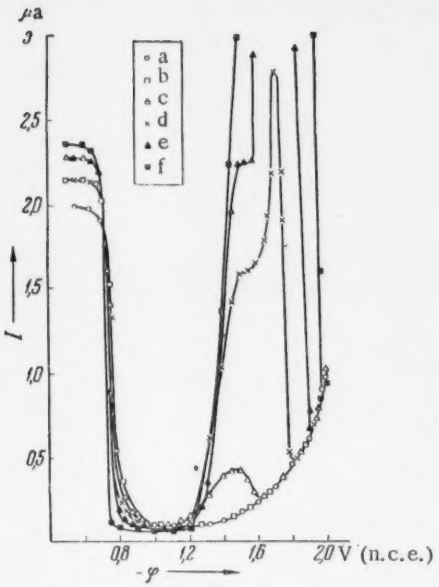

Fig. 3. Polarization curves of reduction of 10^{-3} N K_2PtCl_4 by a dropping mercury electrode with addition of: a) no addition; b) 10^{-5} N $[(C_4H_9)_4N]_2SO_4$; c) 10^{-4} N $[(C_4H_9)_4N]_2SO_4$; d) $5 \cdot 10^{-4}$ N $[(C_4H_9)_4N]_2SO_4$; e) 10^{-3} N $[(C_4H_9)_4N]_2SO_4$; f) $5 \cdot 10^{-3}$ N $[(C_4H_9)_4N]_2SO_4$.

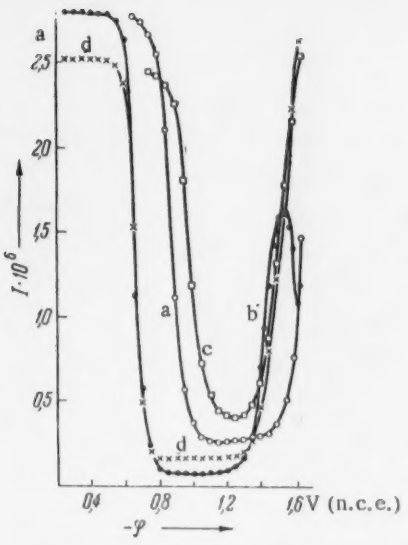

Fig. 4. Polarization curves of reduction of 10^{-3} N K_2PtCl_4 on a dropping mercury electrode with addition of: a) 0.1-N Na_2SO_4; b) 0.1-N Na_2SO_4 + 10^{-3} N $[(C_4H_9)_4N]_2SO_4$; c) 1-N Na_2SO_4; d) 1-N Na_2SO_4 + 10^{-3} N $[(C_4H_9)_4N]_2SO_4$.

The increase of the reaction rate taking place for potentials more negative than −1.2 volts is apparently due to a certain deformation of the $[(C_4H_9)_4N]^+$ cation at the electrode, as the result of which the center of gravity of the charge approaches the surface of the electrode. This is confirmed by the change of the capacitance of the mercury electrode in the presence of the $[(C_4H_9)_4N]^+$ cation: starting from $\varphi = -1.2$ volts, up to the potential for which desorption of $[(C_4H_9)_4N]^+$ takes place, the capacitance increases; this can be due to the deformation of the large organic cation at the surface of the electrode [2]. This explanation is confirmed by the fact that during reduction of the $PtCl_6^{"}$ anion, whose structure is octahedral instead of flat, the $[(C_4H_9)_4N]^+$ accelerates the first stage of the reduction reaction of $PtCl_6^{"}$ in the whole region of adsorption potentials of this cation.

The results on the effect of inorganic and organic cations on electrical reduction of the $PtCl_6^{"}$ anion makes it necessary for us to comment on the work of P. Kivalo and H. Laitinen, who have criticized the theory explaining the anomalous fall of the current on the $I-\varphi$ curves of reduction of anions by electrostatic repulsion of negatively charged particles from the negatively charged surface of the electrode. These authors consider that the reduction of $PtCl_4^{"}$ on a dropping mercury electrode is not an electrochemical process but a purely chemical process: during the first stage of reduction $PtCl_4^{"}$ reacts with mercury, forming Hg_2^{++}, and then Hg_2^{++} is oxidized by $PtCl_4^{"}$ to Hg^{++}, which again forms Hg_2^{++} according to the reaction $Hg^{++} + Hg \rightarrow Hg_2^{++}$. This catalytic cycle is disrupted at more negative potentials because of the rapid electrical reduction of Hg_2^{++}, formed on the surface of the electrolyte during the first stage of the reaction. The incorrectness of the assumption of chemical reduction of $PtCl_6^{"}$ by mercury has already been discussed in the literature [6]. We would like to note that the experimental data we have obtained on the variation of the reduction rate of $PtCl_6^{"}$ as a function of the radius of the cation of the supporting electrolyte and also on the effect of organic cations on this reaction can no longer be explained by the theory put forward by P. Kivalo and H. Laitinen. The fact that the effect of cations on the reduction reaction of $PtCl_4^{"}$ occurs only in the region of adsorption potentials of the organic cation (Figs. 3 and 4) is a direct proof of the correctness of the assumption that the reduction of $PtCl_4^{"}$ is an electrochemical process. These data show that the reduction of $PtCl_4^{"}$ is a surface process and does not occur in the solution.

To conclude, it is our pleasure to thank Academician A.N. Frumkin for his constant consultation and attention to our work.

LITERATURE CITED

[1] T.A. Kryukova, Proc. Acad. Sci. USSR 65, 517 (1949); G.M. Florianovich and A.N. Frumkin, J. Phys. Chem. (USSR) 29, 1827 (1955); T.V. Kalish and A.N. Frumkin, J. Phys. Chem. 28, 473 (1954); A.N. Frumkin and N.V. Nikolaeva-Fedorovich, Bull. of Moscow State Univ., Ser. Math.-Phys.-Chem. No. 4, 169 (1957); S. Siekierski, Roszn. Chem. 30, 1083 (1956).

[2] N.V. Nikolaeva and B.B. Damskin, Conference of the Problems of the Effect of Surface-Active Substances on Electroprecipitation of Metals [in Russian] (Vilnyus, 1957) p. 33; N.V. Nikolaeva-Fedorovich and L.A. Fokina, Proc. Acad. Sci. USSR 118, No. 5 (1957).*

[3] A.N. Frumkin, Progress in Chemistry (USSR) 24, 933 (1955).

[4] D. Grahame, J. Electrochem. Soc. 98, 343 (1951); A.N. Frumkin, B.B. Damaskin and N.V. Nikolaeva-Fedorovich, Proc. Acad. Sci. USSR 115, 751 (1957).**

[5] P. Kivalo and H. Laitinen, J. Am. Chem. Soc. 77, 5205 (1955).

[6] A.N. Frumkin and N.V. Nikolaeva, J. Chem. Phys. 26, 1552 (1957).

M.V. Lomonosov Moscow State University

Received April 7, 1958

*See C.B. translation.

**Original Russian pagination. See C.B. translation.

EFFECT OF OXIDE FILMS AND ADSORPTIONALLY ACTIVE MEDIA ON CREEP OF COPPER WIRE

V.S. Ostrovskii, T.A. Amfiteatrova and B.Ia. Iampol'skii

(Presented by Academician P.A. Rebinder, May 30, 1958)

P.A. Rebinder and his co-workers [1] showed that the adsorption of the outside medium affects the mechanical properties of solids during the process of deformation.

The effect of surface-active substances on metals in process of deformation was studied in nonpolar liquid hydrocarbons; it was shown [2] that these liquids themselves do not affect the mechanical properties of metals during the creep process. Polar media, water in particular, are surface active with respect to some metals; consequently, in order to determine the effect of substances dissolved in these media, one must take into account the effect of the media. Furthermore, if the medium reacts chemically with the metal, forming an oxide film on its surface, for example, these additional products may have a considerable effect on the mechanical properties of the metal.

Roscol and Andrade [3] noted that oxide films formed on monocrystals may strengthen them considerably, increasing the flow limit and rendering further deformation more difficult in the main plastic region when the metal is being stretched at constant rate, or decreasing the rate of plastic flow during the process of stretching under constant load.

Rozhanskii and Rebinder [4] have investigated the role of oxide films in the decrease of resistance to deformation due to adsorption. Likhtman and Ostrovskii [5] have investigated this phenomenon on cadmium monocrystals; they found that the effect of oxide films increases with their thickness and with the decrease of the diameter of the sample, and depends on the orientation of the monocrystal; the maximum effect is produced in the region of angles of initial orientation χ_0 close to 45°. These authors have explained this effect on the basis of the so-called scale factor. Some authors [6] have confirmed the assumption that oxide films of the order of a few-thousand angstroms possess high resistance to rupture, close to the theoretical value.

The presence of such films slows down plastic deformation of monocrystals as long as the load on the sample remains below the value necessary to rupture the brittle oxide film; only beyond this point does displacement along the slip planes of the monocrystal become possible. The calculation of the stress in the oxide film necessary to induce its rupture gives values whose order of magnitude is in agreement with the theoretical values for the resistance of ionic crystals.

Investigations of the effect of oxide films on polycrystalline metals have been made only for thin films, from several microns to tens of microns in thickness [7]. The effect of thin oxide films on the mechanical properties of polycrystals has a special interest. We have shown that the deformation of a polycrystalline copper wire is rendered more difficult in water. Samples of electrolytic copper wire 0.5 mm in diameter were annealed so as to obtain grain sizes (of the order of 0.1 mm) inducing maximum adsorption; they were etched in ammonium persulfate. The stretching was done at constant load below the flow limit on a special apparatus. A more detailed description of the experimental method was given in an earlier work [8].

It was found that when the samples are subjected to deformation in distilled water the initial rate of flow and also the total deformation over a given period of time are considerably lower as compared to the results obtained in air. Figure 1 shows the curves obtained for the creep of copper in air (1) and in water (2). As one can

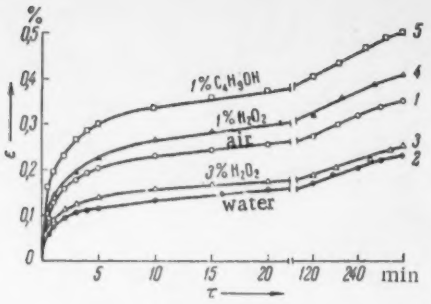

Fig. 1

see, curve 2 is considerably lower than curve 1. When the samples are immersed in water, they become covered with a reddish oxide film several-hundred angstroms in thickness [9]. The formation of the oxide film on the copper surface is apparently due to oxygen from the air dissolved in the water. In fact, when hydrogen is passed through the water, there is no increase of resistance – the curves obtained in air and water coincide. When air is passed through the water, the resistance increases with the period of time during which the air is being passed through the water and reaches a maximum at about 60 minutes.

Rebinder and Venstrem have demonstrated that the resistance of solid metals as well as surface tension decreases at the surface of metal-electrolyte separation as the result of electrocapillarity [11].

V.A. Krongausen has shown in our laboratory that cathodic polarization during the process of deformation of copper eliminates the increase of resistance by removing the oxide film and preventing its formation. Thus, the increase of resistance takes place only in the presence of oxide films; conditions which prevent their formation or eliminate them lead to the disappearance of this phenomenon. Hydrogen peroxide as a more active agent should have a stronger effect, since catalytic decomposition of H_2O_2 with evolution of atomic oxygen takes place on copper. However, because of this active reaction, no continuous film is formed on the metal; instead corrosion occurs and as the result the metal flow even in a 3% H_2O_2 solution is facilitated with respect to its flow in water (Fig. 1, 3). When the H_2O_2 concentration reaches 10%, the curve is above that corresponding to results obtained in air (Fig. 1, 4).

TABLE 1

Medium	v_0	ε_{15},%	$\frac{v_a - v_{H_2O}}{v_{H_2O}}$,%	$\frac{\varepsilon_a - \varepsilon_{H_2O}}{\varepsilon_{H_2O}}$,%	$\frac{v_a - v_{air}}{v_{air}}$,%	$\frac{\varepsilon_a - \varepsilon_{air}}{\varepsilon_{air}}$,%
Air	3,1	0,240				
Water	2,0	0,145			−39,5	−35,5
3% H_2O_2 solution	2,3	0,167	15	15	−30,4	−25,8
10% H_2O_2 solution	3,6	0,287	80	98	+19,5	+16,1
1% C_4H_9OH solution	5,5	0,360	175	148	+50,0	+77,4

Surface-active substances (butyl alcohol for example) which are adsorbed on the metal from an aqueous medium also increase the rate of flow of copper samples with respect not only to their flow in water but also in air (Fig. 1, 5). Table 1 represents the initial flow rate v_0, the magnitude of deformation over a period of 15 minutes ε_{15} (in percent), the value of relative increase (or decrease) of the initial rate of flow and the relative increase (or decrease) of deformation during stretching in active and nonactive media as compared to water and air.

The results show that thin oxide films may have a significant effect on the mechanical properties of monocrystalline and also polycrystalline samples. However, in this particular case, it seems impossible to explain this phenomenon by the increased resistance of thin oxide films since in this case one would have to assume that the stresses leading to the rupture of the oxide films are considerably higher than the theoretical resistance.

The decrease of the creep rate under the effect of thin oxide films can be explained on the basis of the idea of dislocation. During deformation of the samples, the dislocation formed within tends to come out to the surface. The oxide films on the surface prevent this because of the increased potential barrier of closely acting forces repulsing the dislocations from the surface and preventing their outward movement, which is caused by the applied shearing stresses and forces of mirror images. Therefore, the dislocations can reach the surface only under stresses higher than those necessary for metals free of surface oxide films [10]. Not only oxide films but surfaces with modified properties in general, after cold hardening for example, may constitute such barriers. It

seems that the oxide film affects first of all the dislocations created by a source with one fixed edge; such sources are located near the surface and have lower "starting stresses" than sources with two fixed edges. When sources with one fixed edge are blocked, the deformation begins at considerably higher starting stresses of the sources. Under conditions of creep, the retardation of the outward movement of some of the dislocations per unit time signifies the decrease of the rate of flow and the decrease of deformation during a given period of time.

The authors express their gratitude to E.D. Shchukin for his valuable advice during the discussion of the results of this work.

LITERATURE CITED

[1] V.I. Likhtman, P.A. Rebinder and G.V. Karpenko, Effect of Surface-Active Medium on the Processes of Deformation of Metals [in Russian] (Acad. Sci. USSR Press, 1954).

[2] A.B. Taubman and E.K. Venstrem, Third All-Union Conference on Colloidal Chemistry [in Russian] (1956) p. 52.

[3] R. Roscol, Phil. Mag. 21, 399 (1936); E.N. da C. Andrare and C. Henderson, Phil. Trans. Roy. Soc. A, 244, 177 (1951).

[4] V.N. Rozhanskii and P.A. Rebinder, Proc. Acad. Sci. USSR 91, 129 (1953).

[5] V.I. Likhtman and V.S. Ostrovskii, Proc. Acad. Sci. USSR 93, 105 (1953).

[6] J. Beams, J. Breazeale and W. Bart, Phys. Rev. 100, No. 6, 1657 (1955).

[7] L.A. Kochanova and B.Ia. Iampol'skii, Proc. Acad. Sci. USSR 92, 119 (1953).

[8] B.Ia. Iampol'skii and T.A. Amfiteatrova, Physics of Metals and Metal Study 4, No. 1, 131 (1957).

[9] G. Beilby, Proc. Roy. Soc. A 89, 593 (1914).

[10] A.H. Cottrell, Dislocations and Plastic Flow in Crystals (Oxford, 1953).

[11] P.A. Rebinder and E.K. Venstrem, J. Phys. Chem. (USSR) 19, No. 1 (1945); Acta Physicochim. URSS 11, 417 (1944); Proc. Acad. Sci. USSR 68, No. 2 (1949).

M.V. Lomonosov Moscow State University

Received May 9, 1958

ELASTIC PROPERTIES OF DISPERSE SYSTEMS AND THE PHENOMENON OF THIXOTROPY

V.P. Pavlov and G.V. Vinogradov

(Presented by Academician A.V. Topchiev, May 17, 1958)

The shear modulus (g) and the limit of resistance (τ_{lim}) are the most important parameters characterizing the mechanical properties of plastic disperse systems. The measurement of the value of g is of particular importance because the small, relative elastic deformations (γ) under which the measurements are made do not, as a rule, induce significant destruction of the system under investigation.

The measurements were made with an elastoviscosimeter with concentric cylinders [1]. The surfaces forming the concentric clearance had a macroscopic roughness. The field of the shearing stress (τ) was 94% homogeneous. The samples were deformed by rotating a cylindrical core with a constant speed (n) (hard dynamometer) or by twisting an elastic thread connected to the core (soft dynamometer). The modulae of these dynamometers were, respectively, $4.9 \cdot 10^5$ and 29 g·cm/radian. The values of γ are easily determined as the ratio of the linear displacement of the layer of the substance carried with the core and the width of the concentric clearance. The shearing stress acting in the clearance is determined by registering the deformations of the dynamometer. In the experiments described below we have determined the relationship $\tau = f(\gamma)$ and the value of g under static conditions as well as for constant and variable rotation speeds of the core (for small velocities). The experiments were made on different plastic lubricants at 20°C.

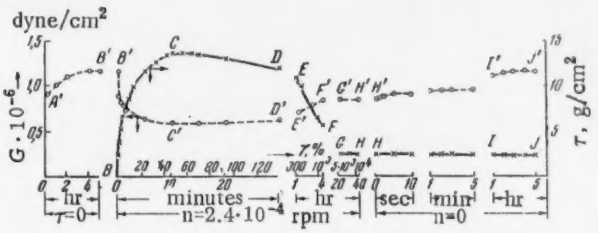

Fig. 1. Variation of shearing stress and shearing modulae as a function of deformation and time of an oily "solid oil."

Curve BC...H in Fig. 1 represents the variation of τ as the function of γ, obtained on a hard dynamometer, for an oily "solid oil" when $n = 2.4 \cdot 10^{-4}$ rpm. Since the different processes under investigation proceed at different speeds, they are represented on different time scales. Taking this into account, and also considering the fact that some processes are very slow, the curves represented in Fig. 1 are discontinuous; intervals in the curves correspond to the passage from one time scale to another or to a certain period of time during which the test was continued but no measurements were made. The segment GH of the curve $\tau = f(\gamma)$ corresponds to the time during which a stationary state of flow of the system and equilibrium shear stress (τ_{equil}) are being achieved with the core rotating at the indicated speed. After 40 hours (point H on curve BC...I) the core was stopped and the system left under stress. Since the pseudo-gels have a low relaxation capacity and the thixotropic regeneration of the oily "solid oil" is rapid, only a small drop of stress occurs in the HI region of the BC...I curve.

The shear modulae of an oily "solid oil" measured immediately after the apparatus was filled, during the process of relaxation in the apparatus, and during testing, are represented in Fig. 1 by the curve A'B'...I'. In these experiments the origin of the time measurement is taken as the moment the elastoviscosimeter is filled with the oil. Section A'B' of the curve A'B'...I represents the relaxation of the "solid oil" during which thixotropic regeneration of the lubricant and the growth of the value of g occur. The value of g was determined during the process of continuous deformation of the system [to which corresponds curve $\tau = f(\gamma)$]; curve B'C'...H' represents the results obtained. The application of stress decreases the shear modulae, which reach minimum values for $\tau = \tau_{lim}$ (point C' of the B'C'...H' curve); after this the value of g slowly increases until the value $\tau = \tau_{equil}$ is reached. From the moment the rotation of the core is stopped (point H' on the curve B'C'...I'), the value of g starts to increase due to the thixotropic regeneration of the structure of the lubricant; five hours after rotation of the core is stopped g reaches the value measured at the beginning of the experiment (point B' on the A'B'...I' curve).

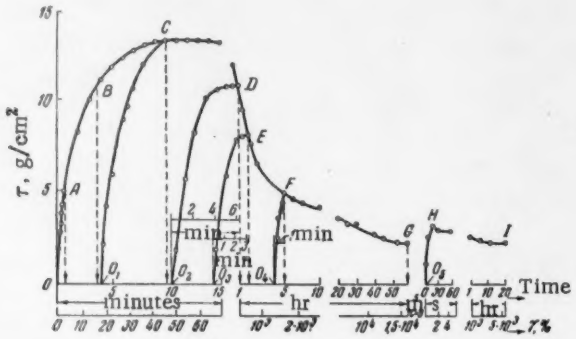

Fig. 2. Variation of shearing stress as a function of deformation for an oily "solid oil" in different successions of tests.

The modulae were measured under continuous slow rotation of the core and also 0.5-1 second after the rotation of the core was stopped (at higher velocities). It was found that with respect to static conditions the values of g decrease by 10% even when n is of the order of 10^{-5} rpm. A seventh-order change of the value of n induces, under the conditions of our experiments, a tenfold decrease of the value of g, while the value of τ_{lim} changes only by a factor of two.

The most important result of the examination of the $\tau = f(\gamma)$ curve, used for the determination of the value of τ_{lim}, is the determination of that stage of the process of deformation of the system, during which the system is destroyed and the resistance to shear undergoes irreversible change. The solution of this problem is clarified in Fig. 2, which refers to the same conditions as in Fig. 1. First the curve OA...G representing the relationship $\tau = f(\gamma)$ is drawn. Then, when τ becomes equal to a certain value τ_A on a new portion of the sample (point A on curve OA...G) the sample is unloaded (dotted arrow descending from point A) and the experiment is started anew. In this, and analogous experiments, the time interval between two consecutive loadings of the sample was five minutes. In the repeated experiment, point O was taken as reference point for measurement of the values of τ and γ; the curve $\tau = f(\gamma)$ coincided with the OA...G curve. A new (third) portion of "solid oil" was measured up to the value of $\tau = \tau_B$, then the load was removed and the experiment repeated. The function $\tau = f(\gamma)$ for this experiment is also represented by curve OA...G. It was shown that investigation of plastic bodies under the condition of continuously increased stresses with $\tau < \tau_{lim}$ does not necessarily induce the lowering of their resistance to shear. The change of the structure of plastic bodies, leading to the decrease of the resistance to shear, starts after the values of τ_{lim} or γ_{lim} (corresponding to τ_{lim}) are reached. In fact, the deformation of a new portion of "solid oil" up to $\gamma = \gamma_C$, then unloading and loading anew, gave the curve $O_1C...G$. In experiments under similar conditions in which samples were not previously deformed to γ_D, γ_E, γ_F, the corresponding curves are represented by O_2D, O_3E, O_4F. For those three experiments, intervals of time during which maximum values of τ are reached (for n = constant) are represented on separate time scales. The results show that preliminary deformation of samples up to $\gamma \geq \gamma_{lim}$ decreases the time necessary to reach τ_{lim} on subsequent experiments.

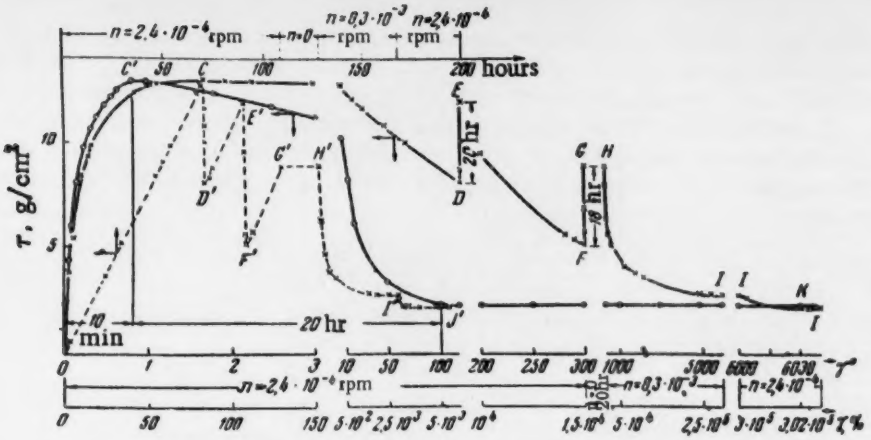

Fig. 3. Variation of the shearing stress as a function of deformation and time for an oily "solid oil" during its test on elastoviscosimeters with hard and soft dynamometers. OC...I – Variation of shearing stress as a function of deformation on a soft dynamometer; OC'K – the same, for a hard dynamometer; OCD'...I' – variation of the shearing stress as a function of time for a soft dynamometer.

The decrease of the resistance limit as the result of deformation for $\gamma > \gamma_{lim}$ occurs for those values of τ lower than those reached in the preceding experiments. Under the conditions of the experiments described, there is no thixotropic regeneration of samples insofar as in each consecutive experiment the (maximum) value of τ reached corresponds to the value of τ reached at the end of the previous experiment. For high degrees of deformation (region FG of the OA...G curve) thixotropic regeneration of plastic bodies takes place after their unloading and relaxation. Thus, after τ_{equil} is reached the load is removed (point G of the OA...G curve) and the sample is allowed to relax five minutes; as the result, one obtains the $O_5H...I$ curve, which has a distinct maximum.

During the process of deformation of plastic bodies the values of $\underline{g}$ and τ_{lim} change differently. Elasticity and resistance to shear are determined by different types of bonds between the particles of the disperse phase; the forces necessary to rupture and re-establish these bonds are different.

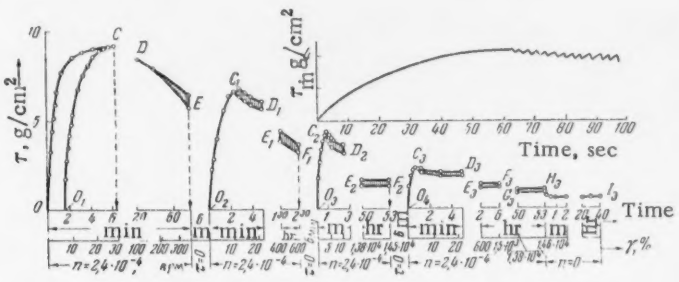

Fig. 4. Variation of the shearing stress as a function of deformation for the plastic hydrocarbon lubricant GOI-54.

Comparison of results obtained with hard and soft dynamometers was very interesting in connection with the discussion between N.V. Mikhailov [2] and A.A. Trapeznikov [3]. This comparison is represented in Fig. 3. The experimental conditions for the hard dynamometer are the same as in the case represented in Fig. 1. The results of the experiment on the soft dynamometer represent the variation of τ as a function of γ and time. For the experiments on the hard dynamometer the time necessary to reach τ_{lim} and τ_{equil} is given.

Figures 1-3 show that τ_{lim} corresponds to high values of γ. In experiments on the hard dynamometer (even for very low values of $\underline{n}$) these values of τ_{lim} are reached very rapidly while τ_{equil} is reached very slowly.

For sufficiently low loading rates, τ is directly proportional to time in the experiments with the soft dynamometer; after the resistance limit is passed, an alternate increase and decrease of the value of τ occurs (broken lines CDEFG and C'D'E'F'G'), and when the value of τ_{lim} is reached very slowly, a considerable increase of deformation (segment CD of the OCD curve) takes place during a short period of time (segment CD' of the broken line OCD'), i.e., rapid destruction of the structure occurs, accompanied by the drop of the value of τ. The segments GH and G'H' correspond to the system under constant load, which, however, is not accompanied by relaxation of stresses in the system.

The present work shows that soft plastic bodies tested on hard and soft dynamometers give real differences of deformation characteristics; they also show that self-induced alternations of the processes of destruction and restitution of structure under low deformation velocities (described for the first time in the literature [4] for aqueous bentonite pastes) and the accompanying jumps of values of τ are of general significance for disperse systems with complex structures.

Depending on the fragility of the system, the jumps in the values of τ during the process of deformation are more or less sharp according to the rate of deformation. Figure 4 represents the results of tests of hydrocarbon plastic lubricant GOI-54, a system more fragile than a "solid oil." The experiments were made on a hard dynamometer. During the first cycle of tests, the OCDE, $O_2C_1D_1E_1F_1$, $O_3C_2D_2E_2F_2$ and $O_4C_3 \ldots I_3$ curves were obtained. After the points E, F_1 and F_2 were reached, the samples were unloaded and were subjected anew to the action of increasing shearing stresses. A small relaxation of stress occurred at point H_3, where the twisting of the core was stopped and the sample remained under load. The curve O_1C was obtained after the value τ_{lim} (point C) was reached. Figure 4 shows that oscillations of the value of τ occur along the dropping branches of the curves of $\tau = f(\gamma)$; the amplitude of these oscillations corresponds to the heights of the hatched areas. The character of oscillations of τ is clearly shown on the upper part of the figure where the $O_3C_2D_2$ curve is represented on a larger scale. The amplitude of oscillations of τ is determined [4] by the competing processes of destruction and regeneration of the structure of plastic bodies.

LITERATURE CITED

[1] V.P. Pavlov, Notes on the Investigations of the Chemistry and Technology of Petroleum and Gas Published During 1956 [in Russian] (Moscow Petroleum Institute Acad. Sci. USSR, 1957) p. 69; V.P. Pavlov and G.V. Vinogradov, Proc. Acad. Sci. USSR 114, 997 (1957).*

[2] N.V. Mikhailov, Colloid J. (USSR) 17, 68 (1955).*

[3] A.A. Trapeznikov, Colloid J. (USSR) 18, 496 (1956).*

[4] N.N. Serb-Serbina and P.A. Rebinder, Colloid J. (USSR) 19, 381 (1957).*

Received May 17, 1958

*Original Russian pagination. See C.B. translation.

EQUILIBRIUM DISTRIBUTION OF DEUTERIUM IN THE HYDROGEN EXCHANGE WITH LIQUID HYDROGEN CHLORIDE

Ia. M. Varshavskii, S. E. Vaisberg, and B. A. Trubitsyn

(Presented by Academician V. A. Kargin June 9, 1958)

The present work represents the first investigation of the deuterium exchange in liquid hydrogen chloride and is devoted to the study of isotopic equilibria in certain systems which include hydrogen chloride.

In previous works we have discovered [1, 2] and analyzed [3] a general rule, which determined the nature of equilibrium distribution of deuterium in isotopic hydrogen exchange reactions and enabled us to predict the value of deuterium distribution coefficient (α) in any system of substances containing hydrogen. The numerous experimental data found in the literature are in good agreement with this rule [3]. The only exception was the value of α for a benzene-hydrogen chloride system [4]; the accuracy of this value, however, was rather doubtful. There were grounds to believe that equilibrium was not attained in the work cited (only direct exchange had been studied), and the obtained $\alpha_{20^\circ} = 1.6$ value was consequently too low. In another, more recent work [5], the experimental determination of deuterium distribution coefficient between aromatic C−H bond in phenol and hydrogen chloride gave a more satisfactory value $\alpha_{50^\circ} = 2.18$. It should be noted that this value was calculated from experimental data on the false assumption that the value of α for the O−H and H−Cl bonds was 1.1. A proper recalculation, however, did not appreciably change this value but gave $\alpha_{50^\circ} = 2.0$. In that work, too, equilibrium was only attained from one side.

Thus, it was interesting to obtain a reliable α value for an isotopic equilibrium between hydrogen chloride and an aromatic C−H bond, and also to compare this value with those of α for O−H and aliphatic C−H bonds, for which there is no experimental data in the literature. We also have to know the respective values in connection with our current investigation of deuterium exchange with liquid hydrogen chloride.

We studied the equilibrium between hydrogen chloride and benzene, cyclopentane, and also water. Experiments were conducted in the liquid phase under pressure; for this we used air-tight ampules with Monel metal or platinum valves ([6], Figs. 3 and 4). After equilibrium was attained, we evaporated the hydrogen chloride, passed the first portion of it through sodium carbonate at 350° [4], and analyzed the water produced after neutralization for deuterium. Evaporation was done very slowly without removing the test tube from the thermostat. On top of this, at the end of exchange experiment we determined the deuterium content in organic substances and water. In experiments with benzene and cyclopentane we burned the hydrocarbons in a stream of hydrogen and determined the isotopic composition of the resulting water. But in experiments with water, after evaporating hydrogen chloride, we neutralized the remaining hydrochloric acid and passed the vapors through sodium carbonate at 350°. In addition to this, we introduced a correction for the difference in deuterium concentration in the original water and hydrogen chloride by titrating to determine their relative contents in the analyzed sample. In all the cases, the isotopic analysis of water was done by the drop method [7].

The isotopic exchange equilibrium was attained from both sides by conducting experiments on direct and reverse exchange (except in the case of cyclopentane). In the isotopic exchange experiments with hydrocarbons aluminum chloride was used as a catalyst. The data obtained are compiled in Table 1.

Despite the fact that experiments were conducted on liquid systems, α values given in Table 1 refer to dissolved (liquid) substance – gaseous hydrogen chloride systems, since at the end of the experiment the deuterium

concentration was determined not in liquid but in the gaseous hydrogen chloride, which was in isotopic equilibrium with the liquid phase. In addition to this, we removed a nelgigible portion of hydrogen chlcride for analysis, just as it was to be evaporated from the ampule. The accuracy of obtained data was ± 5% in α.

Besides a direct experimental determination of α in the water (liquid) – hydrogen chloride (gas) system, its values were also calculated from the spectral data; corrections for the anharmonic vibrations in H_2O, HDO [8], and DCl [9], as well as corrections for the H_2O–HDO vapor pressure ratio [8] were taken into account. The calculated values, $\alpha_{0°} = 2.79$; $\alpha_{25°} = 2.45$; $\alpha_{40°} = 2.32$ agreed well (within the limits of experimental error) with the experimentally determined ones, listed in Table 1. Corresponding exact calculations for systems involving benzene and cyclopentane were not carried out since the literature did not contain corrections for anharmonicity of vibration and vapor pressure ratios of various isotopic forms of these compounds.

TABLE 1

Temperature, °C	Time of exchange (hours)	Initial deuterium concentration, at.%		Final deuterium concentration, at.%		Distribution coefficient α	
		in HCl	in substance	in HCl	in substance		
HCl – water system							
0	6,0	1,10	—	0,80	2,10	2,66	2,65
0	6,0	1,10	—	0,80	1,96	2,48	
0	3,8	—	1,96	0,42	1,14	2,73	
0	4,5	—	1,96	0,43	1,17	2,73	
25	3,2	0,95	—	0,78	1,84	2,38	2,43
25	21,0	1,10	—	0,86	2,04	2,40	
25	22,3	1,10	—	0,97	2,18	2,28	
25	2,5	—	1,96	0,49	1,23	2,52	
25	2,6	—	1,96	0,48	1,23	2,58	
40	2,3	0,95	—	0,70	1,57	2,26	2,34
40	2,1	0,95	—	0,64	1,43	2,25	
40	4,8	1,10	—	0,83	1,81	2,20	
40	4,4	—	1,96	0,50	1,24	2,49	
40	5,1	—	1,96	0,56	1,36	2,48	
HCl – benzene system							
25	3,6	0,95	—	0,52	1,26	2,44	2,47
25	24,0	0,95	—	0,48	1,10	2,31	
25	24,5	1,10	—	0,96	2,27	2,40	
25	20,5	—	1,10	0,29	0,74	2,57	
25	21,0	—	1,26	0,27	0,70	2,61	
HCl – cyclopentane system							
~ 20	530	0,95	—	0,47	1,11	2,38	2,35
~ 20	549	0,95	—	0,49	1,10	2,26	
~ 20	771	1,10	—	0,60	1,44	2,42	

The data obtained indicate that the values of α (at a fixed temperature) in the isotopic exchange between hydrogen chloride and compounds containing O–H, as well as aromatic or aliphatic C–H bonds, are the same for all practical purposes. This fact, and also the amount by which α exceeds unity are in full accord with the general rule for the equilibrium distribution of deuterium [1-3].

We discovered in this work a hydrogen exchange which deserves a special attention; it takes place with a saturated hydrocarbon that does not contain any tertiary carbon atoms (for this we used cyclopentane) in the presence of $AlCl_3$ in a liquid hydrogen chloride medium (as well as in solutions of $AlBr_3$ in HBr and BF_3 in HF [10]).

The comparative ease with which hydrogen exchanges between hydrocarbons and liquid hydrogen chloride points to its possible use (together with other liquid hydrogen halides [11, 12]) as a medium for investigating the reactivity of organic compounds in electrophilic substitution reactions by the method of deuterium exchange. Currently we are conducting research along this line.

LITERATURE CITED

[1] Ia. M. Varshavskii, S. E. Vaisberg, Proc. Acad. Sci. 100, 97 (1955).

[2] Ia. M. Varshavskii, S. E. Vaisberg, J. Phys. Chem. 29, 523 (1955).

[3] Ia. M. Varshavskii, S. E. Vaisberg, Prog. Chem. 26, 1434 (1957).

[4] A. Klit and A. Langseth, Zs. Phys. Chem., A, 176, 65 (1936).

[5] H. Hart, J. Am. Chem. Soc., 72, 2900 (1950).

[6] Ia. M. Varshavskii, M. G. Lozhkina, J. Phys. Chem. 31, 911 (1957).

[7] A. I. Shatenshtein, Ia. M. Varshavskii, J. Anal. Chem. 11, 746 (1956).*

[8] I. Kirschenbaum, Heavy Water (IL, 1953) [Russian Translation].

[9] H. C. Urey, J. Chem. Soc., 1947, 562.

[10] Ia. M. Varshavskii, S. E. Vaisberg, M. G. Lozhkina, J. Phys. Chem. 29, 750 (1955).

[11] A. I. Shatenshtein, V. R. Kalinachenko, Ia. M. Varshavskii, J. Phys. Chem. 30, 2094 (1956).

[12] Ia. M. Varshavskii, M. G. Lozhkina, A. I. Shatenshtein, J. Phys. Chem. 31, 911, 1377 (1957).

L. Ia. Karpov Physicochemical Institute

Received June 9, 1958

*Original Russian pagination. See C.B. translation.

THERMODYNAMIC PROPERTIES OF Cu–Ni AND Fe–Co SOLID SOLUTIONS

Corresponding Member Acad. Sci. USSR Ia. I. Gerasimov, A. A. Vecher, and V. A. Geiderikh

The interest in the thermodynamic properties of copper-nickel and iron-cobalt alloys is connected with their various technical applications. From the electromotive forces (e.m.f.) we determined the free energy, heat, and entropy of formation of Cu–Ni alloys as well as the activity of iron in Fe–Co alloys.

E.m.f. measurements on Cu–Ni alloys were carried out in this voltaic cell,

$$\text{Cu (solid)} \mid \text{Cu}^{+} \text{ (fused) (CuI + KI + NaI)} \mid \text{Cu–Ni (alloy).}$$

The alloys were prepared from powdered copper and nickel by compression and subsequent annealing (up to 100 hours at 1050-1250°C). Current outlets were made of tungsten or molybdenum wires; the experiment was carried out at 620-750° in an argon atmosphere. After the experiment the alloys were analyzed.

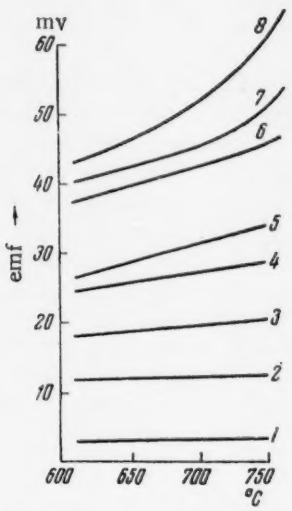

Fig. 1. Electromotive forces of copper-nickel alloys as a function of temperature.
Values of N_{Cu}: 1) 0.93; 2) 0.780; 3) 0.663; 4) 0.568; 5) 0.483; 6) 0.282; 7) 0.191; 8) 0.104.

Experimental results are shown in Fig. 1. The e.m.f. values were quite constant and reproducible within 1.5-2%; from the e.m.f. and its temperature dependence we determined for each alloy the activity (a_{Cu}), relative partial molar heat content L_{Cu}, and the partial molar entropy of mixing for copper (ΔS_{Cu}). Subsequently, by graphically intergating equation

$$g = N_{Ni} \int_0^{N_{Cu}} \bar{g}_{Cu} d \frac{N_{Cu}}{N_{Ni}} \qquad (1)$$

we determined the integral heats and entropies of formation for the alloys in this system. Excess entropy of mixing was calculated according to formula

$$\Delta S^{excess} = \Delta S + R(N_{Ni} \ln N_{Ni} + N_{Cu} \ln N_{Cu}) \qquad (2)$$

and excess free energy at 1000°K according to

$$\Delta Z^{excess} = \Delta H - T\Delta S^{excess}. \qquad (3)$$

The course of activity change for both components is shown in Fig. 2, integral excess values in Fig. 3. Our experimental data for the activity coefficient (γ_{Cu}) and relative partial molar heat contents of copper (L_{Cu}) at 1000°K can be approximately expressed by the following equations, determined by the method of least squares,

$$\lg \gamma_{Cu} = -0{,}016\, N_{Ni} + 0{,}696\, N_{Ni}^2,$$
$$\bar{L}_{Cu} = -1824\, N_{Ni} + 4440\, N_{Ni}^2.$$

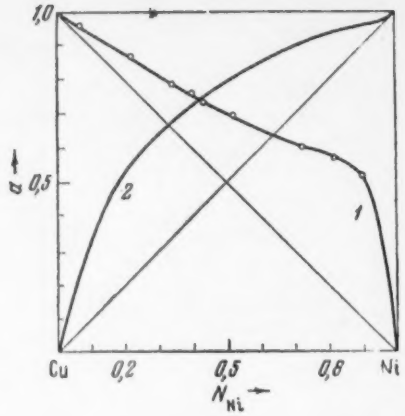

Fig. 2. Changes in the activities of copper (1) and nickel (2) in copper-nickel alloys at 1000°K – experimental data.

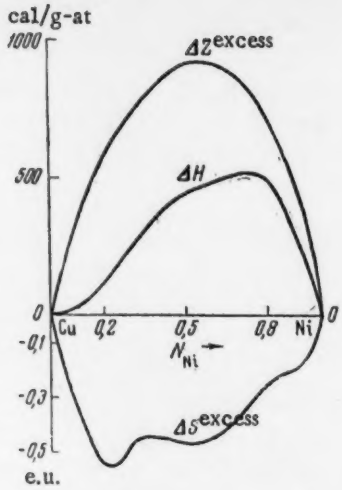

Fig. 3. Heat, excess entropy, and excess free energy of formation for Cu–Ni alloys at 1000°K.

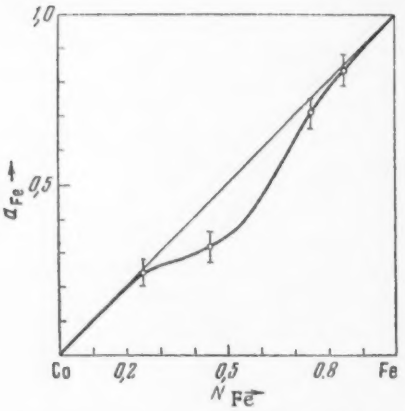

Fig. 4. Change in the activity of iron in cobalt-iron alloys at 1000°K.

Cu–Ni system forms a continuous series of solid solutions [1]. Wagner [2] considers the deviations from ideality small, so that the Cu–Ni system constitutes an exception; for the remaining systems, formed by Cu, Ag, and Au with Fe, Co, and Ni, either do not give solid solutions at all or give solutions which decompose at lower or higher temperatures. On the contrary, it is evident from our data that the Cu–Ni system still exhibits appreciable positive deviations from Raoult's law, though to a lesser extent than Au–Fe [3] and Au–Ni [4] systems. However, excess entropies of mixing for Cu–Ni alloys are negative (see Fig. 3) in contrast to Au–Fe and Au–Ni alloys, which have positive excess entropies of mixing of the order of 1-1.5 e.u./g-at. [3, 4].

The orderly distribution of atoms in Cu–Ni alloys cannot be established by X-ray investigation, since the difference in diffractive powers of copper and nickel is very small. However, the electrical resistance measurements and magnetic properties of copper–nickel alloys [5-7] indicate definite orderliness. Ignoring the question of the extent of orderliness or the composition of alloys showing it, let us note that this orderliness is probably connected with the interaction between free (valence) electrons in copper and nickel. Heat of alloy formation (connected with this interaction), calculated by Varley's method [8], was −0.6 kcal/g-at. for an equiatomic alloy at temperatures from 0-300°K. Consequently, orderliness in Cu–Ni alloys is quite probable. However, according to our data, heats of formation for Cu–Ni alloys are slightly positive. This is very probably caused by a disorganization in the alloy at the experimental temperature,(a lattice deformation) produced when the alloy is formed from components with differing atomic dimensions, and by an increase in volume of Cu–Ni alloy on mixing [9].

Constantan (N_{Cu} = 0.6) entropy calculated from heat capacity [10] was $S_{289°}$ = 7.43 e.u./g-at., whence the excess entropy of mixing came out to be of the order of −1.5 e.u./g at.; thus, the value of excess entropy of mixing gives a strong indication of an orderly arrangement in Cu–Ni alloys. According to our data, $\Delta S^{excess}_{1000°}$ = −0.5 e.u./g-at. for an alloy of corresponding composition. Probably, at higher temperatures a disarrangement takes place in the alloy, and the absolute value of the excess entropy of mixing decreases.

Thus, large negative excess entropies when subtracted from comparatively small positive heats in (3) give positive excess free energies.

It may be seen in Fig. 1 that e.m.f. does not increase linearly with temperature (as is common), but more rapidly. Hence, it follows that: 1) positive deviations from Raoult's law rapidly decrease with increase in temperature; 2) heat and entropy of formation of copper-nickel alloys depend on the temperature (which was already noted before).

It is obvious that further research on the structure of copper-nickel alloys is necessary.

E.m.f. measurements on iron-cobalt alloys were carried out in a cell,

$$Fe\ (solid)\ |\ Fe^{\cdot\cdot}\ (in\ molten\ chloride\ salts)\ |\ Fe-Co\ (alloy)$$

at 650-900°C. In these experiments, the reproducibility of e.m.f. measurements was not too good (about 10%), since e.m.f. would decrease with time, probably due to the reaction

$$Fe^{-}\ (electrolyte) + Co\ \ (alloy) \rightarrow Co^{-}\ (electrolyte) + Fe\ (alloy).$$

Results obtained for the activity of iron in $Fe-Co^{-}$ alloys are compiled in Fig. 4 and agree fairly well with the data [11] obtained by the determination of equilibrium constants.

LITERATURE CITED

[1] M. Hansen, Structures of Binary Alloys (Moscow, 1941) [Russian translation].

[2] K. Wagner, Thermodynamics of Alloys (Moscow, 1957) [Russian translation].

[3] L. L. Siegle, J. Metals, 8, 91 (1956).

[4] L. L. Siegle, B. L. Averbach and M. Cohen, J. Metals, 4, 1320 (1952).

[5] N. V. Grum-Grzhimailo, Bull. Phys. Chem. Anal. Sec. 19, 531 (1949).

[6] N. V. Grum-Grzhimailo, Bull. Phys. Chem. Anal. Sec. 23, 101 (1953).

[7] K. Torkar and H. Mariacher, Planseeber. Pulvermet., 3, 78 (1955).

[8] J. H. O. Varley, Phil. Mag., (7), 45, 887 (1954).

[9] N. P. Allen, J. Inst. Metals, 51, 233 (1933).

[10] A. Eucken and H. Werth, Zs. anorg. Chem., 188, 152 (1930).

[11] T. Satow, S. Kachi and K. Iwase, Sci. Rep. Res. Inst. Tohoku Univ., A, 8, 502 (1956).

M. V. Lomonosov Moscow State University

Received July 1, 1958

THREE-CENTER ORBITALS IN THE STRUCTURE OF CYCLOPROPANE AND OTHER THREE-MEMBERED RING COMPOUNDS

M. E. Diatkina and Corresponding Member Acad. Sci. USSR Ia. K. Syrkin

The idea that three-center orbitals (containing the atomic orbitals of three atoms) may have a real existence in molecules arose in connection with the problem of structure of borohydrides and other electron-deficient compounds, which did not fit within the frame work of usual (localized between two atoms) chemical bond representations [1]. Similar three-center orbitals are also assumed in π-complexes formed between double bonds and positive ions, which provide the third, vacant orbital (in addition to two atomic orbitals, which form the π-bond [2]). Actually, bonds between a platinum atom and an ethylene molecule in compounds of the Zeise salt type can also be represented as three-center orbitals [3]. These examples, referring to widely differing classes of chemical compounds, indicate that the formation of three-center orbitals is not an unusual phenomenon but is quite widespread among various molecules.

We presume that such orbitals can also exist in many other cases, beside the ones enumerated above, and by introducing three-center orbital representations one may come nearer an explanation for the properties of a series of other molecules. This concerns primarily a number of electron-deficient compounds, formed when a proton combines with molecules whose valences are fully saturated. It is known that the reaction $H_2 + H^+ = H_3^+$ is accompanied by liberation of 70 ± 9 kcal/mole [4], so that a triatomic complex H_3^+ with two electrons can exist. V. L. Tal'roze and co-workers [4] discovered a methonium ion CH_5^+, in which the carbon atom is bonded to five hydrogens; the reaction $CH_4 + H^+ \rightarrow CH_5^+$ liberated 121 ± 9 kcal/mole. For H_3^+ the assumption of three-center orbitals is the only possible and widely accepted one. We presume that a similar situation exists also in CH_5^+. There is hardly any other way to explain the structure of CH_5^+. On the other hand, if three-center orbital representations are used, the difficulties can to a large degree be removed. We assume, that three of the C—H bonds (a CH_3 group) are of the usual covalent two-electron and two-center type.

Besides these bonds the C atom has one more orbital and one electron, while the two attached H atoms have one orbital each, so that a three-center orbital may be formed, which could be both of the central and of the open type (according to Eberhardt's, Crawford's, and Lipscomb's classification [1]) depending on the ratio between $\gamma_{H\cdots H}$ and γ_{C-H} integrals. Within this three-center orbital two electrons are distributed (one from the C atom and the other from one of the H atoms, whereas the other proton has no electron). At the same time the molecule would have structure (I).

In our opinion, apart from electron-deficient compounds, three-center orbitals may be possible in other molecules, especially in the ones containing three-membered rings. It is known that such compounds, as for example, cyclopropane and its analogs have certain characteristic properties, which distinguish them from other alicyclic organic compounds. This is most clearly illustrated by the fact that compounds containing cyclopropane rings display certain similarities to unsaturated compounds. We refer, for example, to addition reactions, as well as to a number of anomalies, which can only be explained by introducing assumptions on the "conjugation" of a

cyclopropane ring with attached double bonds or phenyl groups (just as is done in conjugated diene systems). It seems to us that the existing hypothesis on the structure of cyclopropane, which postulates three C−C σ-bonds directed along the sides of a triangle (with a large deviation from the direction in which the wave functions of corresponding hybridized bonding σ-orbitals have a maximum concentration), can not provide a satisfactory explanation for the anomalies enumerated above. There are indications in the literature that a cyclopropane ring behaves like a double bond and for that reason can be conjugated with other double bonds; however, there is still no apparent physical reason why this conjugation of π-bonds with σ-bonds in a ring should be so much more effective than other cases of σ-π-conjugation. This stimulated a search for other hypotheses, which would be able to better represent the properties of three-membered rings.

The specific configuration of a three-membered ring with 60° angles brings to our mind the possiblity of having in this case three-center orbitals. If we assume that each cyclopropane carbon atom uses two hybridized atomic orbitals to form two C−H bonds, then there will still be left two orbitals for each C atom. The fact that the H−C−H angle equals 120° [5] permits us to assume that hybridization takes place in a plane perpendicular to to the plane of the ring; therefore, for the bonds in the ring there remains one sp^2 hybrid orbital, directed from a carbon atom towards the center of the ring (II) and a π-orbital, located in the plane of the ring and perpendicular to the H−C−H plane. The described σ-orbitals are fully suited to form ordinary three-center orbitals of the

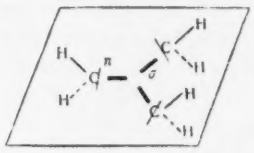

"central" type. Four electrons can be placed in two lowest orbitals (bonding and antibonding). The remaining two electrons can (as we presume) occupy the lower one of the three-center orbitals of the second type, formed from three carbon π-orbitals. Such orbitals are not encountered among borohydrides, but the possibility of their formation appears quite probable. The concern is with the interaction between π-orbitals; their axes are at 120° to each other and located in one plane forming a single molecular orbital, which overlaps all three C atoms along a circumference described around the CCC triangle. We assume, of course, that this interaction is much weaker than the one leading to the formation of a regular three-center σ-orbital of the central type. That is why only one lower three-center orbital seems to be filled. The described π-orbital differs from a regular three-center σ-orbital in that the latter has the electron density concentrated in directions leading from the C atoms to the center of the ring and in the center itself, whereas a three-center π-orbital has the electron density distributed along a circumference, overlapping the triangle formed by C atoms. Such a distribution of electron density differs from the one predicted for cyclopropane on the basis of common ideas about two-center σ-bonds in the fact that with usual bonds the electrons are distributed exclusively along the triangular perimeter, while in the representation we propose a considerable fraction of the electron density to appear not in the perimetric region, but inside the triangle, due to the presence of "central" three-center orbitals filled by four electrons. Evidently, the conugation of a cyclopropane ring with attached double bonds is caused by the presence of a three-center π-orbital, which interacts with the π-orbital of the double bonds. At the same time, it is true that the interacting orbitals are not strictly located in parallel planes (which is generally impossible, if the C−CH=CH_2 or C−Ph bond forms a 60° angle with the plane of the ring). But this, as is known, still is not an obstacle to conjugation [6]. The idea of a conjugated three-center π-orbital is not in conflict with an assumption occasionally put forward, that the conjugation in cyclopropane derivatives is due to a ring "opening", which was represented with the held of such as the following (to be inspected) valence representations:

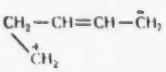

As an inspection of π-complexes indicates [2], such valence representations correspond to (though in a less obvious form) a three-center orbital in the molecular orbital treatment.

The ideas stated should pertain not only to cyclopropane, but also to such analogs of it as ethylene oxide or ethylene imine.

Iron tetracarbonyl $Fe_3(CO)_{12}$ is another example of a molecule which may be based on three-center orbitals. D. A. Brown [7] already showed that the diamagnetism of this compound could only be explained if we assume the existence of Fe—Fe—Fe three-center orbitals. Brown assumed, however, that the molecule has the structure $(CO)_3Fe(CO)_3Fe(CO)_3Fe(CO)_3$, and the three-center orbitals assumed by him were of the "open" type. It has since become known that the molecule does not have the structure shown above, but contains a triangle formed by Fe atoms [8]. At the same time, it is possible to retain the idea of three-center orbitals as well as the electron distribution given by Brown (which results in diamagnetism), but with orbitals not of the open but of the central type as in cyclopropane.

A probable formation of three-center orbitals in cyclopropane and $Fe_3(CO)_{12}$ give grounds for the assumption that this type of orbitals is encountered more frequently than was previously assumed, particularly among three-membered ring compounds.

LITERATURE CITED

[1] W. Lipscomb, W. Eberhardt and B. Crawford, J. Chem. Phys., 22, 989 (1954).

[2] M. J. S. Dewar, J. Chem. Soc., 1946, 406; 1953, 2885.

[3] M. E. Diatkina, J. Inorg. Chem. 3, 2039 (1958).

[4] E. L. Frankevich, V. L. Tal'roze, Proc. Acad. Sci. 119, 1176 (1958).*

[5] H. H. Gunthard, R. C. Lord and T. K. McCubbin, J. Chem. Phys., 26, 768 (1956).

[6] M. E. Diatkina, S. M. Samoilov, J. Phys. Chem. 22, 1944 (1948).

[7] D. A. Brown, J. Inorg. and Nucl. Chem., 5, 289 (1958).

[8] F. Lawrence and R. E. Rundle, J. Chem. Phys., 26, 1751 (1957).

Received July 7, 1958

*Original Russian pagination. See C.B. translation.

ADSORPTION OF WATER VAPOR ON CRYSTALLINE SILVER AND LEAD HALIDE DUST PARTICLES

N.N. Moskvitin, Academician M.M. Dubinin and A.I. Sarakhov

Aerosols of silver and lead iodides have found a practical application as active crystallization centers in the formation of artificial rain from supercooled clouds. Formerly, a hypothesis was proposed that the first step in the formation of artificial rain depended on the adsorption of water vapor on AgI and PbI_2 particles, followed by arrangement of adsorbed molecules into normal ice structure [1-4]. In the opinion of the authors, disturbance of phase equilibrium in the supercooled cloud leads to a rapid crystallization of water vapor and precipitation. Efforts to establish a connection between adsorption properties and the ability of AgI and PbI_2 particles to act as crystallization and condensation nuclei were unsuccessful [4, 5]. This could partially be explained by the fact, that the experimental isotherms for the adsorption of water on hexagonal crystals, such as AgI, PbI_2, et al., which have a lattice similar to that of ice and act as crystallization centers, were not the same, for example, as those for crystals with a cubic lattice, which do not act as crystallization centers (AgCl, CdI_2, et al.). In the present investigation we compared the adsorption isotherms on typical representatives of the above-mentioned crystal groups over a sufficiently wide temperature range.

Water vapor adsorption isotherms were studied with a quartz microbalance [6, 7], which could weigh 1 g with an accuracy of $2.5 \cdot 10^{-7}$ g. In the 10^{-4} to 1 mm of Hg range, the pressure was measured with a Pirani gauge, while for pressures above 0.5 mm of Hg we used a diaphragm manometer with an accuracy of 0.05 mm of Hg. The sample was kept at a constant temperature in a thermostat which could operate in the range of −40° to +60° [8]. The items investigated were spectroscopically pure powders of lead iodide, silver iodide and chloride, with a specific surface of 0.25, 0.2, 0.08 m^2/g, respectively.* The standard preparation of the adsorbents for investigation consisted of initial heating on a balance in vacuo at 110-120° for 8-10 hours. The upper temperature limit was dictated by the fact that at 120° the adsorbents studied still did not undergo sintering or any visible sublimation. Work on AgI and AgCl (substances which undergo photolysis) was carried out in red light. The adsorbents weighed 0.75-0.8 g.

Water adsorption isotherms were measured on AgI and AgCl crystals at 20, 10, 0 and −20°. All the obtained isotherms (type II according to Brunauer's classification) were reversible over the whole measured pressure range and were fully reproducible at all temperatures irregardless of whether or not the samples were preheated before the measurements. Water adsorption isotherms, when plotted in coordinates relative to each adsorbent, practically coincide with each other at 20, 10 and 0°. This means that the heat of water adsorption is close to the heat of condensation.

Water adsorption isotherms on AgI and AgCl can be represented by the polymolecular adsorption equation of Brunauer, Emmet and Teller (BET) in the partial pressure range from 0.05 to 0.4 mm. Using the BET method, we calculated from these isotherms the capacities of statistical monomolecular layers (a_m) and the magnitudes of specific surfaces (see above). Thus, for AgI a_m = 1.32 μmoles/g, and for AgCl a_m = 0.54 μmoles/g. The absolute adsorption isotherms of water on silver iodide and chloride practically coincided. No thick adsorption films were formed on the investigated crystals at temperatures from 20 to −20°. For example, about three monomolecular layers were adsorbed at a partial pressure of 0.8 mm.

*The samples were prepared by precipitation from solutions in the I.I. Angelov Laboratory at the Institute of Pure Chemical Reagents.

At −20° certain peculiarities were observed in the adsorption of water on silver iodide (Fig. 1) and chloride (Fig. 2). These isotherms are drawn through the experimental points and include a correction for the adsorption of water vapor on the glass pan of the balance. The lower isotherms in these graphs were fully reversible if the vapor pressure in the system did not exceed the saturated vapor pressure of ice at −20° (P_s = 0.77 mm of Hg). In our case, the main reason for not getting a pressure over 0.77 mm in the adsorption apparatus was the condensation of excess water vapor on the walls of the balance. Therefore, we called any temporarily artificially produced pressure over 0.77 mm, supersaturation. At a pressure close to 0.77 mm the threshold adsorption value was about 4 μmoles/g on AgI and about 2 μmoles/g on AgCl. When we supersaturated the system, we observed that during the first 15 minutes the adsorbent sharply increased in weight by a few tens of micromoles of water per gram of adsorbent. As the system approached equilibrium, the amount of adsorbed water decreased. The equilibration took 2.5-3 hours, and meanwhile the amount of adsorbed water became the same as the amount normally adsorbed under a water vapor pressure of 0.77 mm (point A in Figs. 1 and 2). After this, the desorption points did not fall any more on the adsorption curve, but fell consistently above (upper curves). The hysteresis loop, formed in this way, was observed every time that supersaturation was produced in the system. Let us note that after supersaturation and subsequent prolonged standing in vacuum at the experimental temperature (−20°), there still remained a certain amount of water (0.6 μmoles/g on AgI and 0.3 μmoles/g on AgCl) held irreversibly on the adsorbent; it could only be removed by pumping at room, or higher, temperatures.

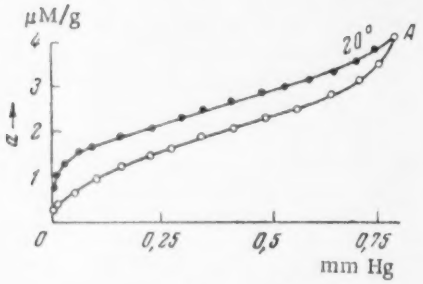

Fig. 1.

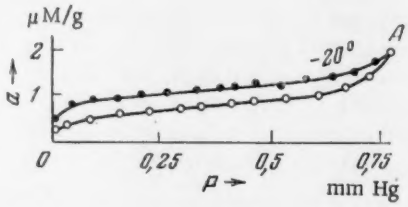

Fig. 2.

The main interest was in the question as to what was the phase composition of water adsorbed on AgI and AgCl at temperatures below 0°. In earlier works [4] an unfounded assumption was made that the water adsorbed on AgI powder at −20° was in the form of ice. We undertook to clarify this problem, and to do this we represented our experimental data in the form of isosteres. In Figs. 3 and 4 we have plotted the respective isosteres for various amounts of adsorption on silver iodide and chloride; these were calculated from isotherms at 20, 10, 0, and −20° (for −20° the reversible adsorption branch was used).

Each isostere in Fig. 3 consists of two straight segments, which intersect at temperatures near 0°. The dotted line in the upper part of the graph represents the function $\log P = f(1/T)$ for water in the solid phase. At 0° the break on this curve corresponds to the melting of ice. The difference in the slopes of the straight segments at the point of phase transition is determined by heat of fusion, equal to 1450 cal/mole. Similarly, it seems, a break on an adsorption isostere could be considered a formal indication that a phase transition took place in the adsorbed water. We think that only a part of the adsorbed water underwent a phase transition, since the heat of adsorption in the second and subsequent monomolecular layers did not approach the heat of fusion for a normal solid phase at −20°. A similar type of isostere could also be explained by the fact that a phase transition probably took place in the first adsorbed layer. Then, the remaining water would be in a quasi-liquid or quasi-crystalline state. One would rather assume that at −20° the water adsorbed on the surface of AgI is in a quasi-crystalline phase, since the field of the adsorbent must strongly orient the polar water molecules so as to produce a two-dimensional ice analog. Such a conclusion would also be supported by the fact that the crystal lattice of silver iodide is almost identical with that of ice.

In Fig. 4 the isosteres, drawn for the adsorption of water vapor on silver chloride, do not have a break. Consequently, the heat of adsorption is practically equal to the heat of condensation at positive as well as negative temperatures. One could naturally assume that at −20° the water was adsorbed on AgCl crystals in the form of a

supercooled liquid. Similar effects, where the liquids were supercooled in an adsorbed state, have been observed before [9-13]. We have already mentioned that, when the experiment is carried out under specific conditions, an unusual hysteresis loop appears at −20°. The presence of desorption branches of the isotherms in Figs. 1 and 2 indicates that at a given pressure the properties of adsorbed water on the adsorption or desorption curves must differ sharply from each other. If we supersaturate the system during the adsorption of water vapor on silver chloride at −20°, then the probability of spontaneous crystallization in the thick adsorption films, that are being formed, greatly increases. This would be all the more correct for silver iodide, since the water adsorbed on its surface is in a quasi-crystalline state. One can present a hypothesis that the difference in the type of isosteres obtained for water vapor on AgI and AgCl (which is attributed to a phase transition in the adsorbed layer which occurs on silver iodide but not on chloride) may have a connection with the different behavior of these aerosols in the artificial seeding of supercooled clouds.

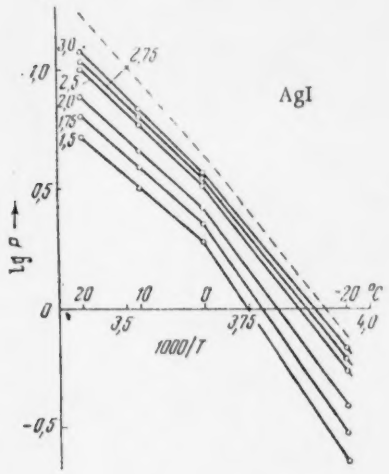

Fig. 3.

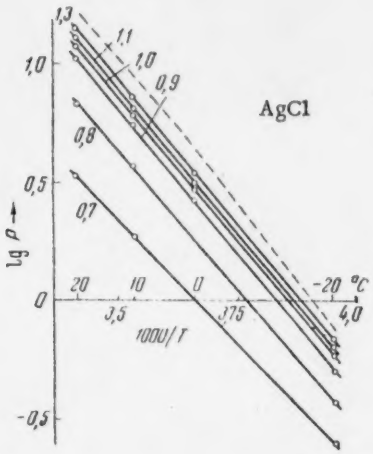

Fig. 4.

In studying the process of water adsorption on lead iodide crystals, we encountered a case where the adsorption equilibrium could not be attained in the system even after 35 days. Most probably it was caused by the fact that another very slow process was finely superimposed on the physical adsorption process. One of such processes, which would complicate the van der Waals adsorption of water on PbI_2, could be hydration. Thus, in the case of water adsorption on PbI_2 we were dealing with a nonequilibrium water-adsorbent system at all the investigated temperatures. That is why we were unable to find any connection between the adsorption behavior of PbI_2 and the ability of its particles to act as crystallization nuclei.

LITERATURE CITED

[1] B. Vonnegut, J. Appl. Phys. 18, 7, 593 (1947).

[2] V. Schaefer, J. Meteor. 11, 417 (1954).

[3] E. Fournier d'Albe, Quart. J. R. Meteor. Soc. 75, 323, 1 (1949).

[4] S. Birstein, J. Meteor. 12, 4, 324 (1955).

[5] L. Coulter and G. Candela, Zs. f. Electrochem. 56, 5, 449 (1952).

[6] B.P. Bering and V.V. Serpinskii, Proc. Acad. Sci. USSR 94, 3, 497 (1954).

[7] A.I. Sarakhov, Proc. Acad. Sci. USSR 112, 3, 464 (1957).*

*Original Russian pagination. See C.B. translation.

[8] M.G. Batrukova, N.N. Moskvitin and A.I. Sarakhov, Zavodskaia Labs. 9, 1149 (1958).

[9] A. Coolidge, J. Am. Chem. Soc. 46, 596 (1924).

[10] J. Jones and R. Gortner, J. Phys. Chem. 36, 387 (1932).

[11] W. Patrick and W. Land, J. Phys. Chem. 38, 1201 (1934).

[12] W. Patrick and W. Kemper, J. Phys. Chem. 42, 369 (1938).

[13] B.N. Vasil'ev, B.P. Bering, M.M. Dubinin and V.V. Serpinskii, Proc. Acad. Sci. USSR 114, 1, 131 (1957).*

Institute of Physical Chemistry
Academy of Sciences, USSR

Received July 3, 1958

* Original Russian pagination. See C.B. translation.

THE EFFECT OF REPLACING HYDROGEN WITH DEUTERIUM ON THE POLARIZABILITY OF MOLECULES

I.B. Rabinovich and Z.V. Volokhova

(Presented by Academician A.N. Frumkin, June 27, 1958)

In a series of works [1, 18] it was shown that gaseous deuterium compounds had smaller polarizabilities than their hydrogen analogs. It was also found, that replacement of hydrogen with deuterium caused a decrease in the polarizabilities of certain liquids: water, hydrogen peroxide [2, 10], benzene, cyclohexane [3], and dibromoethane [4].

In this work we have studied density and the dispersion of light and calculated the electron polarizability (α_0) for twelve liquid deuterium compounds and their hydrogen analogs listed in Table 1. Synthesis of $CDCl_3$ was described in [5], while that of deuteroalcohols in [6]. C_6D_6 and $C_6D_5CH_3$ were prepared as described in [7]. To prepare CD_3NO_2 we repeatedly exchanged nitromethane with a 0.02 M solution of NaOD in D_2O at 110°. The substances were thoroughly purified and dried. Densities (ρ^{20}_4) and refractive indices ($n^{20}D$) of hydrogen compounds agreed with reliable literature data [8] to within $1 \cdot 10^{-4}$ g/cm^3 and $1 \cdot 10^{-4}$, respectively.

Refractive indices were measured in an IPF-23 Pulfrich refractometer with a relative precision of $2 \cdot 10^{-5}$ (at 293±0.05°K) for Hα, D, Hg_z, Hβ and Hg_{s-f} lines. Electron polarizabilities were determined by extrapolating to $\nu = 0$ the $(n^2 + 2)/(n^2 - 1)$ function of ν^2, where ν = frequency of light. As Wulff has shown [9], such an extrapolation is theoretically sound for colorless substances if experimental data in the visible range of light is used. In all the studied substances the above-mentioned function was linear (within the limits of error in measuring n) in the investigated frequency range.

Densities were determined at 5° intervals in the 20-70° range, with an accuracy of $1 \cdot 10^{-4}$ g/cm^3 (for chloroform: 10-40°; for methanol: 10-60°). Molar volumes (V_X) of compounds with x% D were calculated by use of additivity. In Table 1 we have listed only the values of V_X at 20°, but the relative differences in molar volumes of isotopic analogs were the same (to within 0.01%) over the whole indicated temperature range.

All the twelve deuterium compounds studied by us had lower refractive indices and smaller polarizabilities than did the corresponding hydrogen compounds (Table 1).

The lowering in polarizability, when a hydrogen is replaced with deuterium, can be explained by a lowering in the atomic vibrational zero-point energy (ϵ_0), while the electronic potential energy curve and the force constants (f) of the bonds remain practically unchanged [10]. In the simpler case of a diatomic molecule, allowing certain approximations, we can show that a lowering in the vibrational levels of electronic spectra increases the energy of electronic transitions (ϵ_{et}) between the ground (0) and excited (i) levels. Thus, disregarding the difference between the electronic energies of H- and D-compounds in the same level i, and also the difference between rotational energies (its absolute value is small in comparison to the vibrational energy difference), we will get

$$\Delta\varepsilon_{e.t.} = \varepsilon^{0,i}_{e.tD} - \varepsilon^{0,i}_{e.tH} = (\varepsilon_{0,H} - \varepsilon_{i,D})^0 - (\varepsilon_{0,H} - \varepsilon_{0,D})^i. \quad (1)$$

And since, by dropping terms of higher orders we will be left with [10]

$$\varepsilon_{0,H} - \varepsilon_{0,D} = \frac{1}{2}h\omega_{0,H}(1-\zeta) - \frac{1}{4}h\omega_{0,H}\varkappa_0(1-\zeta^2) =$$
$$= \frac{h}{4\pi}\mu_H^{-1/2}f^{1/2}\left(1-\zeta-\frac{\varkappa_0}{2}+\frac{\varkappa_0}{2}\zeta^2\right),$$

where μ is the reduced mass, $\varkappa_0$ is the coefficient of anharmonicity, and $\zeta = (\mu_H/\mu_D)^{1/2}$, then from Eq. (1) we can get

$$\Delta\varepsilon_{e.t.} = \frac{h}{4\pi}\mu_H^{-1/2}[(f^0)^{1/2} - (f')^{1/2}]\left[(1-\zeta) - \frac{\varkappa_0}{2}(1-\zeta^2)\right]. \quad (1')$$

Since $f^0 > f'$; $(1-\zeta)$ and $(1-\zeta^2)$ are positive numbers of the same order, and $\varkappa_0$ is of the order 0.01 [10], then, according to Eq. (1'), we will have .

$$\Delta\varepsilon_{e.t.} > 0 \quad \text{or} \quad \nu_{i,D} > \nu_{i,H}, \quad (2)$$

where ν_i is the electronic transition frequency.

TABLE 1

The Isotope Effect in Electron Polarizability (α_0) and Intermolecular Dispersion Energy (ϵ_d) at 293°K

Substance	D, % atom	nD	V, cm^3/mole	$\alpha_0 \cdot 10^{24}$ cm^3	$\frac{\epsilon_{d,H}-\epsilon_{d,D}}{\epsilon_{d,H}}\times 100$
C_6H_6	0	1,50110	88,87	9,950	0,41
C_6D_6	91	1,49909	88,69	9,896	
$C_6H_5CH_3$	0	1,4968	106,29	11,705	0,47
$C_6D_5CH_3$	76	1,4945	106,18	11,652	
CH_3NO_2	0	1,38166	53,65	4,670	1,00
CD_3NO_2	96	1,37945	53,66	4,640	
$CHBr_2CHBr_2$	0	1,63773	116,42	16,018	0,26
$CDBr_2CDBr_2$	80	1,63631	116,42	15,991	
$CHCl_3$	0	1,44590	80,17	8,258	0,30
$CDCl_3$	98	1,44492	80,19	8,244	
$CH_2OHCHOHCH_2OH$	0	1,47397	73,02	7,751	0,71
$CH_2ODCHODCH_2OD$	96	1,47149	73,13	7,730	
CH_2OHCH_2OH	0	1,43197	55,74	4,473	0,58
CH_2ODCH_2OD	97	1,42994	55,82	4,464	
CH_3OH	0	1,32863	40,48	3,191	0,54
CH_3OD	70	1,32759	40,54	3,186	
C_2H_5OH	0	1,36139	58,36	5,010	0,42
C_2H_5OD	98	1,36060	58,45	5,006	
$CH_3(CH_2)_2OH$	0	1,38542	74,79	6,805	0,37
$CH_3(CH_2)_2OD$	99	1,38445	74,89	6,800	
$(C_3H_3)_2CHOH$	0	1,37758	76,55	6,836	0,36
$(C_3H_3)_2CHOD$	99	1,37672	76,67	6,834	
CH_3COOH	0	1,37200	57,24	5,038	0,43
CH_3COOD	98	1,37090	57,27	5,028	

The results in (2) are probably also accurate for a polyatomic molecule. Evidently, Ingold, Raisin and Wilson [11] are of the same opinion, since to explain the decreased polarizability of benzene, when deuterium replaced hydrogen, they used basically the same type of reasoning (in a more approximate form) as the one we have presented above for a diatomic molecule. Urey and Teal [12] explained the great polarizability of heavy water, as compared with ordinary, by the fact that $\nu_{i,D} > \nu_{i,H}$.

The accuracy of (2) is confirmed by experimental data. Thus, Ingold and Wilson [13] found from the fluorescent spectrum of C_6D_6 and C_6H_6 that $\nu_{i,D}$ is higher than $\nu_{i,H}$ by approximately 200 cm^{-1}. Gero and Schmid [14], on the basis of predissociation phenomena in the CH- and CD-spectra, concluded that the atomic combination energy levels in CD are higher by approximately 350 cm^{-1} than in CH. Frank and Wood [15] estab-

lished that the long-wave absorption limit in D_2O is farther from the violet region than in H_2O and consequently $\nu_{i,D} > \nu_{i,H}$. It was also shown that in methane [16] and ammonia [17] $I_D > I_H$, where I is the ionization potential.

Molecular polarizability can be expressed by the dispersion equation [22]

$$\alpha = \frac{2}{h} \sum \frac{\nu_i P_i^2}{\nu_i^2 - \nu^2}, \tag{3}$$

where P_i^2 is the electronic transition probabilities, ν is the frequency of incident light.

Since the electron clouds of isotopic compounds are identical, $P_{i,D}^2 \approx P_{i,H}^2$. Therefore, according to Eq. (3), for the polarizability α_i in i-th level we will get

$$\frac{\alpha_{i,D}}{\alpha_{i,H}} = \frac{\nu_{i,H} - \nu^2/\nu_{i,H}}{\nu_{i,D} - \nu^2/\nu_{i,D}}. \tag{4}$$

And since $\nu_{i,H} < \nu_{i,D}$, while for colorless substances $\nu_i > \nu$, then it follows from Eq. (4) that $\alpha_{i,D} < \alpha_{i,H}$. And hence it is probable that in general

$$\alpha_D < \alpha_H \tag{5}$$

in agreement with experimental data.

Expanding $(\nu_{i,D} - \nu^2/\nu_{i,D})^{-1}$ into a series and substituting it in Eq. (4), we get

$$\frac{\alpha_{i,D}}{\alpha_{i,H}} = \frac{\nu_{i,H}}{\nu_{i,D}} - \nu^2\left(\frac{1}{\nu_{i,H}\nu_{i,D}} - \frac{\nu_{i,H}}{\nu_{i,D}^3}\right) - \nu^4\left(\frac{1}{\nu_{i,H}\nu_{i,D}^3} - \frac{\nu_{i,H}}{\nu_{i,D}^5}\right) -$$
$$- \nu^6\left(\frac{1}{\nu_{i,H}\nu_{i,D}^5} - \frac{\nu_{i,H}}{\nu_{i,D}^7}\right) - \ldots - \nu^{2n}\left(\frac{1}{\nu_{i,H}\nu_{i,D}^{2n-1}} - \frac{\nu_{i,H}}{\nu_{i,D}^{2n+1}}\right) - \ldots \tag{6}$$

In Eq. (6) all the coefficients of ν^{2n} have the same form, and since $\nu_{i,D} > \nu_{i,H}$ these coefficients are all positive. In view of this, and because all the terms, beginning with the second, on the right side of Eq. (6) have the quantity $(\nu_{i,H}/\nu_{i,D})$ subtracted, the difference between α_D and α_H will increase with increase in ν. This also agrees with the literature and our own experimental data.

For the electron polarizability ($\nu = 0$) we get from Eq. (4)

$$\left(\frac{\alpha_{i,D}}{\alpha_{i,H}}\right)_0 = \frac{\nu_{i,H}}{\nu_{i,D}}. \tag{7}$$

At moderate temperatures, as a consequence of the relation (5), the intermolecular dispersion energy (ε_d) decreases when deuterium replaces hydrogen.* Thus, according to Slater-Kirkwood equation [23],

$$|\varepsilon_d| = \frac{3eh}{8\pi r^6}\left(\frac{n\alpha_0^3}{m}\right)^{1/2}, \tag{8}$$

where n is the total number of electrons in the outer clouds of atoms constituting the molecule, m and e are the mass and charge of the electron, r is the intermolecular distance. To the first approximation $(r_H/r_D)^3 = V_H/V_D$.

$$\frac{\varepsilon_{d,D}}{\varepsilon_{d,H}} = \left(\frac{V_H}{V_D}\right)^2 \left(\frac{\alpha_{0,D}}{\alpha_{0,H}}\right)^{1/2}. \tag{9}$$

*Bell [18] assumes also another approach to the effects of (5). He qualitatively connects (5) with the fact that, as a result of anharmonicity in zero-point atomic vibrations, the increase in the average internuclear distance (relative to its value at the potential curve minimum) is smaller for D-compounds than for H-compounds.

As may be seen in Table 1, the calculations from Eq. (9) show, that among the investigated substances

$$|\varepsilon_{d,D}| < |\varepsilon_{d,H}| \text{ (moderate temperatures).} \quad (10)$$

This can be attributed to the fact, that at moderate temperatures the relative difference in the $\alpha^{3/2}$ values of isotopic analogs is larger than a difference in the V^2 values, so that according to Eq. (9) the $(\epsilon_{d,D}/\epsilon_{d,H})$ ratio will depend on the $(\alpha_{0,D}/\alpha_{0,H})$ ratio.

The result of (10) is in agreement with the fact that replacement of hydrogen by deuterium causes a decrease in the critical temperature [24] (provided it is not in the low-temperature region), and also with the fact that deuterium compounds are more compressible than their hydrogen analogs [6], if we exclude low-temperature regions.

However, at low temperatures the change in the amplitude of zero-point molecular vibration has a pronounced effect on the molar volume. For example, at 19.5°K, V_D of D_2 is 17% smaller than V_H of H_2 [19], while for He^4 and He^3 [20] at 2°K, V_4 is 29% smaller than V_3. In these cases the difference in ϵ_d values of isotopic analogs is (according to [9]) mainly due to the difference in V values, and

$$|\varepsilon_{d,D}| > |\varepsilon_{d,H}| \text{ (low temperatures).} \quad (11)$$

Thus, if we substitute the values of V and α_0 [21] for He^4 and He^3 at 2°K into Eq. (9), then we will get $|\epsilon_{d,4}| > |\epsilon_{d,3}|$ by 45%. It is interesting that the result of this very approximate calculation agrees well with the experimental data on the heats of vaporization of He^4 and He^3 [20]: 22.2 cal/mole* and 11.1 cal/mole, respectively, at 2°K. The result of (11) agrees also with the fact that the critical temperatures of D_2 and He^4 are higher than those of H_2 and He^3, respectively [24].

We are grateful to Prof. L.S. Maiants for giving his appraisal of the results.

LITERATURE CITED

[1] T. Larsen, Zs. Phys. 100, 543 (1936); 105, 164 (1937); 111, 391 (1938); O.E. Frivold et al., Nature 138, 330 (1936); Phys. Zs. 37, 134 (1936).

[2] M.K. Phibbs and P.A. Giguere, Canad. J. Chem. 29, 173 (1951).

[3] J.A. Dixon and R.W. Schiessler, J. Am. Chem. Soc. 76, 2197 (1954).

[4] J. Verhulst and J.C. Jungers, Bull. Soc. Chim. Belg. 58, 73 (1949).

[5] I.B. Rabinovich, P.I. Nikolaev, Z.E. Gochaliev and N.N. Tret'iakova, Proc. Acad. Sci. USSR 110, 241 (1956).

[6] I.B. Rabinovich, V.G. Golov, N.A. Efimova and S.M. Rustamov, Proc. Acad. Sci. USSR 114, 590 (1957).**

[7] I.B. Rabinovich, V.I. Kucheriavyi and P.N. Nikolaev, J. Phys. Chem. 32, No. 2 (1958).

[8] J. Timmermans, Phys.-Chem. Constants of Pure Organic Compounds (New York, 1950).

[9] P. Wulff, Zs. phys. Chem. 21, 368 (1933).

[10] A.I. Brodskii, Isotope Chemistry (Moscow, 1957);*** G. Herzberg, The Spectra and Structure of Diatomic Molecules [Russian translation] (Moscow, 1949).

[11] C.K. Ingold, C.G. Raisin and C.L. Wilson, J. Chem. Soc. 1936, 915.

[12] H.C. Urey and C.K. Teal, Rev. Mod. Phys. 7, 34 (1935).

*This value corresponds to He(I), but in this case it evidently does not matter. As is known, the heat of λ-transformation in liquid helium is insignificant, and between 1.75° and 3.5°K the heat of vaporization changes by 4% only.

**Original Russian pagination. See C.B. translation.

***In Russian.

[13] C.K. Ingold and C.L. Wilson, J. Chem. Soc. 1936, 941.

[14] L. Gero and R. Schmid, Zs. Phys. 118, 210 (1941).

[15] J. Franck and R.W. Wood, Phys. Rev. 45, 667 (1934).

[16] R.E. Honig, J. Chem. Phys. 16, 105 (1948).

[17] H. Neuert, Zs. Naturforsch. 7a, 293 (1952).

[18] R.P. Bell, Trans. Faraday Soc. 38, 422 (1942).

[19] E.C. Kerr, J.Am. Chem. Soc. 74, 824 (1952).

[20] E.C. Kerr, Phys. Rev. 96, 551 (1954); W.H. Keesom, Helium [Russian translation] (Moscow, 1949).

[21] V.P. Peshkov, J. Exptl.-Theoret. Phys. 33, 833 (1957).

[22] M.V. Vol'kenshtein, Structure and Physical Properties of Molecules (Moscow, 1955); Molecular Optics (Moscow, 1951) [In Russian].

[23] J.C. Slater and J.G. Kirkwood, Phys. Rev. 37, 682 (1931).

[24] I.B. Rabinovich and V.A. Gorbushenkov, Proc. Acad. Sci. USSR 120, No. 3 (1958).*

Chemical Institute at N.I. Lobachevskii
Gorki State University

Received June 6, 1958

*Original Russian pagination. See C.B. translation.

EQUILIBRIUM IONIZATION GENERATED BY DUST PARTICLES

Iu.S. Saiasov

(Presented by Academician V.N. Kondrat'ev, June 4, 1958)

As is known, many cases of ionization in carbon flames are basically due to thermal emission of electrons from carbon dust particles, which are usually very homogeneous and are characterized by a mean radius $\underline{r}$ of the order of 10^{-6} cm and a work function $\varphi_0 = 4.35$ ev [1]. Since work functions of charged carbon particles should not differ significantly from φ_0, then at the temperatures we are interested in, the multiple ionization of dust particles may play a significant part, and has to be taken into account in computing the equilibrium concentration of electrons in such systems. Similar calculations have recently been carried out [1, 2] by investigating the infinite series which express the electron concentration in the presence of multiple ionization of particles. In this communication we are presenting a full mathematical solution of the equilibrium ionization problem in systems formed by dust particles, by using the well-studied θ-functions, which enabled us to express the equilibrium concentration of electrons (in a closed form) by an equation whose limiting cases are Saha's equation (accurate at sufficiently low temperatures) and a simple, asymptotic expression found by [1, 2] (accurate at sufficiently high temperatures); the region of intermediate temperatures can also be studied with these functions.

We will assume at first that the particles are identical, and we will introduce the symbols: $\underline{n}$ (cm^{-3}) is the concentration of particles; n_e (cm^{-3}) is the concentration of electrons; n_m^+ (cm^{-3}) is the concentration of positively charged particles + me_0 (e_0 is the charge of the electron, m = 1, 2, . . .); n_m^- (cm^{-3}) is the concentration of negatively charged particles $-me_0$; n_0 (cm^{-3}) is the concentration of neutral particles. The statement of the problem, as put forth below, is in full accord with that used in [2].

Under the conditions that the system be quasi-neutral and the total number of particles be conserved, we can write the following relationships [2]:

$$n_e = \sum_{m=1}^{\infty} m n_m^+ - \sum_{m=1}^{\infty} m n_m^-, \quad n = n_0 + \sum_{m=1}^{\infty} n_m^+ + \sum_{m=1}^{\infty} n_m^-. \tag{1}$$

(Just as in [1, 2], $\underline{m}$ in Eqs. (1) is summed to infinity, since theoretically the particles can have a very large positive or negative charge.)

Equilibrium constant K_m^+ for the single ionization of a particle with charge + $(m-1)e_0$ can be defined by the relationship $n_m^+ = K_m^+ / n_e \cdot n_{m-1}^+$, where [1, 3] $K_m = 2(m_e kT/2\pi h^2)^{3/2} \exp[-\varphi/kT] = K \exp[-(m-1)/2\sigma^2]$, $\varphi = \varphi_0 + (m-1)e_0^2/r$, $K = 2(m_e kT/2\pi h^2)^{3/2} \exp[-\varphi_0/kT]$, $\sigma^2 = rkT/e_0^2$ (T is the absolute temperature, m_e is the mass of electron). The ionization potential of a particle with charge $(m-1)e_0^2/r$, which is evidently valid for spherical and fairly well conducting particles; the statistical weight ratio for the initial and final state of the particle is taken to be one (same as in [1]).

From this it is easy to find a relationship between n_m^+ and the concentration of neutral particles,

$$n_m^+ = r_0 \prod_{i=1}^{m} K_i^+ / n_e = n_0 a^m \exp\left[-\frac{(m-1)m}{2\sigma^2}\right], \quad a = K/n_e.$$

Similarly, by introducing an equilibrium constant for the process of single ionization of a negatively charged particle $-me_0$, $K_m^- = 1/Ke^{-m/2\sigma^2}$, we find a relationship between n_m^- and n_0. $n_m^- = n_0 \prod_{i=1}^{m} K_i^- n_e =$

$= n_0 a^{-m} \exp[-m(m+1)/2\sigma^2]$. Substituting thus determined values of n_m^+ and n_m^- into Eqs. (1), we get the formulas [2]:

$$\frac{n_e}{n} = \frac{\sum_{m=-\infty}^{\infty} m a^m \exp\left[\frac{-m(m-1)}{2\sigma^2}\right]}{\sum_{m=-\infty}^{\infty} a^m \exp\left[\frac{-m(m-1)}{2\sigma^2}\right]}, \quad \frac{n_0}{n} = \frac{1}{\sum_{m=-\infty}^{\infty} a^m \exp\left[\frac{-m(m-1)}{2\sigma^2}\right]}. \tag{2}$$

Applying elementary transformations, we can express n_e/n in the form of elliptic θ-functions. Let us take $\ln a = 2\pi v$. Then,

$$\sum_{m=-\infty}^{\infty} a^m \exp[-m(m-1)/2\sigma^2] = \exp[\pi v + 1/8\sigma^2] \times$$

$$\times \sum_{n=-\infty}^{\infty} \exp[(2n+1)\pi v] \exp\left[-\frac{(n+1/2)^2}{2\sigma^2}\right] = \exp[\pi v + 1/8\sigma^2]\,\theta_2(-iv, \rho),$$

where [4, 5] $\theta_2(x,\rho)$ is an elliptic θ-function, $\theta_2(x,\rho) = \sum_{-\infty}^{\infty} q^{(n+1/2)^2} \exp[(2n+1)\pi x i]$, $q = e^{-\pi\rho}$ i.e., here $\rho = 1/2\pi\sigma^2$. From this we get

$$\frac{n_e}{n} = \frac{1}{2} + \frac{1}{2\pi}\frac{d}{dv}\ln\theta_2(-iv,\rho), \quad \frac{n_0}{n} = \frac{1}{\exp[\pi v + 1/8\sigma^2]\,\theta_2(-iv,\rho)}.$$

Making use of known transformations $\theta_2(iv,\rho) = \rho^{-1/2} e^{\pi v^2/\rho}\,\theta_0(-v/\rho, 1/\rho)$ and $\theta_0(x,\rho) = \theta_3(1/2 - x, \rho)$ [4], we finally get

$$\frac{n_e}{n} = y + \frac{\rho}{2\pi}\frac{d}{dy}\ln\theta_3(y,\rho)\ *, \quad \frac{n_m^{\pm}}{n} = \rho^{-1/2}\exp\left[\frac{-\pi(y \mp m)^2}{\rho}\right] \cdot \frac{1}{\theta_3(y,\rho)}. \tag{3}$$

Here $y = \sigma^2 \ln(K/n_e) + 1/2$, $\rho = 2\pi\sigma^2$, m = 1, 2, . . .

Let us now investigate some limiting cases of Eqs. (3). In the beginning, let $\rho \gtrsim 1$ (sufficiently high T and r). Utilizing a well-known asymptotic expression for $\theta_3(y,\rho)$, $(d/dy)\ln\theta_3(y,\rho)$ (accurate at $\rho \gtrsim 1$ [4]), we easily get in this case**

$$\frac{n_e}{n} = y - 2\rho e^{-\pi\rho}\sin 2\pi y, \quad \frac{n_m^{\pm}}{n} = \frac{1}{\sqrt{2\pi\sigma^2}}\exp\left[-\frac{(y \mp m)^2}{2\sigma^2}\right], \tag{4}$$

where the remainder $2\rho e^{-\pi\rho}\sin 2\pi y$ is always small when $\rho \gtrsim 1$.

Let us note, that according to Eqs. (4), at $\rho \gtrsim 1$ the concentration of particles with a charge m has a Gaussian distribution [2], while y denotes that positive charge of which there is the greatest concentration.

---

*If written in the form of infinite series $\theta_3 = \sum_{m=-\infty}^{\infty} q^{n^2} e^{2\pi n y i}$, $q = e^{-\pi\rho}$, this equation coincides with the one found in [2].

**The equation $n_e/n = \sigma^2 \ln(K/n_e) + 1/2$ was first discovered by A. Einbinder [1]. The proper conditions, $2\pi\sigma^2 \gtrsim 1$, under which it was applicable were pointed out in [2].

When $q = e^{-\pi\rho} \lesssim 1$ (sufficiently low T and r), if we use an asymptotic expression for $d \ln \theta_3(y,\rho)/dy$ (accurate at $e^{-\pi/\rho} \ll 1$ [4]) from which it follows that

$$\frac{\rho}{2\pi}\frac{d\ln\theta_3}{dy} = -y + \sum_{n=1}^{\infty}(-1)^{n-1}\frac{\operatorname{sh}\frac{2\pi n y}{\rho}}{\operatorname{sh}\frac{\pi n}{\rho}} \cong$$

$$\cong -y + \sum_{n=1}^{\infty}(-1)^{n-1}a^n + \sum_{n=1}^{\infty}(-1)^{n-1}(a^n - a^{-n})\,e^{-n/2\sigma^2},$$

then we will get in this case Saha's equation

$$\frac{n_e}{n} = \frac{K/n_e}{1 + K/n_e} + O(\rho) \quad \text{or} \quad \frac{n_e}{K} = -\frac{1}{2} + \sqrt{\frac{1}{4} + \frac{n}{K}} \tag{5}$$

with a correction $O(\rho)$, which has the order $n_e/K e^{1/2\sigma^2}$ at $K/n_e \ll 1$.

Let us note finally, that regardless of the value of σ^2 at $n \to \infty$, n_e is determined by the condition $y \to 0$. Actually, at $n \to \infty, n_e$ should remain finite, and therefore at $n \to \infty, y$ will depend on the equation $y + (\rho/2\pi)d\ln\theta_3/dy = 0$, which as can easily be demonstrated, has a singular solution, $y = 0$. Thus, at $n \to \infty$, $n_e \to n_e^0 = Ke^{1/2\sigma^2}$, i.e., at $\sigma^2 \gg 1, n_e^0 = K$, where K is nothing else but the equilibrium ionization on the surface of a substance with a work function φ_0.

Using tables of θ-functions [5], it is also possible to find values for n_e/n at intermediate parameters for which Eqs. (4) and (5) do not hold. In this manner we determined and plotted in Fig. 1 graphs of $\log n_e/K$ as a function of $\log n/K$ for various values of parameter σ^2, which covered the whole range of r and T values of interest to us. It may be seen from these graphs, that already at $\sigma^2 \gtrsim 0.2$, Einbinder's equation, $n_e/n = \sigma^2 \ln(n_e/K) + 1/2$ is quite closely fulfilled.

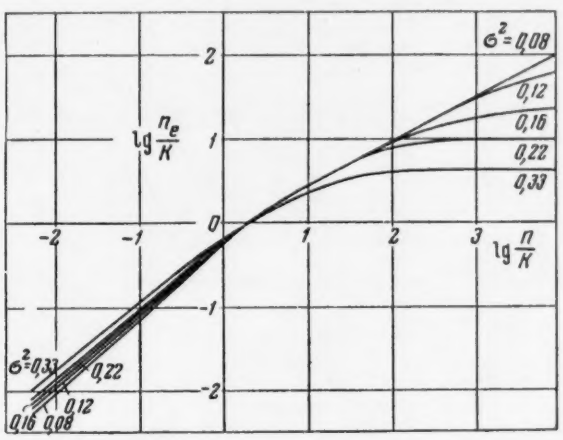

Fig. 1.

In concluding, let us note that the equations derived can easily be generalized to cover the case where the system contains dust particles of various sizes (having different r and φ_0). If we introduce the numbers $n^+_{m_i}$, $n^-_{m_i}$, $n_0^{(i)}$ and $n^{(i)}$, where $n^{\pm}_{m_i}$ is the number of particles of i-th kind with a charge $\pm m$; $n_0^{(i)}$ is the number of neutral particles; $n^{(i)}$ is the total number of particles of i-th kind; n is the total number of all the particles, then using expressions for $K^{\pm}_{m_i}$ and relationships

$$n_e = \sum_i \left(\sum_{m_i=1}^{\infty} (m_i n_{m_i}^{+} - m_i n_{mi}^{-}) \right), \qquad n^{(i)} = n_0^{(i)} + \sum_{m_i=1}^{\infty} n_{m_i}^{+} + \sum_{m_i=1}^{\infty} n_{m_i}^{-},$$

it is easy to find an equation for n_e, which is a simple generalization of Eq. (3),

$$\frac{n_e}{n} = \sum_i \frac{n^{(i)}}{n} \left(y_i + \frac{\rho_i}{2\pi} \frac{d \ln \theta_3 (y_i, \rho_i)}{dy_i} \right), \tag{6}$$

where numbers y_i, ρ_i refer to particles of i-th kind,

$$\rho_i = 2\pi\sigma_i^2, \quad \sigma_i^2 = r_i kT / e_0^2, \quad y_i = \sigma^2 \ln \frac{K_i}{n_e} + \frac{1}{2}.$$

Equation (6) makes it easy to find n_e/n in a case where the system contains several kinds of dust particles with widely differing properties. Let us assume, in particular, that the dust particles differ only in their radii, while their densities are a continuous function of radii and obey Gauss's theorem, i.e., $dn/n = n^{(i)}/n = 1/\sqrt{2\pi\kappa^2} \times$ $\times \exp[-(r-R)^2/2\kappa^2]dr$ (we assumed that $R^2/2\kappa^2 \gg 1$). If $\rho_0 = 2\pi(kTR/e_0^2) \gtrsim 1$, then we will use, of course, the previously derived equation, $y + (\rho/2\pi)(d/dy) \ln \theta_3(y,\rho) \cong y - 2\rho e^{-\pi\rho} \sin 2\pi y$, and then the concentration of electrons

$$\frac{n_e}{n} = \frac{1}{\sqrt{2\pi\kappa^2}} \int_0^{\infty} \exp\left[-\frac{(r-R)^2}{2\kappa^2} \right] (y - 2\rho e^{-\pi\rho} \sin 2\pi y)\, dr \cong$$

$$\cong \sigma_0^2 \ln \frac{K}{n_e} + \frac{1}{2} - \frac{2}{\sqrt{2\pi\kappa^2}} \int_0^{\infty} \rho \sin 2\pi y \exp\left[-\pi\rho - \frac{(r-R)^2}{2\kappa^2} \right] dr,$$

$$\sigma_0^2 = RkT / e_0^2, \quad \rho_0 = 2\pi\sigma_0^2, \quad \rho = 2\pi\sigma^2.$$

Since the exponent in the integral above has a minimum, equal to $-[\pi\rho_0 - (\pi^2/2)\rho_0^2(\kappa^2/R^2)]$, then at $\pi\rho_0 - (\pi^2/2)\rho_0^2(\kappa^2/R^2) \gg 1$ it can be solved by the method of steepest descent. In this manner we get

$$\frac{n_e}{n} = \sigma_0^2 \ln \frac{K}{n_e} + \frac{1}{2} - 2\rho_m \sin 2\pi y_m \exp\left[-\pi\rho_0 \left(1 - \frac{\pi}{2} \rho_0 \frac{\kappa^2}{R^2} \right) \right], \tag{7}$$

$$\rho_m = 2\pi\sigma_m^2 = \rho_0 - \pi\rho_0^2 \frac{\kappa^2}{R^2}, \quad y_m = \sigma_m^2 \ln \frac{K}{n_e} + \frac{1}{2}.$$

It follows from Eq. (7), that Einbinder's equation is applicable to the case where the radii of dust particles are not constant, but are distributed according to Gauss's theorem and if the distribution range K is small enough, namely, obeys the condition that $\pi\rho_0 - (\pi^2/2)\rho_0^2(\kappa^2/R^2) \gg 1$, and $2\kappa^2/R^2 \ll 1$.

I would like to express my gratitude to Prof. A.S. Kompaneits for his appraisal of the work.

LITERATURE CITED

[1] H. Einbinder, J. Chem. Phys. 26, 948 (1957).

[2] A.A. Arshinov and A.K. Musin, Proc. Acad. Sci. USSR 120, No. 4 (1958).*

[3] L.D. Landau and E.M. Lifshits, Statistical Physics (1951) p. 331 [in Russian].

[4] A.M. Zhuravskii, Handbook of Elliptic Functions [in Russian] (Izd. AN SSSR, 1941).

[5] E. Jahnke and F. Emde, Tables of Functions [Russian translation] (1948).

Received May 23, 1958

*See C.B. translation.

THE EFFECT OF CONCENTRATION ON THE DEGREE OF RADIOLYTIC TRANSFORMATION OF AQUEOUS SODIUM NITRATE

V. A. Sharpatyi, V. D. Orekhov and M. A. Proskurnin

(Presented by Academician A. N. Frumkin, June 5, 1958)

The formation of radiolytic reaction products in aqueous solutions depends primarily on the reaction of H and OH radicals with the molecules of dissolved substances. By properly combining the conditions of irradiation and the composition of solution one can achieve a yield of reaction products corresponding to a full use of radiolized water molecules (on the order of 12-13 moles per 100 ev) [1].

We studied the dependence of accumulated nitrite yield in alkaline (pH = 14) solutions of sodium nitrate on the concentration of the latter (from 10^{-7} to 6 M, Fig. 1, Curve 1).* The curve giving dependence of $G_{NO_2^-}$ on [$NaNO_3$] has four distinct sections. In the $NaNO_3$ concentration range from 10^{-7} to $5 \cdot 10^{-4}$ M, $G_{NO_2^-}$ increases with increase in the nitrate contents of solution and reaches a certain constant value (~ 4.3 equiv/ ev) in the region of $5 \cdot 10^{-4} - 10^{-2}$ M sodium nitrate. In more concentrated solutions a further increase in $G_{NO_2^-}$ is observed which is proportional to the logarithm of $NaNO_3$ concentration; this has also been observed by Mahlman and Schweitzer in 0.1 – 5 M $NaNO_3$ solutions [2]. In 1 M and more concentrated $NaNO_3$ solutions, $G_{NO_2^-}$ remains constant (~9equiv/100 ev).

When a conjugate acceptor of OH-radicals, glycerin [10^{-3} M], is introduced into the nitrate solution, under similar irradiation conditions it does not change the shape of $G_{NO_2^-}$ vs. [$NaNO_3$] function in the initial part of the curve $5 \cdot 10^{-4}$ M $NaNO_3$. However, the presence of glycerin in solution shortens the length of the first plateau in the curve. At $NaNO_3$ concentrations in excess of $5 \cdot 10^{-3}$ M the curve of $G_{NO_2^-}$ vs [$NaNO_3$] is steeper than in corresponding cases without glycerin (Fig. 1, 2). In 1–6 M $NaNO_3$ solutions containing glycerin, a higher limiting value of $G_{NO_2^-}$ is attained (~ 12 equiv/ev).

Comparing the yields of gaseous products formed in 1 M sodium nitrate solutions without and with glycerin we see that G_{H_2} decreases from 0.06 moles/100 ev to 0.04 moles/100 ev, and oxygen yield correspondingly from 0.40 to 0. The cited experimental data agree with the current hypothesis concerning the course of conjugate reactions – oxidation of glycerin and reduction of sodium nitrate, in aqueous solutions; the data also confirm that it is possible to have the H and OH radicals participate in the oxidation-reduction reaction instead of recombining.

It should be noted that in the presence of glycerin, the value obtained for the limiting yield in the reduction of nitrate ion by H atoms, 12 equiv/ 100 ev in 1 – 6 M $NaNO_3$ solution (assuming that the same number of OH radicals takes part in oxidation of glycerin), corresponds to the use of 12 radical pairs (12 molecules of water) in the oxidation-reduction reactions. This value agrees with the results of Firestone ($G_{H \text{ and } OH}$ = 11.7 ± ± 0.6) [4], who studied the isotopic exchange between H and D atoms in water vapor by the use of initiating radiation. Under these experimental conditions, in comparison to the liquid phase where the Frank-Rabinovich cell effect appears, there was a considerable decrease in the density of reaction medium, and consequently the diffusion of H and OH radicals (formed from excited water molecules) noticeably increased. In this manner the degree of free radical participation in the exchange reactions increased.

*We used in this work a Co^{60} γ-ray source in 30 equiv. of Ra; the yield of $NaNO_2$ was determined from the initial sections of curves on which accumulation of $NaNO_2$ was plotted vs. dosage in the 0 – 25,000 r interval. NO_2^- was determined colorimetrically by diazotizing sulfanilic acid and coupling it with phenol.

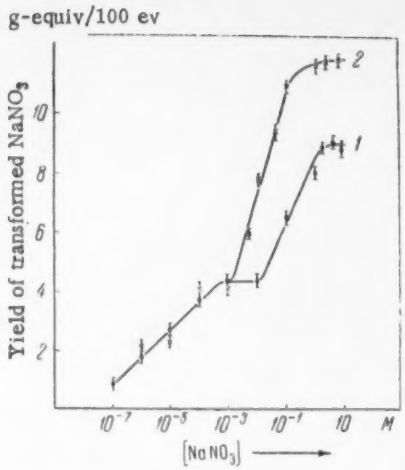

Fig. 1. G_{NaNO_2} (equiv/100 ev) as a function of the $NaNO_3$ concentration in an alkaline solution (pH = 14).

In the $10^{-4} - 10^{-2}$ M $NaNO_3$ concentration range (Fig. 1, 1), a constant $G_{NO_2^-} \sim 4$ equiv/100 ev is attained; this obviously is connected with the practically full binding of H radicals (formed from ionized water molecules) by nitrate ions. The NO_3^- concentration needed to bind the H atoms completely slightly exceeds the value of local H atom concentration along the track of ionizing particle; this is determined by the reactivity of NO_3^- in relation to H atoms. In works [6, 7] it was shown, that for solutions of certain compounds these limiting concentrations can vary within the range $10^{-5} - 10^{-2}$ M. $G_{NO_2^-} = 9$ equiv/100 ev and its continuation in 2 – 6 M nitrate solutions exceeds the yield possible by the full use of radicals from ionized water, and cannot be solely due to the direct action of γ-rays on NO_3^- • (as has been shown before [3, 8] by irradiating frozen $NaNO_3$ solutions of the same concentrations).

During such a reaction, the action of direct γ-radiation cannot be responsible for a $G_{NO_2^-}$ in excess of 10-15% of the total nitrate reduction yield. This conclusion is confirmed by experiments with molten crystal-hydrate nitrate salts [5], where the NO_3^- concentration was of the order of 10 M. Under these conditions of irradiation the effect of direct γ-ray action on NO_3^- assumes considerable importance, yet at the same time $G_{NO_2^-}$ drops to 1-1.5 equiv/100 ev.

As was shown above, introduction of glycerin into dilute $NaNO_3$ solutions ($10^{-7} - 10^{-5}$ M) does not have any effect on the course of $G_{NO_2^-}$ vs. $[NaNO_3]$ function (Curves 1 and 2 in Fig. 1 coincide). Such an agreement could be due to insufficient accuracy of NO_2^- determination in dilute solutions (~ 20%). Under these conditions one would expect to attain the constant yield (4 equiv/100 ev) at lower NO_3^- concentrations, since glycerin ($1 \cdot 10^{-3}$ M) would make it easier to involve H atoms in the reaction.

In concluding let us note that the method used in this work, which involves changing the concentration of dissolved substance ($NaNO_3$) and introduction of a conjugate acceptor (glycerin), enabled us to fix the limits of radiolytic conditions within which the action of ionized and excited water molecules is apparent.

LITERATURE CITED

[1] M. A. Proskurnin, V. D. Orekhov and E. V. Barelko, Progr. Chem. 24, 584 (1955).

[2] H. A. Mahlman and G. K. Schweitzer, J. Inorg. and Nucl. Chem. 5, 213 (1958).

[3] V. A. Sharpatyi, V. D. Orekhov and M. A. Proskurnin, Coll. The Action of Ionizing Radiation on Inorganic and Organic Systems, Izd. AN SSSR, 1958, p. 43 [in Russian].

[4] R. F. Firestone, J. Am. Chem. Soc. 21, 5593 (1957).

[5] M. A. Proskurnin and Ia. M. Kolotyrkin, Proc. of the 2nd International Conference on the Peaceful Uses of Atomic Energy, Geneva, 1958 [in Russian].

[6] H. Fricke and E. J. Hart, J. Chem. Phys. 6, 229 (1938).

[7] Z. M. Bacq, Fundamentals of Radiobiology, London, 1955.

[8] V. A. Sharpatyi, Trans. of All-Union Conf. on Radiation Chemistry, Izd. AN SSSR 1958, p. 111 [in Russian].

L. Ia. Karpov Physicochemical
Scientific Research Institute

Received June 3, 1958

• Mahlman and Schweitzer explained the increased NO_2^- yield in acidic nitrate solutions (0.1 – 5 M) by direct action of radiation on NO_3^-.

RADIOLYSIS OF HEPTANE

A.M. Brodskii, Iu.A. Kolbanovskii, E.D. Filatova

and A.S. Chernysheva

(Presented by Academician S.I. Mironov, June 4, 1958)

We have investigated in this paper γ-radiolysis of normal heptane in liquid phase and radiolysis of a dibenzylsulfide solution in heptane. The primary aims of the research were: to establish precise radiolysis kinetics for the initial components, in particular, to determine the effect of interrupted exposure, and also to establish the exact composition and yield of gases formed over a wide (more than three orders of magnitude) range of radiation dosage.

Dibenzyl sulfide ($5.011 \cdot 10^{-4}$ M)* was added to heptane in order to elucidate the behavior characteristics of aromatic sulfur compounds in radiation fields and to determine the effect of such admixtures on the radiolysis of paraffins.

We used the following radiation sources: a) for small doses – x-ray set-up RUP-3, operating conditions: potential 300 kv, tube** current 5 ma, focusing-coil current 0.75 a. Under these conditions the output dosage in the irradiated cell (determined with a ferrous-sulfate dosimeter) was about $3 \cdot 10^{15}$ ev/cm$^3 \cdot$ sec; b) for large dosages irradiation was done in Co^{60} set-ups.

The following technique was applied to the study of radiolysis kinetics at small dosages. An annular pyrex cell was placed next to the anode of the tube. The upper part of the cell was connected through a short tube to a diaphragm manometer, the readings of which were recorded with the help of a differential photoelectric cell on a self-recording potentiometer EPP-09.*** The sensitivity in pressure readings was $5 \cdot 10^{-2}$ mm Hg, recorded on 1 mm of EPP-09 tape. Irradiation was carried out in two cells with liquid capacities of 30 and 8 ml, respectively. During irradiation the temperature was maintained at $9 \pm 0.05°$ in a Hoeppler ultrathermostat; temperature constancy was regulated automatically. During irradiation with Co^{60}, the compound was placed in special ampules made of zirconium glass.

Commercial heptane was purified till it became almost completely transparent to ultraviolet light. Mass-spectrometric analysis**** did not detect any of the possible higher or lower paraffins. Dibenzyl sulfide was synthesized in the usual way and recrystallized many times; its constants and ultraviolet spectrum agreed with the listed ones. Before irradiation all the samples were repeatedly frozen and pumped on with a diffusion pump so as to remove all the dissolved air. Gas-liquid chromatography was used in gas analysis; the method roughly resembled the one described in [2]. This highly sensitive method is capable of analyzing 0.5 cm^3 of gas (up to C_5 inclusively) with a relative precision of 2-5% for each component. One should note that analysis and yield determination of gaseous radiolysis products required a careful and systematic treatment, since even small systematic errors in gas analysis could lead to contradictory results [3, 4].

*All the subsequent data refer to solutions of this concentration.

**We used a BPV-400 tube with a circular radiation outlet.

***Our scheme was a modification of G.I. Kosourov's method [1].

****The authors are grateful to G.D. Gal'pern and T.S. Novozhilova for performing the spectral measurements, and to R.A. Khmel'nitskii for mass-spectrometric analysis.

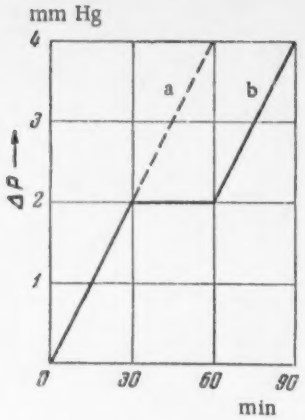

Fig. 1. Radiolysis kinetics at small dosages: a) uninterrupted irradiations; b) interrupted irradiation.

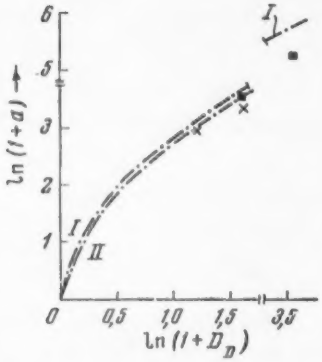

Fig. 2. Kinetics of hydrogen and methane evolution during radiolysis. Uninterrupted curve sections near the origin correspond to experimental data at low dosages. The curves obey the linear gas-evolution rule: I and squares – pure heptane; II and crosses – heptane solution of dibenzyl sulfide; $\underline{a}$ – in cm^3/10 ml; D_D – in $ev \cdot 10^{-21}$.

When irradiation was interrupted, gas evolution stopped immediately. After irradiation was resumed, the gas evolution line was actually a continuation of the original line (Fig. 1). Thus, even with very highly accurate measurements, no radiation "hysteresis" was detected in the gas evolution. Direct quantitative gas measurements in our method showed that the amount of hydrogen and methane dissolved in heptane was not large and that Henry's law was obeyed. In Fig. 2 we have shown the dependence of hydrogen and methane yields on the dosage, in pure heptane and with dibenzyl sulfide. For the purpose of combining the data which covered a wide range of integral doses, and at the same time to preserve the shape of the curve in regular coordinates at small degrees of radiolysis, we plotted the abscissa and ordinate as $\ln(1 + a)$ and $\ln(1 + D_D/10^{21})$, respectively, where $\underline{a}$ is the yield of methane and hydrogen in cm^3 per 10 ml of substance, and D_D is the dosage on the basis of a ferrous-sulfate dosimeter. Deviations from linearity, characteristic of curves in Fig. 2, began at integral dosages of the order $D_D = 10^{21}$ ev/ml. We can also see in Fig. 2, that dibenzyl sulfide protects heptane from radiolysis: the yield of hydrogen-methane mixture was decreased by approximately 10% in the linear part of the curve.

To determine the absolute values of radiochemical yields, the (G)-doses (obtained with a ferrous-sulfate dosimeter) were converted into doses in n-heptane by considering that absorption is directly proportional to the density and effective atomic number of heptane divided by the density and atomic number of the dosimeter system.

Thus, the dosage in heptane $D_{C_7H_{16}} = D_D \frac{\rho_{C_7H_{16}} \bar{Z}_{C_7H_{16}}}{\rho_D \bar{Z}_D}$, where $\bar{Z} = \sqrt[2,94]{\frac{\Sigma n \bar{Z}^{3.94}}{\Sigma nZ}}$ and ρ_i is the density [5]. Since our measurements showed that, at a 10^{21} ev/ml dosage, nonlinear effects already took place, while at lower dosages only the yields of hydrogen and methane could be measured precisely, the G-values are given only for these gases: $G(H_2) = 4.9$; $G(CH_4) = 0.22$. The value $G(H_2) = 4.9$ is sufficiently close to that listed in [4] [$G(H_2) = 4.7$]. It should be noted that the yield of methane listed in [4], $G(CH_4) = 0.09$, and also the conservation of linearity in the yield as a function of dosage did not agree with our data,* as may be seen for pure heptane in Table 1.

We will now proceed to investigate the C_2–C_5 gas fraction which in pure heptane attained 20.5% (moles) of over-all gas yield at the integral dosage $D_D = 3.25 \cdot 10^{22}$ ev/ml. In Table 2 the results of gas analysis are listed (in mole %).

The following remarks should be made in connection with the above-mentioned data.

1. Nonlinear effects appear at the integral doses of $D_D = 10^{21}$ ev/ml and show up in all the components. Nonlinearity, particularly in methane, can easily be explained if we assume interaction between CH_3 radicals and radiolysis products; this is in accord with the usual representations for the course of such a process.

2. In radiolysis of alkanes the process of direct C–C bond rupture, with the formation of alkyl radicals as

*Deviations from linearity take place with hydrogen and methane, – to a greater degree with methane. The indicated discrepancy between the results could be explained by inaccuracy in determinations of small quantities of methane by the mass-spectroscopic method, used in [4]. In fact, all of Dewhurst's analyses are in the nonlinear region.

TABLE 1

D_D (ev/ml)	Yield of 1st fraction (cm^3/10 ml)	Composition of 1st fraction	
		H_2 (mole %)	CH_4 (mole %)
$1.6 \cdot 10^{19}$	0.15	Analysis was not carried out	
$3.2 \cdot 10^{19}$	0.30	95.9	4.1
$4 \cdot 10^{21}$	34	96.6	3.4
$3.25 \cdot 10^{22}$	193	98	2

well as direct formation of final saturated and unsaturated products, plays an extremely important role. This part of radiolysis resembles thermal cracking of hydrocarbons under conditions of short-lived but powerful thermal shock.

3. The presence of acetylene in gaseous radiolysis products should be noted (it is the first time that acetylene was detected in radiolysis of alkanes); its relative amount decreases with increase in integral dosage. The concentrations of other lower olefins also decreased in the course of radiolysis, which attested to the great role of secondary reactions among lower olefins. In general, the gas composition indicated that, in the course of radiolysis, the liquid phase became impoverished in hydrogen.

TABLE 2

Composition of Gaseous Radiolysis Products

Components	D_D (ev/ml)				
	n-heptane			solution of dibenzyl sulfide in heptane	
	$3.2 \cdot 10^{19}$*	$4 \cdot 10^{21}$*	$3.25 \cdot 10^{22}$	$2.4 \cdot 10^{22}$	$4 \cdot 10^{22}$
Hydrogen	95,9	96,6	79,5	70,1	73,27
Methane	4,1	3,4	1,6	2,37	1,54
Ethane	} 97,2	} 97,2	3,2	6,46	} 8,03
Ethylene			0,22	2,30	
Acetylene		2,8	0,02	4,37	0,09
Propane			4,57	3,30	5,27
Propylene			0,32	1,41	0,85
n-Butane			4,49	3,98	3,31
iso-Butane			0,09	—	—
iso-Butene	} 0,18	} 0,18	} 0,18	} 1,53	} 1,36
n-Butene-1					
n-Butene-2			0,26	—	—
iso-Pentane	} 0,22	} 0,22	} 0,22	—	—
3-Methylbutane-1				—	—
n-Pentane			4,83	4,18	6,29
2-Methylbutene-1			0,3	—	—
2-Methylbutene-2			0,2	—	—
Hydrogen sulfide			—	—	—
Total yield of gases (cm^3/10 ml)			234,5	24,9	36,6

*The compositions in this column are those of individual fractions. Other analyses were not done in these experiments.

4. An important fact is the extensive collection of gaseous radiolysis products, among which there are comparatively many isomeric structures (probably of secondary origin). As far as we know, the complete composition of gaseous radiolysis products is being listed for the first time.

5. Hydrogen sulfide was not found among the gases produced in radiolysis of dibenzyl sulfide in heptane. This indicated that the decomposition of dibenzyl sulfide with the formation of hydrogen sulfide did not exceed 10% of the whole dibenzyl sulfide in the cases under investigation. Therefore, it is possible that the shielding effect in this case was basically due to an excitation energy transfer.

The authors express their gratitude to Academician S.I. Mironov and to Corresponding Member Acad. Sci. USSR K.P. Lavrovskii for their valuable advice, and to N.N. Naimushin for his help in carrying out gas analyses.

LITERATURE CITED

[1] G.I. Kosourov, Pribory i Tekhnika Eksperimenta No. 3, 90 (1956).

[2] A.M. Brodskii, R.A. Kalinenko and K.P. Lavrovskii, Coll.: Problems in Kinetics and Catalysis [in Russian] (Izd. AN SSSR, 1957) p. 9;* A.M. Brodskii, K.P. Lavrovskii et al., Chem. and Technology of Fuels and Oils No. 11 (1958).

[3] L.S. Polak, A.V. Topchiev and N.Ia. Cherniak, Proc. Acad. Sci. USSR 119, 307 (1958).**

[4] H.A. Dewhurst, J. Phys. Chem. 61, 1466 (1957).

[5] M. Day and G. Shtein, Coll.: Radiation Chemistry [Russian translation] (IL, 1953) p. 235.

Petroleum Institute
Academy of Sciences, USSR

Received June 3, 1958

*In Russian.

**Original Russian pagination. See C.B. translation.

COMBUSTION IN AN ADIABATICALLY HEATED GASEOUS MIXTURE

S. G. Zaitsev and R. I. Soloukhin

(Presented by Academician V. N. Kondrat'ev, June 11, 1958)

In the works [1-4] devoted to the study of combustion of homogeneous gaseous mixtures under conditions of rapid adiabatic heating, the following pecularities were observed in the combustion phenomenon: existence of a finite induction period and appearance of combustion centers during the initial stage of the process. However, it was not possible to conduct a detailed study of the appearance and growth of combustion centers due to a lack of recording equipment with high enough resolving power.

In this work we have investigated the formation and propagation of an exothermic reaction in a homogeneous gas medium heated adiabatically to temperatures of 600-1400° at a pressure of 1-3 atm. The experiments were conducted in a shock-tube [5]. The cross section of the internal bore was 40 × 40 mm, length of the low pressure chamber 2 m, length of the high-pressure chamber 0.7 m. In the low-pressure chamber (containing the studied mixture) a shock wave S was produced which spread down the bore and was normally reflected from the end-face of the chamber. The wave intensity was chosen so that the temperature T_2 behind the reflected shock wave R was within the studied range. Meanwhile, temperature T_1 behind the S wave did not exceed 500°. At the end of the chamber, where the normal reflection of wave S took place, the side walls were made of plane-parallel optical glass plates. The length of this section was 158 mm, and density changes in it were recorded by Schlieren technique using an IAB-451 apparatus; a high-frequency frame exposure (Fig. 1) as well as a track method (Fig. 2) were used. Piezometers [6] were built into the upper wall and the end-face of the chamber.

Investigation of combustion processes was carried out with hydrogen-oxygen mixtures. Schlieren photographs of the studied gas state, as well as pressures registered on the chamber walls indicated that the gas behind wave R experienced small pressure and density disturbances. The amplitude of pressure fluctuations did not exceed 5% of its absolute value. Density fluctuations did not exceed 0.5% of its absolute value. Let us note, however, that the above-mentioned density and pressure disturbances behind the reflected wave R have been observed in inert gases, air and nitrogen. Therefore, the nature of these disturbances was in no way connected with the specific chemical properties of the reacting gaseous mixture.

By making use of pressure P_0, temperature T_0 in front of the S wave and also of its velocity of propagation (determined by Schlieren-photography), we could calculate pressure P_2 and temperature T_2 of the studied mixture under the conditions behind wave R with the help of well-known gas dynamics formulas. The calculated pressure agreed with the experimentally measured one. On the basis of this, we used the calculated value of temperature T_2 in describing the process. Within the investigated region experimentally observed optical density disturbances did not exceed 0.5%; temperature fluctuations corresponding to these variations did not exceed 10°. Let us note, that as a result of the interaction between reflected shock from R and the boundary flow-layer [7], which follows behind the wave S, the surface of front R undergoes a deformation leading to an observable front widening on the Schlieren photographs (Figs. 1, 2).

Combustion process in an adiabatically heated mixture occurs in the following way. The observable reaction, accompanied by intense light emission and a sharp change in thermodynamic parameters of the gaseous mixture, first originates at one or several points within the studied space (reaction centers). At first, the gaseous region where an observable reaction takes place (combustion center) occupies a small volume which increases

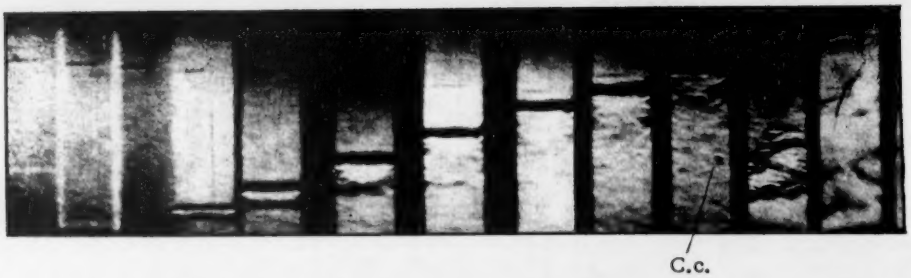

Fig. 1. Schlieren photograph of the combustion process. Exposure frequency was 35,000 frames per second.
1) C.c. = combustion center.

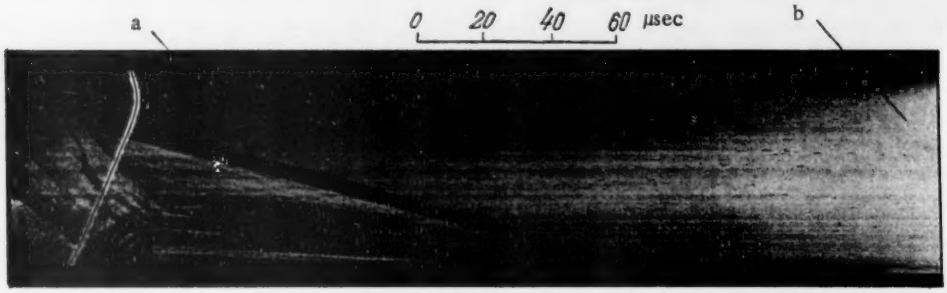

Fig. 2. Schleieren photograph of the combustion process by the continuous track method.
1) a = Wave R track; 2) b = wave S track.

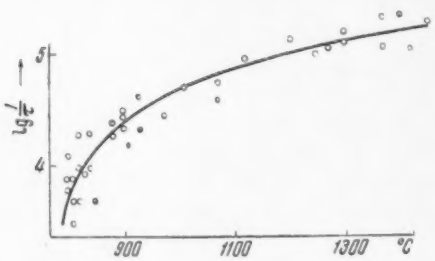

Fig. 3. Combustion delay in a $H_2 + O_2$ mixture as a function of temperature.

with time. At a mixture temperature of 900° the velocity of the combustion center front is 180-200 m/sec. Subsequently, as several combustion centers merge within the investigated space, appearance of detonations is observed. Front velocity of the newly formed region increases to the order of 2000 m/sec. In Fig. 1 the reaction center was recorded on the tenth frame; on the following frame a combustion region was recorded. The velocity of its front was 1900 m/sec. Quantitative study of the above-described process was done with the help of Schlieren photographs by the continuous track method. In Fig. 2 we have presented a typical photograph of this process, obtained by this method. The absolute error in the velocity determinations for waves S, R, explosive, and normal combustion did not exceed 20 m/sec; error in determining the moment of appearance of active centers did not exceed ± 2 μ sec.

The probability of a reaction center originating at a fixed point of the investigated space depends on the time intervals τ_1 and τ_2, spent by the selected part of the gas volume at temperatures T_1 and T_2, respectively. Wave S raises the gas temperature from T_0 to T_2, while wave R raises it from T_1 to T_2. The delay in the combustion of a mixture, the temperature of which has been raised instantaneously from T_0 to T_2, is measured by the time interval τ between the time heat was applied to the mixture and the moment the first reaction center appeared in it. Within a mixture layer that is spread over a distance $\underline{x}$ from the end of the chamber, as $\underline{x}$ increases the time interval $\tau_2(x)$, between the moment temperature is instantaneously raised from T_1 to T_2 and the first appearance of a reaction center, decreases; i.e., it decreases with increase in time spent by the

investigated volume at temperature T_1. We determined τ (equal to $\tau_2(0)$) using the experimental values of $\tau_2(x)$, obtained from the Schlieren photographs of the process. Experimental values of $\log 1/\tau$ are plotted in Fig. 3 as a function of temperature T. Changes in the magnitude of $\log 1/\tau$ with respect to pressure in the region of 1 to 3 atm are small in comparison with its absolute value. Experimentally determined values for the combustion delay period are in satisfactory agreement with the values of induction period calculated on the basis of chain-reaction theory [8, 9].

It seems to us, that the combustion process develops in the following way under the above-described conditions. After the gas temperature has been raised, an increase in the concentration of active intermediate products takes place within the heated volume [7]. Within specific points of space, at the end of induction period, arise conditions which lead to an avalanche-like increase in reaction rate (in this same part of space), and a reaction center is formed. Further propagation of the reaction from the center to the adjoining mixture layers is determined by the processes of normal flame-front propagation. Due to the fact that in an adiabatically heated mixture a system of centers always appears, the combustion of some volume elements occurs under conditions where they are surrounded on all sides by combustion fronts. This leads to the formation of localized explosions, accompanied by the appearance of shock bursts among the combustion products; this is observed experimentally. When these shock bursts pass into the region of unburned gas, they form detonation fronts.

In concluding, the authors consider it a pleasant duty to express their deep gratitude to A. S. Predvoditelev, E. V. Stupochenko and T. V. Bazhenova for their constant attention to the work and valuable remarks.

LITERATURE CITED

[1] L. B. Zel'dovich and I. Ia. Shliapintokh, Proc. Acad. Sci. 65, No. 6, 871 (1949).

[2] J. Livengood and W. Leary, Ind. and Eng. Chem. 43, No. 12, 2797 (1951).

[3] A. Ederton, O. Saunders, A. LeFêbre and N. Moore, 4 Sympos. on Combustion, paper No. 51, Baltimore, 1953.

[4] M. Steinberg and W. Kaskan, 5 Sympos. on Combustion, paper No. 74, N. Y., 1955.

[5] R. I. Soloukhin, Trans. of the 4th Conference of the Institute of Power Engineering, Moscow, 1959.*

[6] S. G. Zaitsev, Exper. Instr. and Tech. No. 6 (1958).

[7] H. Mark, J. Aeronaut Sci. 24, 4, 304 (1957).

[8] N. N. Semenov, Chain Reactions, Leningrad, 1934.*

[9] A. B. Nalbandian and V. V. Voevodskii, Hydrogen Oxidation and Combustion Mechanism, Moscow-Leningrad, 1949.*

G. M. Krzhizhanovskii Power
Institute, Academy of Science, USSR

Received June 11, 1958

PREPARATION AND ELECTROCHEMICAL PROPERTIES OF CRYSTALLINE MODIFICATIONS OF LEAD DIOXIDE

I. G. Kiseleva and B. N. Kabanov

(Presented by Academician A. N. Frumkin June 10, 1958)

The phenomenon of polymorphism in lead dioxide has been described in several works [1-5]. It was established that PbO_2 exists in two modifications: tetragonal (β-form) and rhombic (α-form). The formation of one or the other modification depends on the conditions under which it is prepared. Thus, the α-form is obtained in anodic plating from a neutral or alkaline solution of lead salts, during oxidation of $PbSO_4$ in dilute H_2SO_4 solutions, and under pressure from β-form; oxidation of $PbSO_4$ in concentrated H_2SO_4 solutions gives β-form.

Analysis of the available data showed that the conditions for obtaining either α - or β-form under normal pressure essentially differed in the fact that PbO_2 was formed in the presence or absence of H_2SO_4. Therefore, one could assume that the formation of different crystalline forms is connected with the adsorption of sulfuric acid, which, as has previously been shown, is very strongly attached to PbO_2 and in large amounts, too [6].

To confirm this assumption, we measured the comparative adsorbing abilities and studied the structures of PbO_2 electrodes obtained under various conditions. The results are presented in Table 1. Adsorptions were measured radiochemically by the activity changes in the electrodes; structures were studied by X-ray crystallography.* The initial PbO_2 electrodes were plated in the form of smooth deposits on gold from a 15% $Pb(NO_3)_2$ solution at $2 \cdot 10^{-4}$ amp/ cm^2 current density.

In agreement with the literature data, the deposits we obtained from a neutral solution or from oxidation of $PbSO_4$ in 0.01 N H_2SO_4 consisted mainly of α-PbO_2. As a result of electrochemical recrystallization of the electrode in 8 N H_2SO_4 (a cathodic reduction to $PbSO_4$ with a subsequent anodic oxidation to PbO_2), an irreversible adsorption of H_2SO_4 on PbO_2 took place and a conversion of α-PbO_2 to β-PbO_2.** The amount of adsorption in 8 N H_2SO_4 was from $6 \cdot 10^{-8}$ to $40 \cdot 10^{-8}$ M/ cm^2, depending on the thickness of the PbO_2 layer. Adsorbed H_2SO_4 could be removed from the PbO_2 deposit by displacement from the electrode with the help of adsorbing cobalt [6]. We carried out a structural X-ray analysis on lead dioxide which was deposited in 8 N H_2SO_4 and polarized anodically for 10-15 hours in a solution of 8 N H_2SO_4 + 5% $CoSO_4$. It turned out that desorption of H_2SO_4 was accompanied by a change from β-PbO_2 to α-PbO_2.

As regards the nature of H_2SO_4 adsorption on PbO_2 we can assume that H_2SO_4 is absorbed within the electrode space on the inter-crystal surface. Good evidence of this is the large magnitude of adsorption and its dependence on the thickness of PbO_2 layer (Table 1). Besides, we established, that appreciable irreversible adsorption occurred only in the process where PbO_2 was made from $PbSO_4$, but none was detected after extensive anodic polarization of PbO_2 in H_2SO_4.*** This seems to indicate that sulfuric acid is not adsorbed on an

* We express our gratitude to E. V. Semenova for performing the X-ray structural analysis on lead dioxide samples.

** It should be noted that under these conditions neither one of the modifications obtained was pure. In all the cases we had a mixture of both crystalline forms, but the mixture plated from a neutral solution was primarily α-form, while that from an acid β. These deposits we call by convention α-PbO_2 and β-PbO_2 respectively.

*** If $CoSO_4$ was present in solution, the change in crystal modification and H_2SO_4 adsorption during uninterrupted anodic polarization could be explained by recrystallization, which proceeded as follows: β-$PbO_2 \rightarrow PbSO_4 \rightarrow \alpha$-$PbO_2$. In the presence of $CoSO_4$ this process was accelerated on account of lowered oxygen overvoltage and a consequent approach of electrode potential to its standard value. It was also possible that preferential reduction of β-PbO_2 at the expense of oxygen evolution was primarily responsible for this.

TABLE 1

PbO_2 from solution of	Form of PbO_2	Thickness of PbO_2 layer in μ	H_2SO_4 adsorption in moles		
			moles/cm² on visible surface	moles/cm³	moles/cm² on inter-crystal surface
$Pb(NO_3)_2$	α	2–30	—	—	—
0.01 N H_2SO_4	α	20	$0{,}0_1 \cdot 10^{-8}$		
8 N H_2SO_4	β	2	$6 \cdot 10^{-8}$	$3 \cdot 10^{-4}$	$3 \cdot 10^{-11}$
8 N H_2SO_4	β	20	$40 \cdot 10^{-8}$	$2 \cdot 10^{-4}$	$2 \cdot 10^{-11}$
8 N H_2SO_4 + + $CoSO_4$	β → α	Coated electrode	Desorption (*)		

already deposited lead dioxide but in the process of dioxide formation.* It is interesting to note that the crystals of PbO_2 formed in 8 N H_2SO_4 were 100 times finer (on the basis of linear measurements) than the ones formed in $Pb(NO_3)_2$ or 0.01 N H_2SO_4 solutions. This can be explained by a well-known phenomenon – crystal growth hampered by chemisorption.

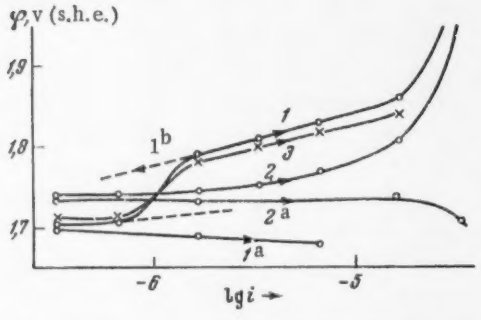

Fig. 1. Overvoltage curves. 1 and 1a) α-PbO_2 from a $Pb(NO_3)_2$ solution; 2)and 2a) β-PbO_2 from 8 N H_2SO_4; 3) α-PbO_2 from 8 N H_2SO_4 + 5% $CoSO_4$.

It is known that a series of properties undergo a change when the crystalline modification of a substance is changed. In connection with this, it was interesting to compare the electrochemical behavior of α-PbO_2 and β-PbO_2. For this purpose we measured the rates of anodic PbO_2 formation from $PbSO_4$ and cathodic reduction of PbO_2 on smooth tetragonal and rhombic PbO_2 electrodes. These reaction rates were measured by taking overvoltage curves in 8 N H_2SO_4. To measure the overvoltage, we partially discharged the electrode, i.e., part of PbO_2 was reduced to $PbSO_4$. The curves showing φ as a function of log i, for two different PbO_2 modifications, are shown in Fig. 1.**. Anodic curves which were taken rapidly and at small current densities, as well as cathodic ones, run parallel to each other separated by 30-40 mv. Decomposition current was almost the same on both modifications. The shape of a curve depended on the deviation of $PbSO_4$ concentration next to the electrode surface from the concentration in a saturated solution. However, in the region of 10^{-6} – $3 \cdot 10^{-6}$ amp/cm² the overvoltage on α-PbO_2 in the anodic process increased (at a fixed current density), with time, by approximately 80 mv. Therefore, a curve plotted comparatively slowly (during 3-4 hours) had an anomalous appearance (Fig. 1, 1) and when it was measured in the reverse direction (from large to small current densities), hysteresis was observed (dotted line, Curve 1b). After PbO_2 was anodically polarized for 10-15 hours in 8 N H_2SO_4 + + $CoSO_4$ (H_2SO_4 was desorbed and β-PbO_2 converted to α-PbO_2), oxidation of $PbSO_4$ was retarded and the overvoltage curve (Fig. 1, 3) proceeded in almost the same way as on α-PbO_2 obtained from a neutral solution.

Slowed oxidation of $PbSO_4$ on α-PbO_2 in 8 N H_2SO_4 was probably connected with hindered electrocrystallization [9], which could be explained by H_2SO_4 adsorption. It is known that anodic oxidation of Pb^{++} in 8 N H_2SO_4 leads to to the formation of β-PbO_2. If the PbO_2 electrode is of the same modification, then the electrocrystallization process proceeds with ease, since there is a continuing growth of an already-present crystal lattice [10]. However, in the case of an α-PbO_2 electrode, on which H_2SO_4 has not yet had a chance to be adsorbed, a deposit of α-PbO_2 is readily formed on active centers. Gradually the number of active centers decreases, probably because of specific H_2SO_4 adsorption (which takes place very slowly), with the result that plating of α-PbO_2 gradually stops. Subsequently,

* Absorption of H_2SO_4 cannot be explained by the formation of a stoichiometric compound between H_2SO_4 and PbO_2 [7], since the amount of H_2SO_4 absorbed would then have to be twice as large as the experimental.

** All the curves were taken on the same electrode in the order in which they are numbered.

only β-PbO_2 can form at an already increased overvoltage. In this case the overvoltage increase is due not only to the formation of a deposit on a surface that is foreign to the forming PbO_2, but also to the adsorption of sulfuric acid on this same surface. That is why the rate of the process did not increase, as one would have expected, after the first layers of deposit were formed. Evidently, the attained increase in potential promotes very large specific H_2SO_4 adsorption, which in turn hinders the growth of PbO_2 nuclei that are being formed, and the process continues at a reduced rate.

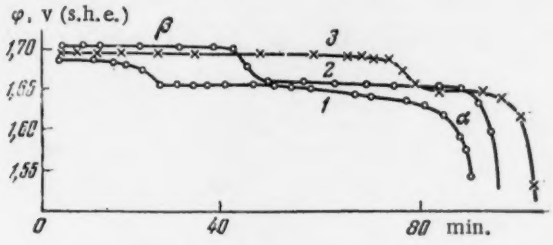

Fig. 2. Reduction of PbO_2 (discharge curves). 1) 25% β-PbO_2; 2) 50% β-PbO_2; 3) 75% β-PbO_2.

Judging from the Curves 1a and 2a (Fig. 1), the reduction of α-PbO_2 at a given potential proceeds at an incomparably slower rate than that of β-PbO_2. Accordingly, when an electrode composed of both PbO_2 modifications was discharged there appeared two delays on the potential vs. time discharge curve; these delays differed in potential by approximately 30 mv (Fig. 2). α-PbO_2 plated from a neutral $Pb(NO_3)_2$ solution or 0.01 N H_2SO_4 served asstarting material for preparing such electrodes. Partial reduction of PbO_2 followed by subsequent oxidation of the resulting $PbSO_4$ in 8 N H_2SO_4, converted the reduced α-PbO_2 fraction into β-PbO_2. The length of the first plateau depended on the amount of β-PbO_2. In Curves 1, 2, and 3 of Fig. 2 a partial preliminary discharge of α-PbO_2 comprised 25, 50, and 75%, respectively, of the bulk.

Similar phenomena were observed in the experiments of Rüetschi and Cahan [4]. However, the authors were inclined to explain it by a difference in discharge potentials of α-PbO_2 and β-PbO_2, as well as by the phenomenon of passivation. Burbank [5] came to the conclusion that the discharge was retarded by α-PbO_2 on the basis of the experimental fact that among corrosion products of lead coated with a mixture of α-PbO_2 and β-PbO_2, one finds α-PbO_2 together with $PbSO_4$.

Therefore, on the basis of the investigation carried out, we can consider the chemical adsorption of sulfuric acid on the surface of PbO_2 to be responsible for the retardation of the $PbO_2 \rightarrow PbSO_4$ process and the formation of β-form. The effect of H_2SO_4 adsorption on the rate of another anodic process on PbO_2 (oxygen evolution) has already been previously established [8].

In concluding, we should note that a further study of the conditions under which various lead dioxide modifications are formed and of their properties is of some practical value. Thus, for instance, when lead dioxide was plated on gold we observed a considerable difference between the mechanical strength of α-PbO_2 and β-PbO_2 deposits. Besides, it is known that PbO_2 from 0.1 N H_2SO_4 is harder than PbO_2 from 8 N H_2SO_4 [11]. Hence, it is possible that so-called "sliding" of the active mass on a positive electrode in a lead storage battery is connected with decreased durability, on account of α-PbO_2 conversion to β-PbO_2 in the process of recharging [3].

LITERATURE CITED

[1] M. Kamayama and T. Fukumoto, J. Soc. Chem. Japan, 49, 155 (1946).

[2] A. I. Zaslavskii, Iu. D. Kondrashov, S. S. Tokachev, Proc. Acad. Sci. 75, 559 (1950).

[3] H. Bode and E. Voss, Zs. f. Electrochem., 60, 1053 (1956).

[4] P. Rüetschi and B. D. Cahan, J. Electrochem. Soc., 104, 406 (1957).

[5] J. Burbank and A. C. Simon, J. Electrochem. Soc., 100, 11 (1953).

[6] I. G. Kiseleva, B. N. Kabanov, Proc. Acad. Sci. 108, 864 (1956).

[7] R. Von Konow, Tekn. Fören. Finl. Förhand., 74, No. 12, 257 (1954).

[8] B. N. Kabanov, I. G. Kiseleva, D. I. Leikis, Proc. Acad. Sci. 99, 804 (1954).

[9] M. Fleischmann and H. R. Thirsk, Trans. Farad. Soc. 51, 71 (1955).

[10] P. D. Dankov, Trans. of the 2nd Confer. on Metal Corrosion, 1943, p. 121.•

[11] D. I. Leikis, E. K. Venstrem, Proc. Acad. Sci. 112, 971 (1957).••

Electrochemical Institute
Acad. of Sci. USSR

Received June 10, 1958

• In Russian.

•• Original Russian pagination. See C. B. Translation.

INTERACTION OF SHOCK WAVES WITH FLAME FRONTS

S.M. Kogarko, V.I. Skobelkin and A.N. Kazakov

(Presented by Academician V.N. Kondrat'ev, June 21, 1958)

We are investigating the problem of strengthening shock waves during their interaction with a flame front by changing the normal combustion process in the shock wave.

Let p_i = pressure, ρ = density, T_i = temperature, c_i = velocity of sound, u_i = gas velocity relative to a fixed coordinate system.

A flame front with velocity λ_0 (relative to the gas particles) spreads through a burning gas changing its parameters from p_0, ρ_0, T_0 and u_0 to p_1, ρ_1, T_1 and u_1. Toward the flame front (or behind it) moves a shock wave with amplitude $\Delta p_0 = \frac{p'_0 - p_0}{p_0}$, and behind it a gas in a state with parameters p'_0, ρ'_0, T'_0 and u'_1, is formed.

Let us assume that the length of the shock wave is sufficiently large in comparison with the reaction zone (i.e., the time spent by the reaction zone within the shock wave is longer than the reaction time). Such a shock wave interacts with the flame front in the following way.

1. On the flame front the shock wave undergoes a change, just like on a boundary separating two media. There arise refractions and reflections of the wave [1]. The refractive index will depend on the conditions under which the shock wave passes over from a medium with parameters p_0, ρ_0, T_0 into one with parameters p_1, ρ_1, T_1, or in the reverse direction [2]. The flame front can here be regarded, approximately, as a contact discontinuity.

For weak shock waves being propagated from a cold gas to a hot one the refractive index is $\xi_- = \frac{2}{1+\sqrt{T_1/T_0}}$; for waves propagating in the reverse direction, $\xi_+ = \frac{2\sqrt{T_1/T_0}}{1+\sqrt{T_1/T_0}}$.

2. In going through a flame front, a shock wave compresses the gas in the reaction zone and raises the gas temperature within the zone to $T^* > T_1$. A temperature rise in the reaction zone increases the reaction rate, which, in turn, results in an increased velocity of flame propagation.

Such an increase in the flame propagation velocity occurs quite rapidly (time of the same order as reaction time). Therefore, the above-described process can be considered as a sort of detonation in the gas flow behind the shock-wave front; it results in the formation of two supplementary (reinforcing) shock waves, which are propagated in directions opposite to the flame front.

The shock wave front travels with a subsonic velocity (relative to the excited gas), and, consequently, any kind of turbulence in the flow behind the shock front is capable of overtaking it and changing it.

The increase in the velocity of flame propagation does not occur instantaneously after the arrival of the shock wave, but after a certain relaxation time; during this time the suddenly changed (by the shock wave) conditions in the flow of reaction do not produce any substantial changes in the diffusion and temperature currents coming out of the reaction zone. The relaxation time is of the same order as that of the reaction [3].

Figure 1 is a schematic representation of the reinforcement a shock wave undergoes when passing through a flame front.

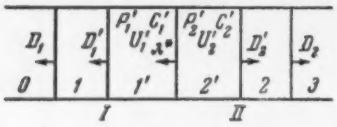

Fig. 1

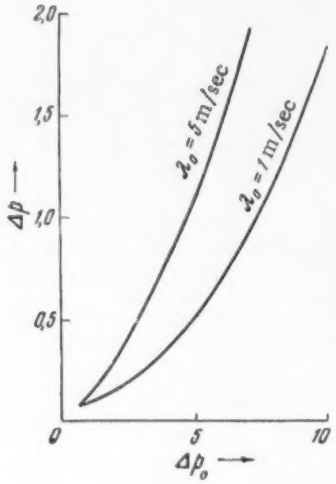

Fig. 2

States 1 and 2 originate when a shock wave is refracted and reflected from a flame front; 1' and 2' – reinforcing shock waves; 0 and – original states of the system.

By making use of the relations on the shock front, it is possible to express all the quantities in regions 1' and 2' in terms of M_1 and M_2 respectively [4], where $M_1 = (v_{01})/C_1$ and $M_2 = (v_{02})/C_2$; v_{01} and v_{02} are the gas velocities relative to the surfaces of discontinuities I and II; C_1 and C_2 are determined from the velocity of sound in the fuel gas, C_0.

Expressing $\Delta p_1 = \frac{p'_1 - p_1}{p_1}$, $\Delta p_2 = \frac{p'_2 - p_2}{p_2}$, u'_1 and u'_2 in terms of M_1 and M_2, and substituting them in equations

$$p'_1 = p'_2$$
$$u'_2 = u'_1 + \frac{(\gamma - 1)\, Q\lambda^*}{C'^2_1}, \qquad (1)$$

which are correct on the flame front, we get $M_1 = M_2 = M$ and an equation involving M,

$$M^6 + \lambda_0 AM^5 + a_1 M^4 - a_2 AM^3 - a_3 M^2 + \\ + a_4 M + a_4 = 0, \qquad (2)$$

in which all the coefficients are expressed in terms of initial parameters:

$$A = \frac{(\gamma - 1)\, Q}{(1 - \mu^2)\, C_1^2 \left(1 + \frac{C_2}{C_1}\right)}; \quad \mu^2 = \frac{\gamma - 1}{\gamma + 1};$$
$$a_1 = \frac{1 - \mu^2 - 3\mu^4}{\mu^2 + \mu^4}; \quad a_2 = \frac{\lambda^* - \lambda_0 + 2\mu^4 \lambda_0}{\mu^2 + \mu^4}$$
$$a_3 = \frac{1 + \mu^2 - 3\mu^4}{\mu^2 + \mu^4}; \quad a_4 = \frac{1 - \mu^2}{1 + \mu^2}.$$

To calculate the new flame propagation velocity λ^*, we make use of Zel'dovich's theory [5],

$$\frac{\lambda^*}{\lambda_0} = \frac{T_2^*}{T_2} \sqrt{\frac{T_2 - T_0}{T_2^* - T_0}} \exp \frac{E}{2RT_2} \left(1 - \frac{T_2}{T_2^*}\right). \qquad (3)$$

The ratio $\frac{T_2^*}{T_2} = \frac{1 + \Delta p_0 + (1 + \Delta p_0)^2 \mu^2}{1 + \Delta p_0 + \mu^2}$ was here obtained from a Hugoniot adiabatic curve (T_2 = combustion temperature, E = activation energy, R = gas constant, Q = heat of combustion).

It follows from Equations (2) and (3), that the amplitude of reinforcing shock wave depends on the amplitude of the original shock wave Δp_0, and also on the kinetic properties of the combustible mixture (reaction rate, heat capacity of the fuel, activation energy, etc.).

In Fig. 2 we have drawn a graph showing the dependence of the amplitude of the reinforcing shock wave on the degree of compression in the reaction zone, for two flame propagation velocities (λ_0 = 1 m/sec and λ_0 = = 5 m/sec).

The total reinforcement of the shock wave depends on the relaxation process [3], which we have not investigated in this communication, and after relaxation on the final change in the normal flame propagation velocity in the shock wave. For weak waves, mainly, the relaxation reinforcement is important.

LITERATURE CITED

[1] N.E. Kochin, Coll. Works 1-2 [in Russian] (Izd. AN SSSR, 1949).

[2] G.M. Bam-Zelikovich, Coll. Theor. Hydrodyn. No. 4 (1949); No. 9 (1952).

[3] S.M. Kogarko and V.I. Skobelkin, Proc. Acad. Sci. USSR 120, No. 6 (1958).*

[4] R. Courant and K.O. Friederichs, Supersonic Flow and Shock Waves [Russian translation] (IL, 1950).

[5] Ia.B. Zel'dovich, J. Phys. Chem. 14, No. 3 (1948).

Institute of Chemical Physics
Academy of Sciences, USSR

Received June 11, 1958

*See C.B. translation.

THE ROLE OF SURFACE PROPERTIES OF A SEMICONDUCTOR IN ADHESION PHENOMENA

V.P. Smilga and Corresponding Member Acad. Sci. USSR B.V. Deriagin

In [1-3] we had examined the electrostatic force components at the metal-nonconductor [1, 2] and semiconductor-metal [3] points of contact. The existence of appreciable electric fields at the intersolid boundary can,under certain conditions, lead to a useful effective coupling force between two solids, with values of the order of several kilograms per square centimeter. However, in those calculations we did not allow for the presence of surface states on the semiconductor. Meanwhile, it was very interesting to calculate their effect. It was easy to see that if the electrostatic component of adhesive force was going to attain a value of the order of tens of kilograms per square centimeter (value corresponding to the adhesive force of commercial glue), then it was necessary that the electric field at the metal-semiconductor boundary attain the magnitude of several million volts per centimeter; a very unlikely case for a metal-semiconductor contact without surface states.

On the other hand, precisely such fields appear at the boundary between two metals in contact; of this,one can easily be convinced by simple calculations. When two dissimilar metals are pulled apart,the electrostatic component of adhesive force may fail to manifest itself, since (due to the great conductivity) the charges will flow from separated parts to the ones still in contact (of course, a simultaneous separation along all the surface of contact is never realized). However, if the conductivity were insignificantly small and no similar charge recombination took place, then there would be a very appreciable adhesion between the two metals. (Let us note that in double layer a charge recombination through the tunnel effect, though it would decrease the adhesive force, would yet be considerably less effective than the recombination resulting from significant conductivity of the solids being separated.) One would expect, in connection with the things just said, that a semiconductor with a large number of surface states would be a very favorable object for getting appreciable adhesion, since, on one hand, "metallization" of the semiconductor surface would take place (a trap for electric charges is formed on the surface), while on the other hand, a large number of experimental facts [4] indicate that the surface conductivity of semiconductors is very small. Irregardless of the considerations stated, it is necessary to take surface states into account so as to bring the theoretical system nearer to reality.

As we know, surface states can be caused by a break in the regular structure (I.E. Tamm's surface zones) as well as by the presence on the surface of a great number of foreign centers.

In the system under examination we will only consider the surface levels of the second type; moreover, we will assume that there are two types of surface states – donors and acceptors. In essence, this system conforms with that of Bardeen and Brattain [4], which was proposed to explain the rectifying properties of germanium. The model used has the advantage that it permits a good classification of regular qualitative properties, and at the same time has a very general character. Just as in [2, 3] a semiconductor with only one type of carriers is being examined.

Before we proceed to the solution of the problem, let us note one more feature of general interest to the problem of surface states and adhesion. From a microscopic point of view the electrostatic theory of adhesion should analyze the donor-acceptor bond between contact surfaces. It is quite evident that the study of density redistribution in the electron gas at the contact of two solids is completely similar to the problem of electron-density determination in any kind of heteropolar molecule; there is, however, one very essential difference, this being that in the case of solids we can apply statistical methods and carry out a phenomenological description of the effect, whereas a determination of electronic densities in a molecule requires difficult quantum-mechanical

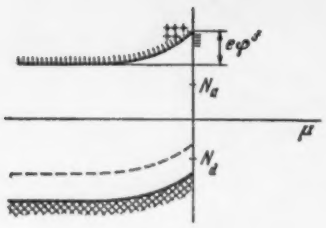

Fig. 1

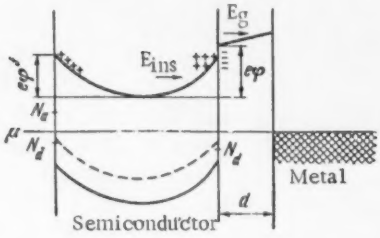

Fig. 2

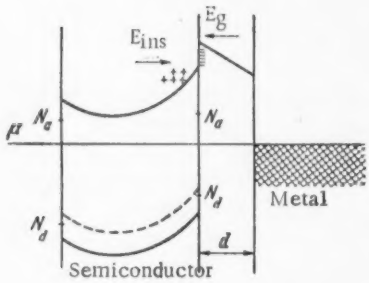

Fig. 3

computations. Introduction of surface states does not change anything in the method of calculation; therefore, we are able to analyze the donor-acceptor chemical coupling phenomenologically and consider the effect of functional donor or acceptor groups introduced on the surface.

Perhaps it should be noted, that a similar linkage between two glued solids is of a particular interest due to the long-distance character of the forces (the field of the charged surface is constant), which leads, first, to a greater binding strength with respect to sudden loads (these produce small voids which are covered up after the load is removed), and second, to an increase in shearing work proportional to the square of the number of individual donor-acceptor bonds.

Statement and solution of the problem. We are analyzing a semiconductor with one type of carriers (to be more definite, we will later on analyze an electron semiconductor). Arrangement of surface levels may be seen in Fig. 1 (i.e., we assumed that there are only two types of levels on the surface, the acceptor levels are located above, while the donor levels are located below the Fermi level). The system in Fig. 1 corresponds to a case where the surface is negatively charged. Here μ = Fermi level, N_a and N_d are acceptor and donor levels on the surface, $e\varphi^f$ is the degree of zone curvature on the free semiconductor surface. In the case where the semiconductor is in contact with a metal through a small gap d the zonal diagram looks as shown in Fig. 2. Here we have shown a case where the work function of a metal is greater than that of the semiconductor and the field strength is the same on both sides of the semiconductor surface. Generally, the sign of the surface charge is not specified. In Fig. 2, E_g and E_{ins} define the electric fields in the gap and in the semiconductor, respectively.

Another case is also possible. The case drawn in Fig. 3 is interesting for the reason that the electric field has a different sign on each side of the semiconductor surface. It will be convenient for us to separate all the cases of semiconductor-metal contacts into two groups: 1) the electric field has the same sign on both sides of the semiconductor surface, and 2) the electric field has different directions on the reverse side of the semiconductor surface.

For further analysis it is convenient to introduce a number V_k^0, equal to the contact potential difference between the given metal and an identical (to the given one) semiconductor (but without surface states).

$$eV_k^0 = \varphi_M - \varphi_{sc}^0. \tag{1}$$

Here e = charge of the electron, φ_M = work function of a metal, φ_{sc}^0 = work function of a semiconductor without surface states. It is easy to see, that for the case represented in Fig. 2, we have

$$eV_k^0 = edE_g + e\varphi. \tag{2}$$

For the case corresponding to Fig. 3

$$|eV_k^0| = |-edE_g + e\varphi|. \tag{3}$$

If we assume the semiconductor conduction zone to be far removed from the Fermi level, then the Poisson equation for the analyzed model will look as follows,

$$d^2\varphi/dx^2 = \varkappa^2 \operatorname{sh}\tilde{\varphi}, \quad \tilde{\varphi} = e\varphi/kT, \tag{4}$$

$\varkappa$ = inverse Debye length.

On the semiconductor surface bordering on the metal we have

$$E_g - \epsilon E_{ins} = 4\pi\sigma, \tag{5}$$

where σ = semiconductor surface charge (the direction from semiconductor into vacuum is considered positive). We will pick a point inside the semiconductor, where $d\varphi/dx = 0$, to be the origin of potential energy readings, $\varphi = 0$.

It is evident from Eq. (5) that for the case in Fig. 2 the surface is positively charged when $E_g > \epsilon E_{ins}$ and negatively charged when $E_g < \epsilon E_{ins}$. For the case in Fig. 3 the surface is always negatively charged (or always positively, if the metal has a negative charge). The surface charge is equal to

$$\sigma = (p_d - n_a), \tag{6}$$

where p_d = number of free donor centers on the surface, n_a = number of filled acceptor centers on the surface. As is known,

$$p_d = \frac{N_d}{1 + \exp[(\mu - e\varphi - E_d)/kT]}, \quad n_a = \frac{N_d}{1 + \exp[(E_a + e\varphi - \mu)/kT]}. \tag{7}$$

Here E_a and E_d are the energies of acceptor and donor planes, respectively. For the origin of energy readings we have chosen the top of the normal zone inside the semiconductor (behind the layer of space charge). Correspondingly, N_a and N_d are the acceptor and donor levels on the surface.

Let us now analyze the case in the absence of contact with metal, where the semiconductor surface is uncharged. In this case $p_d^f = n_a^f$ and $\varphi^f = 0$ (index f denotes that a free surface is being analyzed).

From Eq. (7), on the free surface, we get

$$\frac{N_d}{1 + \exp[(\mu - E_d)/kT]} = \frac{N_a}{1 + \exp[(\mu - E_a)/kT]} = C. \tag{8}$$

According to Eq. (8), C is the number of ionized centers of one or the other type on the free semiconductor surface. After the semiconductor is brought in contact with metal through a small gap d (gap was introduced for convenience and generality of analysis), the arrangement of zones looks as shown in Fig. 2. In our case V_k^0 is equal to V_k – the contact potential difference between the metal and semiconductor with surface states (in a general case, V_k^0 and V_k are related through the equation $V_k = V_k^0 - \varphi^f$).

In order to simplify the analysis, we will consider the distance of donor and receptor levels from the Fermi plane to be much greater than kT, before,as well as after,contact. Then (8) and (7) take the form

$$N_d \exp\left(-\frac{\mu - E_d}{kT}\right) = N_a \exp\left(-\frac{E_a - \mu}{kT}\right) = C, \tag{9}$$

$$p_d = Ce^{e\varphi/kT}, \qquad n_a = Ce^{e\varphi/kT}. \tag{10}$$

From Eq. (5) we get

$$eE_g - e\varepsilon E_{ins} = 4\pi e^2 (p_d - n_a) = 2\pi e^2 C \operatorname{sh}\tilde{\varphi}. \tag{11}$$

The field on the inner side of the semiconductor surface is obtained by integrating Eq. (4) under conditions $\varphi = 0$ at $d\varphi/dx = 0$. Then,

$$\frac{eE}{kT} = \frac{d\tilde{\varphi}}{dx} = 2\varkappa \operatorname{sh}\tilde{\varphi}. \tag{12}$$

From Eqs. (11) and (12) we get

$$eE_g = 2\varkappa kT\varepsilon \operatorname{sh} {}^1/_2\tilde{\varphi} + 2\pi e^2 C \operatorname{sh} \tilde{\varphi}; \tag{13}$$

and from (2) and (4)

$$V_k = 2d\left(\frac{\varkappa kT\varepsilon}{e} \operatorname{sh} \frac{\tilde{\varphi}}{2} + C\pi e \operatorname{sh} \tilde{\varphi}\right) + \frac{kT}{e}\tilde{\varphi}. \tag{14}$$

We will find the field in the gap by considering that

$$d = 5 \cdot 10^{-8} \text{ cm}, \ \varkappa = 10^4 \text{ cm}^{-1}, \ kT = 4.16 \cdot 10^{-14} \text{ erg (300°K)}, \ \varepsilon = 10. \tag{15}$$

The values of V_k and C are varied. The results of numerical solutions of Eqs. (13) and (14) are presented in Table 1 (calculated with an accuracy of 5%; E in v/cm).

Table 1 shows that the field in the gap rapidly increases with C – the number of ionized centers before contact. If we assume that the number of surface levels in 10^{15}-10^{16}, then the selected values will correspond to having from 10^{-2}-10^{-3} to 10^{-5}-10^{-6} of the total number of foreign centers ionized, i.e., to a perfectly real case.

TABLE 1

V_k	$C = 10^{10}$	$C = 10^{12}$	$C = 10^{13}$
0.1	$1.7 \cdot 10^5$	$1.35 \cdot 10^6$	$1.87 \cdot 10^6$
0.3	$2.7 \cdot 10^6$	$4.7 \cdot 10^6$	$5.75 \cdot 10^6$
0.5	$6.3 \cdot 10^6$	$8.4 \cdot 10^6$	$1 \cdot 10^7$

Data in Table 1 show that fields appear at the contact which provides an adhesive force of the order of tens of kilograms per square centimeter. If we calculate the adhesive force using formula $F = E^2/8\pi$, we get F = = 40 kg/cm^2 when $E = 10^7$ v/cm. One can also see that the larger the number of ionized centers on the free semiconductor surface, the more intense is the screening action of the surface and a more substantial part of the contact potential difference will fall in the gap.

In this work we have only touched upon the principal highlights in the analysis of this problem, but the chosen examples already show, that in the presence of a large number of surface states at the metal-semiconductor boundary there actually appear electric fields which provide substantial adhesion. Besides, this result is obvious enough if we remember that, when two metals come in contact, fields of the order of 10^7 v/cm appear at the boundary, while surface states "metallize" the semiconductor surface in the sense that there appears on the surface a trap of electric charges.

LITERATURE CITED

[1] B.V. Deriagin and N.A. Krotova, Adhesion [in Russian] (Izd. AN SSSR, 1949); Proc. Acad. Sci. USSR 61, 849 (1948); Progr. Phys. Sci. 36, 387 (1948); B.V. Deriagin, Research 8, 2, 70 (1955); L.P. Morozova and N.A. Krotova, Colloid J. 20, 59 (1958)*; Proc. Acad. Sci. USSR 115, 747 (1957).*

[2] S.M. Skinner, R.L. Savage and J.E. Rutzler, J. Appl. Phys. 24, 4, 438 (1953); S.M. Skinner, J. Appl. Phys. 26, 5, 498 (1955).

[3] V.B. Sandomirskii and V.P. Smilga, J. Tech. Phys. (USSR) (in print); B.V. Deriagin and V.P. Smilga, Proc. Acad. Sci. USSR 121, No. 5 (1958).**

[4] W. Brattain and J. Bardeen, Surface Properties of Germanium, Problems in Semiconductor Physics [Russian translation] (IL, 1957); J. Bardeen, Phys. Rev. 71, 10, 717 (1947).

Received July 16, 1958

*Original Russian pagination. See C.B. translation.

**See C.B. translation.

P.M.R. SPECTRA OF SOME POLYMERS IRRADIATED AT 77°K

Iu.D. Tsvetkov, N.N. Bubnov, M.A. Makul'skii, Iu.S. Lazurkin

and Corresponding Member Acad. Sci. USSR V.V. Voevodskii

In order to solve certain problems connected with the structure and chemical properties of organic radicals in the solid phase and to study the mechanism of chemical transformations arising in organic solids under the action of penetrating radiation, we undertook a paramagnetic resonance (p.m.r.) investigation of free radicals formed during irradiation of a series of polymers and substances, initially at 77°K. There is evidence in the literature, that this sort of experiment had been conducted in a series of laboratories [1, 2], however, a somewhat fuller systematic investigation with a comparison between the p.m.r. spectra of various irradiated substances had not been published.

We have investigated polyethylene, polyvinyl chloride, Teflon (polytetrafluoroethylene), polydimethylsiloxane, polyisobutylene, polymethylmethacrylate, polystyrene, polybutylmethacrylate, and natural rubber. After irradiation at 77°K in a nuclear reactor [3] (irradiated for about 1.5 hours, dose 40 megarads*), the cylindrical specimens (d = 5 mm, l = 15 mm) were transferred without unfreezing into special Dewar flasks and placed in a cylindrical resonance cavity (type H_{011}, $Q \approx 5000$) of a high-frequency modulated spectrometer. The p.m.r. signal was recorded as a first derivative. The band widths listed below were measured between the extremes of the first derivative with the help of a nuclear meter.**

Samples of all the analyzed substances, when stored at 77°K without unfreezing, gave a very intense p.m.r. signal with a g-factor close to 2.0036. Under the above-described irradiation conditions the total concentration of radicals varied from $\sim 10^{17}$ cm^{-3} (for polystyrene) to $\sim 10^{20}$ cm^{-3} (for polyethylene). At a klystron potential of ~50-100 mvolt, in the majority of cases we observed a saturation of the p.m.r. signal. When the samples were warmed up to room temperature, we observed a change in the signals of all the samples. When some samples were warmed up the signal disappeared completely (polyisobutylene, polydimethylsiloxane, natural rubber), while in the cases of polyethylene, Teflon, polyvinyl chloride, polymethylmethacrylate, and polybutylmethacrylate, the nature and the hyperfine structure of the signal changed very sharply. After the polymethacrylate and polyethylene samples were frozen again, the signal remained unchanged (same as at room temperature), but the spectrum of Teflon underwent fully reproducible and reversible changes on repeated cooling and warming (see below).

Comparison of all the data obtained shows that the type of spectra obtained with frozen samples can be fully and satisfactorily explained if we assume that the initial chemical process during irradiation is a rupture of one of the C–H bonds in the main chain, but if these are absent (as in the case of polysiloxane, for example), a rupture of a C–H bond in a side chain. We found no direct evidence that the rupture of the main chain was the initial and irreversible chemical consequence of irradiation.

If one is interested in a comparison with results obtained on irradiating frozen unbranched, saturated hydrocarbons and cyclohexane [4], then the study of irradiated polyethylene will be of the greatest interest. Polyethylene p.m.r. spectrum, taken at 77°K (Fig. 1a), consisted of six components separated by 26±3 oersteds. Cyclohexane irradiated at 77°K also had a spectrum consisting of six components. Under the same conditions, hexadecane spectrum also had an even number of components. In all these cases, the even nature of the spectrum can be connected with the formation of the radical

*Ethylene used as standard.

**In original, "Iadernyi datchik," – Publisher's note.

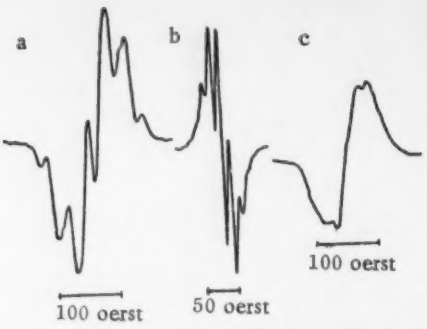

Fig. 1. P.m.r. spectra of irradiated polyethylene (77°K) (a); polyethylene (300°K) (b); and polyvinyl chloride (77°K) (c).

$$\sim CH_2 - \dot{C}H - CH_2 \sim. \quad (1)$$

Primary rupture of a C–C bond or a secondary chain rupture in (1), with the formation of $\sim CH{=}CH_2$, would lead to the creation of the radical

$$\sim CH_2 - \dot{C}H_2, \quad (2)$$

in the spectrum of which we should observe an odd number of components (as actually happens in cases where the primary process is the rupture of a C–H bond in a methyl group of a saturated hydrocarbon [4].

When the polyethylene sample, irradiated at 77°K, was warmed up to room temperature, there occurred, as we already mentioned before, a very sharp change in the spectrum (Fig. 1b). It consisted of an odd number of components and with approximately half as large a separation (14±1 oerst). When the sample was stored at room temperature the spectral intensity gradually diminished, and in about an hour it disappeared almost entirely. The spectral change on warming indicates that, when the temperature is raised, the free radical (1) undergoes some sort of an intrinsic change. The simplest explanation for these spectral changes would be an assumption that the reaction proceeds as follows at room temperature,

$$\sim CH_2 - \dot{C}H - CH_2 - CH_2 - CH_2 \sim \rightarrow \sim CH_2 - CH = CH_2 + \dot{C}H_2 - CH_2 \sim.$$

However, a few objections could be raised against making this explanation the only one. As a most obvious objection, one can point to the very large C–C bond energy in alkyl radicals (27 kcal/mole [5]) and to the incomprehensible decrease in hyperfine splitting from 26 to 14 oerst. In view of this, we tried to formulate another possible explanation for the data obtained. According to this hypothesis, when the initially formed radical (1) is warmed up, it interacts with a neighboring polyethylene molecule to form a hydrogen bridge between the two adjoining chains,

$$\begin{array}{l} \sim CH_2 - CH_2 - CH_2 \sim \\ \\ \sim CH_2 - \dot{C}H - CH_2 \sim \end{array} \quad \rightarrow \quad \begin{array}{l} \sim CH_2 - \overset{\bullet}{C}H - CH_2 \sim \\ \quad\quad\quad\quad\quad\; | \\ \quad\quad\quad\quad\quad\; H \\ \quad\quad\quad\quad\quad\; | \\ \sim CH_2 - \underset{\bullet}{C}H - CH_2 \sim \end{array} \quad (3)$$

Moreover, the decreased hyperfine splitting to approximately one half of its initial value could be understood if we assumed that the spin density of the unpaired electron was almost equally distributed between the tagged (with a star) C atoms, but almost zero near the bridge hydrogen. Then, an even number of protons would participate in the splitting, and the number of components would be odd, which fact was experimentally observed. System (3) is not stable, and in about an hour at room temperature two neighboring molecules "hook-up" directly, while the comparatively weakly bonded bridge hydrogen is removed. Of course, the proposed hypothesis requires some direct experimental confirmation.

Let us now compare our results from the study of polyethylene with the data on polyvinyl chloride. As may be seen from the spectrum (Fig. 1c), here we observe two bands with approximately the same g-factor, without any kind of hyperfine structure, and with widths equal to approximately 79±2 and 44±2 oerst. Let us analyze the possible ways by which the free radical could have formed with the main chain left intact. Two of these involve C–H bond rupture:

$$\sim CHCl - \dot{C}H - CHCl \sim \quad (4)$$

and

$$\sim CH_2 - \dot{C}Cl - CH_2 \sim. \quad (5)$$

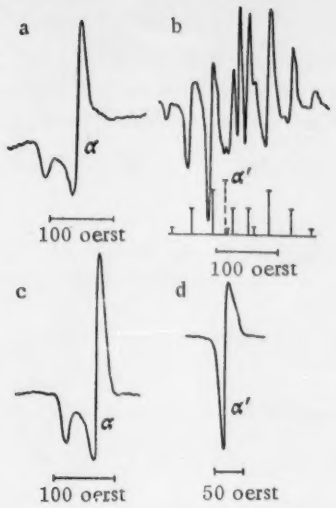

Fig. 2. P.m.r. spectra of Teflon irradiated at 77°K. 1) a = sample of 77°K before warming; 2) b = sample warmed up in vacuum (300°K); 3) c = sample b frozen in vacuum (77°K); 4) d = sample warmed up in air (300°K).

The free valence in both radicals is located in the immediate vicinity of Cl atoms. When free spin interacts with nuclei of H and Cl ($I = {}^3/_2$), a very large number of unresolved hyperfine structure components can arise; spin-nucleus interaction, in this case nuclei of H or Cl ($I = {}^3/_2$), may give rise to a very large number of unresolved hyperfine structure components, which would explain the great width of observed p.m.r. bands. Formation of a stable radical through the rupture of a C–Cl bond,

$$\sim CH_2 - \dot{C}H - CH_2 \sim \qquad (6)$$

is obviously unlikely, since it is much harder to remove a Cl than an H atom to any appreciable distance. Beside, if radicals (6), which are structurally very similar to polyethylene radicals (1), were present in the investigated system in any appreciable concentrations, then the corresponding hyperfine structure should have appeared in the resulting spectrum; it would have been superimposed on the bands of the remaining radicals. In the present case, however, the observed spectrum does not exclude the possibility of having formed free radicals by breaking the C–C bond in the principal chain.

The results obtained in the investigation of Teflon are very interesting. First of all, we should note, that if Teflon is irradiated at room temperature, as a result of disintegration [6] its mechanical properties change sharply (it changes into a rigid, highly brittle material), even at doses below 1 megarad; no such changes occur, even with ~40 megarad, when it is irradiated at 77°K then warmed up. Analysis of the p.m.r. spectrum leads to the following results. The initial spectrum of 77°K (Fig. 2a) consists of an unsymmetrical (about 50 oerst wide) band (α) superimposed on another very wide band. When Teflon is warmed up to room temperature in vacuum or under nitrogen (Fig. 2b), band α changes into a narrower asymmetric band α', while the wide band disappears; at the same time, a compound spectrum is observed, which (as is shown in the figure) consists of two quintuplets with the intensity ratio 1:4:6:4:1 superimposed on each other. The appearance of this spectrum is, evidently, due to the formation of radical

$$\sim CF_2 - \dot{C}F - CF_2 \sim. \qquad (7)$$

On second freezing, band α was retained (Fig. 2c) but the broad one was not observed. During successive cooling and warming, if oxygen was excluded, the spectra would undergo a reversible transition between forms 2b and 2c. In the presence of oxygen the compound spectrum of radical (7) became gradually weaker at room temperature, while the intensity of band α' increased (Fig. 2d); intensity of band α also increased correspondingly on cooling. Though the presence of an asymmetric line in irradiated Teflon has already been observed before [2], yet as far as we know, the other spectral peculiarities had not been recorded. It seems to us that the observed picture can be explained in the following way. When Teflon is irradiated at 77°K, radicals of type (7) and F atoms are formed, which explains the appearance of a wide diffuse band in spectrum 2a. The small amount of oxygen dissolved in Teflon reacts with radical (7) to form a certain number of peroxide radicals, which also explains the appearance of band α. When the sample is warmed up, the fluorine atoms either recombine with, or break, the C–C bonds, leading to a partial disintegration of (7), and the spectrum of radical (7) appears better defined. When oxygen is present, it diffuses among radicals (7), converting them into very stable peroxide radicals. And, consequently, an increase in the intensity of band α takes place. The change in the form of band α on cooling can be explained if we assume that at 77°K the peroxide group C–O–O is frozen, while at room temperature a free rotation around C–O bond takes place. Calculations done on this assumption showed that the C–O–O angle in a peroxide radical of the type studied is 75±15°.

The proposed scheme fails to explain why the spectrum of radical (7) disappears on freezing. That the radical itself does not disappear is obvious from the reversibility of this phenomenon.

Therefore, when Teflon is irradiated at low temperatures, it is possible to obtain a fully satisfactory (in its mechanical properties) material, containing a large quantity of (~0.1%) of fluoroalkyl or peroxide-free radicals.

Beside, it is very interesting to note, that absorption bands of type α were observed with other organic compounds irradiated in the presence of air [7]. We also observed bands of this type in finely dispersed polyethylene, irradiated in the presence of air. It seems very likely that the appearance of such bands as a result of irradiation could serve as a direct indication of peroxide radical formation.

LITERATURE CITED

[1] E.E. Schneider, Disc. Faraday Soc. 19, 158 (1955); J. Uebersfeld, Compt. rend. 239, 240 (1954).

[2] W.B. Ard, H. Shields and W. Gordy, J. Chem. Phys. 23, 1727 (1955).

[3] Coll. Reactor Construction and Theory, Proc. of the Sov. Delegation at the Geneva Conference [in Russian] (Izd. AN SSSR, 1955) p. 91.

[4] N.Ia. Cherniak, N.N. Bubnov, et al., Proc. Acad. Sci. USSR 120, 346 (1958).*

[5] V.V. Voevodskii, Trans. of the Kiev Conference on the Problems in Org. Reaction Mechanisms [in Russian] (Kiev, 1953) p. 58.

[6] J.W. Ryan, Mod. Plast. 31, 51 (1953).

[7] G. McCormick and W. Gordy, Bull. Am. Phys. Soc. 1, 200 (1956); H.N. Rexroad and W. Gordy, Bull. Am. Phys. Soc. 1, 200 (1956).

Institute of Chemical Physics
Academy of Sciences, USSR

Received July 24, 1958

*Original Russian pagination. See C.B. translation.